Bull. Spec. Astrophys. Obs., 1996, 40, 5–124

Investigation of RATAN–600 RC radio sources

Parijskij Yu. N.[a], **Goss W.M.**[b], **Kopylov A.I.**[a], **Soboleva N.S.**[a], **Temirova A.V.**[a], **Verkhodanov O.V.**[a], **Zhelenkova O.P.**[a], **Naugolnaya M.N.**[a]

[a] Special Astrophysical Observatory of the Russian AS, Nizhnij Arkhyz 357147, Russia
[b] National Radio Astronomical observatory, P.O. Box 0, Socorro, New Mexico 87801, USA

Received January 19, 1996; accepted February 20, 1996.

Abstract. We use the RATAN–600 radio telescope for picking up the most distant objects in the Universe. As a first step, about 100 steep spectrum FRII radio galaxies (SS FRII RG) from the RATAN–600 RC catalog (Parijskij et al., 1991; 1992) were mapped by the VLA and identified with optical objects down to 24–25 R mag. All the VLA images and all the deep CCD images of the RC SS fields, collected up to now, are given. An updated list of calibrators with the known redshifts of the same SS FRII class RGs was compiled to estimate photometric redshifts, redshifts from angular size – redshift relations and by the radio "standard candle" method. The mean redshift of the RC SS FRII RG list happened to be greater than 2. $BVRI$ photometry was made, and by standard model fittings we estimated "color" redshifts and the ages of stellar systems of the parent gE galaxies in 14 cases. Several objects were found in which active star formation began in the first billion years after the Big Bang. We believe that more than 10000 of such old active galaxies are available on the sky and all of them are in the range of present day optical and radio facilities.

Key words: radio galaxies: general – observations – cosmology

1. Introduction

In the experiment "Cold" conducted at the RATAN–600 radio telescope in 1980–1981 a strip of the sky, 24–hours long and 0.3 deg wide, centered at "the sky object No.1", SS433 (declination about $+5^0$) was observed at frequencies from 1 GHz to 22 GHz. The best receiver at 3.9 GHz had an rms sensitivity of about 3–5 mJy (1–2 mK) per beam in a single daily scan. About 100 daily records were collected for the whole 24–hours right ascention range. The "coldest" part of this strip has been observed practically every year ever since. In these selected regions of the strip about 300 daily multi–frequency scans are available at present. We had in mind a threefold goal.

- Very deep cross–cut of the Galaxy and SS433 monitoring.
- Cosmic microwave anisotropy experiment on all scales down to a resolution limit of 1 arcmin (up to l=3000 Legandre term).
- Detection of discrete radio sources at a flux density level below the lowest one, reached by Effelsberg group in 1979 (14 mJy at 6 cm).

The results related to the first two objectives were discussed by Parijskij and Korolkov (1986). The preliminary results on the source statistics were published by Berlin et al. (1984) and discussed also by Parijskij and Korolkov (1986). The first catalog of the radio sources discovered at the most sensitive frequency, 3.9 GHz, after the first year of monitoring the "Cold" selected area in two azimuths $(0°, 30°)$ appeared in (Parijskij et al., 1991; 1992) under the name RC (RATAN–600 Cold). 1145 objects down to a few mJy were included in the list, most of them being new ones, having no identification in any published radio, infrared, optical, X–ray catalogs (Bursov et al., 1993). Great efforts were made to improve the positional accuracy of the catalog and final errors of about 4.5 arcsec were reached for objects in the central part of the strip. It means that the RC catalog has an area of the error box by an order of magnitude less than that of Zelenchuk Sky Survey (Z) (Amirkhanian et al., 1989) and Green Bank (GB) Survey with a flux density limit of RC catalog by a factor of 5–10 deeper. About 20% of sources (with steep spectra or strong enough) were successfully identified with the UTRAO objects (Reich et al., 1991), but most of the sources waited for much better position information. The RC catalog fills the gap between the very deep sub–mJy class VLA and WSRT surveys of very small regions of the sky and GB and Z class surveys of very large areas. There are many interesting directions of investigation of radio sources in this gap. As a first step, we decided to use the RATAN–600 for picking

up the most distant population of radio sources in the 1–50 mJy range, where the $log(N/N_0) - log(S)$ curve has maximum slope. Now it has been proved not only by theory (Longair, 1974), but also by direct redshift measurements in different flux density regions from Jy to μJy populations. To get maximum information about distant radio sources discovered in the experiment "Cold" the BIG TRIO project was suggested (Goss et al., 1992,1994), and we describe here the present status of that project. The RATAN–600 is used as one of the best wide field searching survey instrument, the VLA – as the best imaging system, the 6 m Russian optical telescope – as one of the world best instrument for deep optical identification and spectroscopy. In the first two Sections we present the method of preliminary selection of candidates for the very distant objects from the radio surveys which we use. Then we give all the VLA maps obtained up to now for the selected RC object fields and all available optical CCD images of these fields. Next Section is concerned with our first attempt to estimate redshifts of the identified objects and ages of stellar population of the parent galaxies. Astrophysical aspects of the results obtained up to now we give in the last Section together with some future prospects of the project. Apart from the program connected with picking up the most distant galaxies, several other programs based on the RC catalog are in progress: variability of radio sources at the RC catalog flux levels (practically unexplored) on time scales from 1 day to 15 years, complete spectral information and selection of physically different subgroups of radio objects, including QSRs, BL Lac, UCSS and GPS objects. We hope to contact with VLA, VLBI, X–ray and other investigators at some step of data reduction to get as much information as possible. We shall publish the results of these next steps of the RC catalog data reduction as soon as they appear.

2. Strategy of radio selection of distant galaxies

It is clear now for all groups, working with Early Universe objects, that blind optical searches for high–redshift objects are very inefficient (it is better to say, have a zero efficiency) and we have to find some preliminary selection rule of picking up the most probable candidates and only then we can ask for very expensive observing time at big optical telescopes. All attempts to escape the step of preliminary selection were a failure. Direct spectroscopy of all objects in the fields of the best optical telescopes up to $m_I = 22.5$ gave the median $z = 0.56$ and none with $z > 1.4$ (Crampton et al., 1995). In the famous 3C catalog only one object has $z > 2$, and the mean $z = 0.57$. The same situation is with the IRAS, Einstein and ROSAT data, the mean z of even weak populations in these catalogs is much smaller than 1. Optimization of the radio flux density range only was not of great help. Even in the "deepest" range, 1-50 mJy, VLA attempts to compile a list of 2–10 mJy sources at 6 cm gave the mean $z = 0.1$ only. Recent combined radio–optical record in the deepness of the sky survey (8.8 μJy in radio, 25.6 R mag in optics) was unsuccessful again: the mean z of 7 measured galaxies ($I < 20.5$ mag) being only 0.25 with estimates that for fainter objects ($I < 22.5$ mag) visible by HST and associated with μJy population of radio sources z should be lower than 0.8 (Windhorst et al., 1995).

The main cause of this situation may be explained in the following way. Even in a non–evolving Universe the number of sky objects of any nature at $z > 1$ is smaller than that at z of about 1 because of geometry of every not very empty Universe. For the radio Universe this is discussed, e.g. in J.Condon's review (1988). Practically, only very luminous objects can be observed at very high redshifts in optics (and in radio as well), which have spatial densities by a few orders of magnitude lower than normal galaxies. It means, that the expected angular separations between potentially observable objects (say, 1–2 deg, see below) are two orders of magnitude greater than the field of view of any big instruments (about 1 arcmin for HST and VLA). (The situation may be better only in an empty Universe and only when $R = 27 - 28$ objects can be observed spectroscopically (Yoshi and Peterson, 1991), or with the next century generation of very wide field instrumentation in Astronomy and Radio Astronomy.)

Several selection rules have been proposed in the last decade. These include:

- Looking around distant QSOs at the prescribed z as deep as possible (Djorgovski method, Djorgovski et al., 1985).
- Use of Lyman α forest in the absorption spectra of the most distant QSOs and identifying absorption features of individual galaxies.
- Method of selection of $z > 3$ objects with Lyman continuum cut–off appearing in the optical domain.
- Looking for 100–micron peak of IR emission from dusty galaxies, shifted in the submm-mm-cm region. This gives a way practically unlimited by distance (K–correction is strongly positive for these objects and dominates over the "distance" losses, see Parijskij and Korolkov, 1986).

But in reality, the rule of preselection of steep spectrum FRII objects happened to be far more efficient than any others (McCarthy, 1993). In some sense, due to a new role of that class of radio sources, classical radio astronomy of Cygnus–A type objects now experiences the epoch of "Second Birth". Indeed,

it was well known even in the 50s that the most powerful class of Cygnus–A type radio sources can be detected at very high redshifts. The main barrier was not an instrumental, but psychological one: up to the 80s it was generally adopted in astronomy that the epoch of galaxy formation can not be much earlier, than at $z = 1$. The last decade have drastically changed this point of view. In the summer of 1995, the absolute record of the published highest-z galaxies was $z = 4.41$, which is close to the QSR record, $z = 4.46$. Whereas the QSO record was 5.2. In the late 70s, it was realized that steep spectra radio sources are most difficult to identify with optical objects, they are very often invisible on the POSS prints. Later it was proved that they are at the greater redshifts. Since that time a radio preselection of SS RG has become the main and practically incompetitive tool in the attempts to find the most distant galaxies. Except a few galaxies found by methods 2 and 3, all 200 galaxies with $z > 1$ were discovered through the SS RG approach. Kapahi and Kulkarni (1990) suggested that the strong recomendation of Longair (1974) to use FRII RG should be combined with the steep spectrum selection rule and demonstrated the efficiency of this approach. In the BIG TRIO project we have added two criteria:

- Optimization of the flux density range of the selected radio sources.
- Optical identification program may be about 100% efficient if we take into account that (from the experiment) the radio luminosity is as a rule lower than optical.

Moreover, only for the FRII RG this ratio is approaching 1 and can be used for classification of objects prior the spectroscopy or morphology investigations. QSRs have far stronger optical luminosity, being about the same in radio power. FRI, Sy and normal galaxies have much lower radio power, being only slightly less luminous in optics.

Many investigators point out that up to now only in radio galaxies it has been possible to observe a good enough spectral content of the light from stellar population. And it is possible to trace back the history of the stellar population and recover the epoch of the beginning of the star formation, the most important parameter for cosmology. It is interesting to note here that in some sense the FRII SS approach is the "antipode" of the classical Tinsley way of selection of very young objects with signs of the first burst of star formation. Here we are looking for the oldest stellar systems at the high redshift. Indeed, the following properties of the FRII objects are normally suggested.

1. Parent galaxies are of gE type with a very advanced stellar evolution history.

2. Being the most powerful radio emitters, they should have the most advanced giant black hole evolution history, which includes the process of normal star formation in the protogalaxy, formation of the very dense central star cluster, growth of black hole from stellar mass to half billion solar masses, through Eddington limited QSO activity.

3. FRII–class radio sources belong to the objects with the most advanced radio structure, not only because of the big sizes (up to a few Mpc), but also because of the large energy content in the bubbles, accumulated during a rather extended period of nuclear activity.

4. Steep spectra normally appear due to the aging of the relativistic electrons in the bubbles. It also takes time.

5. Most popular cosmological alternatives of galaxy formation suggest that such objects as giant ellipticals of 10^{12} solar masses may appear through multiple (10^4 times) merging process in hierarchical cosmology or they have to wait the completion of fragmentation process of protocluster cloud. Both variants have finite time scale.

There are also several important observational "marvels" in FRII class. Let us recall them.

- Being the most powerful population of the radio sky, with the present–day facilities they can be detected at any distances up to the recombination epoch.
- In the optical domain they are much more luminous than any other galaxies (only QSOs are brighter) and also can be observed with the best present–day optical instrumentation up to $z = 5 - 10$.
- As we demonstrate below the "standard candle" method can be used to estimate redshift of these objects with a 7–10 % accuracy up to at least $z = 1.5 - 2$.
- Direct redshift measurements are much easier owing to the strong narrow lines with a line luminosity about equal to the luminosity in the continuum. It means that if an object is identified its redshift is also measurable.
- Angular sizes of the gE are normally 2–5 arcsec at $z \sim 2$ and ground–based optical facilities can be used as well as space–borne, the latter may be very efficient in the imaging of these objects.

3. Redshift estimations

Only a few quanta per minute can be caught from a high–z galaxy even of the gE class. That is why we have to be as carefully as possible in the final selection of candidates for the first generation galaxies. No more than 1–2 of such weak objects per night can be investigated spectroscopically by the best optical telescopes. In this Section we discuss different ways

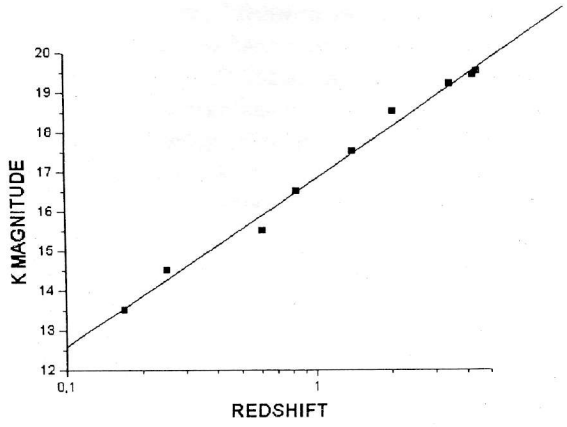

Figure 1: $K - z$ *relation*

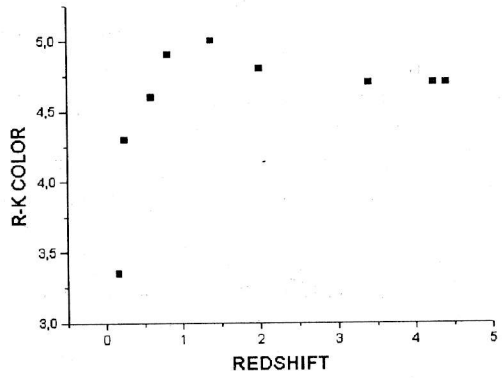

Figure 2: R–K *color index vs* z

of preliminary estimation of redshift after the optical identification of objects which in its turn remain in the list after the radio selection process. The last step will be related to the "age" selection by multi-color photometry and only then we can go to the deep spectroscopy of candidates for the objects with the closest to the Big Bang epoch of the first star formation. Only a few percent of the original catalog can survive in that long way...

3.1. Photometric redshift calibration

It has been known for over 10 years that up to $z = 1$ the gE, responsible for the FRII radio galaxies type, can be considered as the "standard candle" in R and K bands with very small dispersion in absolute magnitudes (e.g., $R = -23.2 \pm 0.3$ (McCarthy, 1993). Physical reason for this is unclear, but it helps greatly in estimation of redshift with an accuracy up to 7% without spectroscopy. At higher redshifts, in which we are interested here, the situation is not so good. But at least in the K–band, less sensitive to the young stellar population, there is a strong relationship between K mag and z. To demonstrate this, we have collected all the published data and show them averaged in several redshift bins in Fig.1.

A simple linear fit yields

$$K = (21.33 \pm 0.09) + (4.6 \pm 0.16) \times log\ z$$

with a correlation coefficient $R = 0.995$ for all the objects with $0.5 < z < 4.41$.

Such a simple behaviour of the $K - z$ relation has not been understood either as yet – it is not easy to compensate all z–dependent effects of different signs, such as luminosity evolution and Geometry of the World, K–corrections even for non–evolving spectral energy distribution (SED) etc. If only R mag was available, (as in our project up to now), we used K–calibration and $R - K$ color index, slowly variable

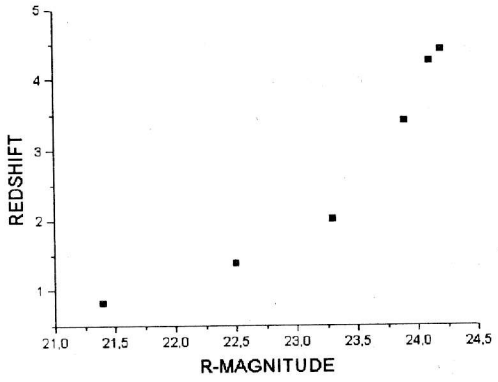

Figure 3: $R - z$ *relation*

with z, as it is shown in Fig. 2. The final R–z relation is shown in Fig. 3.

The present–day $R - z$–calibration curve differs slightly from the curve we have used in our previous publications (Kopylov et al., 1995a,b). Here we present the SS FRII $R - z$–calibration curve from Dunlop et al. (1989) for $0 < z < 1.5$ and updated points for the $2 < z < 4.41$ part of the curve, which include the last year records. Linear regression gives the following solution:

$$R = (21.90 \pm 0.12) + (3.68 \pm 0.28) \times log\ z.$$

This curve was used in the calculation of the photometric redshifts. We estimate that the accuracy of the $z > 3$ part of the curve is not better than 30% because of the small statistics and (very possibly) higher real physical dispersion in the early galaxy stellar content because UV from short–living stars penetrates into the R band.

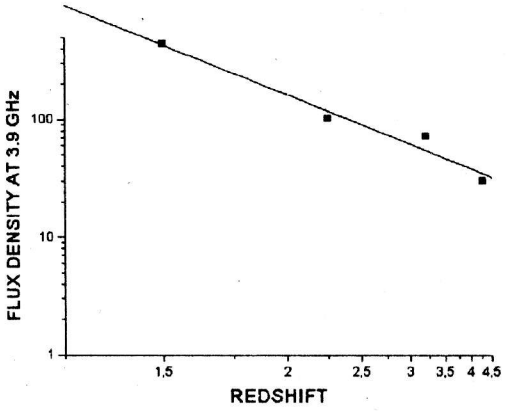

Figure 4: *Flux density vs redshift*

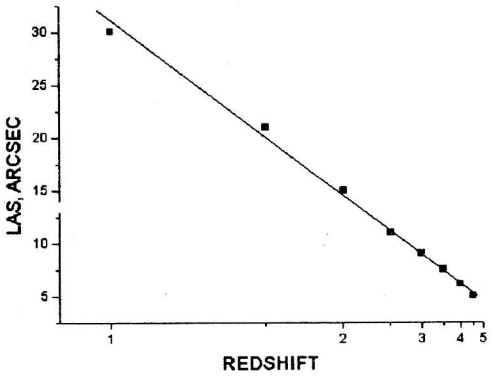

Figure 5: *L.A.S. – z relation*

3.2. Radio "standard candle" method

If we collect all information about the "flux density–redshift" relation for the SS FRII RG we can realize that there is a correlation between these values, which can be used for z–determination, see Fig. 4.

It can be shown (Kopylov et al., 1995a,b) that there is a very small dispersion in the radio luminosities of all high-z doubles discovered so far and listed, e.g., in the Nilsson et al. (1993). If we select the SS FRII RG subgroup, the dispersion will be even better, all 17 well studied objects in that list have $logL(erg/s) = 45.61 \pm 0.35$. It means that, in principle, we can try to use that class of radio sources as "standard candle" of about a maximum radio luminosity observable in the nearby Universe. There are certainly many selection effects which can mimic the "standard candle" situation, but even in this case z estimations from radio flux may be useful. We can understand the fact as follows. The FRII class has normally a radio luminosity "not greater but very close to" the upper limit for any radio objects. It is a mystery that this limit is just the optical luminosity of the parent galaxy. The fact that the lobes energy content of the FRII RG is very close to M_c, where M_c is the critical mass of black hole, $5 \cdot 10^8 M_\odot$, at which its luminosity reaches the Eddington limit, is much more understandable than the correlation with normal star population in old galaxies. Only in the case when the ratio of mass of the nuclear black hole to the mass of galaxy is equal to the ratio of efficiency of stellar interior nuclear reactions to efficiency of black hole gravitation energy release we can expect some correlation of the kind observed. It is interesting that the real situation is not far from this.

For the "standard candle" there is a well known (e.g., Longair, 1974) model–dependent expression, connecting the flux density and the redshift. For $\Omega_0 = 1$, $\lambda_0 = 0$ it looks as follows:

$$S = P_0/\{(4c^2/H_0^2)[1-(1-z)^{-1/2}](1+z)^{1+\alpha}\},$$

where P_0 is the radio luminosity, H_0 is the Hubble constant, α is the spectral index, $S \sim \nu^{-\alpha}$. We calculated $S(z)$ behaviour for the FRII RG–like Cygnus–A, (see Parijskij and Korolkov, 1986). The SS FRII RG objects as well as Cygnus–A can be observed with the RATAN–600 at any redshift even in the transit mode and very easily with the VLA, where long integration times can be used. This formula makes it possible to estimate redshift from the "radio Hubble" $S - z$ relation.

3.3. Redshifts from the LAS

The redshift–angular size relation for the "standard rod" case has been discussed in radio astronomy since 1958 (Hoyle, 1959), but no agreement between radio astronomers on its behaviour either from the observational point of view or from the theoretical interpretation has been reached so far. As was stressed most strongly by Kapahi (1986), there is linear "*log θ–log z*" relation, and only the Euclidean Universe can explain it. The Dutch group (Windhorst, 1984; Oort, 1987; Neser, 1995) suggested the linear size to be variable with z, which compensates the effects of the General Relativity Theory (GR). Kellermann (1993) and Gurvits (1993) indicated that sub–galactic double VLBI structures follow the standard GR predictions. Using RC sample, we feel that there may be two populations of FRII doubles: the one that follows GR predictions and may not be due to the differences in the surrounding medium. We do not want to get into this problem, but just present the observational data collected for the FRII SS RGs, see Fig. 5, which we used as a secondary redshift calibration curve before direct spectroscopy.

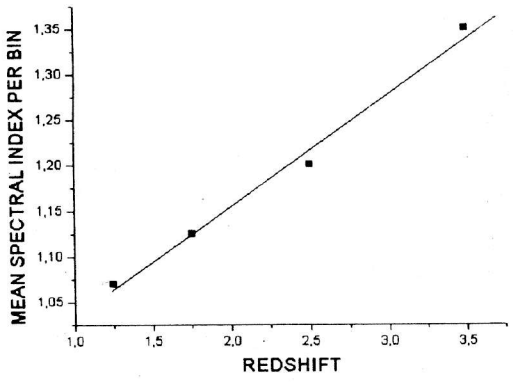

Figure 6: *Redshift vs spectral index*

3.4. "Color" redshifts

"Radio colors", the shapes of spectra of radio sources, are used by numerous groups for preselection of distant radio populations and, as we have discussed earlier, we use this information in the first selection step. A few years ago we realized, independently of other groups (e.g., Oort, 1987), that inside steep spectrum populations there is a statistically meaningful redshift–spectrum index correlation. We demonstrate it in Fig. 6.

The simplest physical interpretation of this correlation is "spectrum curvature effect" (e.g., Soboleva et al., 1977) .

There are several suggestions in literature for using multi–color optical photometry for redshift estimations (Benn et al., 1988). This calibration may be used up to $z = 1$ with an rms error less than 15%. For greater z there are no observational calibrations yet and we decided to use the predictions from the available evolutionary models for our class of gE galaxies. The results of this approach are given below.

4. Ages of the parent galaxies

Even with direct spectroscopical redshifts, we have to find a way of estimating the epoch of parent galaxy formation, the most crucial value for evolution of galaxies. It will be recalled here that gE, related to the FRII RG in a first approximation, look like radio quiet gE, and only careful morphological and spectroscopic studies may reveal some peculiarity. In QSOs the stellar population light is much lower ($< 1\%$) than that of a nuclear excited region, and classical stellar system evolution models can not be used to trace its history back to the moment of the first burst of star formation. We collect now all suggestions related to the problem of age of FRII RG parent galaxies.

4.1. Age from radio data

1. Statistics approach (Schmidt, 1966). If all gE pass through the RG phase, the mean age of the RG can be estimated from the equation

$$T/T_o = N_{RG}/N,$$

where T is the age of the RG, T_o is the age of the gE, (close to the age of the Universe), N_{RG}, the spatial density of the RG, N, the spatial density of the gE.

2. The age from L.A.S.: the minimum value is just the linear size of the radio structure divided by the velocity of bubble expansion. In the early 60s it was suggested that v/c for the bubble velocities is close to 1 (Ryle and Longair, 1967). But later it became clear that it is not the case, and $v/c \ll 1$ (Parijskij and Soboleva, 1980) and the value of $v/c = 0.03 - 0.05$ is much closer to reality. X–ray data confirm the low–velocity solution.

3. The age from the energy consideration:

$$t = E/(dE/dt),$$

or

$$t = \frac{Bubbles\ energy\ content}{Eddington\ nuclear\ luminosity\ limit}.$$

4. The age from the spectral breaking due to the electron aging in the magnetic (or CMB electromagnetic) fields is found from the equation:

$$f_{break} = B^{-3}t^{-2}GHz,$$

where B is the magnetic field strength in Gauss, t is the age in years (e.g., Kellermann, 1973).

The detailed multi–frequency mapping of the bridge between bubbles can also be used to estimate the breaking frequency in the regions far from the main source of relativistic electron generation, that is from the "hot spots", even if this fact is not well visible from the integrated spectrum (Daly, 1992, 1994). In our case of the most distant objects it should be remembered that for very extended RG the Compton losses dominate over the synchrotron ones and the age of a radio structure depends strongly on the redshift, because the density of the CMB energy increases as $(1+z)^4$. In our case of SS FRII RG it is generally believed that the very fact of steep spectrum indicates that we are dealing with an old radio structure. We collected all information about the radio spectra of all RC objects, and it can be used to estimate the age of their radio structures. This method is equivalent to the optical one from multi–color photometry (see below).

4.2. Optical age estimates

There are several models of evolution of the synthetic spectra of the stellar population of early galaxies

Table 1: *Redshifts and ages of the RC radio galaxy subsample*

Name	δt	z_{cc}	z_{ph}	z_{LAS}	z_{sp}	z_{mn}	z_{sf}	z_{g_0}	T_{cc}	T_{mn}	T_{sf}	T_{bh_0}	T_{g_0}
0837+0446	0.4	2.3	1.2	3	1.0	1.9	2.4	5.0	1.7	2.1	1.6	1.3	0.7
	0.6	2.7	1.2	3	1.0	2.0	2.8	7.5	1.4	2.0	1.4	1.0	0.4
0934+0505	0.9	3.4	3.9	3	1.3	2.9	7.6	23.3	1.1	1.3	0.4	0.7	0.1
	1.1	1.7	3.9	3	1.3	2.5	7.0	3.0	2.2	1.5	0.4	1.8	1.2
1031+0443	0.9	0.6	1.2	1.0	2.3	1.3	1.9	0.9	4.9	2.9	2.0	4.5	3.9
1152+0449	1.1	1.2	1.4	3	1.0	1.6	2.9	1.9	3.1	2.4	1.3	2.7	2.1
1219+0446	0.9	2.4	1.2	0.5	2.6	1.7	2.7	5.6	1.6	2.3	1.4	1.2	0.6
1333+0452	1.1	1.2	1.4	0.5	4	1.9	3.5	1.9	3.1	2.1	1.0	2.7	2.1
1357+0453	0.9	0.6	0.5	2.3	1.0	1.1	1.6	0.9	4.9	3.3	2.4	4.5	3.9
	1.1	0.5	0.5	2.3	1.0	1.1	1.7	0.7	5.4	3.3	2.2	5.0	4.4
1436+0501	0.35	1.2	2.1	2.1	2.8	2.1	2.5	1.9	3.1	1.9	1.5	2.7	2.1
1510+0438	1.7	0.6	1.4	3	1.0	1.5	4.3	0.9	4.9	2.5	0.8	4.5	3.9
1626+0448	0.6	2.7	1.5	3	2.8	2.5	3.9	7.5	1.4	1.5	0.9	1.0	0.4
1646+0501	1.7	0.6	0.6	2.0	1.9	1.3	3.1	0.9	4.9	2.9	1.2	4.5	3.9
1703+0502	0.6	3.0	1.9	3	2.5	2.6	4.1	10.7	1.2	1.5	0.9	0.8	0.2
	0.9	2.0	1.9	3	2.5	2.4	4.7	3.9	1.9	1.6	0.7	1.5	0.9
1740+0502	0.9	0.4	1.2	3	2.4	1.7	2.9	0.6	6.0	2.2	1.3	5.6	5.0
	0.4	3.8	1.2	3	2.4	2.6	3.3	99.9	0.9	1.5	1.1	0.5	0.0
2013+5080	0.33	2.5	0.4	2.7	1.0	1.7	2.0	6.1	1.5	2.3	2.0	1.1	0.5

from the very beginning, that is from the moment of the first "star burst". We used the Chambers–Charlott calculations (1990) for the SED, but other models can be used as well. These models predict the $UBVRIK$ fluxes as a function of age using the improved Bruzual method. Our $BVRI$ photometry results were used, and an agreement with model prediction can be achieved by proper adjusting of the redshifts and ages. We illustrate the process in Fig.7 (p.33). at the end of this paper. In this figure positions of optical photometrical ($BVRI$) points on the SED curves for the different ages of radio galaxies are estimated using the least square method for the tabular defined functions (Verkhodanov, 1996). The best model fittings, defined by the minimization of the sum of squares of discrepancies, are shown in Fig.7 and used in Table 1.

Morphology studies can also be used to estimate the "dynamical age" of the stellar system. The relaxation time for the system can be estimated from the Chandrasekhar formula:

$$t_{relax} = (2/3)^{1/2} \frac{v^3}{3\pi G^2 m n \lambda},$$

where $\lambda = ln(n/2)$. For the central dense stellar cluster the following values are usually adopted: $m = 1M_{\odot}, n = 10/pc, v = 225\ km/s$. It gives $t_{relax} = 3 \cdot 10^8$ yr. The relaxation of the whole giant galaxy system takes a few rotation periods, that is about 0.3–0.6 Gyr.

It is generally believed that in the relaxed (old) systems the surface brightness of the galaxy drops as $r^{1/4}$ and this is confirmed by accurate photometry of gE.

Spectroscopy methods. There is some problem in separation of age and chemical abundances. Recently it has been found that Balmer–γ line 4340 Å (Jones and Worthey, 1995) can be used to separate these effects. For our selected SS FRII objects this line is expected to appear in K–band.

In Table 1 we have tried to use all kinds of the redshift estimates mentioned in Section 3 to find the epoch of formation of gE, responsible for the FRII RG. Ages, calculated with the Chambers–Charlott model (1990), were used to estimate the epoch (and redshifts) of the last burst of star formation. Mean value happened to be $z_{sf} = 3.3$ (corresponding to the first Gyr after the Big Bang) with a big dispersion. The time of the galaxies formation for the FRII class of objects may be estimated from z_{RG}, if we take into account the extra time needed to form giant black holes (3×10^8 solar masses), working as the energy sources of these objects. In classical theory this time is determined by the fundamental constants only, being 0.4 Gyr. We used this value to estimate independently the epoch of the beginning of central black hole formation in our objects. Normally, we have to wait for about 3 galaxy rotations before the central star cluster may be formed, where a black hole can find the fuel. Inspite of the great uncertainties, all these values are not extra-ordinary ones and will be checked later by direct redshift measurements.

In Table 1 z_{cc} is the estimated redshift of the RG using Chambers–Charlott (1990) models for SED

of gE and δt is the appropriate age (Gyr) of star population for the best model fittings of the observed $BVRI$ fluxes, T_{cc} is the corresponding cosmic time (Gyr) of the radio source (for the flat Universe, $H_0 = 75\ km/s/Mpc$), z_{ph} is the photometrical z, z_{LAS} is z estimated using the object radio size, z_{sp} is z estimated from the "spectral index–redshift" relation, z_{mn} is the mean of all types of redshift estimates (z_{ph}, z_{cc}, z_{LAS}, z_{sp}), T_{mn} is the corresponding cosmic time of the radio source, z_{sf} is the redshift of the beginning of the last burst of star formation in the RG, T_{sf} is the corresponding moment in Gyr, T_{bh_0} is the time of the beginning of the giant black hole formation in the galactic centre (see the paper), z_{g_0} is the redshift of the galaxy gas component formation, which happened 3 galaxy rotation periods earlier than the black hole began to appear, and T_{g_0} is the corresponding cosmic time.

4.3. Age of FRII RG and the black hole evolution time scale

Beginning from the pioneer Hills work (1975), it has been generally believed that radio activity began after the maximum luminosity stage of the black hole evolution. In his evolution picture, the time of growth of a primary black hole of about 10 solar masses in the central dense stellar cluster to about $3.2 \cdot 10^9 M_\odot$ (when maximum optical luminosity is reached) depends on the fundamental physical constants only:

$$t_{edd} = \sigma_{Tompson} c / 4\pi G m = 0.4 Gyr.$$

Here m is the proton mass (see Rees, 1984).

After that time the energy resources depend not on the internal processes in the central cluster, but mainly on the outside accretion rate, the time scale of which has not been so well determined and may be triggered by the gravitational interaction with the nearby galaxies.

We shall collect time scales of all processes for the well studied subsample of RC objects later, getting all information we need from the radio and optical observations of radio galaxies from our list.

4.4. Coming back to recombination epoch

Star formation process can begin only after the collapse of protogalaxy cloud from rarefied state to a density, comparable to the density of the Milky Way, about $1/cm^3$. It takes time. Peebles (1980) uses the formula

$$t_{max} = (6\pi G \rho_b(t_{max}))^{-1/2},$$

(where ρ_b is the barionic density of the Universe) to estimate the time required to reach protoobject maximum size in the expanding close Universe, after which it will be gravitationally isolated from the expanding surroundings and may collapse to the density, adequate for the star formation process. As was mentioned by Gurevich and Chernin (1983), this time is exactly the same, as that, spent for the expansion. Before the moment t_{max} the density of the protoobject relative to the mean surroundings increases as $1/(1+z)$, but up to the redshift

$$z = (3/5) \cdot (1 + 1/\Omega_0)$$

only. It means that for small Ω_0 (0.03 from He/H abundance) a maximum possible relative density increase from recombination ($z = 1000$) is about 30 (Peebles, 1980). This discussion will be used later in attempts to playing back the evolution of protogalaxies down to the recombination time, for which we have some observational restriction from the RATAN–600 (and some from the USA) anisotropy experiments.

5. VLA maps of the selected RC objects

In this Section we present all available radio images of radio sources from the RC catalog. All maps were made with the help of the VLA at different configurations. All the radio data, obtained from the VLA maps, RATAN-600 observations and from literature, are collected in Table 2.

Column **1**: The source name according to RATAN–600 RC catalog.
Columns **2,3**: Right ascension and declination of objects for the epoch 1950.0 determined from the VLA observation.
Column **4**: The VLA beamsize, in arcsec.
Column **5**: The VLA central frequency, in MHz.
Column **6**: The largest angular size of the source measured between peaks of components in arcsec.
Column **7**: The angular size of the components of the source, in arcsec.
Column **8**: Flux densities of components at the VLA central frequency, in mJy.
Column **9**: Total flux density of the object at the VLA central frequency and an expected one from the integrated spectrum of the source (in brackets), in mJy.
Column **10**: The extrapolated flux density of the object at 3.9 GHz, in mJy.
Column **11**: Spectral index ($S \sim \nu^{-\alpha}$) calculated by least square fit, rejecting points strongly falling out.
Columns **12,13**: Galactic longitude and latitude.
Column **14**: The limiting optical magnitude calculated from the condition: optical luminosity equals to radio luminosity (see Section 3.2 of the paper).
Column **15**: Structure classification: P–point, Ext–extended, Df–diffuse, CJ–core with jet, C–core, WC–weak core, BC–bright core, D–double, T–triple, M–multiple; FRII–Fanaroff–Rily II type structure. The sources marked with asterisk have individual notes below the table.

Table 2: *The list of RC sources having the VLA images.*

RC name	R.A. 1950.0	Dec 1950.0	Beam	Freq	LAS	Comp. size	Comp. f.d.	f.d.(integ) at VLA	f.d. 3.9GHz	α	l	b	m_{lim}	Morphol.
1	2	3	4	5	6	7	8	9	10	11	12	13	14	15
	h m s	$^\circ$ $'$ $''$	$''\times''$	MHz	$''$	$''\times''$	mJy	mJy	mJy		$^\circ$	$^\circ$	^{m}	
0015+0503a	00 12 36.809	4 50 05.6	9.25×4.66	1425.0	20.6	4.6×2.8	30	92	18.9	.84-1.07	106	-57	23.7	D,FRII
	37.995	49 55.0				4.6×4.6	62							
0015+0503b	00 12 44.17	4 47 12.0	9.25×4.66	1425.0	9.8	<4.7×3.3	5.2	7.6			106	-57		D,FRII
	44.78	17.0				<1.1×3.3	2.4							
0015+0501	00 12 48.498	4 44 53.3	9.25×4.66	1425.0	16.3	10.0×4.6	75	91(99)	36.3	1.03	106	-57	22.9	D,FRII
	48.90	37.7				7.6×4.6	16							
0029+0509	00 26 29.101	4 53 00.03	1.1	4885.1		point		(415)	430	0.14	113	-57	19.2	P,*
0034+0513	00 31 31.23	4 58 29.2	1.34×1.24	4860.1	12.1	1.1×1.0	65	86(68)	80	1.05	115	-57	22.1	D,*
	32.014	25.2				0.7×2.2	21							
	00 31 31.669	4 58 26.0	9.88×4.61	1425.0		15.4×3.4		248(235)						
0038+0449	00 36 00.01	4 34 22.4	1.33×1.28	4860.1	3.3	0.35×0.15	51	68	94.6	0.902	117	-58	21.9	D,FRII
	00.08	19.3				0.6×0.3	17.5							
	00 36 00.04	4 34 21.7	9.84×4.59	1425.0				230						
0039+0454	00 37 16.871	4 39 08.98	1.1	4885.1	16.9	1.0×0.7		(230)	300	0.99	117	-58	20.6	D,FRII,*
	17.650	38 59.11				2.3×1.5								
0042+0504	00 39 51.87	4 48 56.8	10.73×4.51	1425.0	24.8	7.9×3.6	167	203	80	0.895	119	-58	22.1	D,FRII,*
	53.27	49 10.8				4.0×3.8	36							
0043+0502	00 41 11.907	4 46 31.07	1.1	4885.1		point		(146)	151	-0.05	119	-57	19.9	P,*
0103+0524	01 00 53.657	5 05 26.34	0.35	4819.56		0.5		(183)	212	0.82(C)	128	-57	21.0	P,*
0105+0501	01 02 58.786	4 45 10.16	1.51×1.43	1425.0	7.6	1.0	50.0	79(97)	32.9	1.10	130	-58	23.0	D,FRII
	59.13	04.6				1.3	29.0							
0110+0500	01 07 36.09	4 43 33.8	10.79×4.57	1425.0	74.4	9.2×10.4	40	250	84	0.902	132	-58	22.0	T,WC,FRII
	37.53	51.1				12.6×9.2	26							
	40.105	44 18.1				22.0×13.5	184							
0117+0503	01 15 06.37	4 47 03.0	1.51×1.46	1425.0		<0.5	30	30(40)	12	1.02	135	-57	24.1	P
0126+0502	01 23 39.8	4 46 28.11	14.8×5.2	1425.0	18.0	11.2×3.4	75	150	51.4	1.065	139	-57	22.5	D,FRII,*
	40.5	42.1				11.2×9.9	75							
0133+0459	01 30 45.10	4 43 56.17	0.78×0.79	8439.9		<0.2		17(23)	62.4	1.13	142	-56	22.3	D
	01 30 45.096	4 43 56.24	1.51×1.43	1425.0				238(217)						
0135+0450	01 33 00.987	4 33 13.33	1.52×1.41	1425.0	7.8	0.7	170	273(264)	92.0	0.973	143	-56	21.9	T,BC
	1.262	15.08				0.8	92							
	1.483	16.00				1.5	11							
0137+0539	01 34 39.87	5 19 39.1	1.32×1.22	4860.1		0.7×0.2	39	39(52)	66.0	0.98	143	-55	22.3	D
			15.0×5.2	1425.0				128(183)						
0143+0505	01 40 57.43	4 52 49.4	1.35×1.26	4860.1	7.4	0.8	3.2	39(46)	55.0	1.03	146	-55	22.5	D,FRII,*
	57.71	55.5				0.5	34							

1	2 h m s	3 ° ′ ″	4 ″×″	5 MHz	6 ″	7 ″×″	8 mJy	9 mJy	10 mJy	11	12 °	13 °	14 m	15
	01 40 57.695	4 52 54.72	14.9×5.2	1425.0		<4.0		136(160)						
0152+0508	01 49 52.94	4 52 02.5	1.36×1.3	4860.1	26.9	2.0	13	23.5	52.8	0.825	150	-55	22.3	D,FRII
	54.58	51 50.66				2.0	10.5							
	01 49 53.25	4 51 56.8	45.	1400.				75						
0152+0453	01 50 16.44	4 39 01.7	14.9×5.1	1425.0	122.5	<8.0	92	155(180)	52.8	1.15	150	-55	22.5	T,WC,FRII
	22.58	40 23.9				9.2×6.5	63							
0153+0455	01 51 20.54	4 41 19.7	1.47×1.35	4860.1		1.1		61	73	0.76	150	-55	22.1	P
0154+0459	01 52 11.19	4 44 42.1	1.61×1.42	1425.0		0.6	84	84(89.5)	31.2	1.01	151	-54	23.1	P
0159+0448	01 56 59.052	4 31 01.	15.1×5.2	1425.0	14.7	7.7×5.9	95	145(139)	50	0.99	153	-54	22.6	D,FRII
	57 00.0	30 57.2				7.7×5.9	50							
0209+0501a	02 06 35.77	4 46 42.1	15.1×5.2	1425.0		10.4×3.2	87		33	1.16	156	-53	23.0	P
	02 06 35.8	4 46 42.0	1.6×1.3	4860.1			21.4	(23)						
0209+0501b	02 06 44.375	4 47 30.5	1.6×1.3	4860.1	18.06	1.5	7.5	15	18	0.91	156	-53	23.7	D,FRII
	45.079	33.												
	45.517	35.75				1.5	7.5							
	02 06 44.89	4 47 33.2	15.1×5.2	1425.0		21.3×5.8		47						
0213+0516	02 10 59.126	5 04 04.4	15.1×5.2	1425.0	35.8	5.1×4.4	157	390	147	0.959	157	-52	21.4	T,BC,FRII
	59.3	18.9				15.5×6.5	99							
	59.65	38.7				5.1×4.4	134							
0215+0522	02 13 17.801	5 10 31.35	0.35	4819.56		0.3		(200)	200	0.0	158	-52	19.7	P
0225+0506	02 22 32.498	4 55 06.4	1.61×1.42	1425.0		0.2	215	215(206)	69	1.06	162	-51	22.2	P
0226+0512	02 23 42.536	4 33 08.18	1.47×1.40	1425.0	10.7	0.9×1.9	69	260(230)	82	0.97	162	-51	22.1	D,FRII,*
	43.076	01.66				0.6×0.97	191							
0234+0446	02 31 30.039	4 33 35.62	0.35	4819.56		0.3		(354)	354	0.0	165	-50	19.0	P,*
0250+0512	02 48 15.71	5 03 52.35	0.85×0.78	8439.9	1.1	0.3	6.6	13(28)	70	1.32	169	-47	21.9	D,FRII
	15.77	52.83				0.3	6.6							
	02 48 15.72	5 03 52.48	1.48×1.40	1425.0		1.5 × <0.2		238(280)						
0302+0456	03 00 18.172	4 43 31.28	1.89×1.64	1425.0	27.2	2.0×1.9	85	157(150)	50	0.9	173	-45	22.6	D,FRII
	19.6	47.30				2.3×2.0	72							
0308+0454	03 05 56.11	4 42 44.3	0.89×0.78	8439.9	1.03	0.4	9	12	27	0.95	174	-44	23.3	CJ or D
	56.17	43.79				0.3	3							
	03 05 56.12	4 42 44.0	1.45×1.43	1425.0		1.4 × <0.35		68						
0311+0507	03 09 09.887	4 56 47.1	1.45×1.43	1425.0		1.2 × <0.2		475	120	1.36	175	-43	21.3	CJ
0318+0456	03 15 59.0	4 30 48.33	5.44×4.83	1425.0	76.2	5.9×4.1	182	490	152	1.13	177	-42	21.3	T,BC,FRII
	16 01.13	48.33				4.4×3.6	30							
	04.07	45.0				4.9×4.1	278							
0318+0506	03 16 19.574	4 48 27.17	0.35	4885.1	13.9	2.2×1.6		(80)	96	0.92	176	-42	21.9	T,*
	20.039	21.67				1.3×1.3								
	20.174	17.25				1.9×3.1								
0319+0504	03 16 48.077	4 54 01.28	0.35	4885.1		0.7	42	(66)	80	0.85	177	-42	22.1	CJ
0324+0442	03 21 29.39	4 31 25.4	5.46×4.84	1425.0	11.8	3.3	328	385	129	1.02	178	-41	21.6	CJ,*

1	2 h m s	3 ° ′ ″	4 ″ × ″	5 MHz	6 ″	7 ″ × ″	8 mJy	9 mJy	10 mJy	11	12 °	13 °	14 m	15
	30.07	32.				5.3×7.8	57							
0343+0458	03 40 52.297	4 48 35.85	0.35	4819.56	34.4			(665)	1153	0.82	182	-38	19.2	*
	50.746	11.17												
0350+0506	03 48 15.56	4 57 21.13	0.35	4819.56		0.2		(325)	366	0.52	183	-36	20.1	P
0355+0449	03 52 34.381	4 31 55.91	1.45×1.33	1425.0	2.4	0.24×0.24	118	254(279)	46	1.9(1.4)	184	-35	21.1	D,FRII
	34.498	57.37				0.36×0.83	136							
0406+0453	04 03 48.01	4 40 03.0	1.49×1.45	1464.9	21.8	0.7	55	125(214)	79	1.02	186	-33	22.1	T,BC,FRII
	48.22	39 49.7				point	4.4							
	48.48	39 42.5				0.7	66							
0427+0457	04 25 08.556	4 50 30.53	0.35	4819.56		0.45		(770)	800	0.17	190	-29	18.6	P
0444+0501	04 41 38.5	4 55 58.5	5.55×4.44	1464.9	10.8	1.1×4.5	113	177(200)	69	1.09	192	-25	22.2	D,FRII
	39.0	51.				3.0×5.3	64							
0446+0525	04 43 43.05	5 35 38.4	1.2	4885.1	19.1			(74)	100	1.11	192	-24	21.8	D,FRII,*
	43.37	20.												
0457+0452	04 55 14.17	4 49 40.4	1.27×1.26	1464.9	34.	<0.5	3.2	35(185)	56	1.12	194	-22	22.4	D,FRII
	15.18	10.4				1.0	31.5							
0458+0506	04 55 35.38	4 59 31.97	4.74×4.64	1425.0	26.1	10.3×7.0	155	283(279)	95	1.02	194	-22	21.9	T,WC,FRII
	36.198	42.49				5.7×3.2	48							
	36.734	48.79				4.7×9.8	80							
0459+0456	04 56 23.14	4 51 00.2	1.51×1.46	1464.9	63.8	1.1	34	127(209)	76	0.95	195	-22	22.2	D,FRII
	26.38	41.5				0.6	93							
0505+0459	05 02 43.846	4 55 40.51		4885.1		point		(750)	750	0.0	195	-21	18.2	P,*
0506+0508	05 03 45.55	5 04 20.9	0.41×0.37	4860.1	0.8	0.2	41	47	70	0.88	195	-21	22.2	D,FRII
	45.56	21.6				0.2	6							
	05 03 45.56	5 04 21.1	5.38×4.21	1464.9				150(173)						
0519+0510	05 16 34.971	5 11 59.56	4.88×4.56	1425.0	40.9	8.7×13.6	160	340(303)	120	0.95	197	-18	21.7	M,*
	35.706	43.22				1.5×8.2	41							
	36.485	39.0				2.8×6.4	40							
	37.43	40.78				5.0×3.0	98							
0552+0451	05 50 16.88	4 46 49.8	0.39×0.37	4860.1	1.6	<0.4	36	48(51)	65	1.18	202	-11	22.2	D,FRII
	16.98	50.3				<0.4	11.7							
	05 50 16.92	4 46 49.9	5.19×3.95	1464.9				160(204)						
0619+0506	06 16 20.459	5 07 47.69	0.35	4885.1	2.4			(315)	362	0.62	206	-5	20.2	*
	06 16 20.49	5 07 47.8	45.	1400.				692(693)						
0621+0452	06 18 50.65	4 54 26.0	4.64×4.12	1464.9		0.5		62	39	flat	205	-4	21.5	P
0621+0437	06 19 12.052	4 39 42.06	0.35	4885.1				(355)	422	0.77	205	-4	20.2	*
	06 19 12.58	4 39 49.4	45.	1400.			483	1057(1070)						
	14.62	40 15.7					574							
0625+0437	06 23 12.723	4 37 28.84	0.35	4885.1	1.8			285	357	0.87	206	-4	20.5	D
	12.758	27.08												
0646+0439	06 43 06.81	4 48 09.2	4.10×3.93	1464.9		0.5		30	>73		208	1		P

1	2 h m s	3 ° ′ ″	4 ″×″	5 MHz	6 ″	7 ″×″	8 mJy	9 mJy	10 mJy	11	12 °	13 °	14 m	15
0646+0449	06 43 35.71	4 47 20.9	4.10×3.93	1464.9		0.5		75	28	1.01	208	1	23.2	P
0653+0508	06 50 47.147	5 12 54.02	1.1	4885.1	47.1			(148)	167	0.5	209	3	20.9	P,*
	47.839	36.6				0.73								
	48.809	14.56												
0707+0455a	07 04 56.46	5 01 10.1	4.36×4.05	1464.9		0.5		1.7	6	-1.	210	6	20.7	P
0707+0455b	07 05 06.61	5 00 13.1	4.36×4.05	1464.9		6.0×4.6	9.7				210	6		E×t
0707+0455c	07 05 07.92	4 59 01.3	4.36×4.05	1464.9		7.2×4.6	18.9							E×t
0743+0455	07 40 36.21	5 03 05.5	1.55×1.46	1464.9	20.5	1.2	65	90(112)	37	1.07	214	14	22.9	D,FRII
	37.41	02 56.0				1.1	24.8							
0744+0500	07 42 13.45	5 07 36.	4.86×4.12	1425.0	10.8	5.1×5.1	15	87(93)	27	1.201	214	14	23.1	D,FRII
	13.59	25.				0.74×2.7	72							
0756+0450	07 53 31.20	4 47 17.1	4.16×3.99	1464.9				50.4	14	1.16	215	16	23.9	P
			1.50×1.38	1425.0		0.7								
0759+0454	07 57 04.38	5 03 27.7	4.22×4.63	1464.9		0.5		13.0	14	0.0	216	17	22.6	P,*
	04.38	27.8	0.48×0.48	4860.1				9(13)						
0809+0500	08 07 08.44	5 10 01.5	1.63×1.50	1464.9		1.2		27	31	0.	217	20	21.7	P,*
0820+0454	08 18 18.09	5 03 50.2	1.39×1.25	4860.1	1.7	0.4	114	135	166	1.0	219	22	21.3	D,FRII
	18.20	51.23				0.4	21							
	08 18 18.11	5 03 50.5	4.90×4.28	1425.0		1.2		457						
0836+0511	08 34 09.36	5 23 40.1	4.91×4.38	1425.0	13.5	7.9×2.9	194	320(303)	109	1.05	221	26	21.7	D,FRII
	09.96	30.0				3.9×3.6	126							
0837+0446	08 34 51.27	4 54 51.3	1.73×1.51	1464.9	3.9	0.4	117	136(148)	54	1.0	221	26	22.5	D,FRII
	51.34	54.9				0.6	19.8							
0845+0434	08 42 39.20	4 50 44.6	0.56×0.52	4860.1		point		219	240	0.48	222	27	20.5	P
	39.27	45.4	4.27×4.19	1464.9				305(389)						
0845+0444	08 42 53.25	4 53 53.5	0.38×0.37	4860.1	4.6	point	6.7	13.6	135	1.14	222	27	21.4	T
	53.55	53.0				0.4	6.9	(105)						
	08 42 53.28	4 53 52.9	4.27×4.19	1464.9				370(427)						
0902+0444	08 59 49.464	4 55 01.62	0.35	4885.1		0.35		(102)	105	0.17	225	31	20.8	P
0906+0459a	09 03 34.34	5 14 55.5	4.28×4.14	1464.9		5.2×2.7	53.3		38		225	32		E×t
0906+0459b	09 03 35.59	5 13 36.4	4.28×4.14	1464.9		point	10.6				225	32		P
0906+0459c	09 03 35.89	5 12 18.1	4.28×4.14	1464.9		9.6×2.8	27.4				225	32		E×t
0907+0439	09 04 42.519	4 48 26.45	0.35	4885.1		0.25		(95)	116	0.92	225	32	21.7	P,*
0908+0451	09 05 42.38	5 03 03.85	4.85×4.62	1425.0	34.5	9.1×7.8	218	320(300)	109	0.92	225	33	22.8	D,FRII
	44.51	18.5				8.1×6.3	102							
0909+0445	09 07 13.531	4 56 36.92	0.53×0.40	4860.1		0.12		56	64	1.0	225	33	22.3	P
	09 07 13.51	4 56 37.0	1.93×1.57	1464.9		0.3		173(200)						
0927+0457	09 25 07.65	5 09 25.7	4.21×4.15	1464.9	15.	5.5	30.5	55(72)	39	0.67	228	37	23.7	D,FRII
	09 25 08.18	14.1				5.1	24.1							
0934+0505	09 31 48.08	5 17 12.1	2.05×1.59	1464.9	5.	0.8	42.7	82(94)	36	1.07	229	38	22.9	D,FRII
	48.36	9.3				0.9	39							

1	2 h m s	3 ° ′ ″	4 ″×″	5 MHz	6 ″	7 ″×″	8 mJy	9 mJy	10 mJy	11	12 °	13 °	14 m	15
0936+0504	09 33 32.733	5 17 16.59	0.35	4885.1	2.28	0.7×0.8		(130)	156	0.83	229	39	21.3	T
	32.790	18.67				0.8×0.8								
	32.838	16.82				1.1×1.1								
0937+0450	09 34 32.787	5 03 48.92	0.35	4885.1	2.78	1.1×1.2		(160)	200	0.89	230	39	21.1	*
	32.846	47.66				0.94								
0942+0441	09 39 36.63	4 55 06.32	0.35	4885.1		0.3		(80)	80	0.0	231	40	20.7	P
0942+0447	09 40 02.79	4 58 12.35	1.34×1.22	4860.1	19.95			25	43	0.88	231	40	22.8	T,BC
	03.46	07.4				<0.3	3.1							
	03.99	01.7												
0945+0454	09 42 49.638	5 08 04.14	1.34×1.2	4860.1	4.5	<0.3	13.5	22	30	1.01	231	40	23.2	D,FRII
	49.911	06.74				<0.3	8.5							
0949+0454	09 47 04.9	5 08 46.7	1.2	4885.1		point		(86)	90	0.68	231	41	21.8	*
1011+0502	10 09 28.15	5 21 04.0	1.35×1.2	4860.1		0.2		49	70	1.04	236	46	22.2	CJ
	10 09 28.15	5 21 04.0	14.7 ×4.8	1385.1		point		212						
1015+0452	10 12 39.179	5 08 02.24	0.35	4835.1	1.46	0.41×0.37	54	78(105)	130	0.69	237	47	21.4	D,FRII
	39.195	00.80					24							
1016+0514	10 13 26.626	5 28 00.48	1.1	4885.1		point		(450)	450	0.0	237	47	18.8	CJ,*
1031+0443	10 28 42.0	4 58 20.5	4.21×4.17	1464.9	33.	6.25×2.7	229	645(616)	191	1.20	240	50	21.0	D,FRII
	43.57	40.7				19.1×2.7	416							
1038+0514	10 36 10.833	5 28 06.64	1.1	4885.1		point(0.56)		(500)	500	0.0	242	52	18.7	P,[Law]
1043+0443	10 41 09.00	4 55 47.8	4.22×4.09	1464.9	48.	7.4×4.3	32	90(127)	37	1.14	244	52	22.9	D,FRII
	10.98	56 26.4				4.1×3.5	58							
1045+0455	10 43 16.056	5 11 37.84	1.1	4885.1	2.8			(125)	150	0.87	244	53	21.4	D,FRII,*
	10 43 16.093	5 11 40.61												
1049+0506	10 46 56.298	5 21 25.53		4885.1	8.36	<0.8		(115)	150	0.80	245	54	21.4	T,C,FRII,*
	56.636	25.12				<0.8								
	56.853	25.03												
1051+0449	10 48 50.266	5 05 39.86		4885.1	1.7	<0.5		(105)	132	0.92	246	54	21.6	D,FRII
	50.312	41.23				<0.5								
1057+0456b	10 55 15.321	5 12 24.04	0.35	4835.1		0.5		50(100)	105	0.29	247	55	21.0	E×t
1100+0444	10 57 36.216	5 00 08.31	0.35	4819.56		0.32		(200)	250	0.88	248	55	20.8	P
1102+0459	11 00 12.224	5 15 33.60	0.35	4885.1		0.48×0.41		66(98)	120	0.86	248	56	21.6	*
1103+0451	11 01 14.7	5 08 15.	5.42×3.79	1489.9		<20		(90)	21	1.4	249	56	23.1	E×t
1113+0436	11 11 22.72	4 54 19.6	4.84×3.91	1489.9	29.	5.1×7.4	19	130(144)	52	0.98	253	58	22.6	D
	23.11	18.5				6.4×8.9	21							
	24.55	20.6				9.2×4.8	90							
1123+0450	11 21 18.604	5 06 44.28	0.35	4835.1		0.52		78(87)	102	0.86	256	59	21.8	E×t
1124+0456	11 22 02.637	5 12 55.13		4885.1	12.			(320)	400	0.94	256	60	20.3	D,FRII,*
	02.948	47.2												
1125+0446	11 23 05.748	5 03 21.40	0.35	4885.1		0.72		52(65)	75	0.64	256	60	22.0	CJ
1131+0455	11 29 21.843	5 12 22.32	0.35	4819.56	2.06	0.6×0.9		(202)	250	0.75	259	69	20.8	*

1	2 h m s	3 ° ′ ″	4 ″×″	5 MHz	6 ″	7 ″×″	8 mJy	9 mJy	10 mJy	11	12 °	13 °	14 m	15
	21.9	22.86				0.8×0.9								
	21.959	23.41				0.7×1.1								
1142+0429	11 39 34.689	4 54 12.00	0.35	4885.1		0.68×0.56		(82)	109	1.45	264	62	21.2	E×t
1142+0455	11 39 45.231	5 11 42.76	0.35	4835.1	18.7	0.67×0.55		93(86)	108	1.	263	62	21.8	T,C,FRII
	45.77	36.69				0.7								
	46.19	31.47												
	11 39 45.543	5 11 39.6	14.2×4.9	1385.1		11.2×7.0	227	280(300)						
	46.068	32.4				11.7×6.6	53							
1145+0455	11 42 47.133	5 12 06.29	0.35	4819.56		1.22		(427)	472	0.51	265	63	19.8	CJ,*
1146+0458	11 43 57.585	5 14 58.91	1.1	4819.56		0.43		(202)	215	0.22	265	63	20.1	P
1148+0455	11 46 11.577	5 12 24.04	0.35	4885.1	32.9			(163)	210	1.08	266	63	21.0	T,FRII,*
	12.382	14.79				0.6×1.3								
	13.5	06.35												
1150+0459	11 48 17.806	5 15 40.56	0.35	4885.1		0.3		135(130)	164	0.9	267	64	21.3	P
1152+0449	11 49 49.53	5 04 56.0	4.60×4.1	1464.9	7.	3.4×4.1	43	77(84)	29	1.0	268	64	23.2	D,FRII
	50.0	58.0				3.4×2.6	34							
1154+0431	11 52 19.6	4 41 02.	4.84×3.91	1489.9				(715)	273	0.97	270	64	20.8	D,FRII,*
	11 52 19.330	4 40 53.73	0.35×0.35	4819.56	6.75	<0.3								
	19.735	56.14				<0.3								
1155+0444	11 52 45.34	5 00 05.8	5.29×4.07	1489.9	13.	<2.3	80	131(148)	54	1.0	270	64	22.5	D,FRII
	45.49	18.9				<3.1	48.5							
1213+0500	12 10 53.793	5 16 35.0	14.2×4.9	1455.3	46.7	5.9×6.4	73	188(215)	74	1.12	279	66	22.1	D,FRII
	56.337	17 01.0				7.6×3.8	115							
1218+0515	12 16 14.552	5 31 07.6		4885.1	18.8			(260)	300	0.61	282	67	20.4	*
	15.567	11.93												
1219+0446	12 17 05.64	5 04 19.6	4.82×3.92	1489.9	118.	<1.8	53	67	23	1.23	283	66	23.3	D,FRII
	11.64	03 02.0				3.0	14.5							
1221+0504	12 19 19.101	5 26 54.0		4885.1		<1		(220)	240	0.38	284	67	20.3	P,[Law]
1226+0438	12 24 22.730	4 45 27.21	0.35	4819.56		1.0		(195)	240	0.98	287	67	20.9	*
1235+0453	12 32 34.440	5 09 51.64	0.35	4885.1		0.43×0.37		36(46)	49	0.4	292	67	22.1	E×t
1235+0435a	12 33 13.71	4 48 30.2	5.00×3.94	1489.9		<1.7	9.3				293	67		P
1235+0435b	12 33 16.47	4 49 26.2	5.00×3.94	1489.9	4.1	4.9×4.6	80	116(124)	45	0.98	293	67	22.7	D,FRII
	16.69	28.7				3.4×5.0	36							
1239+0443	12 36 59.90	4 59 33.27		4885.1		<1.0		(346)	361	0.11	295	67	19.3	P,*
1257+0458	12 55 23.401	5 15 29.1		4885.1	1.7			(130)	152	0.64	307	68	21.2	M,*
	23.434	27.85												
	23.439	29.50												
1318+0436	13 15 57.645	4 45 55.90	0.35	4819.56		0.36		(235)	215	-0.49	320	66	18.3	P
1322+0449	13 19 31.74	5 04 30.7	4.74×3.77	1489.9	7.	6.7×3.3	54	107(124)	47	0.96	323	67	22.7	D
	31.95	25.2				6.7×3.3	53							
1333+0451	13 30 32.32	5 07 09.3	0.39×0.38	4860.1	1.	0.4		7.7	11	1.3	329	65	24.0	P

1	2 h m s	3 ° ′ ″	4 ″×″	5 MHz	6 ″	7 ″×″	8 mJy	9 mJy	10 mJy	11	12 °	13 °	14 m	15
	13 30 32.35	5 07 08.5	4.79×4.54	1464.9				36						
1333+0452	13 30 53.71	5 07 30.	4.79×4.54	1464.9	54.	4.6×7.1	35	52(57)	16	1.4	329	65	23.4	D,FRII
	56.62	03.				4.6×9.7	17							
1339+0445	13 37 05.66	5 10 31.7	4.79×4.54	1464.9	34.	14.4×3.7	34	95(122)	41	1.07	332	65	22.8	T,WC
	6.70	16.2				8.9×3.7	14							
	7.03	5.8				5.9×5.0	47							
1340+0448	13 37 55.83	5 01 35.6	1.37×1.09	1477.4		3.0		>3.5	7	inv,fl	333	65		E×t,*
1347+0441	13 44 37.55	4 57 16.2	1.22×0.95	1477.4	4.2	<0.5	26	60(104)	43	0.98	336	64	22.8	T,BC
	37.61	16.7				<0.5	34							
	37.82	16.3												
1347+0435	13 45 17.771	4 52 58.1		4885.1	8.3			(82)	100	0.85	336	64	21.8	*
	17.918	56.2												
	18.176	54.5												
1351+0437	13 49 06.357	4 50 29.53	0.35	4819.56	0.83			(220)	256	0.84	330	63	20.8	D,FRII
	06.413	29.62												
1356+0457	13 53 39.5	5 13 20.		1490	3.47		14		44	0.43	341	63	22.3	*
	50.4	17 28.												
1357+0453	13 55 06.285	5 07 43.49	15.6×4.8	1455.3	12.4	7.0×4.3	116	240(286)	109	0.95	341	63	21.8	D,FRII
	06.5	55.77				7.0×4.3	124							
1424+0442	14 21 38.933	4 48 26.06	0.35	4819.56		<0.35		(300)	300	0.0	351	58	19.2	P,*
1429+0501	14 26 45.26	5 14 50.7	1.32×1.15	1477.4	11.1		1.2	18(188)	82	0.92	354	58	22.1	CJ
	45.76	42.9					17							
1436+0501	14 34 04.66	5 15 10.8	6.79×6.06	1464.9	15.	10.2×3.6		163	48	1.25	356	57	22.5	*
1439+0455	14 37 15.34	5 08 32.9	1.4 ×1.11	1477.4	17.9	1.4	61	93(133)	40	1.15	357	56	22.8	D,FRII
	16.2	43.9				3.4	32							
1446+0507	14 43 46.018	5 20 01.87	1.1	4885.1	68.	1.7×2.1		(108)	121	0.88	359	55	21.6	T,WC,FRII,*
	50.14	23.1				6.1×4.9								
1450+0509	14 48 03.329	5 20 43.28	0.35	4885.1		0.2		(150)	150	0.0	0	54	20.0	P
1454+0440	14 51 45.867	4 50 26.52	0.35	4885.1	30.85		17	90(165)	195	0.82	1	53	21.1	D,FRII
	46.935	52.56					72							
1503+0502	15 01 16.8	5 13 21.	6.64×4.88	1425.0					56					
1503+0456	15 01 30.11	5 08 30.7	1.97×1.37	4860.1		0.6		60(48)	61	1.04	4	51	22.4	P or CJ
	15 01 30.13	5 08 30.7	6.64×4.88	1425.0		1.6	194	194(150)						
1510+0438	15 07 42.91	4 50 53.3	1.40×1.11	1477.4	3.4	1.7	26	71(158)	67	0.9	6	48	22.3	D
	43.05	50.8					45							
1518+0451	15 16 25.76	5 02 06.4	1.39×1.13	1477.4		<0.5		44	24	0.61	6	48	23.2	P
1521+0434	15 18 44.732	4 41 06.07	0.35	4819.56		0.4		(1050)	1400	1.24(C)	7	48	18.8	P
1526+0514	15 23 29.5	5 20 21.3	1.1	4885.1	6.8			(105)	128	0.84	9	47	21.6	D,*
	30.800	49.39												
1543+0452	15 41 04.951	5 01 45.66				0.4		(260)	260	0.04	12	43	19.7	CJ,*
1544+0459	15 41 49.821	5 07 45.6	0.35	4885.1		0.48×0.42		47(50)	50	0.0	13	43	21.2	P

1	2 h m s	3 ° ′ ″	4 ″×″	5 MHz	6 ″	7 ″×″	8 mJy	9 mJy	10 mJy	11	12 °	13 °	14 m	15
1550+0524	15 48 06.961	5 36 11.18				point		(2150)	2200	0.12	14	42	17.4	P,*
1551+0458	15 49 18.90	5 08 29.7	5.4×4.87	1425.0	11.6	3.0	95	228	70	1.10	14	42	22.2	D,FRII
	19.58	24.0				3.0	131							
1559+0502	15 56 38.456	5 10 18.16	0.35	4819.56		0.4		(152)	167	0.75	15	40	21.2	*
1609+0456	16 06 54.63	5 07 51.5	1.48×1.18	1477.4	6.3	0.7	33	42(100)	30	1.15	16	38	23.1	D,FRII
	54.92	46.8				0.9	9.1							
1616+0459	16 14 09.078	5 06 54.32	0.35	4885.1		0.6		906(1050)	840	-0.89	18	36	15.7	CJ,*
1620+0446	16 18 03.955	4 54 46.81	1.1	4885.1	32.8	2.7×2.1		(36)	43	0.82	18	36	22.7	T,C,FRII
	04.711	42.29				1.2×1.3								
	05.601	36.94				2.1×3.2								
1626+0448	16 24 21.64	4 55 32.9	0.44×0.41	4860.1	2.4	0.2	19.2	36	46	1.26	19	34	22.5	T,FRII
	21.72	33.4				<0.2	0.68							
	21.80	33.6				0.2	15.9							
	16 24 21.73	4 55 33.1	4.32×4.12	1464.9				141						
1638+0450	16 36 03.762	4 55 49.36		4885.1	1.92			(145)	180	0.9	21	32	21.2	T,BC,FRII
	03.794	50.05												
	13.817	50.98												
1646+0501	16 44 24.44	5 06 28.5	2.09×1.3	1477.4	15.7	5.2×4.7	57	122(132)	54	0.92	23	30	22.5	D,FRII
	25.52	29.4				5.2×5.2	49							
1653+0443	16 51 27.74	4 48 24.08	4.93×4.73	1425.0	70.5	14.0×7.0	387	590(251)	92	0.98	23	28	21.9	D,FRII
	30.89	47 31.2				15.2×7.0	203							
1658+0454	16 55 43.34	4 58 04.9	0.43×0.41	4860.1		<0.2		17(23)	31	1.25	23	27	22.9	P
			4.26×4.1	1464.9				73(108)						
1658+0514	16 56 05.628	5 19 47.09	0.35	4885.1	2.25	0.4		1446(1610)	1640	0.12	24	27	17.7	*
	05.756	46.4				<0.3								
1703+0502	17 01 01.28	5 06 19.5	0.43×0.41	4860.1	1.8		77.3	108	175	1.18	25	26	21.1	D,FRII
	1.3	21.3					30.4							
	17 01 01.3	5 06 20.0	4.21×4.05	1464.9				458(539)						
1706+0502	17 03 57.811	5 06 31.14	4.91×4.75	1425.0	44.9	1.8	462	778(758)	257	1.01	25	26	20.8	D,FRII
	04 00.581	48.29				4.0	316							
1714+0449	17 12 10.889	4 51 21.92	0.35	4885.1		0.52×0.51		(100)	100	0.0	26	24	20.4	P
1720+0455	17 17 36.00	4 56 48.0	0.43×0.41	4860.1		<0.5		13(15)	19	1.22	27	22	23.5	P
			4.21×4.05	1464.9				47(64)						
1722+0442	17 19 45.03	4 46 01.5	4.83×4.72	1425.0	21.9	7.0×4.8	272	(800)	300	0.99	27	22	20.6	D,FRII
	46.37	10.5				4.5×4.2	493							
1725+0457	17 23 04.52	5 00 05.2	0.43×0.4	4860.1	∼1	0.3		20	27	1.26	29	21	23.1	P
			4.21×4.03	1464.9		point		91						
1726+0504	17 23 56.892	5 07 14.28	0.35	4885.1		0.39×0.38		152(135)	135	0.0	28	21	20.1	P
1728+0429	17 25 56.367	4 29 27.92		4885.1		point		(610)	600	-0.12	27	20	18.2	P,*
1735+0454	17 33 13.49	4 57 04.5	4.23×4.05	1464.9	4.	9 × <1	28	78	30	1.0	29	19	23.2	D

1	2 h m s	3 ° ′ ″	4 ″×″	5 MHz	6 ″	7 ″×″	8 mJy	9 mJy	10 mJy	11	12 °	13 °	14 m	15
	13.54	9.0					49							
1740+0502	17 38 06.03	5 04 11.1	4.31×4.09	1464.9	4.			90(100)	32	1.2	28	18	23.0	CJ
1754+0459	17 51 49.58	5 00 09.9	0.4	4885.1		point		(390)	420	0.35	31	15	19.6	P,*
1806+0527	18 03 46.29	5 24 46.89	1.2	4885.1	49.			246	280	0.82	33	13	20.7	T,BC,*
	46.66	25 12.2				point								
	46.79	25 31.9												
1829+0451	18 27 30.6	4 50 24.2	4.25×4.18	1464.9		0.5		92	25	1.27	35	7	23.1	P,*
1935+0457	19 33 19.31	4 50 04.25	4.30×4.29	1464.9	19.	4.9×3.4		60	17	1.28	42	-8	23.6	D,FRII
	20.57	07.66				7.6×3.4								
2005+0506	20 03 13.83	4 56 00.9	4.30×4.23	1464.9	>3			36	16	0.83	46	-14	23.8	D
2012+0458	20 09 37.3	4 48 27.0	4.74×4.33	1489.9		point		24	13	0.65	47	-15	23.9	P
2012+0457	20 09 57.33	4 48 40.2	4.74×4.33	1489.9	84.6		4.9	8.5	30		47	-16		D
	10 00.15	4 47 24.3					3.6							
2013+0508	20 10 54.53	5 01 21.3	4.72×4.3	1489.9	10.		49.9	85(125)	51	0.96	47	-16	22.6	D,FRII
	54.91	29.67					35.5							
2029+0456	20 27 13.550	4 45 53.24	1.1	4885.1	28.9			(49)	61	0.92	49	-19	22.4	T,BC,FRII,*
	14.179	06.24				0.7×0.7								
	14.772	15.48												
2036+0451	20 34 25.24	4 39 20.4	4.33×4.33	1464.9	56.	11.5×2.1	53	158(200)	75	1.02	50	-21	22.2	T,C,FRII
	26.16	22.7				5.4×4.0								
	27.46	22.7				<2.1×2.7	2.							
	28.9	23.2				8.3×4.0	102.5							
2044+0444	20 42 15.527	4 33 09.98	0.35	4885.1	2.42			(250)	300	0.7	51	-22	20.5	CJ,*
	15.650	08.23												
2048+0453	20 45 32.102	4 42 19.92	0.35	4885.1		0.16		(115)	125	0.48	52	-23	21.2	P
2110+0505a	21 08 15.80	4 53 48.8	4.66×4.23	1489.9			3.4		16		55	-28		P
2110+0456	21 08 22.223	4 43 23.47	0.35	4819.56	2.72			145	168	0.78	55	-28	21.2	D,FRII
	22.382	24.67												
2110+0505b	21 08 26.01	4 54 49.7	4.66×4.23	1489.9		<1.7			16					P,*
2111+0501	21 08 59.19	4 50 56.2		1489.9					9		56	-28		P
2113+0445	21 11 00.342	4 32 53.80	0.35	4885.1		0.6		101(220)	270	0.79 D	56	-29	20.7	
2116+0507	21 13 49.325	4 54 53.28	0.35	4885.1	5.23		55	93(95)	160	0.8	56	-29	21.3	D,FRII,*
	49.437	52.80					28							
2117+0503	21 14 50.762	4 50 27.54	0.35	4885.1		0.25		(206)	211	0.18	57	-31	20.0	P,*
2125+0447	21 22 58.823	4 28 35.94	0.35	4819.56		0.27		(220)	220	0.0	65	-39	19.6	P
2143+0511	21 41 24.662	4 58 41.7	4.7×4.3	1489.9					31					
2144+0513	21 41 56.67	4 57 26.0	1.32×1.22	4860.1		1.76×0.78		61	72	1.06	61	-34	22.2	CJ,*
	21 41 56.65	4 57 26.1	4.7×4.3	1489.9		<2		172(200)						
2204+0442	22 01 46.463	4 25 27.56	0.35	4885.1		2.08		375(590)	600	0.46	68	-41	19.4	CJ,*
2217+0514	22 15 00.431	5 03 53.68	0.35	4885.1	0.88	0.41×0.37		(85)	95	0.62	70	-42	21.7	D,FRII
	00.472	54.40												

1	2 h m s	3 ° ′ ″	4 ″ × ″	5 MHz	6 ″	7 ″ × ″	8 mJy	9 mJy	10 mJy	11	12 °	13 °	14 m	15
2219+0458	22 16 34.74	4 43 39.1	1.34×1.24	4860.1	4.7	1.0×0.9	29	38	48	1.04	68	-41	22.6	D,FRII
	34.791	43.77				2.6×0.4	9							
	22 16 34.74	4 43 39.9	5.77×4.88	1425.0				122(138)						
2224+0513	22 21 46.38	4 58 54.9	1.1	4885.1	36.1	2.0×1.74		(125)	145	0.78	70	-42	21.4	D,*
	46.73	19.2				1.76×1.38								
2225+0523	22 22 43.404	5 11 52.95	1.1	4885.1	2.7	1.22×0.42		(246)	310	0.99	75	-46	20.6	CJ,*
	43.51	55.27				1.85×0.42								
2236+0454	22 34 18.27	4 39 24.9	6.13×4.77	1425.0	40.2	2.0	25	160(143)	42.3	1.15	72	-44	22.7	D,FRII
	20.58	44.8				point	134							
2245+0501	22 43 21.742	4 45 08.33	0.35	4819.56		0.32		(380)	400	0.32	77	-47	19.6	P,*
2247+0507	22 44 43.22	4 52 19.3	1.33×1.23	4860.1	5.6	0.9	38	106	110	0.98	75	-46	21.8	D,FRII
	43.42	14.6				0.4	57							
	22 44 43.33	4 52 16.4	6.30×4.77	1425.0				343						
2251+0502	22 49 22.234	4 46 37.8	0.35	4885.1		0.3		136(130)	160	0.81	79	-48	21.3	P
2258+0517	22 55 52.463	5 00 34.4	1.1	4885.1		point		(195)	203	0.20	83	-50	20.1	P,*
2312+0517	23 10 17.931	5 00 45.47	0.35	4885.1		1.67		(1000)	1253	0.72	94	-54	19.0	Dif
2320+0459	23 18 11.96	4 42 47.5	6.98×4.78	1425.0	15.2	4.8×2.4	100	157(177)	64	0.94	85	-51	22.3	D,FRII
	12.09	43 02.2				5.0×4.6	57							
2320+0512	23 18 12.03	4 57 16.	6.98×4.78	1425.0				(266)	266	0.0	85	-51	19.4	P,*
2343+0520	23 41 17.320	5 06 05.64	1.1	4885.1	15.6	3.4×3.1		(120)	170	0.86	94	-54	21.3	T,C,FRII,*
	17.543	06 00.99				1.2×0.8								
	17.911	05 55.69				1.2×0.8								
2348+0507	23 45 58.484	4 50 55.35	0.35	4885.1	4.7	<0.4	49	98(108)	140	0.95	95	-54	21.5	D,FRII
	58.618	51.08				<0.4	44							
2357+0501	23 55 22.89	4 44 47.4	1.32×1.26	4860.1		0.3 × <0.1		44	54	1.17	99	-55	22.4	P
	23 55 22.99	4 44 47.5	8.08×4.64	1425.0				179						

VLA maps of the selected radio sources are shown in Fig. 8 at the end of the paper (p.48). The scales in arcsec are shown by bars.

Notes on individual sources

0029+0509: The identification given by Lawrence et al. (1986); stellar source B=20.0, R=19.0, shifted by 0.6 arcsec from the radio position.

0034+0514: The shape of the object suggests "precession" ‹ Tect.

0039+0454: Lawrence et al., 1986 also give on POSS an empty field at the radio source position.

0042+0504: Probably a quasar.

0043+0502: The same as in the case of 0039+0454.

0103+0524: Chigo (1977) identified the source with a V=19.5 magnitude optical object.

0126+0502: Probably a quasar.

0143+0505: The first optical candidate is probably a quasar, the second one is the galaxy near the N-component of the radio image.

0226+0512: Probably a quasar.

0234+0446: The source was identified by Bugaenko et al. (1993), U=18.4, U–B=–0.7, B–V=0.3, V–R< –0.6. According to Veron-Cetty, Veron (1993) this quasar with V=18.5 is at the redshift $z = 2.06$.

0318+0506: In Lawrence et al. (1986) the source seems double, the NE component is lost on the VLA snapshot map.

0324+0442: This source is identical to the USS source 0321+045 observed with a better resolution by Röttgering et al. (1994). Our bright component is split on three ones marked in the CCD image (Fig.9). The middle component is the brightest one. It coincides with our bright component within 0.5 arcsec.

0343+0458: The centroid of the double source of UTRAO catalog is between the two listed components, although the position of the second component is under a question. The redshift of the source is $z = 0.358$ (Spinrad et al., 1985). Veron–Cetty, Veron (1993) gives for this galaxy V=19.17, B–V=0.35, U–B=–0.5.

0446+0525: The weak core is possible. Accoriding to Lawrence et al. (1986) the field is also empty.

0505+0459: According to Bugaenko et al. (1993) the colors of the source are U=19.0, U-B=0.0, B–V> –0.2.

0519+0510: Complicated structure, indicating either precession of object or repeated activity which leads to the second ejection from a core.

0619+0506: Bad cleaning of the VLA map. It's difficult to determine the source structure.

0621+0437: Bad cleaning of the map. The centroid of the asymmetric double source of the UTRAO catalog (R.A.= $6^h19^m13^s.71$, Dec= $4°40'04''.33$) is shifted to NE. Weak extended structures are lost on the VLA maps with a high resolution, so the real radio structure of the object most likely differs from that in the mentioned map and in Lawrence et al. (1986). An empty field on POSS of Lawrence et al. (1986) agrees with our statement. The VLA data with the 45 arcsec resolution at 1400 MHz (NRAO/VLA Sky Survey (NVSS) radio source catalog) show two radio components (see Table 2). The centroid of this source coincides with the UTRAO coordinates. The object is identified with the optical galaxy with m_R equal approximately to 18.5.

0653+0508: This source is a point one in Lawrence et al. (1986) and in UTRAO catalog. Identification in Lawrence et al. (1986) agrees with the mentioned one in Table 2.

0759+0454: Empty field is not excluded.

0809+0500: The source is identified with the one of three unresolved galaxies. On the POSS some filaments emerged from this galaxy are seen.

0907+0439: Identification in Lawrence et al. (1986) agrees with the mentioned one in Table 3.

0937+0450:
The centroid of the double UTRAO catalog source has R.A.=$9^h34^m33^s.356$, Dec= $5°03'38''.58$, so the extended component and possibly the second one are lost on the VLA map. Only one component is on the mentioned map.

0949+0454: The position and the radio image of the source have been taken from Lawrence et al. (1986). The identification agrees with ours.

1016+0514: The source in Lawrence et al. (1986) is a point one and identified with the stellar object with B=20.0, R=20.5 shifted by 0.3 arcsec from the radio source.

1045+0455: Empty field on POSS is in agreement with Lawrence et al. (1986).

1049+0506: The source was identified with the quasar with V=18.94, B-V=0.24, U-B=–0.88 at the redshift $z = 1.115$ (Veron-Cetty, Veron, 1993).

1102+0459: The double source in the UTRAO catalog (with centroid R.A.=$11^h00^m11^s.117$ and Dec=$5°03'38''.58$) is situated near the weak point component (R.A.=$11^h00^m11^s.02$ and Dec = $5°15'21''.19$) which most likely is a core of this object. There is only the NE component on the VLA map.

1124+0456: Bad cleaning of the VLA map. Weak extensive details are possibly lost.

1131+0455: The well known gravitational lens.

1145+0455: Bugaenko et al. (1993) identified this source with the object with U=18.5, U–B=0.2, B–V=0.0, V–R< 0.5. Veron-Cetty, Veron (1993) give for this quasar V=19.5, the redshift $z = 1.342$.

1148+0459: The central component is a core with a jet. This source is a cometary one in Lawrence et al. (1986). Identification (empty field on POSS) agrees with ours.

1154+0431: Probably a quasar.

1218+0515: Complicated structure source. The

source is elongated in one direction; probably a core exists.

1226+0438: The centroid of the asymmetrical double source from the UTRAO catalog has R.A.=$12^h24^m21^s.94$, Dec=4°45′40″.84, so only SE component of the object is possibly seen on the VLA map. That's why the identification in Lawrence et al. (1986) with the stellar object with B=21.0, R=20.5, shifted by 0.4 arcsec, is probably unreal.

1239+0443: The identification in Lawrence et al. (1986) (empty field on POSS) differs form ours (see Table 3).

1257+0458: Bad cleaning of the VLA map. The real image of the object is unknown.

1340+0448: The point source coincides with the IRAS source in the box of errors and with the optical galaxy REIZ 3561 (MCG +01-35-028; ZWG 045.068).

1347+0435: Bad cleaning of the VLA map; complicated morphology.

1356+0457: Complicated structure; there are two bright components. The object is identified with the galaxy NGC 5364 (Hummel, 1980; Dressel, Condon, 1978; Condon, 1987).

1424+0442: Identified by Bugaenko et al. (1993) with the object with U=18.0, U–B= –0.3, B–V=0.2, V–R=1.0.

1436+0501: Complicated structure; precession of the object is possible.

1446+0507: Bad cleaning of the VLA map. Extended structure of the object is possibly lost. The identification of Lawrence et al.(1986) (empty field) differs from ours.

1526+0514: Bad cleaning of the VLA map. The centroid of the double UTRAO catalog source has R.A.= $15^h23^m30^s.515$, Dec=5°20′41″.1. This source has a cometary structure in Lawrence et al. (1986) and the identification is also an empty field.

1543+0452: Bugaenko et al. (1993) give for the identified object U=15.1. It is Zwicky galaxy.

1550+0524: Veron-Cetty, Veron (1991) give for this source $z = 1.422$ and V=17.7.

1559+0502: Bad cleaning of the VLA map. There is a bright core with weak components around it.

1616+0459: Veron-Cetty, Veron (1991) give for this quasar V=19.5 and redshift $z = 3.209$.

1658+0514: Although the source is double, the second component is very weak, so this object is either a core with a jet or these are two independent sources. Veron-Cetty, Veron (1991) give for this quasar redshift $z = 0.879$, V=16.54, B–V=0.46, U–B=–0.6. This quasar is also an X–ray source.

1728+0429: The source is identified with a quasar with V=16.99, B–V=0.44, U–B=–0.56 at the redshift $z = 0.293$. This source is also an X–ray source (Veron-Cetty, Veron, 1993).

1754+0459: The position and the radio image of the object have been taken from Lawrence et al. (1986); they give an empty field or possible identification with the object with $m = 17.5$. Our measurement demonstrates the reality of the last identification.

1806+0527: The coordinates and the radio map of the source have been taken from Lawrence et al. (1986). The source may be a core with two jets or a double source of FRII type.

1829+0451: Side by side is the object with R=20.0 with the coordinates: R.A.=$18^h27^m30^s.78$, Dec=4°50′25″.3.

2029+0456: Lawrence et al. (1986) identified this source with the fuzzy object, shifted by 1.4 arcsec, with B=21.0, R=20.5.

2044+0444: Bad cleaning of the VLA map.

2110+0505b: Borisov (1991) identified this source with the quasar with $z = 2.95$.

2116+0507: This source is identified with a quasar with V=20.37 at the redshift $z = 1.001$. The source radiates in the X–ray band (Veron-Cetty, Veron 1993).

2117+0503: Identification of Lawrence et al. (1986) (empty field) agrees with ours.

2204+0442: Bugaenko et al. (1993) identified this source with the object with U=12.6, U–B=0.4, B–V=1.9, V–R=0.8. Veron-Cetty, Veron (1993) give for this galaxy V=15.2, B–V=1.0, U–B=0.22 and the redshift $z = 0.098$.

2144+0513: The first optical candidate is probably a quasar, the second one is a galaxy.

2224+0513: An extended component is possibly lost. Lawrence et al. (1986) give for this source an empty field.

2225+0523: This source has a cometary structure in Lawrence et al. (1986); the identification with the stellar object shifted by 0.3 arcsec with B=18.0, R=18.5. Veron-Cetty and Veron (1991) give the redshift $z = 2.323$. **2245+0501**: Bugaenko et al. (1993) give for the identified object U=19.3, U–B= 0.0, B–V=0.3, V–R=1.5.

2258+0517: Lawrence et al. (1986) give for this source an empty field.

2320+0512: The source is identified with the quasar with V=19 at the redshift $z = 0.623$ (Veron-Cetty Veron, 1993).

2343+0520: Lawrence et al. (1986) identified this source with the stellar object shifted by 0.9 arcsec with B=19.5, R=20.0.

6. Optical identification of RC objects: POSS and 6 m optical telescope CCD observations

6.1. Inspection of the Palomar (POSS) prints

Before deep optical observations with the best in Russia facilities, we examined the prints of POSS as carefully as it was possible and developed different vari-

ants of position measurements, adequate to the simple facilities available. As a result, we achieved sub-arcsecond accuracy of positioning optical objects at POSS even at the limiting magnitudes. Recently, we got access to the INTERNET system and realized soon the efficiency of standard international APM sky catalog facilities to contact with POSS glass copies. But we should say that in some cases the results of optical identification through APM gate may be misleading:

- Weak objects and objects in the crowdy fields may be missed.
- We don't have very repeatable results of the positioning for weak objects, which amounts to 1 arcsec.
- For close pairs only centroid position is given and identification is not possible. That is why we preserve our own method of resolving the uncertainties if they appear.

The results of the identifications done with the help of POSS are listed in Table 3. As we expected, only a small part of the RC population is visible on the POSS (most of them are flat spectrum). It confirms the status of the 1–50 mJy population as the most distant one. Steep spectrum population was selected from the unidentified object list and was observed (after VLA mapping) with the 6 m telescope.

6.2. 6 m CCD images

In this Section all available CCD images of the fields around the RC steep spectrum objects are collected.

The procedure of observations consisted of the receipt of two or more snapshots for each object with the 400^s–600^s exposures with the small (10″–20″) telescope shift between exposures to garantee a possibility of correcting CCD defects and "ghosts" of residual luminescence left by bright stars. After that snapshots were summed up with their corresponding registration by common objects. Snapshots of the bright twilight sky were used for pixel to pixel correction of the nonuniformity of the CCD response. To make this the telescope was directed on blank sky areas free from bright stars and shifted between exposures also. The standard stars from the Landolt lists (Landolt, 1983, 1992) were used for photometric calibration. The data reduction was done with the ESO–MIDAS and partly with the PCVISTA package. The detailed description of CCD is given in the paper of Kopylov et al. (1995b).

CCD images of the selected radio sources are shown in Fig.9 at the end of the paper (p.79).

Positions of the radio source components are marked with big crosses, the central core components (if present) are marked with small crosses and positions of the radio centroid are shown by points.

6.3. Results of optical identification of the RC catalog objects

In Table 3 we give:

Column **1**: The source name according to the RATAN–600 RC catalog.

Columns **2,3**: The right ascension and declination of the candidate for optical identification for the epoch 1950.0.

Column **4**: The observed optical magnitude in R–band. Asterisks denote the magnitude estimates made using the E–plates of POSS.

Column **5**: Correction for absorption by the Galaxy dust in R–band estimated from Burstein and Heiles (1982).

Column **6**: R–magnitude corrected for absorption in the Galaxy.

Column **7**: Difference between limiting optical magnitude calculated from the condition $L_{rad} = L_{opt}$, (as it's given in Column 14 of Table 2) and R–magnitude, corrected for absorption in the Galaxy.

Columns **8,9**: Right ascension and declination position difference of the optical candidate and centroid (or core) of the radio source, in arcsec.

Table 3: *Results of optical identification of the RC catalog sources*

RC name 1	R.A.$_{opt}$ 2 h m s	Dec$_{opt}$ 3 ° ′ ″	m_R 4 m	A_R 5 m	m^o_R 6 m	m_{lim}-m^o_R 7 m	Δ R.A. 8 ″	Δ Dec 9 ″
0015+0503a	00 12 37.49	+4 49 59.5	22.0	0.10	21.9	1.8	-1.8	0.1
0015+0503b	00 12 44.41	+4 47 14.0	21.4	0.10	21.3		0.9	0.6
0015+0501	00 12 48.68	+4 44 42.1	20.6	0.10	20.5	2.2	1.6	-8.5
	00 12 48.42	+4 44 52.9	20.7		20.6	2.1	-2.2	2.3
0029+0509	00 26 29.10	+4 52 59.8	18.1*	0.03	18.1	1.1	-0.1	-0.2
0034+0513	00 31 31.62	+4 58 26.1	23.3	0.03	23.3	-1.2	-0.7	0.1

Table 3: *Results of optical identification of the RC catalog sources (continued)*

1	2 h m s	3 ° ′ ″	4 m	5 m	6 m	7 m	8 ″	9 ″
0038+0449	00 35 59.99	+4 34 21.6	21.2	<0.03	21.2	0.7	-0.8	-0.1
0039+0454			>20.2*	0.00	>20.2			
0042+0504	00 39 52.37	+4 48 58.7	19.0	<0.03	19.0	3.1	3.0	-1.1
0043+0502			>20.2*	0.00	>20.2			
0103+0524			>20.2*	0.10	>20.1			
0105+0501	01 02 59.12	+4 45 06.8	22.2	<0.03	22.2	0.8	3.1	-1.3
	01 02 58.70	+4 45 10.4	22.3		22.3	0.7	-3.1	2.3
0110+0500	01 07 37.90	+4 43 51.5	19.4	<0.03	19.4	2.6	5.6	0.4
	01 07 37.68	+4 43 48.2	19.8		19.8	2.2	2.3	-2.9
0117+0503	01 15 06.48	+4 47 02.9	21.0	0.03	21.0	3.1	1.1	-0.3
0126+0502	01 23 40.27	+4 46 35.8	18.1	<0.03	18.1	4.4	1.8	0.7
0133+0459	01 30 45.19	+4 43 57.2	21.8	<0.03	21.8	0.5	1.4	1.0
0135+0450	01 33 01.25	+4 33 15.3	18.4	<0.03	18.4	3.5	-0.2	0.2
0137+0539	01 34 39.89	+5 19 39.6	23.3	<0.03	23.3	-1.0	0.3	0.7
0143+0505	01 40 57.60	+4 52 53.4	20.6	<0.03	20.6	1.9	-1.5	-1.3
	01 40 57.65	+4 52 56.9	20.3		20.3	2.2	-0.8	2.2
0152+0508	01 49 52.52	+4 51 51.7	19.9*	0.10	19.8	2.5	-6.6	-0.3
0152+0453	01 50 20.40	+4 39 42.2	22.6	0.10	22.5	0.0	-2.7	0.3
0153+0455			>20.2*	0.10	>20.1			
0154+0459	01 52 11.18	+4 44 42.0	22.6	0.10	22.5	0.6	-0.2	0.0
0159+0448	01 56 59.42	+4 30 58.9	20.9	0.10	20.8	1.8	0.6	-0.8
0209+0501a	02 06 35.77	+4 46 42.1	18.5*	0.10	18.4	4.6	0.0	0.6
0209+0501b	02 06 45.00	+4 47 33.0	22.8	0.10	22.7	1.0	1.7	-0.2
0213+0516	02 10 59.18	+5 04 19.4	22.1	0.10	22.0	-0.6	-1.8	0.5
	02 10 59.35	+5 04 21.1	22.5		22.4	-1.0	0.8	2.2
0215+0522			>20.2*	0.10	>20.1			
0225+0506	02 22 32.47	+4 55 06.6	22.1	0.03	22.1	0.1	-0.4	0.2
0226+0512	02 23 42.82	+4 33 04.4	20.1	0.03	20.1	2.0	0.2	-0.1
0234+0446	02 31 29.99	+4 33 35.4	18.0*	0.10	17.9	1.1	-0.7	-0.2
0250+0512			>23.0	0.15	>22.8	<-0.9		
0302+0456	03 00 18.84	+4 43 38.9	24.6	0.30	24.3	-1.7	0.3	0.3
0308+0454			>23.0	0.35	>22.6	<-0.7		
0311+0507	03 09 09.89	+4 56 48.6	22.9	0.40	22.5	-1.2	0.1	1.5
0318+0456	03 16 01.28	+4 30 47.4	24.0	0.30	23.7	-2.4	2.3	-0.9
0318+0506			>20.2*	0.40	>19.8			
0319+0504			>20.2*	0.30	>19.0			
0324+0442	03 21 29.4	+4 31 27.1	22.4	0.30	22.1	-0.5	-1.4	0.7
0343+0458	03 40 51.47	+4 48 21.6	18.2*	0.45	17.8	1.4	1.7	4.6
0350+0506			>20.2*	0.54	>19.7			
0355+0449	03 52 34.39	+4 31 57.0	24.2	0.42	23.8	-2.9	-0.9	0.2
0406+0453	04 03 48.18	+4 39 50.1	24.9	0.41	24.5	-2.4	-0.7	0.4
0427+0457	04 25 08.59	+4 50 30.1	19.1*	0.50	18.6	0.0	0.5	-0.3
0444+0501	04 41 38.70	+4 55 55.2	23.0	0.41	22.6	-0.4	0.4	-0.6
0446+0525			>20.2*	0.30	>19.9			
0457+0452	04 55 14.66	+4 49 19.7	19.4	0.23	19.2	3.2	-6.4	5.9
0458+0506	04 55 36.12	+4 59 43.6	15.1	0.28	14.8	7.1	-1.2	1.1
0459+0456	04 56 25.03	+4 51 25.5	20.9	0.23	20.7	1.5	-7.3	-5.0
	04 56 25.27	+4 51 27.4	22.1		21.9	0.3	-3.6	-3.0

Table 3: *Results of optical identification of the RC catalog sources (continued)*

1	2	3	4	5	6	7	8	9
	h m s	o ′ ″	m	m	m	m	″	″
0505+0459	05 02 43.79	+4 55 40.7	18.2*	0.27	17.9	0.3	-0.8	0.2
0506+0558	05 03 45.46	+5 04 21.5	21.6	0.27	21.3	0.9	-1.5	0.4
0519+0510	05 16 35.10	+5 11 45.7	20.9	0.59	20.3	1.4	-12.7	-4.0
	05 16 37.10	+5 11 38.3	17.3		16.7	5.0	17.2	-11.4
0552+0451			>25.5	1.68	>23.8	<-1.6		
0619+0506			>20.2*	>2.0	>18.2			
0621+0437	06 19 13.75	+4 40 02.2	18.5*	>2.0	<16.5	>5.0	0.6	-2.1
0621+0452			>20.2*	>2.0	>18.2			
0625+0437	06 23 12.71	+4 37 28.9	19.8*	>2.0	<17.8	>2.7	-0.2	0.1
0646+0439			>20.2*	>2.0	>18.2			
0646+0449			>20.2*	>2.0	>18.2			
0653+0508			>20.2*	>2.0	>18.2			
0707+0455a			>20.2*	>1.0	>19.2			
0707+0455b	07 05 06.66	+5 00 11.8	19.0*	>1.0	<18.0		0.8	-1.3
0707+0455c			>20.2*	>1.0	>19.2			
0743+0455	07 40 36.58	+5 03 03.6	23.6	0.12	23.5	-0.6	0.6	0.8
0744+0500			>24.5	0.20	>24.3	<-1.2		
0756+0450			>25.0	0.07	>24.9	<-1.0		
0759+0454	07 57 04.35	+5.03 26.0	20.0*	0.10	19.9	2.7	-0.5	-1.8
0809+0500	08 07 08.25	+5 10 04.0	14.3*	0.03	14.3	7.4	2.9	2.5
0820+0454	08 18 18.18	+5 03 50.2	19.3	0.00	19.3	2.0	1.1	-0.2
0836+0511	08 34 09.52	+5 23 37.9	22.6	0.00	22.6	-0.9	-1.2	1.8
	08 34 09.54	+5 23 33.8	24.2		24.2	-2.5	-0.9	-2.3
0837+0446	08 34 51.25	+4 54 53.0	22.2	0.07	22.1	0.4	-0.4	1.2
0845+0434			>20.2*	0.03	>20.2			
0845+0444	08 42 53.22	+4 53 53.0	21.4	0.09	21.3	0.1	-0.9	0.1
0902+0444	08 59 49.46	+4 55 01.6	17.9*	0.00	17.9	2.9	-0.1	0.0
0906+0459a			>20.2*	0.03	>20.2			
0906+0459b			>20.2*	0.03	>20.2			
0906+0459c	09 03 35.92	+5 12 19.2	19.2*	0.03	19.2		0.5	1.1
0907+0439			>20.2*	0.00	>20.2			
0908+0451	09 05 43.29	+5 03 08.3	19.6	0.00	19.6	3.2	3.5	-0.1
0909+0445	09 07 13.48	+4 56 37.4	20.6	0.08	20.5	1.8	-0.5	0.4
0927+0457	09 25 07.91	+5 09 19.8	16.9*	0.00	16.9	5.8	-0.6	0.9
0934+0505	09 31 48.17	+5 17 11.0	24.1	0.06	24.0	-1.1	-0.6	0.3
0936+0504			>20.2*	0.00	>20.2			
0937+0450			>20.2*	0.00	>20.2			
0942+0441			>20.2*	0.00	>20.2			
0942+0447			>20.2*	0.00	>20.2			
0945+0454			>20.2*	0.00	>20.2			
0949+0454			>20.2*	0.00	>20.2			
1011+0502	10 09 28.02	+5 21 04.6	22.4	0.00	22.4	-0.2	-2.0	0.6
1015+0452			>20.2*	0.10	>20.2			
1016+0514	10 13 26.66	+5 28 00.4	19.1*	0.10	19.0	-0.2	0.5	-0.1
1031+0443	10 28 42.96	+4 58 33.8	22.2	0.06	22.1	-1.1	-0.1	0.3
1038+0514	10 36 10.83	+5 28 06.5	18.7*	0.00	18.7	0.0	-0.1	-0.1
1043+0443	10 41 10.69	+4 56 10.8	23.0	0.00	23.0	-0.1	6.1	-1.9
	10 41 09.74	+4 56 03.3	23.4		23.4	-0.5	-8.1	-9.4

Table 3: *Results of optical identification of the RC catalog sources (continued)*

1	2 h m s	3 ° ′ ″	4 m	5 m	6 m	7 m	8 ″	9 ″
1045+0455			>20.2*	0.00	>20.2			
1049+0506	10 46 56.56	+5 21 24.9	18.9*	0.00	18.9	2.5	-1.1	-0.2
1051+0449			>20.2*	0.00	>20.2			
1057+0456			>20.2*	0.10	>20.1			
1100+0444	10 57 36.17	+5 00 07.9	18.0*	0.10	17.9	2.9	-0.7	-0.4
1102+0459	10 00 10.99	+5 15 22.8	19.8*	0.00	19.8	1.8	-0.5	1.6
1103+0451	11 01 14.38	+5 08 01.3	15.7*	0.00	15.7	7.4	4.8	-0.7
1113+0436	11 11 23.83	+4 54 19.2	22.4	0.10	22.3	0.3	-3.4	-1.0
	11 11 22.91	+4 54 19.7	23.1		23.0	-0.4	-17.1	-0.4
1123+0450			>20.2*	0.10	>20.1			
1124+0456	11 22 02.72	+5 12 48.0	17.1*	0.00	17.1	3.2	<1.0	<0.2
1125+0446			>20.2*	0.00	>20.2			
1131+0455			>20.2*	0.00	>20.2			
1142+0429	11 39 34.69	+4 54 11.5	15.2*	0.03	15.2	6.0	0.0	-0.5
1142+0455	11 39 45.84	+5 11 34.7	21.0	0.00	21.0	0.8	1.1	-2.0
1145+0455	11 42 47.10	+5 12 06.1	18.7*	0.03	18.7	1.1	-0.5	-0.2
1146+0458	11 43 57.58	+5 14 59.2	19.8*	0.03	19.8	0.3	-0.1	0.3
1148+0455			>20.2*	0.03	>20.2			
1150+0459			>20.2*	0.03	>20.2			
1152+0449	11 49 49.68	+5 04 55.6	22.5	0.07	22.4	0.8	-0.9	-1.3
1154+0431	11 52 19.58	+4 40 54.2	19.9	0.00	19.9	0.9	0.7	-0.7
1155+0444	11 52 45.32	+5 00 13.1	18.6	0.07	18.5	4.0	-1.2	2.4
1213+0500	12 10 55.68	+5 16 51.3	21.8	0.00	21.8	0.3	4.9	0.4
1218+0515			>20.2*	0.00	>20.2			
1219+0446	12 17 08.50	+5 03 36.4	22.0	0.06	21.9	1.4	23.5	-26.4
	12 17 11.68	+5 03 01.0	17.6		17.5	5.8	71.2	-61.9
1221+0504			>20.2*	0.00	>20.2			
1226+0438			>20.2*	0.00	>20.2			
1235+0452	12 32 34.22	+5 09 51.1	18.3*	0.00	18.3	3.8	-3.3	-0.5
1235+0435a	12 33 13.72	+4 48 29.9	21.7	0.06	21.6		0.1	-0.2
1235+0435b	12 33 16.57	+4 49 27.6	21.5	0.06	21.4	1.3	0.7	0.9
1239+0443	12 36 59.93	+4 59 33.0	19.0*	0.00	19.0	0.3	0.5	-0.3
1257+0458			>20.2*	0.00	>20.2			
1318+0436	13 15 57.70	+4 45 55.8	19.9*	0.00	19.9	-1.6	0.8	-0.1
1322+0449	13 19 31.70	+5 04 31.0	20.4	0.06	20.3	2.4	-2.1	2.9
1333+0451	13 30 32.30	+5 07 08.8	23.4	0.05	23.3	0.7	0.8	0.3
1333+0452	13 30 54.80	+5 07 20.9	23.3	0.05	23.2	0.2	2.1	-0.3
1339+0445	13 37 06.52	+5 10 15.5	22.7	0.06	22.6	0.2	0.3	-0.4
1340+0448	13 37 55.88	+5 01 35.2	10.0*	0.00	10.0		0.8	-0.4
1347+0441	13 44 37.69	+4 57 14.9	23.5	0.06	23.4	-0.6	1.2	-1.8
1347+0435			>20.2*	0.06	>20.1			
1351+0437			>20.2*	0.03	>20.2			
1356+0457	13 53 41.27	+5 15 46.8	10.0*	0.00	10.0	12.3	1.1	-9.8
1357+0453	13 55 06.46	+5 07 51.8	20.8	0.00	20.8	1.0	0.9	2.3
1424+0442	14 21 38.86	+4 48 26.1	18.6*	0.00	18.6	0.6	-1.1	0.0
1429+0501			>24.0	0.06	>23.9	<-1.8		
1436+0501	14 34 04.92	+5 15 13.3	22.9	0.06	22.8	-0.3	3.9	2.5
	14 34 05.08	+5 15 10.9	22.4		22.3	0.2	6.3	0.1

Table 3: *Results of optical identification of the RC catalog sources (continued)*

1	2 h m s	3 ° ′ ″	4 m	5 m	6 m	7 m	8 ″	9 ″
1439+0455			>25.0	0.06	>24.9	<-2.1		
1446+0507	14 43 48.26	+5 20 14.6	19.3*	0.00	19.3	2.3	0.0	0.0
1450+0509			>20.2*	0.00	>20.2			
1454+0440			>20.2*	0.03	>20.2			
1503+0502			>20.2*	0.03	>20.2			
1503+0456	15 01 30.14	+5 08 30.4	22.8	0.00	22.8	-0.4	0.2	-0.3
1510+0438	15 07 42.97	+4 50 51.8	22.1	0.06	22.0	0.3	-0.5	0.1
1518+0451			>20.2*	0.03	>20.2			
1521+0434	15 18 44.61	+4 41 04.6	20.0*	0.00	20.0	-1.2	-1.8	-1.5
1526+0514			>20.2*	0.00	>20.2			
1543+0452	15 41 04.93	+5 01 45.6	8.9*	0.10	8.8	10.9	-0.3	-0.1
1544+0459	15 41 49.78	+5 07 45.4	17.4*	0.10	17.3	3.9	-0.6	-0.2
1550+0524	15 48 06.95	+5 36 11.2	17.4*	0.17	17.2	0.2	-0.2	0.0
1551+0458	15 49 19.28	+5 08 27.0	23.6	0.17	23.4	-1.2	0.3	0.6
1559+0502			>20.2*	0.15	>20.0			
1609+0456			>24.5	0.14	>24.4	<-1.3		
1616+0459	16 14 09.07	+5 06 53.9	19.6*	0.20	19.4	-3.7	-0.1	-0.4
1620+0446			>20.2*	0.20	>20.0			
1626+0448	16 24 21.72	+4 55 32.5	22.9	0.18	22.70	-0.2	-0.1	-0.9
1638+0450			>20.2*	0.25	>19.9			
1646+0501	16 44 25.13	+5 06 29.4	21.2	0.27	20.9	1.6	2.8	0.5
1653+0443	16 51 29.00	+4 47 55.4	21.4	0.30	21.1	0.8	2.7	-10.5
	16 51 29.00	+4 48 08.6	23.7		23.4	-1.5	2.7	2.7
1658+0454			>24.5	0.27	>24.2	<-1.3		
1658+0514	16 56 05.62	+5 19 46.7	16.0*	0.30	15.7	2.0	-0.1	-0.4
1703+0502	17 01 01.27	+5 06 21.4	23.5	0.27	23.2	-2.1	-0.4	1.4
1706+0502	17 03 59.26	+5 06 41.1	22.9	0.30	22.6	1.8	4.8	3.0
	17 03 59.01	+5 06 37.0	24.6		24.3	3.5	1.1	-1.1
1714+0449	17 12 10.88	+4 51 20.9	17.8*	0.35	17.4	3.0	-0.1	-1.0
1720+0455	17 17 35.93	+4 56 47.8	20.6	0.27	20.3	3.2	-1.0	-0.3
1722+0442	17 19 45.73	+4 46 06.7	20.7	0.30	20.4	0.2	-2.4	-0.6
1725+0457			>24.0	0.27	>23.7	<-0.6		
1726+0504			>20.2*	0.30	>19.9			
1728+0429	17 25 56.29	+4 29 28.1	16.6*	0.30	16.3	1.9	-1.2	0.2
1735+0454	17 33 13.70	+4 57 06.7	23.2	0.39	22.8	0.4	2.7	-0.7
1740+0502	17 38 06.06	+5 04 12.5	22.6	0.41	22.2	0.8	0.5	1.4
1754+0459	17 51 49.47	+5 00 09.8	17.5*	0.59	16.9	2.7	-1.7	-0.1
1806+0527			>20.2*	0.79	>19.4			
1829+0451			>20.2*	>1.5	>18.7			
1935+0457			>20.2*	>1.5	>18.7			
2005+0506			>20.2*	0.72	>19.5			
2012+0458			>20.2*	0.50	>19.7			
2012+0457			>20.2*	0.50	>19.7			
2013+0508	20 10 54.69	+5 01 24.1	21.1	0.46	20.6	2.0	0.0	-0.7
2029+0456			>20.2*	0.40	>19.8			
2036+0451	20 34 27.45	+4 39 23.0	19.0	0.27	18.7	3.5	-0.1	0.3
2044+0444			>20.2*	0.38	>19.8			
2048+0453	20 45 32.07	+4 42 19.0	19.4*	0.35	19.0	2.2	-0.5	-0.9

Table 3: *Results of optical identification of the RC catalog sources (continued)*

1	2 h m s	3 ° ′ ″	4 m	5 m	6 m	7 m	8 ″	9 ″
2110+0505a			>20.2*	0.25	>19.9			
2110+0456			>20.2*	0.25	>19.9			
2110+0505b			18.0*	0.25	17.7			
2111+0501	21 08 58.68	+4 51 03.7	20.0*	0.25	19.7		-4.8	3.7
2113+0445	21 11 03.76	+4 32 56.5	20.2*	0.23	20.0	0.7	2.5	0.7
2116+0507	21 13 49.48	+4 54 53.3	18.5*	0.23	18.3	3.0	0.6	0.5
2117+0503			>20.2*	0.20	>20.0			
2125+0447			>20.2*	0.15	>20.0			
2143+0511			>20.2*	0.18	>20.0			
2144+0513	21 41 56.73	+4 57 26.3	18.8	0.18	18.6	3.6	0.9	0.3
	21 41 56.61	+4 57 25.2	21.5		21.3	0.9	-0.9	-0.8
2204+0442	22 01 46.52	+4 25 27.2	13.7*	0.15	13.5	5.9	0.9	0.4
2217+0514			>20.2*	0.20	>20.0			
2219+0458	22 16 34.8	+4 43 41.5	23.8	0.20	23.6	-1.0	0.9	1.6
2224+0513	22 21 46.56	+4 58 33.5	21.3	0.20	21.1	0.3	0.0	-3.6
2225+0523	22 22 43.47	+5 11 53.6	17.5*	0.03	17.5	3.1	0.0	0.0
2236+0454	22 34 19.41	+4 39 34.2	22.2	0.17	22.0	0.7	-12.2	7.5
2245+0501	22 43 21.83	+4 45 08.7	18.4*	0.00	18.4	1.2	1.3	0.4
2247+0507	22 44 43.26	+4 52 18.6	22.1	0.17	21.9	-0.1	-1.2	2.1
2251+0502			>20.2*	0.00	>20.2			
2258+0517	22 55 52.45	+5 00 35.0	19.6*	0.00	19.6	0.5	-0.2	0.6
2312+0517			>20.2*	0.20	>20.0			
2320+0459	23 18 11.96	+4 42 58.4	20.4	0.10	20.3	2.0	-0.7	5.6
2320+0512			>20.2*	0.10	>20.1			
2343+0520	23 41 17.55	+5 06 01.2	18.4*	0.03	18.4	2.9	0.1	0.2
2348+0507	23 45 58.56	+4 50 53.2	22.8	0.03	22.8	-1.3	0.1	-0.0
2357+0501			>24.0	0.17	>23.8	<-1.4		

7. Conclusions

The RATAN–600 may be used as one of the main sources of 5–50 mJy objects at cm wavelengths. This flux density range, being of special interest for cosmology, was under-explored earlier. RC catalog (1145 objects in the 100 square degree strip) is a mixture of objects of different nature and without optical identification it is not easy to classify them. VLA mapping has helped us greatly (200 images have been obtained up to now) but even with 1 arcsec positional accuracy the majority of the RC objects have not been identified with any objects listed in the best optical (POSS), IR (IRAS), X–ray (Einstein, ROSAT) and radio (GB) sky surveys.

We began deep optical identification program of all RC objects with steep spectrum (SS) radio sources class with FRII morphology. Up to now only for that class we could select complete subgroup of the SS objects (objects even with normal spectra are invisible at longer/shorter wavelengths and cannot be classified through their spectra). The improved "SS FRII" Longair–Lilly method of picking up distant RG happened to be very efficient in this flux density range. We collected about 90 SS objects and almost all o them were mapped at VLA and optically identifie at the 6 m telescope down to $R = 24 - 25$ mag. Fo all identified objects we estimated redshifts using up dated calibrators. The mean photometric redshift o RGs in our list is larger than that, obtained by othe groups (3C, PKS, B2, B3, 8C, Deep WSRT combine with VLA and 4m-5m class optical telescopes; VL very deep surveys combined with HST). We demon strated that the mean multi–color ($BVRI$) age of th stellar systems of the parent galaxies is of order of Gyr, and that at least in some objects active star for mation had begun in the first Gyr after the Big Bang Such distant objects must have high (up to 6 order of magnitude) density contrast and modern cosmolo gy has to explain this very early appearance of dens and massive (Tera–solar masses) protogalaxies with quickly formed massive black holes inside it to pro duce FRII structures. We hope that the suggestion made by Loeb (1993), and Gnedin with Ostriker an Rees (1995) may be useful to create the improve formation theory of this class of active objects. Fro our 100 square degree "Cold" selected area sampl we can estimate that more than 10 000 very early ob

jects, born before the QSO epoch, and available on the sky, are accessible for the present day optical and radio facilities. They can help us to penetrate into the "Dark Age" of the Universe, between the recombination epoch and the epoch of appearance of QSOs. Apart from the normal FRII RG class, some objects with SS happened to be of quite different nature. 10 were not resolved even with VLA in "A" configuration at 3.7 cm, being less than 0.2–0.1 arcsec (CSS class). Several objects have "subgalactic" doubles, with sizes less than 2–3 arcsec, and are of separate interest. A few of them are very complex and can not be considered as FRII objects. One QSR at $z = 2.95$ of FRII type radio structure was found spectroscopically. It has the biggest linear size ever observed at $z > 2$ and we successfully used the object as the "probe particle" of the geometry of the Universe. The ratio of the X–ray flux density to the radio flux density happened to be the most sensitive indicator of the World Geometry if a very distant and a very large radio source is used. Future activity, connected with the BIG TRIO project will be concentrated on the direct spectroscopy of the most probable candidates into the first galaxy generation carefully selected from our RC list. Optical morphology in continuum and line emission will be very important and we hope to use all the best optical facilities for that kind of observations. Radio activity will be concerned with gathering complete spectral information about all RC objects, and the RATAN–600 has greately advanced in this direction (Bursov, 1996). 15–years multi–frequency monitoring of the Cold strip gives us unprecedented possibility to pick up population of highly variable objects in the Early Universe with different time scales from 15 years to 1 day.

Acknowledgements. Authors are thankful to Prof. B. Burke and his collaborators A. Fletcher, S. Conner, F. Crawford, J. Cartwright. for providing the MIT–Green Bank–VLA survey data and for assistance in preparation of some maps, to A.G. Gubanov for assistance in identification with APM sky catalog, and to P. Teerikorpi, K. Nilson and T. Pursimo for collaboration. This work was supported by grants of Russian Fundamental Research Foundation 95-02-03783 and 96-02-106597A and "Astronomy" program project 2-296.

References

Amirkhanyan V.R., Gorshkov A.G., Larionov M.G., Kapustkin A.A., Konnikova V.K., Lazutkin A.N., Nikanorov A.S., Sidorenkov V.N., Ugolkova L.S.: 1989, Zelenchuk Survey of Radio Sources between the Declination 0–14°, Moscow State University.

Benn C.R., Wall J.V., Vigotti M., Grueff G.: 1988, Mon. Not. R. Astron. Soc., **235**, No. 2, 465.

Benn C.R., Wall J.V.: 1995, Mon. Not. R. Astron. Soc., **272**, 678.

Berlin A.B., Gassanov L.G., Golnev V.Ja., Korolkov D.V., Parijskij Y.N.: 1984, Soobshch. Spets. Astrofiz. Obs., **41**, 1; **42**, 1.

Borisov N.: 1991, private communication.

Bugaenko O.I., Gorshkov A.G., Esipov V.F., Konnikova V.K., Novikov S.B.: 1993, Pis'ma Astron. Zh., **19**, 13.

Burstein D., Heiles C.: 1982, Astron. J., **87**, 1165.

Bursov N.N., Chepurnov A.V., Lipovka N.S., Soboleva N.S., Temirova A.V.: 1993, Astron. Astrophys., **101**, 447.

Bursov N.N.: 1996, Astron. Zh.(Russian), in press.

Chambers K.C., Charlot S.: 1990, Astrophys. J., **348**, L1.

Chigo F.D.: 1977, Astrophys. J. Suppl. Ser., **35**, 359.

Condon J.J.: 1987, Astrophys. J. Suppl. Ser., **65**, 485.

Condon J.J.: 1988, in: Galactic and Extragalactic Radio Astronomy, eds.: G.L.Verschuur, K.Kellermann, 641. Springer-Verlag.

Condon J.J, Cotton W.D., Greisen E.W., Yin Q.F., Perly R.A., Broderick J.J.: 1995, The NRAO VLA Sky Survey. I. Goals, Methods, and First Results. Preprint.

Crampton D., Le Févre O., Lilly S.J., Hammer F.: 1995, Astrophys. J., **455**, 96.

Daly R.: 1992, Astrophys. J., **386**, L9.

Daly R.: 1994, Astrophys. J., **426**, 38.

Djorgovski S., Spinrad H., McCarthy P., Strauss M.: 1985, Astrophys. J.Let., **299**, L1

Dressel L., Condon J.J.: 1978, Astrophys. J. Suppl. Ser., **36**, 53.

Dunlop J.S., Peacock J.A., Sanders A., Lilly S.J., Heasley J.N., Simon A.J.K.: 1989, Mon. Not. R. Astron. Soc., **238**, 1171-1231.

Gnedin N., Ostriker J., Rees M.: 1995, Astrophys. J., **438**, 40.

Goss W.M., Parijskij Y.N., Kopylov A.I., Zhelenkova O.P., Naugolnaya M.N., Soboleva N.S., Temirova A.V., Vitkovskij Val.V.: 1994, Turkish J. of Physics, **18**, 894.

Goss W.M., Parijskij Y.N., Soboleva N.S., Temirova A.V., Vitkovskij Val.V., Zhelenkova O.P., Naugolnaya M .N.: 1992, Astron. Zh., **69**, 673.

Gurevich L.E., Chernin A.D.: 1983, in: Proiskhozhdenie Galaktik i Zvezd (in Russian), Nauka, Moscow.

Gurvits L.: 1993, in: Sub–Arcsecond Radio Astronomy, eds.: R.J.Davies, R.J.Booth, Cambridge University Press, 380.

Longair M.: 1974, IAU Symp. No. 63, 130, ed.: M.Longair, England, D.Reidel Publ. Comp.

Hills J.S.: 1975; Nature, **254**, 295.

Hoyle F.: 1959, Paris Symp.on Radioastronomy, ed. R. Bracewell, Stanford Univ.Press, 512.

Hummel E.: 1980, Astron. Astrophys. Suppl. Ser., **41**, 151.

Jones L.A., Worthey G.: 1995, Astrophys. J., **46**, L31.

Kapahi V.K.: 1986, in: High Lights of Astronomy, ed. J.Swings, 371.

Kapahi V.K., Kulkarni V.K.: 1990, Astron. J., **99**, 1397.

Kellermann K.I.: 1973, in: Galactic and Extragalactic Radio Astronomy, MIR, Moscow, 1976, 496.

Kellermann K.I.: 1993, Preprint NRAO -93/200.

Kopylov A.I., Goss W.M., Parijskij Y.N., Soboleva N.S., Zhelenkova O.P., Temirova A.V., Vitkovskij Val. V., Naugolnaya M.N., Verkhodanov O.V.: 1995a, Astron. Zh., **72**, 437.

Kopylov A.I., Goss W.M., Parijskij Y.N., Soboleva N.S., Zhelenkova O.P., Vitkovskij Val.V., Naugolnaya M.N.,

Verkhodanov O.V.: 1995b, Astron. Zh., **72**, 613.
Landolt A.U.: 1983, Astron. J., **88**, 439.
Landolt A.U.: 1992, Astron. J., **104**, 340.
Lawrence C.W., Bennett C.L., Hewitt J.N., Langston G.I., Klotz S.E., Burke B.F.: 1986, Astrophys. J. Suppl. Ser., **61**, 105.
Loeb A.: 1993, Astrophys. J., **404**, L37.
Longair M.: 1974, in: Confrontation of Cosmological Theories with Observational Data, Reidel, Dordrecht.
McCarthy P.J.: 1993, Annu. Rev. Astron. Astrophys., **31**, 639.
Neser M.: 1995, Astrophys. J., **76**, 451.
Nilsson K., Valtonen M.J., Jaakkola T.: 1993, Astrophys. J., **413**, 453.
Oort M.J.A.: 1987, Ph.D., Leiden.
Parijskij Y., Korolkov D.: 1986, Ap.Space Phys. Rev., **5**, 40.
Parijskij Y.N., Bursov N.N., Lipovka N.M., Soboleva N.S., Temirova A.V.: 1991, Astron. Astrophys. Suppl. Ser., **87**, 1.
Parijskij Y.N., Bursov N.N., Lipovka N.M., Soboleva N.S., Temirova A.V., Chepurnov A.V.: 1992, Astron. Astrophys. Suppl. Ser., **96**, 583.
Parijskij Y.N., Soboleva N.S.: 1980, Pis'ma Astron. Zh., **6**, N0. 2, 67.
Parijskij Yu.N., Soboleva N.S., Temirova A.V., Kopylov A.I.: 1994, Astron. Zh., **71**, No. 5, 1.
Peebles P.: 1980, The Large Scale Structure of the Universe, Prinston Univ. Press, Prinston, 90.
Reich P., Soboleva N.S., Temirova A.V.: 1991, Astron. Astrophys. Suppl. Ser., **91**, 337.
Rees M.: 1984, Annu. Rev. Astron. Astrophys., **22**, 471.
Röttgering H.J.A., Lacy M., Miley G.K., Chambers K.C., Saunders R.: 1994, Astron. Astrophys. Suppl. Ser., **108**, 79.
Ryle M., Longair M.S.: 1967, Mon. Not. R. Astron. Soc., **136**, 123.
Schmidt, M.: 1966, Astrophys. J., **16**, 7.
Soboleva N.S., Berlin A.B., Golnev V.Ja.,Timofeeva G.M.: 1977, Astron. Zh., **54**, 945.
Spinrad H., Djorgovski S., Marr J., Aquilar L.: 1985, Publ. Astr. Soc. Pacific, **97**, 932.
Verkhodanov O.V.: 1996, Bull. Spec. Astrophys. Obs., **41**, in press.
Veron-Cetty M.P., Veron P.: 1993, ESO Scientific Report, **13**.
Veron-Cetty M.P., Veron P.: 1991, ESO Scientific Report, **11**.
Windhorst R.A.: 1984, Ph.D., Leiden.
Windhorst R.A., Fomalont E.B., Kellermann K.I., Partridge R.B., Richard E., Franklin B.E.,Pascarelle S.M., Griffith R.E.: 1995, Nature, **375**, 471.
Yoshy Y., Peterson B.: 1991, Astrophys. J., **372**, 8.

Figure 7: *Positions of optical photometrical points BVRI on the curves of the spectral energy distribution for different ages of radio galaxies*

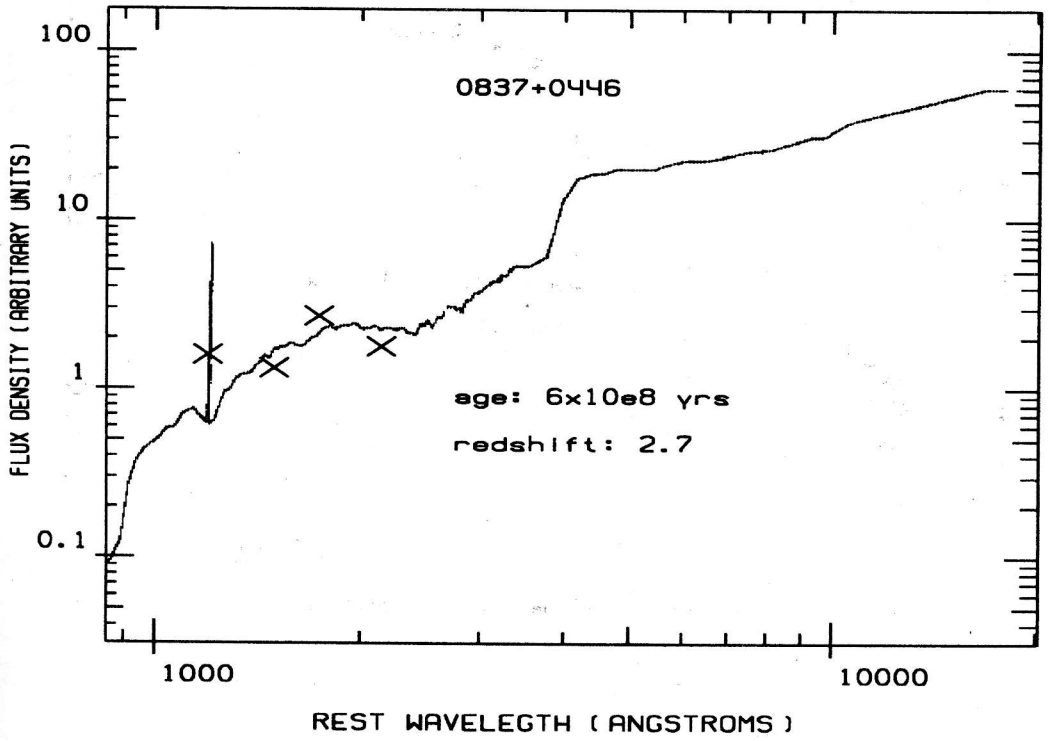

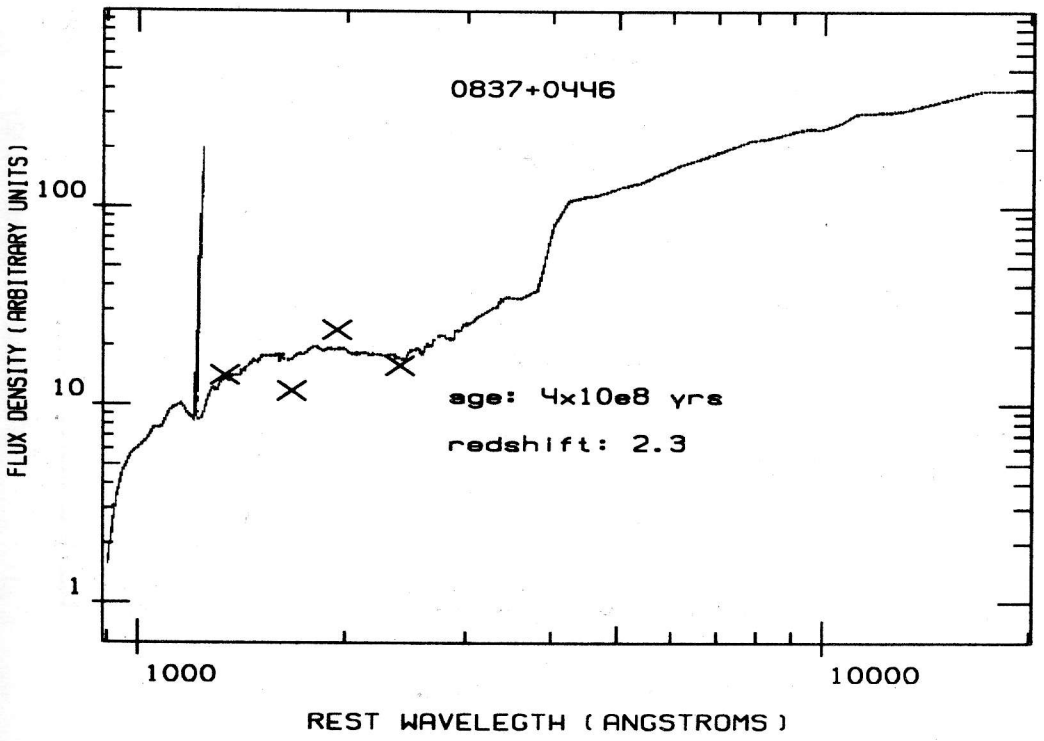

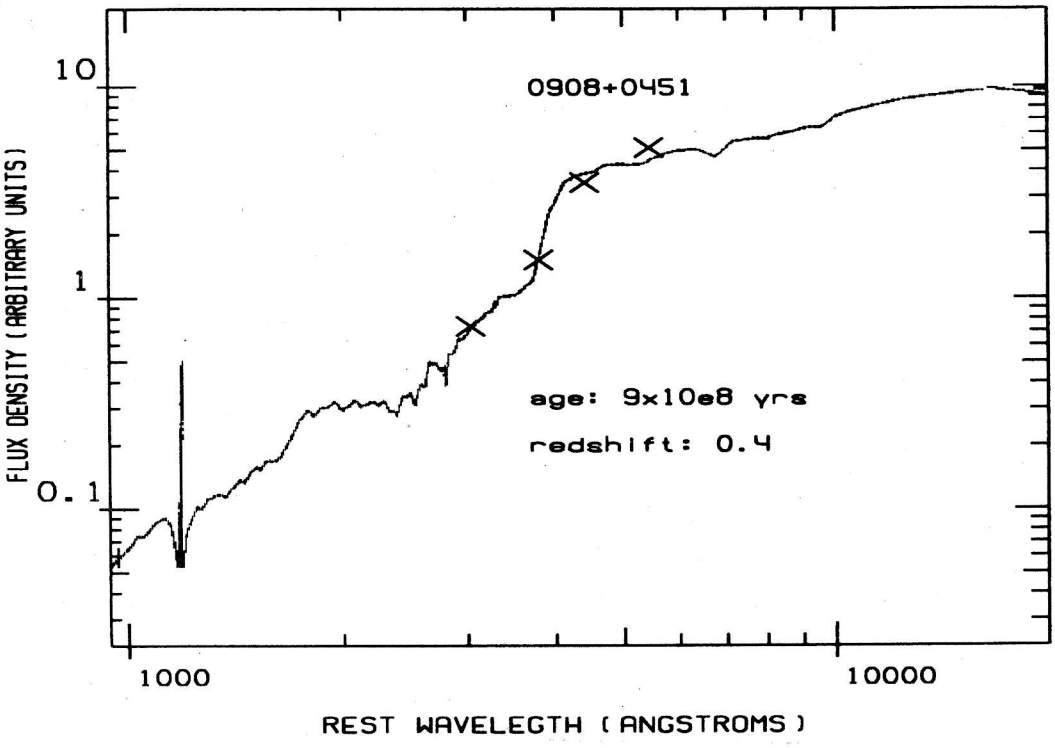
10
1
0.1
0908+0451
age: 9x10e8 yrs
redshift: 0.4
FLUX DENSITY (ARBITRARY UNITS)
1000
10000
REST WAVELEGTH (ANGSTROMS)

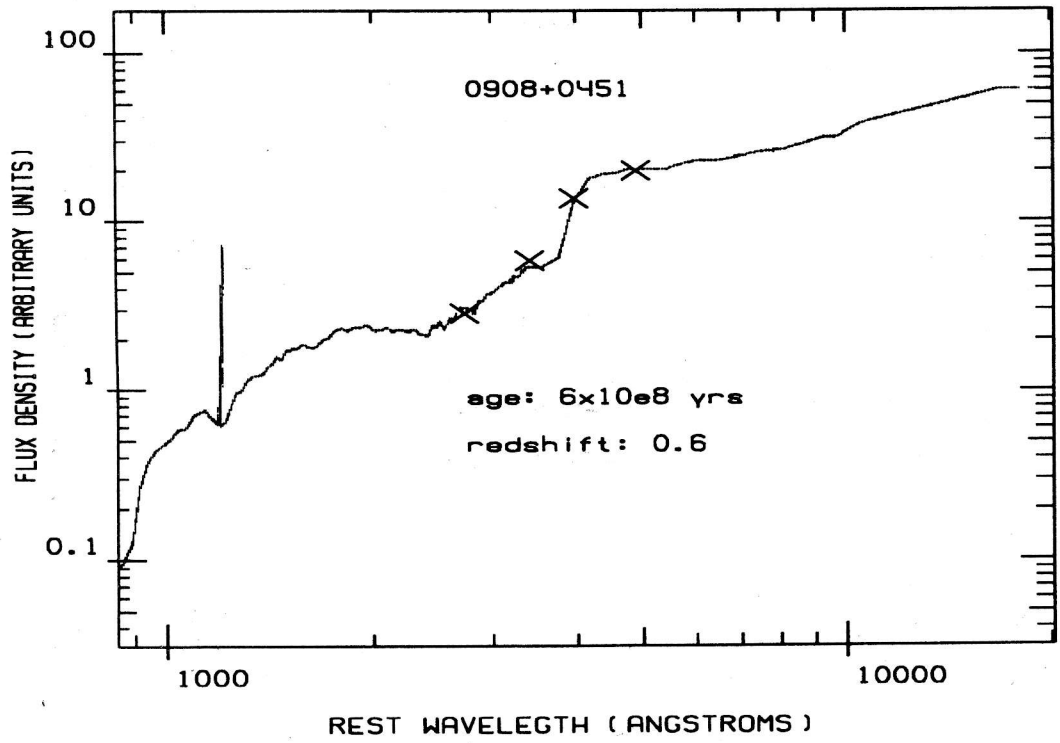
100
10
1
0.1
0908+0451
age: 6x10e8 yrs
redshift: 0.6
FLUX DENSITY (ARBITRARY UNITS)
1000
10000
REST WAVELEGTH (ANGSTROMS)

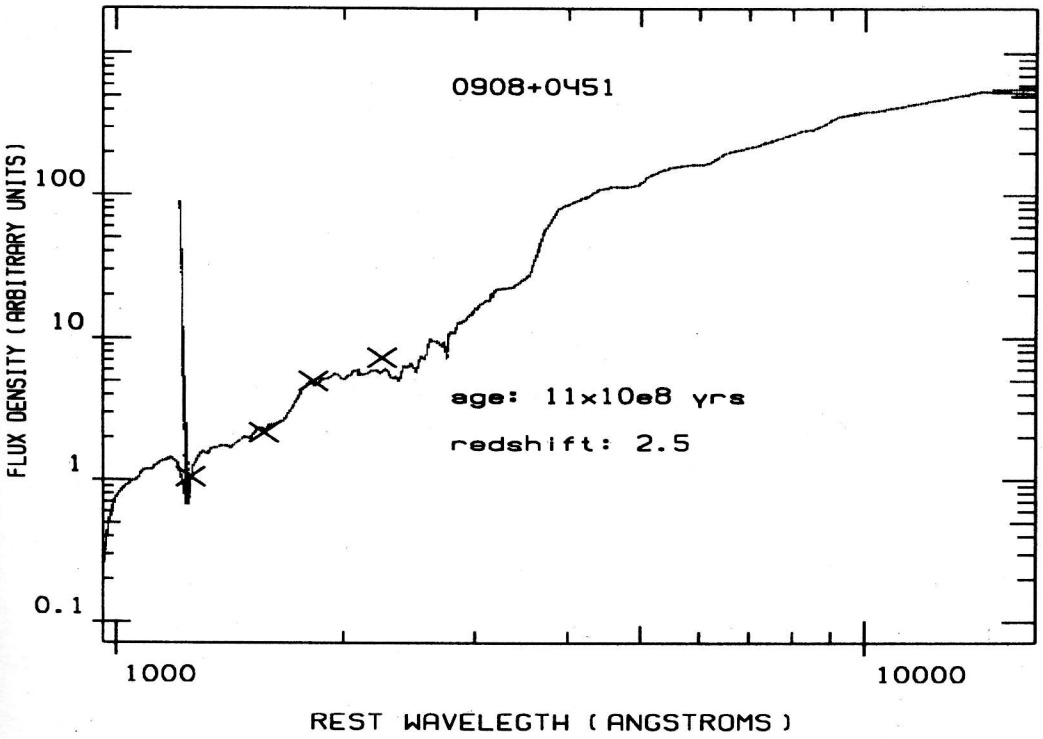
0908+0451
FLUX DENSITY (ARBITRARY UNITS)
100
10
1
0.1
age: 11x10e8 yrs
redshift: 2.5
1000
10000
REST WAVELEGTH (ANGSTROMS)

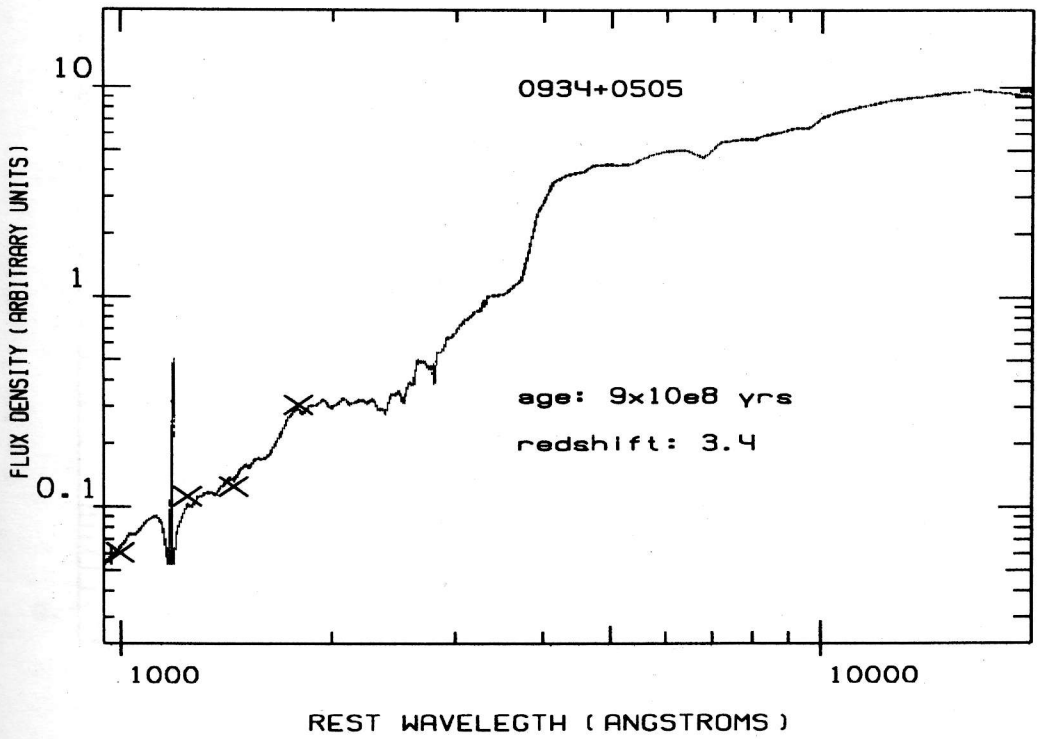
0934+0505
FLUX DENSITY (ARBITRARY UNITS)
10
1
0.1
age: 9x10e8 yrs
redshift: 3.4
1000
10000
REST WAVELEGTH (ANGSTROMS)

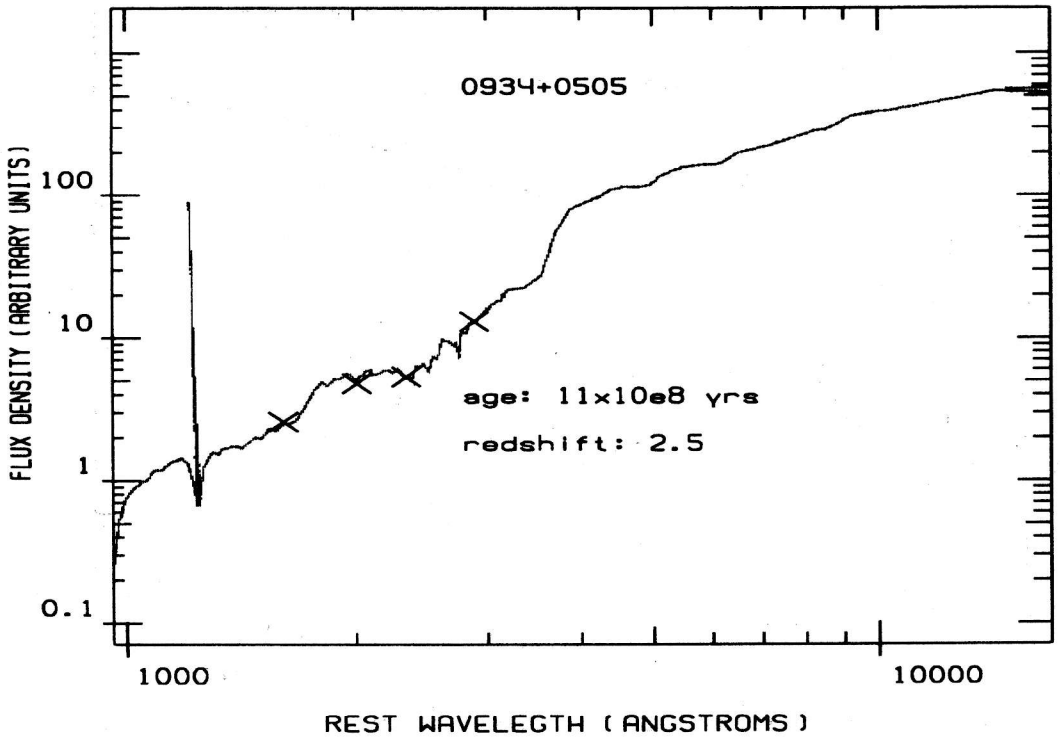
0934+0505
age: 11x10e8 yrs
redshift: 2.5
FLUX DENSITY (ARBITRARY UNITS)
100
10
1
0.1
1000
10000
REST WAVELEGTH (ANGSTROMS)

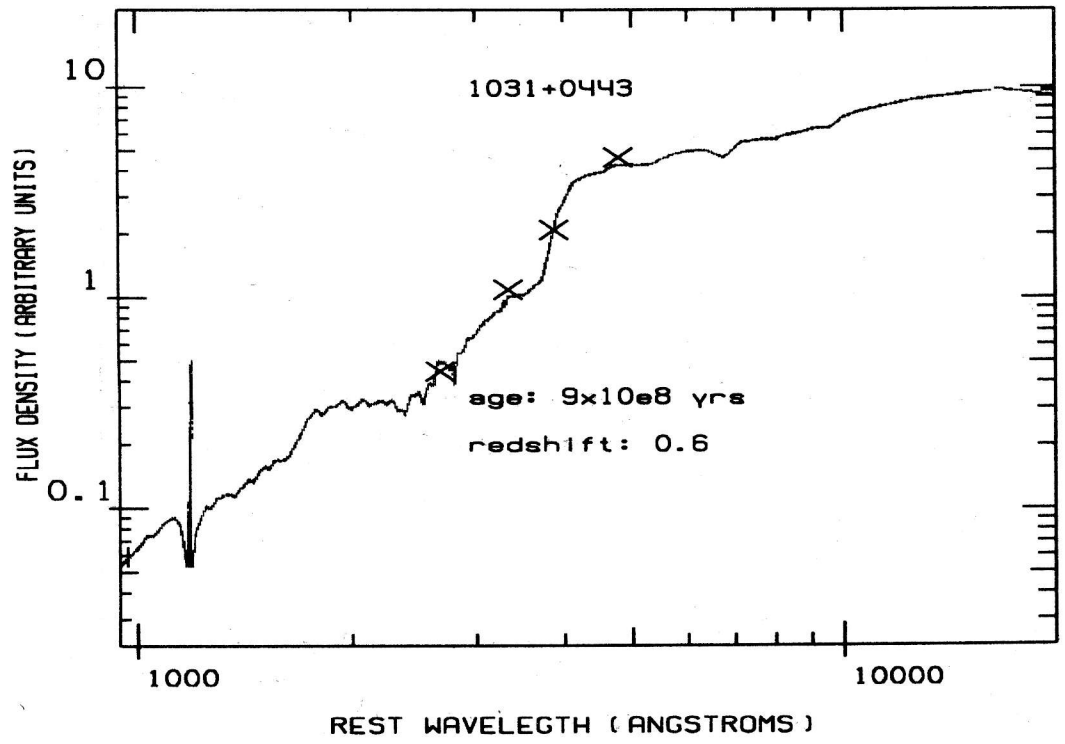
1031+0443
age: 9x10e8 yrs
redshift: 0.6
FLUX DENSITY (ARBITRARY UNITS)
10
1
0.1
1000
10000
REST WAVELEGTH (ANGSTROMS)

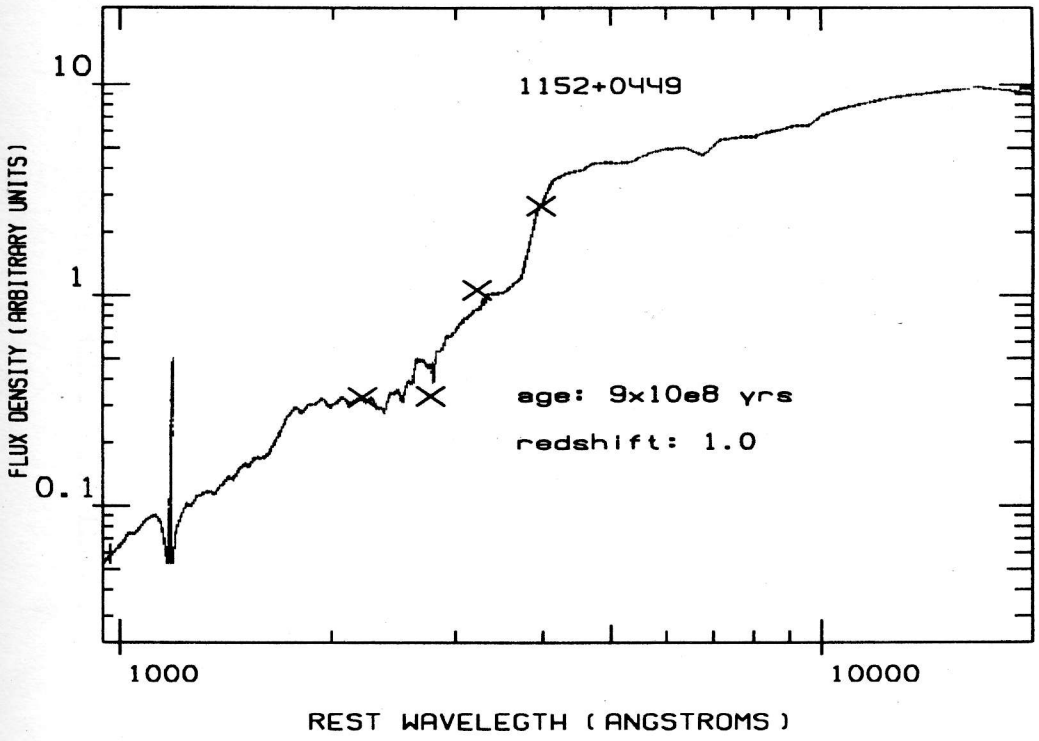
1152+0449
age: 9x10e8 yrs
redshift: 1.0
10
1
0.1
1000
10000
FLUX DENSITY (ARBITRARY UNITS)
REST WAVELEGTH (ANGSTROMS)

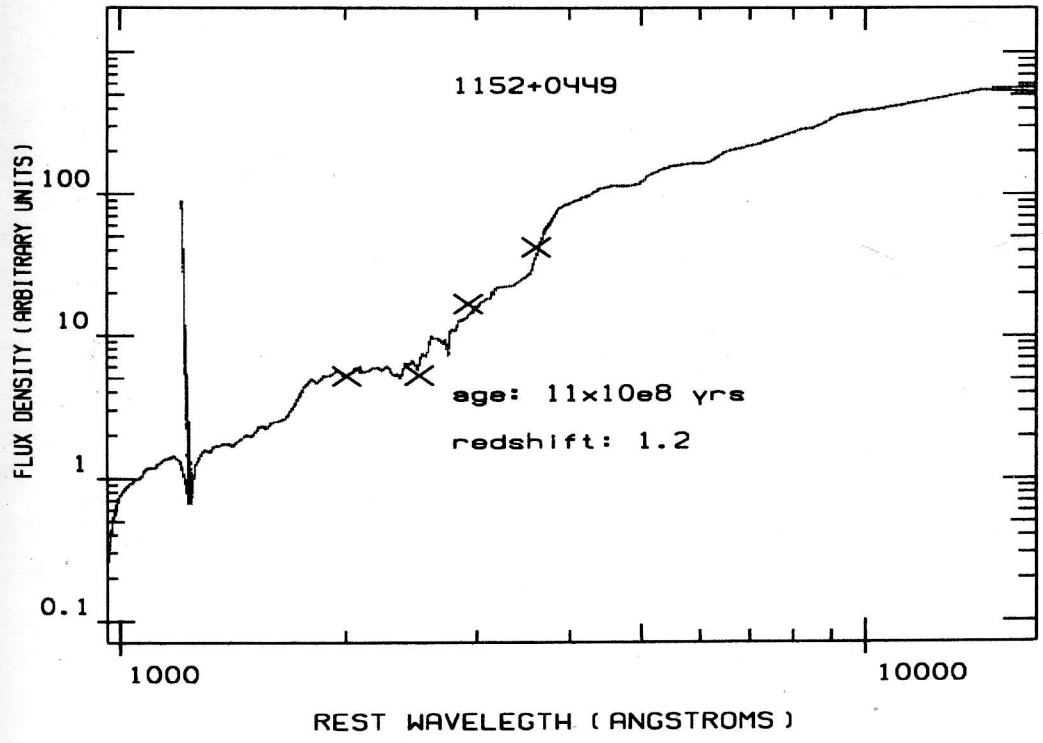
1152+0449
age: 11x10e8 yrs
redshift: 1.2
100
10
1
0.1
1000
10000
FLUX DENSITY (ARBITRARY UNITS)
REST WAVELEGTH (ANGSTROMS)

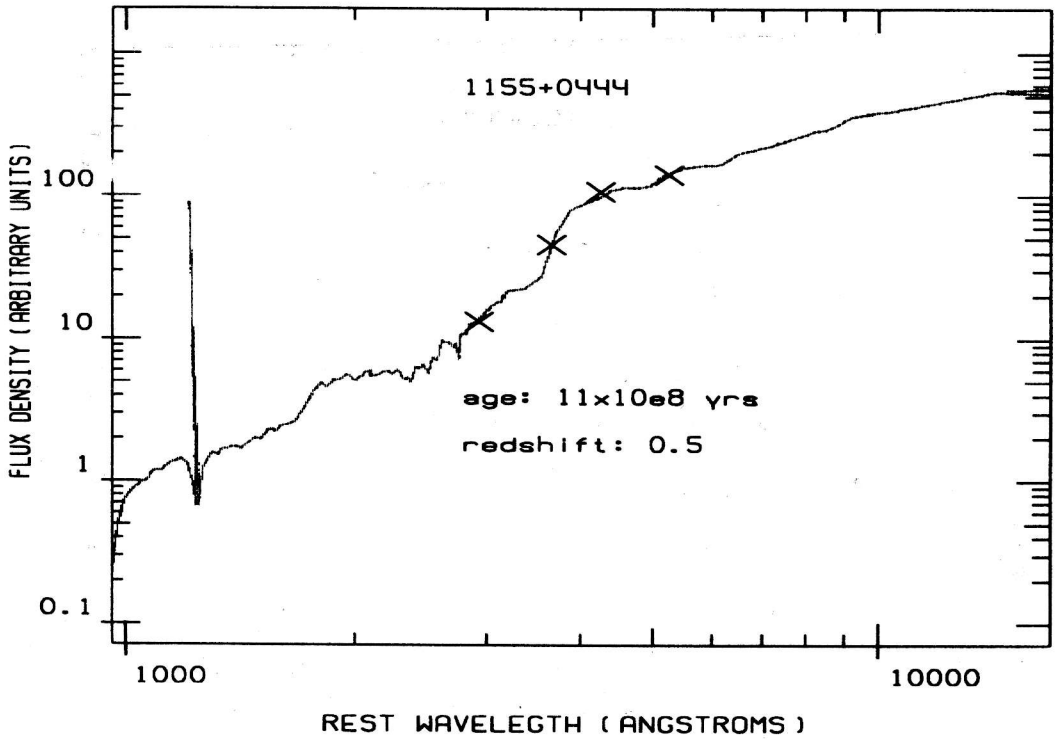
1155+0444
FLUX DENSITY (ARBITRARY UNITS)
100
10
1
0.1
age: 11x10e8 yrs
redshift: 0.5
1000
10000
REST WAVELEGTH (ANGSTROMS)

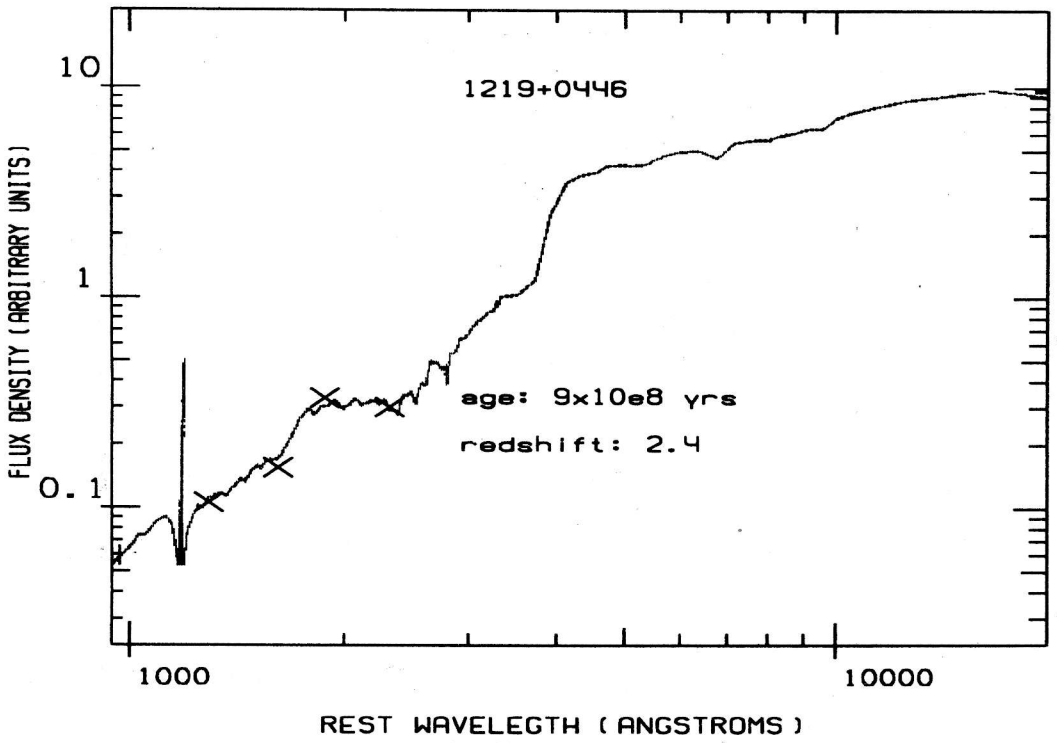
1219+0446
FLUX DENSITY (ARBITRARY UNITS)
10
1
0.1
age: 9x10e8 yrs
redshift: 2.4
1000
10000
REST WAVELEGTH (ANGSTROMS)

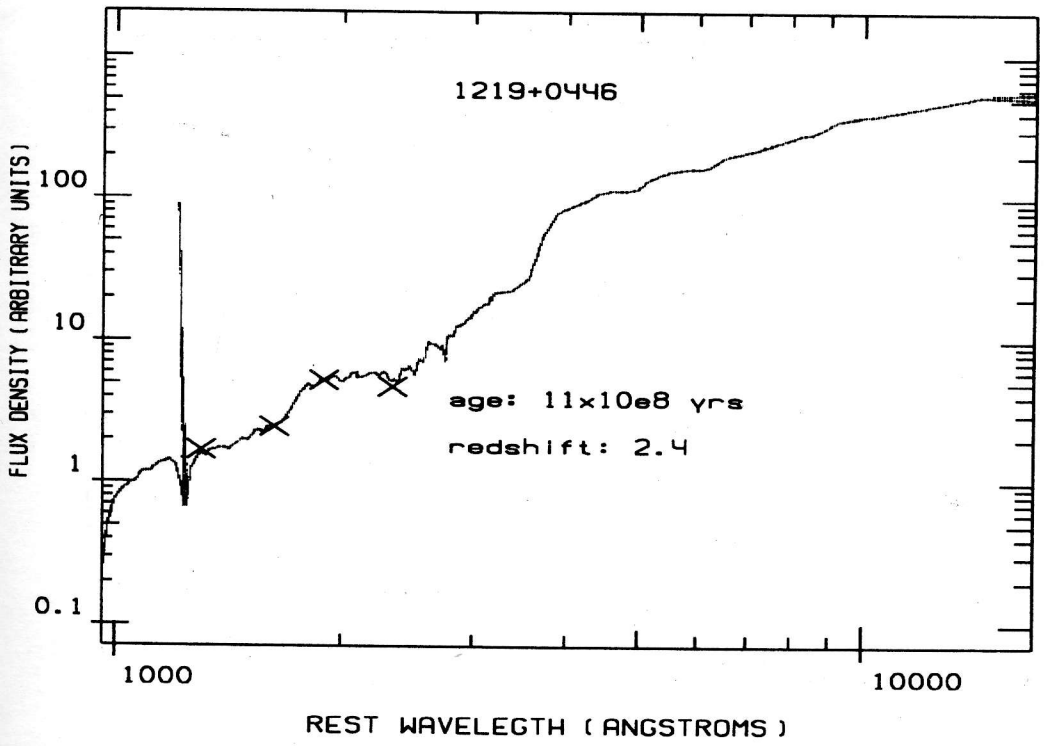
1219+0446
FLUX DENSITY (ARBITRARY UNITS)
100
10
1
0.1
age: 11x10e8 yrs
redshift: 2.4
1000
10000
REST WAVELEGTH (ANGSTROMS)

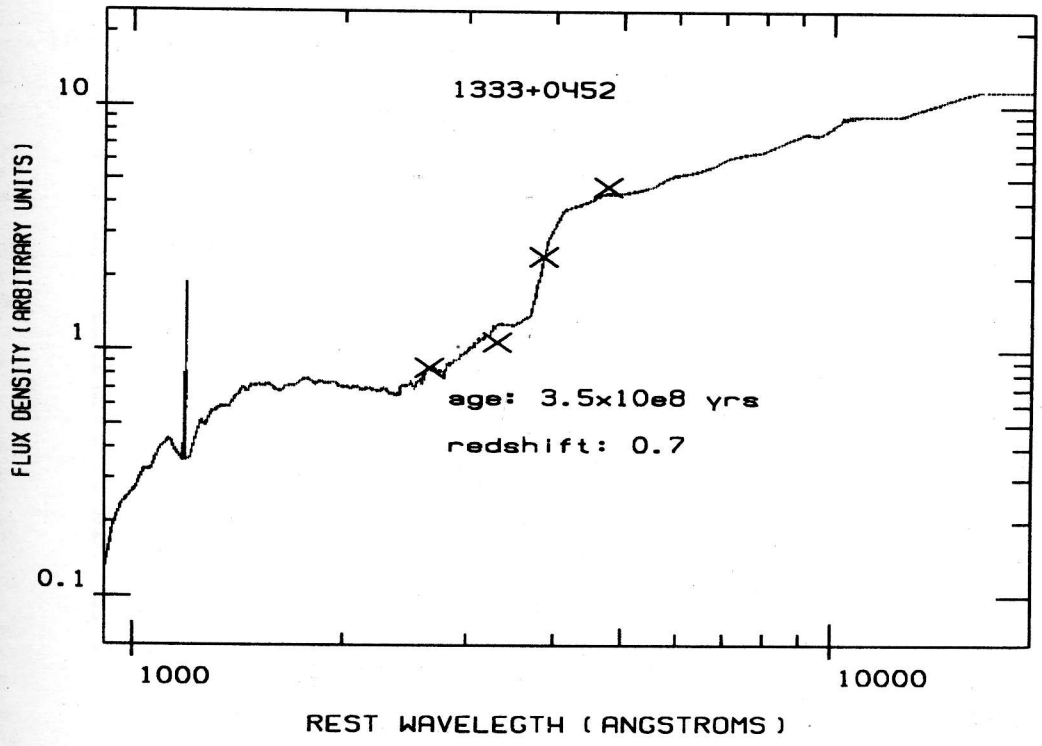
1333+0452
FLUX DENSITY (ARBITRARY UNITS)
10
1
0.1
age: 3.5x10e8 yrs
redshift: 0.7
1000
10000
REST WAVELEGTH (ANGSTROMS)

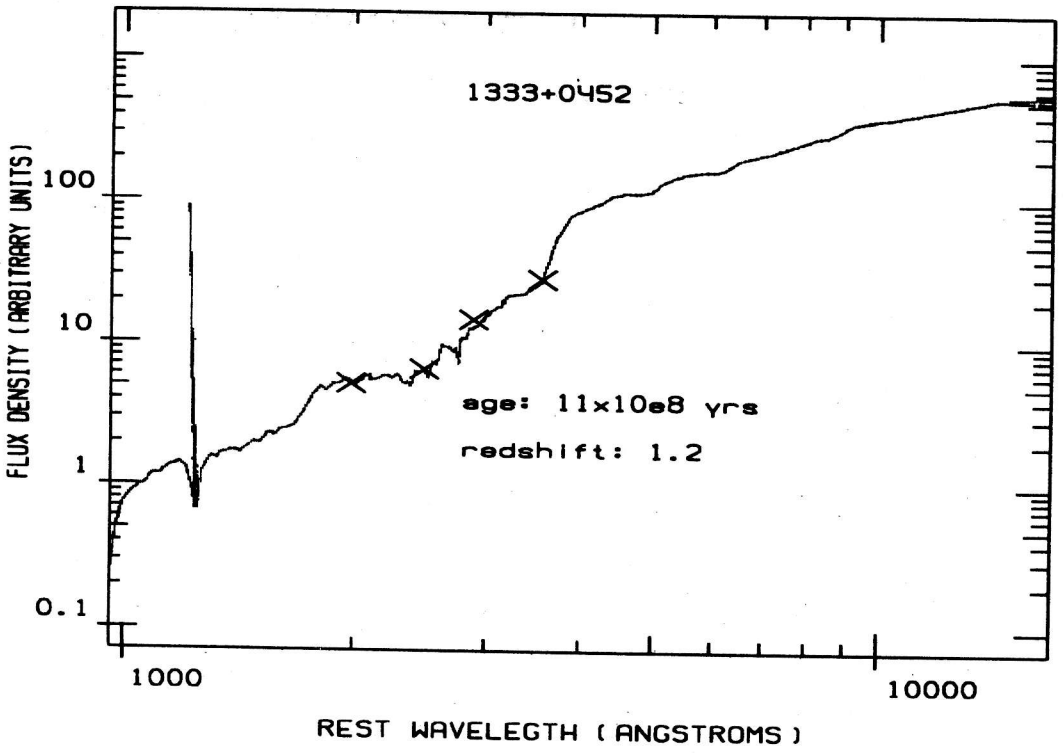
1333+0452
FLUX DENSITY (ARBITRARY UNITS)
100
10
1
0.1
age: 11x10e8 yrs
redshift: 1.2
1000
10000
REST WAVELEGTH (ANGSTROMS)

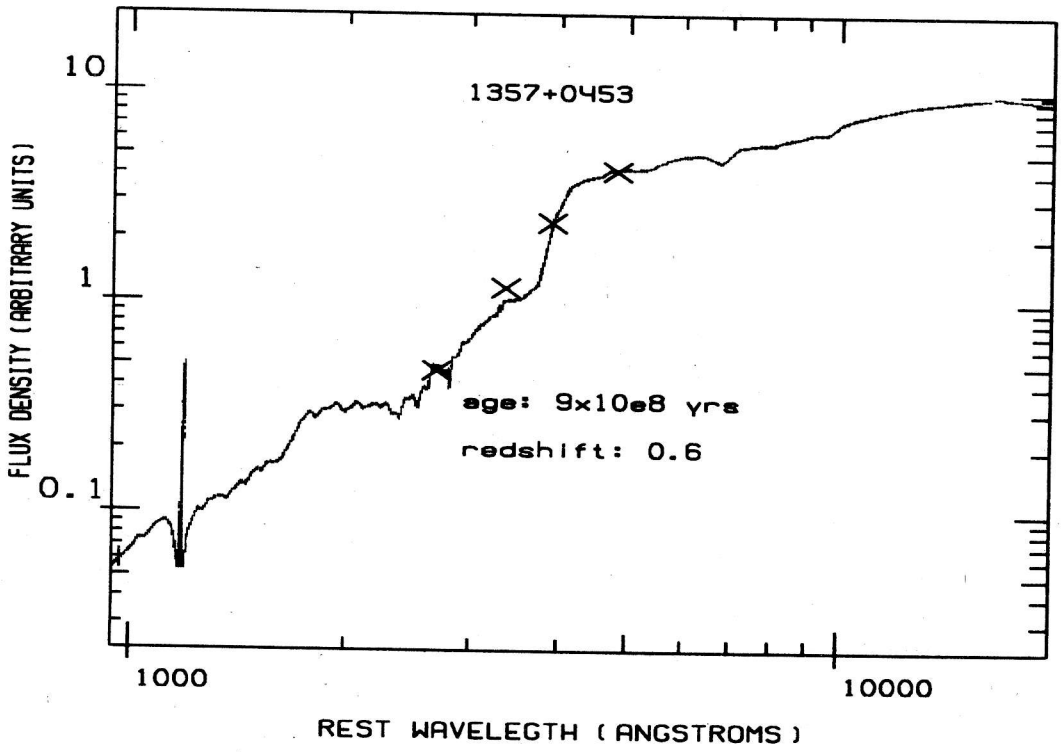
1357+0453
FLUX DENSITY (ARBITRARY UNITS)
10
1
0.1
age: 9x10e8 yrs
redshift: 0.6
1000
10000
REST WAVELEGTH (ANGSTROMS)

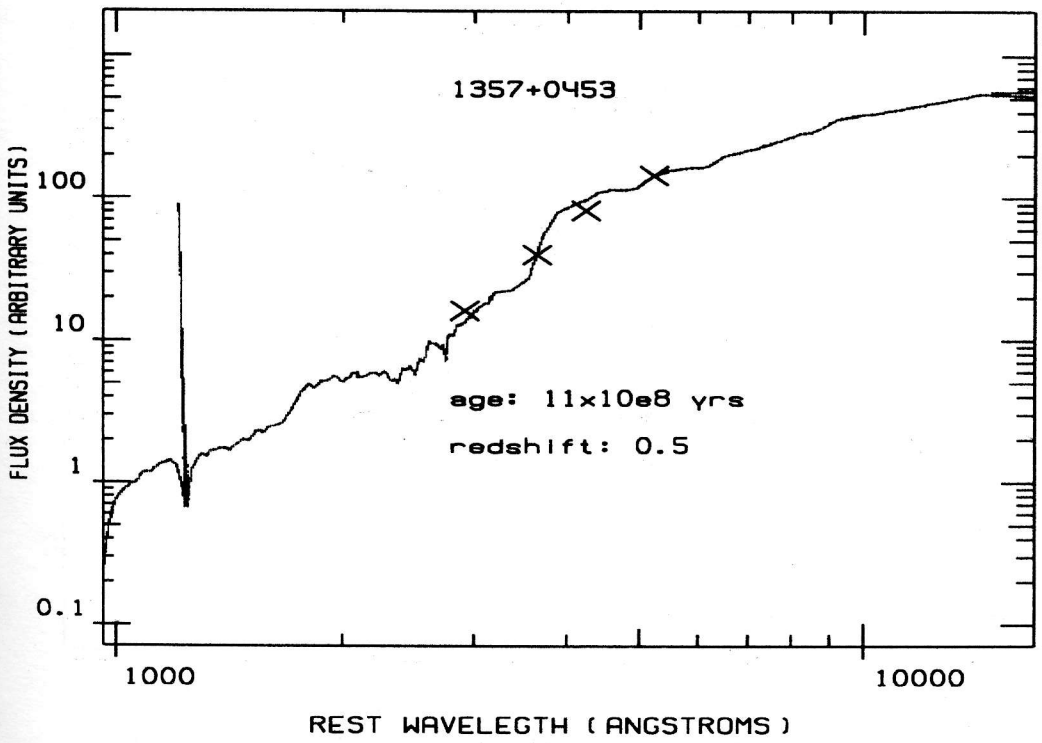
1357+0453
FLUX DENSITY (ARBITRARY UNITS)
100
10
1
0.1
age: 11x10e8 yrs
redshift: 0.5
1000
10000
REST WAVELEGTH (ANGSTROMS)

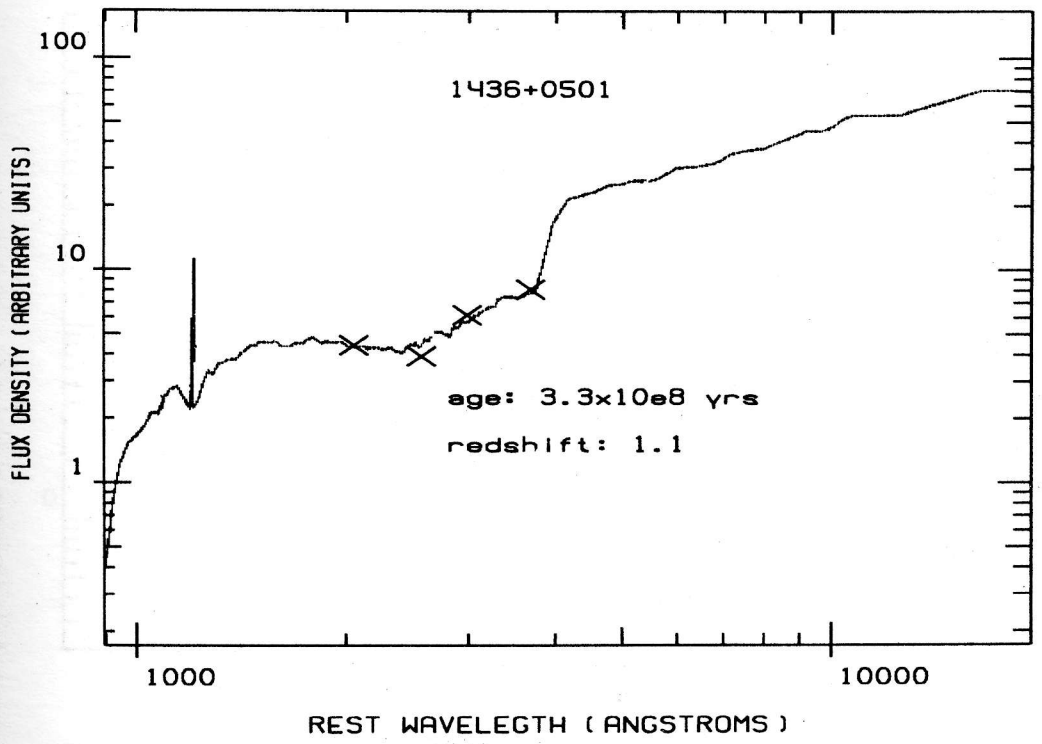
1436+0501
FLUX DENSITY (ARBITRARY UNITS)
100
10
1
age: 3.3x10e8 yrs
redshift: 1.1
1000
10000
REST WAVELEGTH (ANGSTROMS)

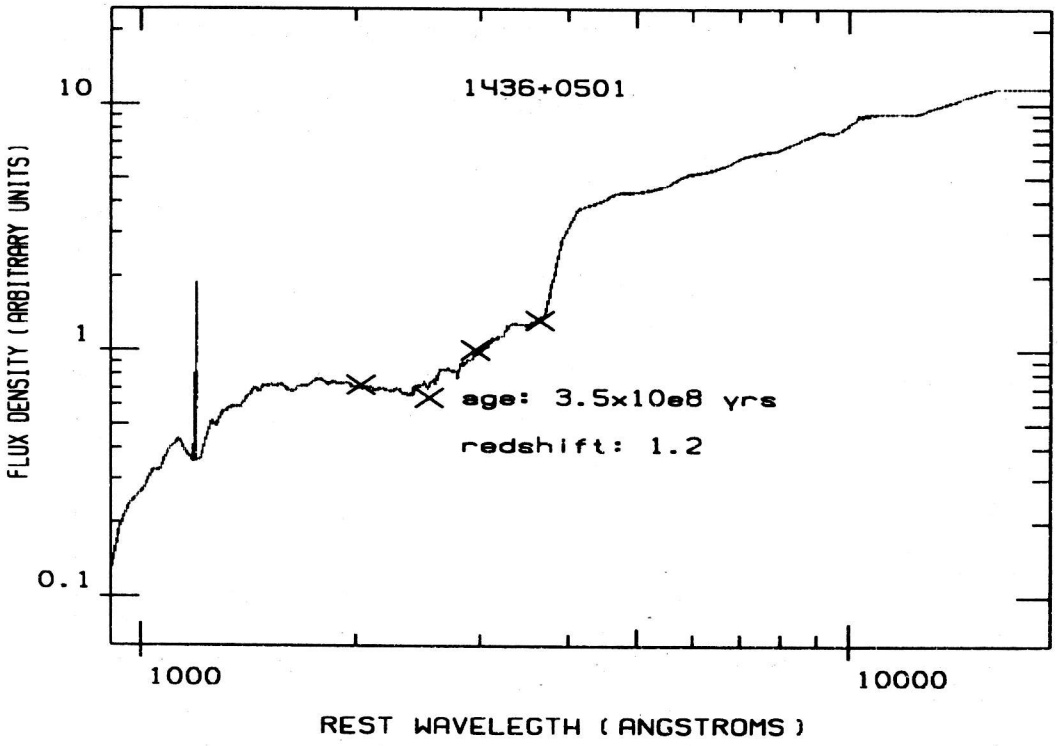
1436+0501
age: 3.5x10e8 yrs
redshift: 1.2
10
1
0.1
1000
10000
FLUX DENSITY (ARBITRARY UNITS)
REST WAVELEGTH (ANGSTROMS)

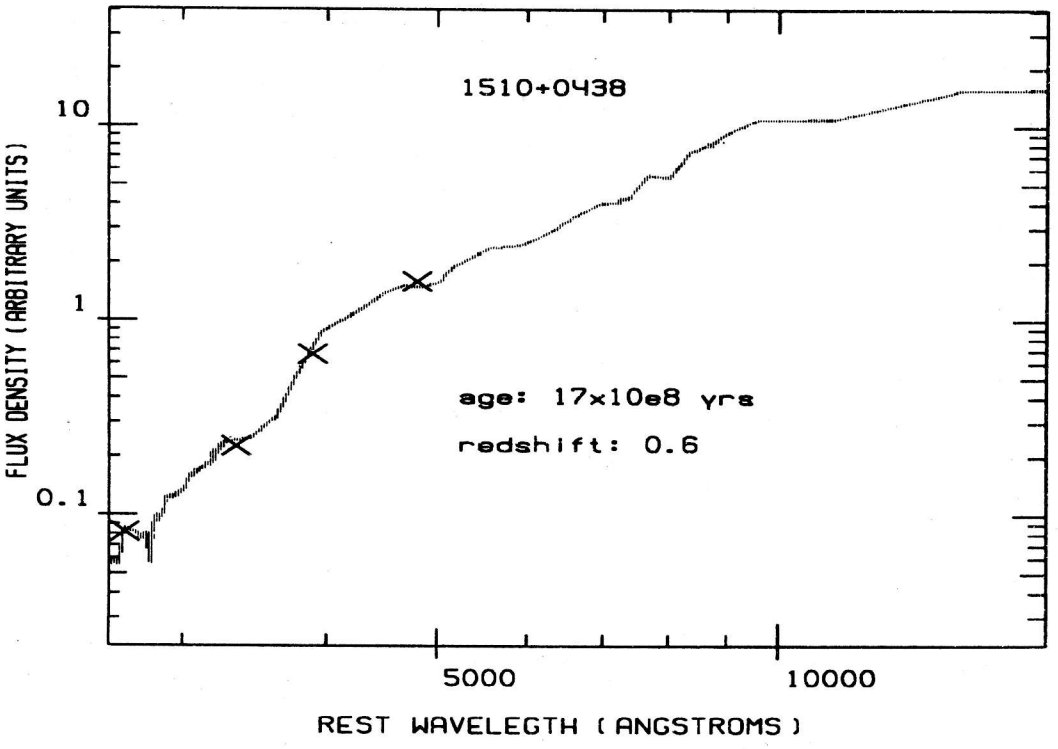
1510+0438
age: 17x10e8 yrs
redshift: 0.6
10
1
0.1
5000
10000
FLUX DENSITY (ARBITRARY UNITS)
REST WAVELEGTH (ANGSTROMS)

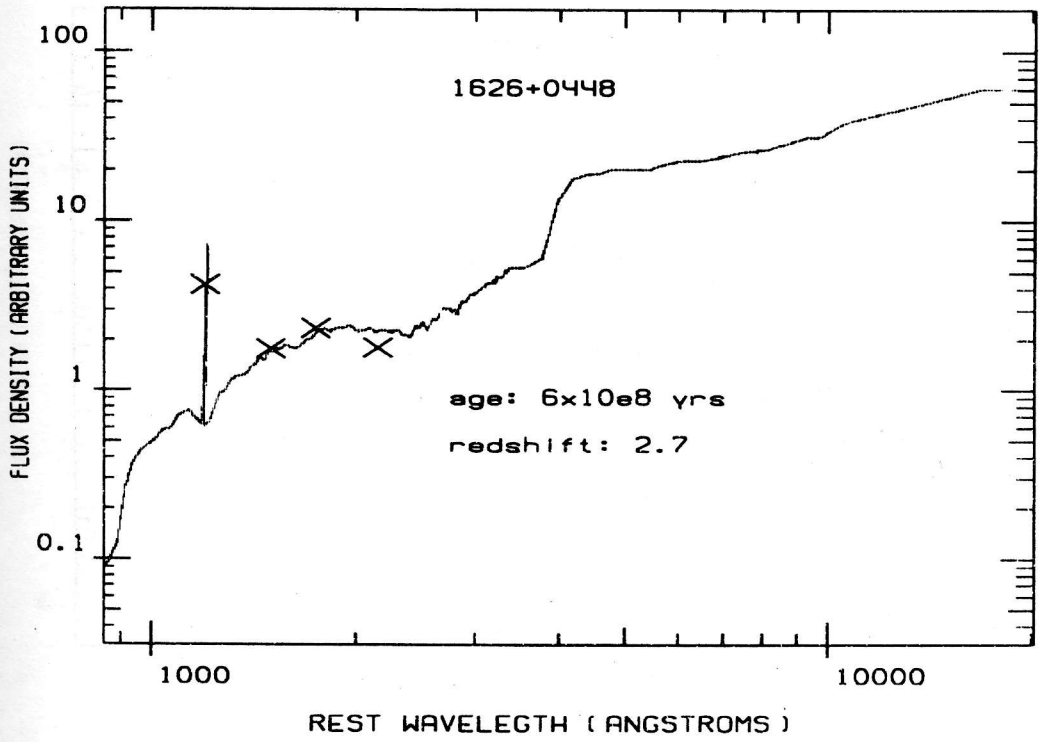
100
10
1
0.1
FLUX DENSITY (ARBITRARY UNITS)
1626+0448
age: 6x10e8 yrs
redshift: 2.7
1000
10000
REST WAVELEGTH (ANGSTROMS)

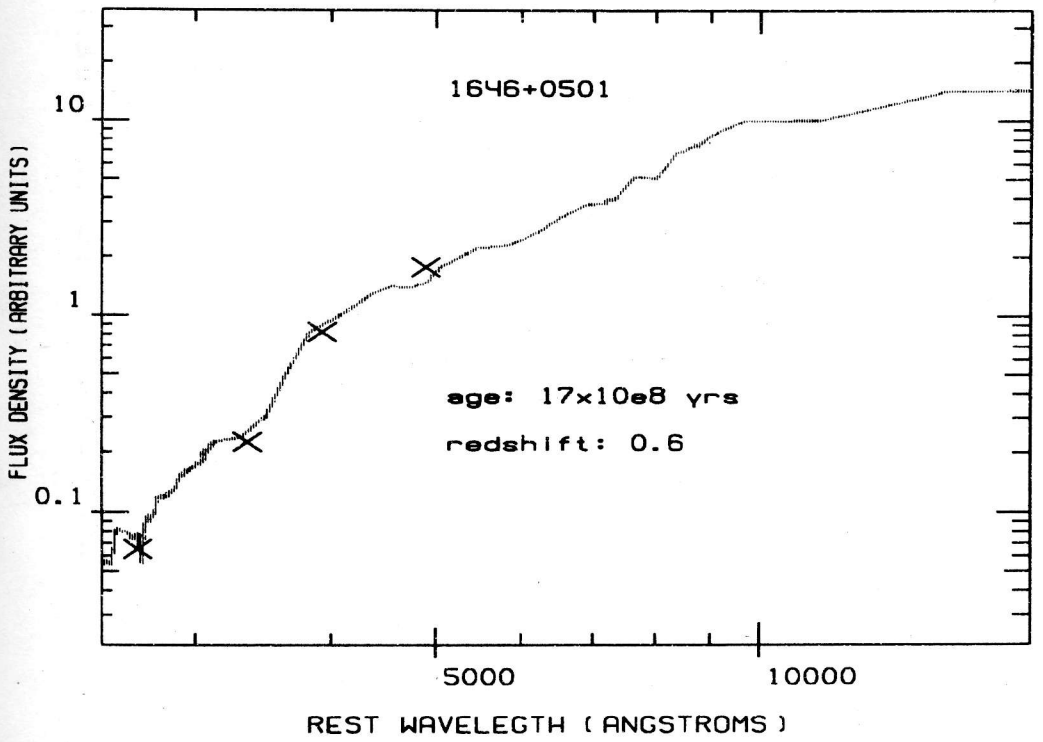
10
1
0.1
FLUX DENSITY (ARBITRARY UNITS)
1646+0501
age: 17x10e8 yrs
redshift: 0.6
5000
10000
REST WAVELEGTH (ANGSTROMS)

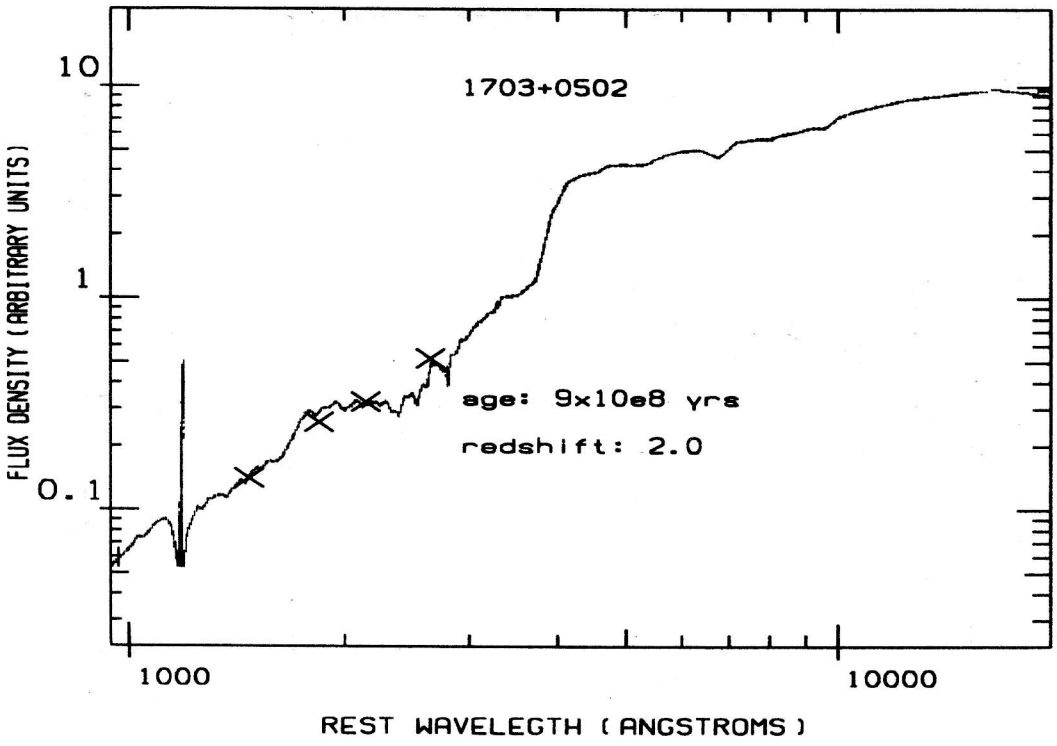
10
1
0.1
FLUX DENSITY (ARBITRARY UNITS)
1703+0502
age: 9x10e8 yrs
redshift: 2.0
1000
10000
REST WAVELEGTH (ANGSTROMS)

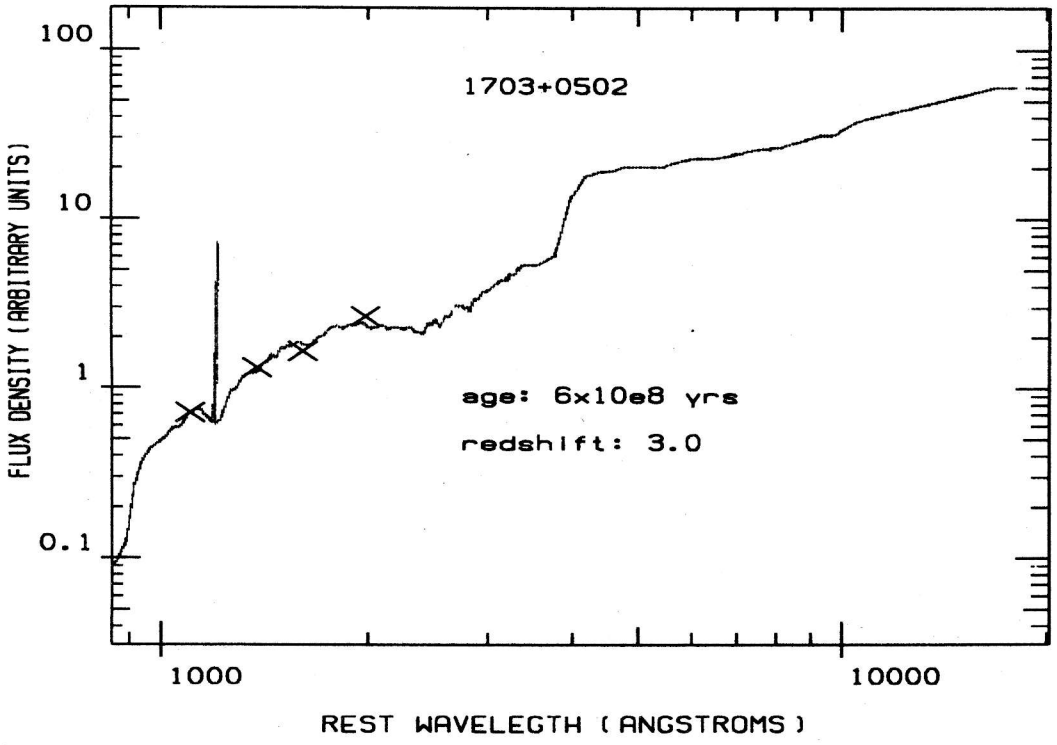
100
10
1
0.1
FLUX DENSITY (ARBITRARY UNITS)
1703+0502
age: 6x10e8 yrs
redshift: 3.0
1000
10000
REST WAVELEGTH (ANGSTROMS)

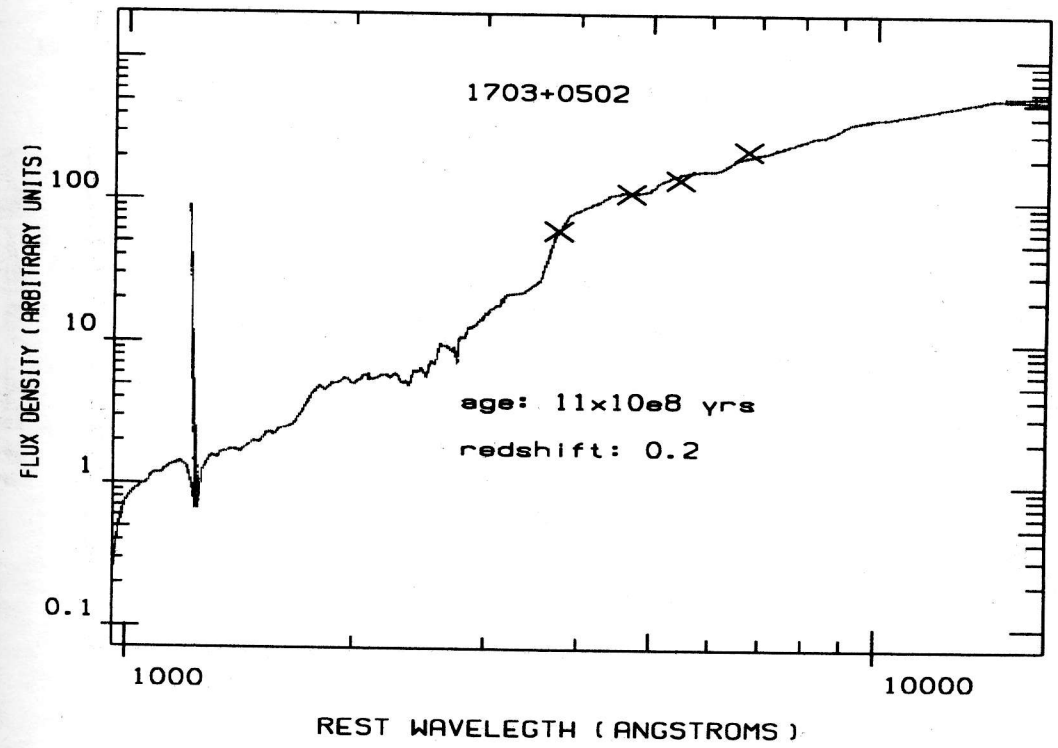
1703+0502
FLUX DENSITY (ARBITRARY UNITS)
100
10
1
0.1
age: 11x10e8 yrs
redshift: 0.2
1000
10000
REST WAVELEGTH (ANGSTROMS)

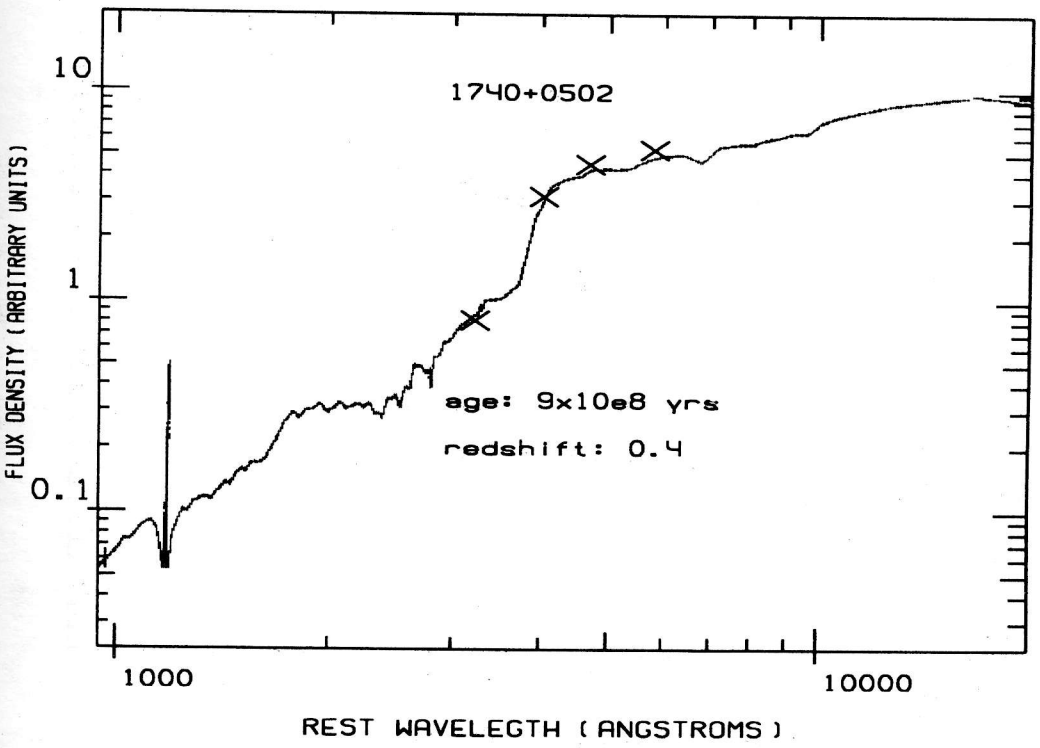
1740+0502
FLUX DENSITY (ARBITRARY UNITS)
10
1
0.1
age: 9x10e8 yrs
redshift: 0.4
1000
10000
REST WAVELEGTH (ANGSTROMS)

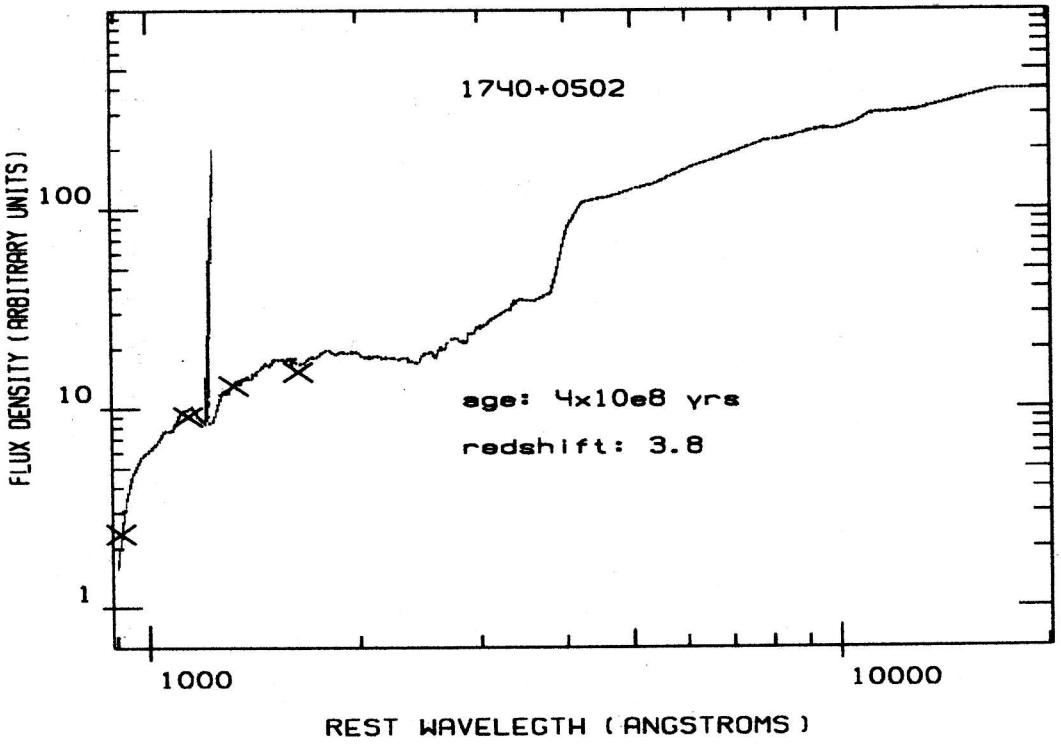
1740+0502
age: 4x10e8 yrs
redshift: 3.8
FLUX DENSITY (ARBITRARY UNITS)
100
10
1
1000
10000
REST WAVELEGTH (ANGSTROMS)

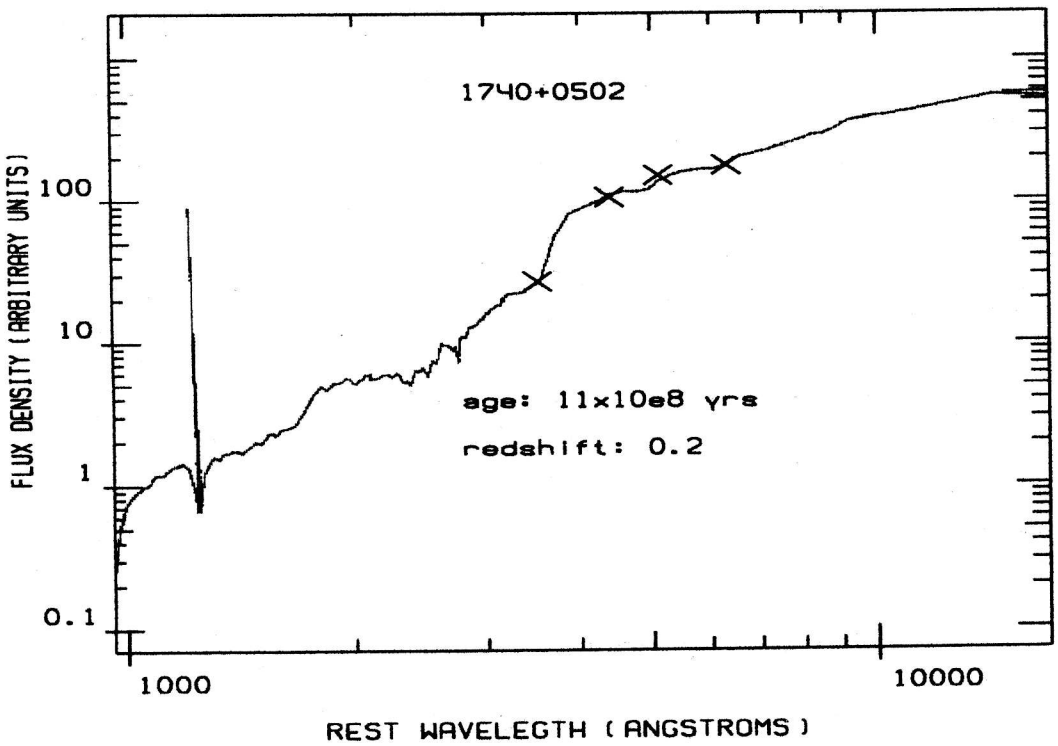
1740+0502
age: 11x10e8 yrs
redshift: 0.2
FLUX DENSITY (ARBITRARY UNITS)
100
10
1
0.1
1000
10000
REST WAVELEGTH (ANGSTROMS)

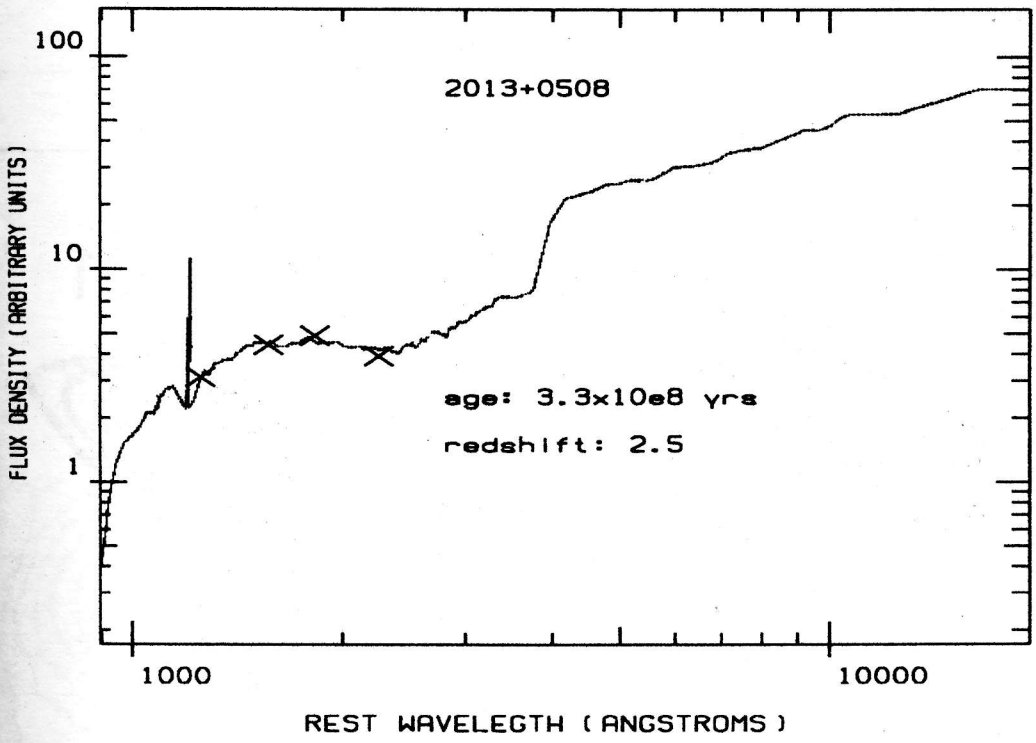
100
10
1
FLUX DENSITY (ARBITRARY UNITS)
2013+0508
age: 3.3x10e8 yrs
redshift: 2.5
1000
10000
REST WAVELEGTH (ANGSTROMS)

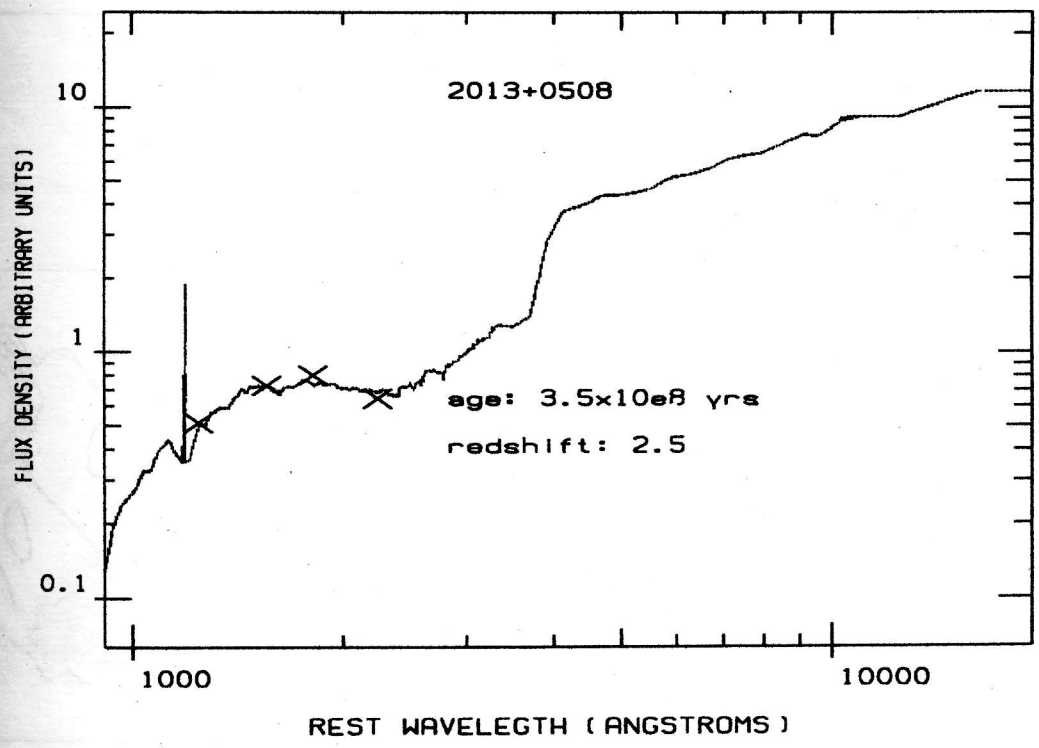
10
1
0.1
FLUX DENSITY (ARBITRARY UNITS)
2013+0508
age: 3.5x10e8 yrs
redshift: 2.5
1000
10000
REST WAVELEGTH (ANGSTROMS)

Figure 8: *VLA maps of RC sources*

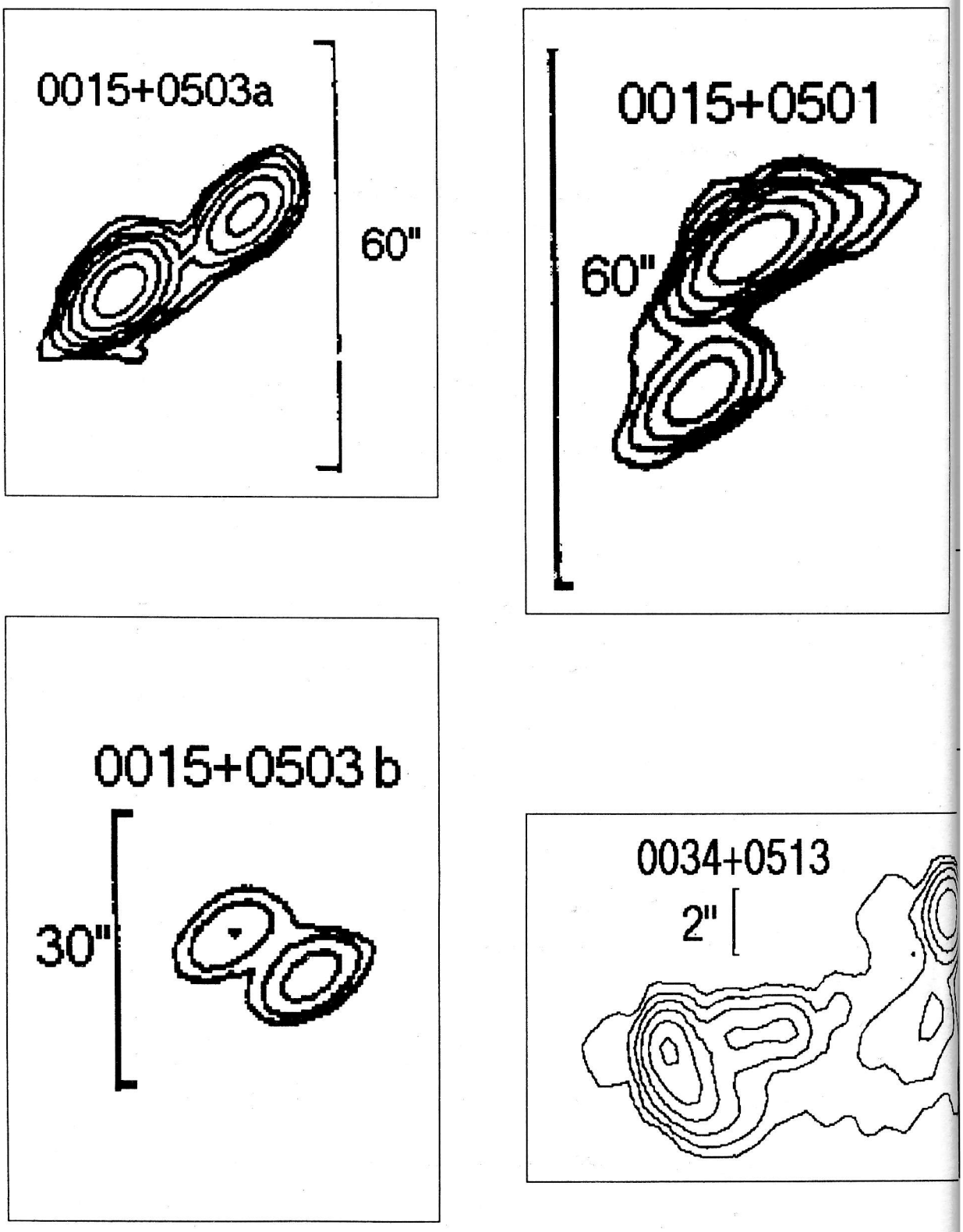

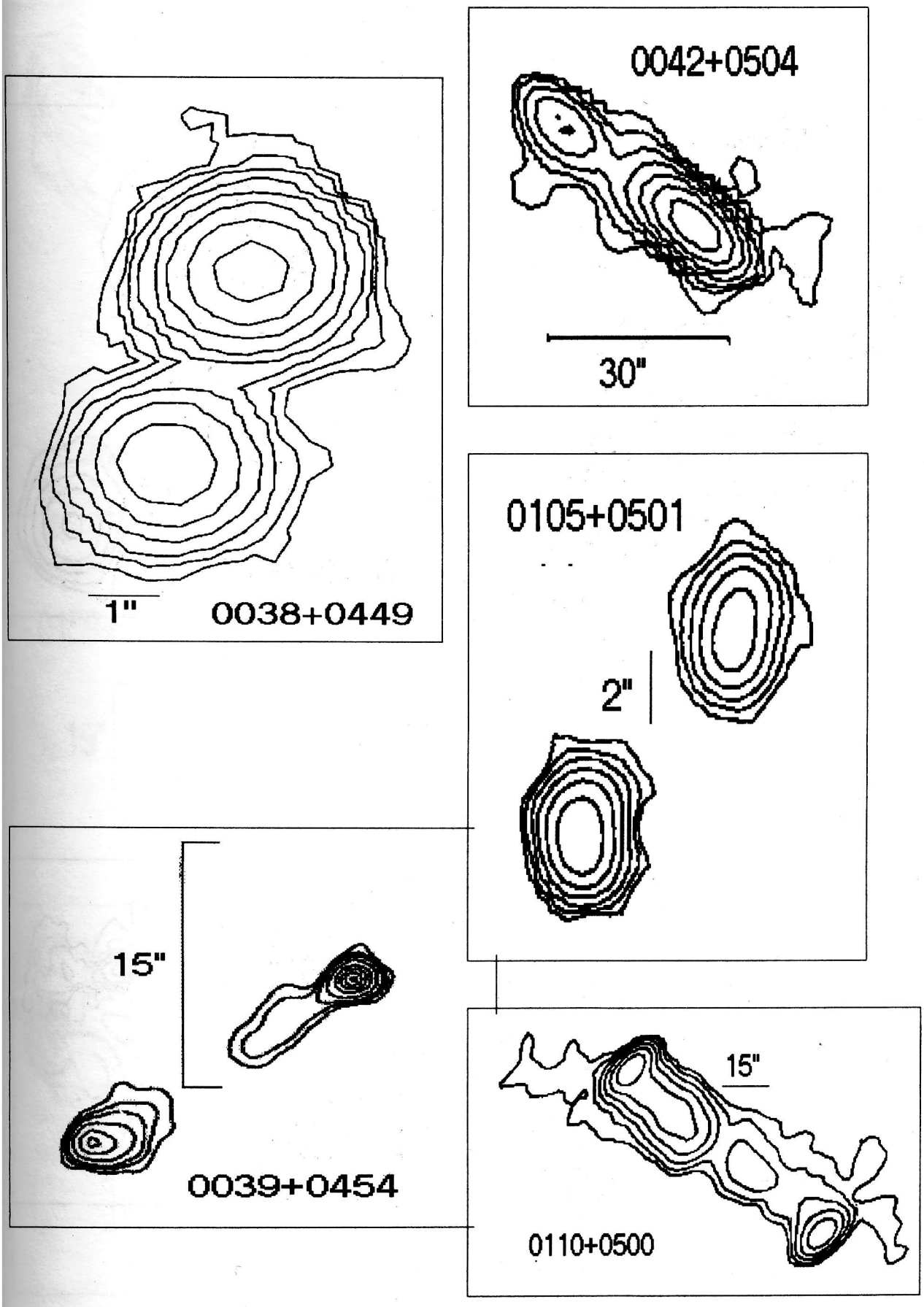
0042+0504
30"
1"
0038+0449
0105+0501
2"
15"
0039+0454
15"
0110+0500

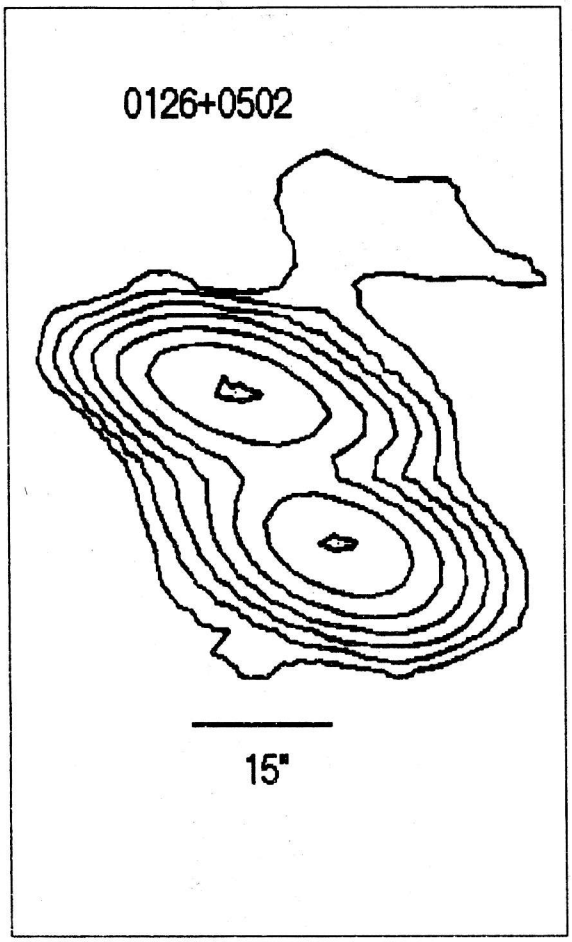
0126+0502
15"

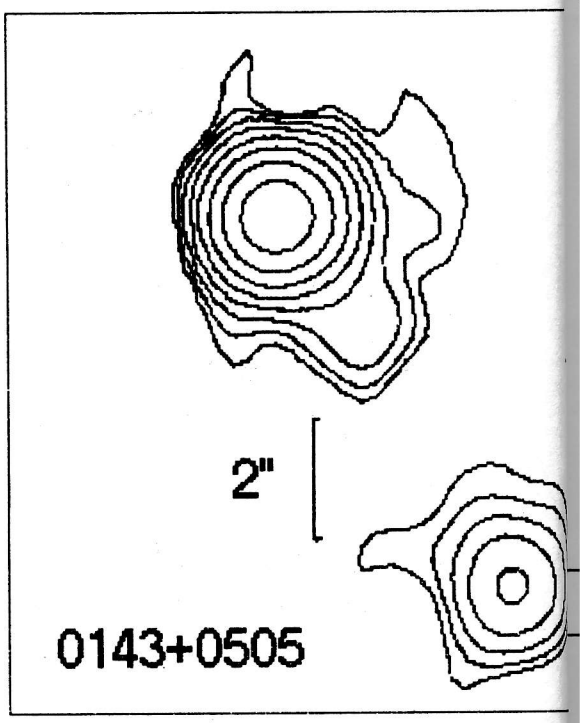
2"
0143+0505

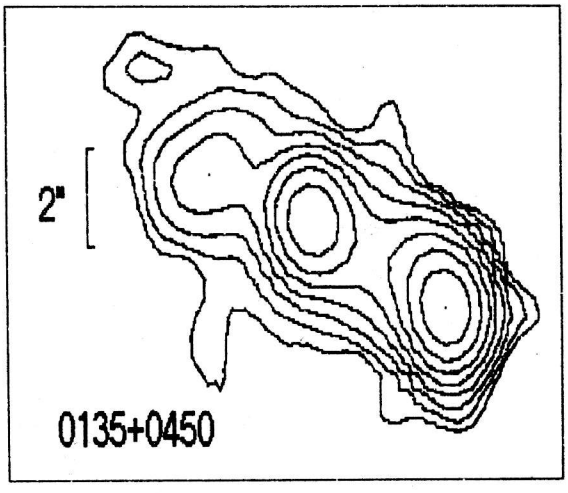
2"
0135+0450

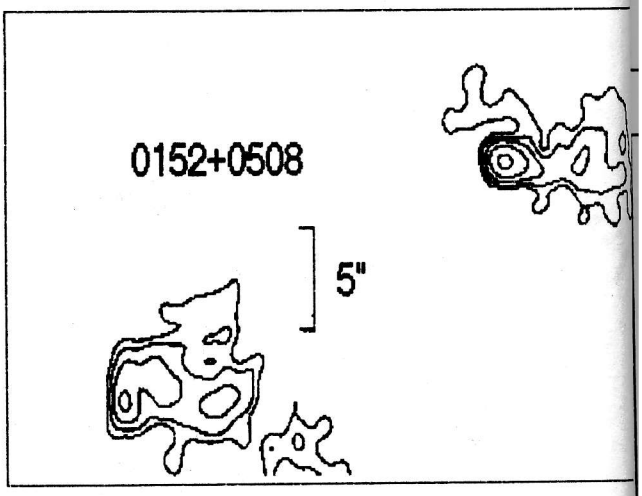
0152+0508
5"

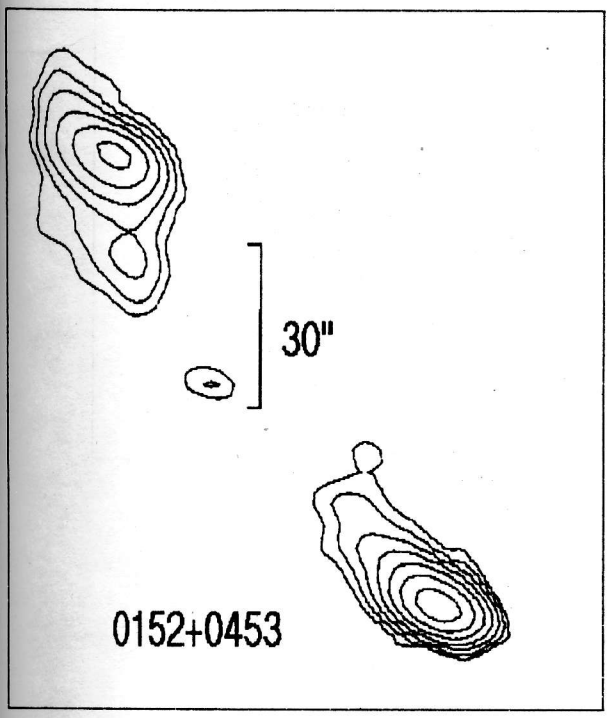
30"
0152+0453

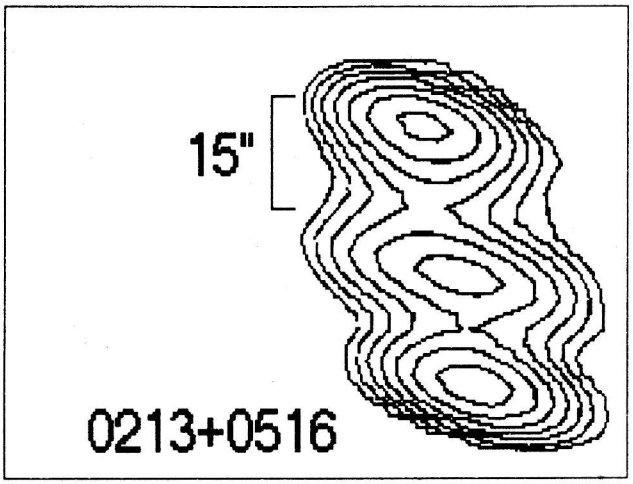
15"
0213+0516

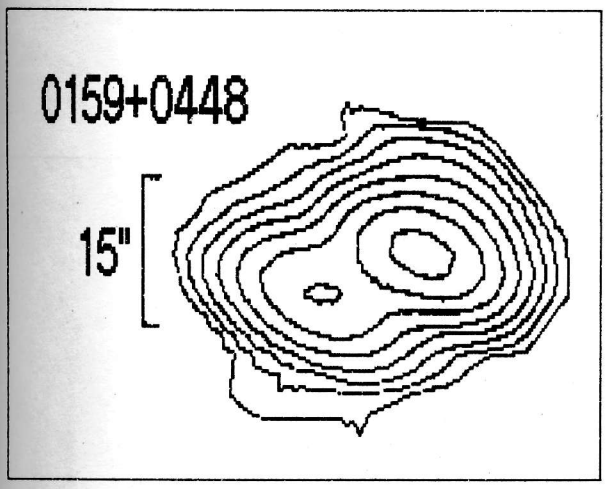
0159+0448
15"

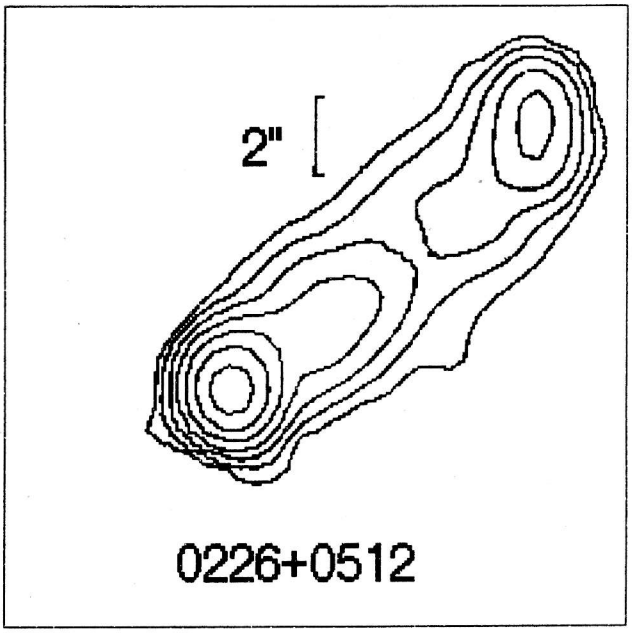
2"
0226+0512

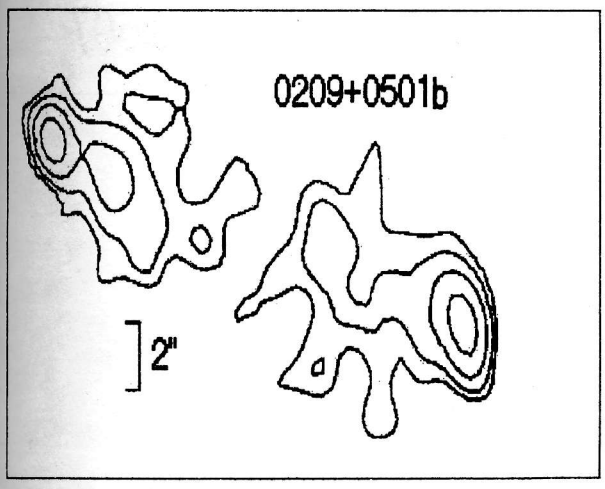
0209+0501b
2"

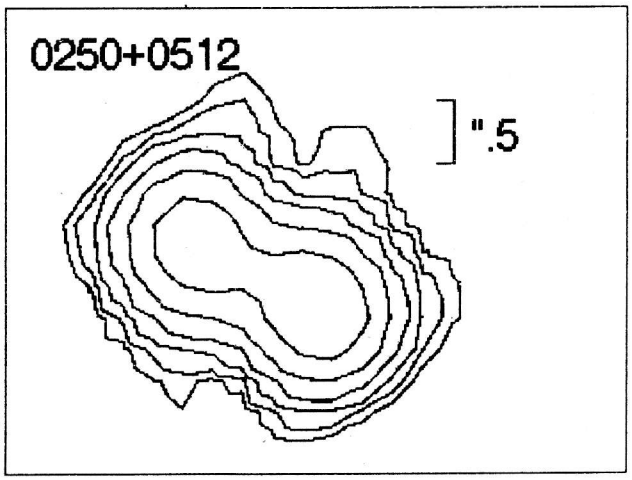
0250+0512
".5

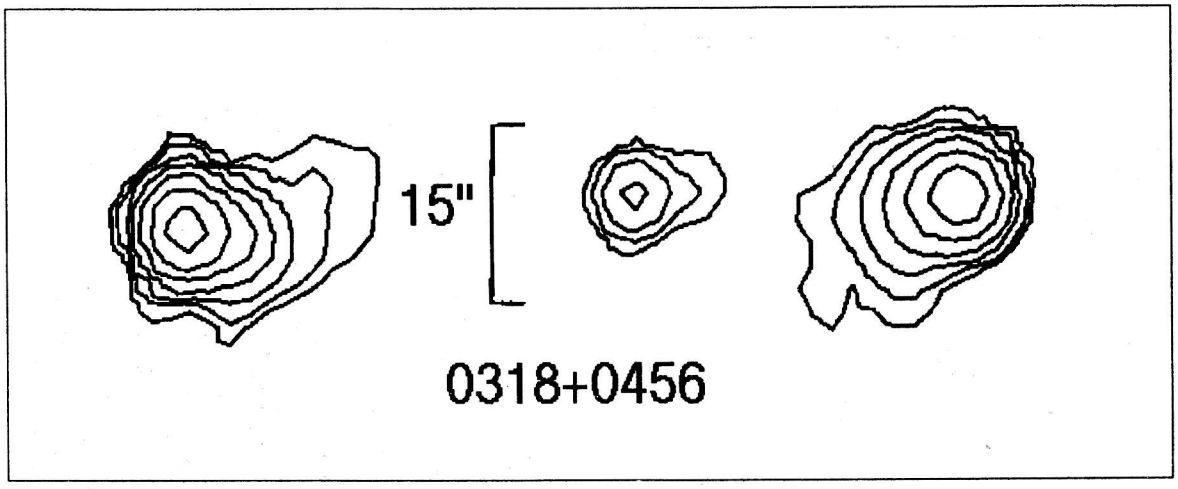
15"
0318+0456

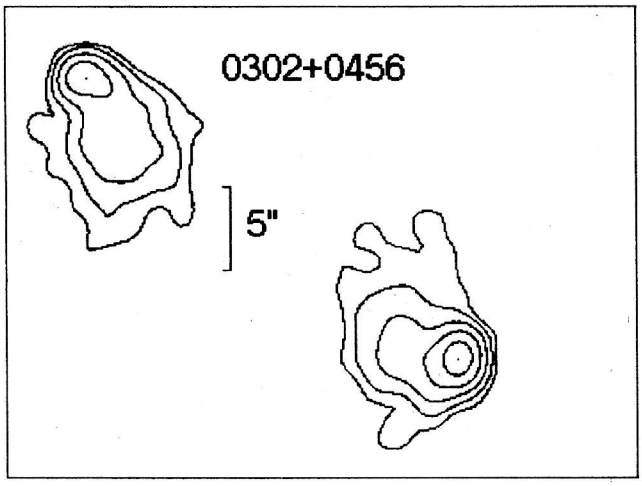
0302+0456
5"

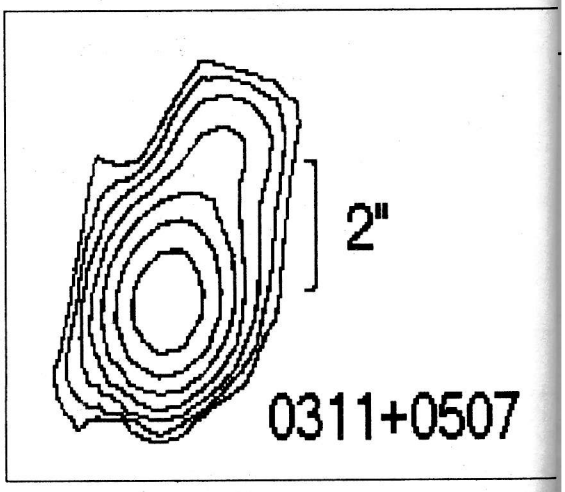
2"
0311+0507

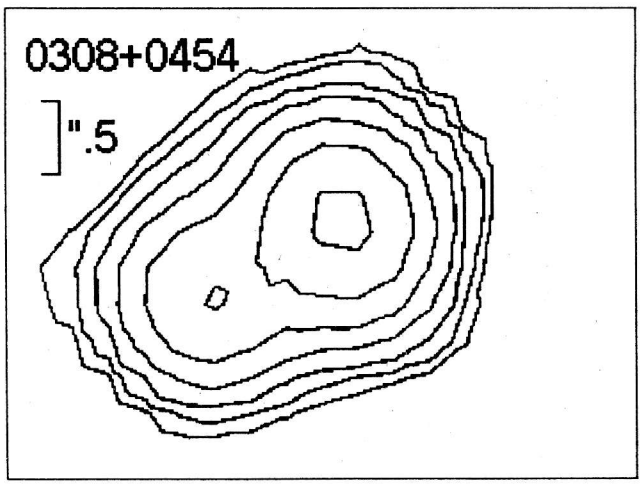
0308+0454
".5

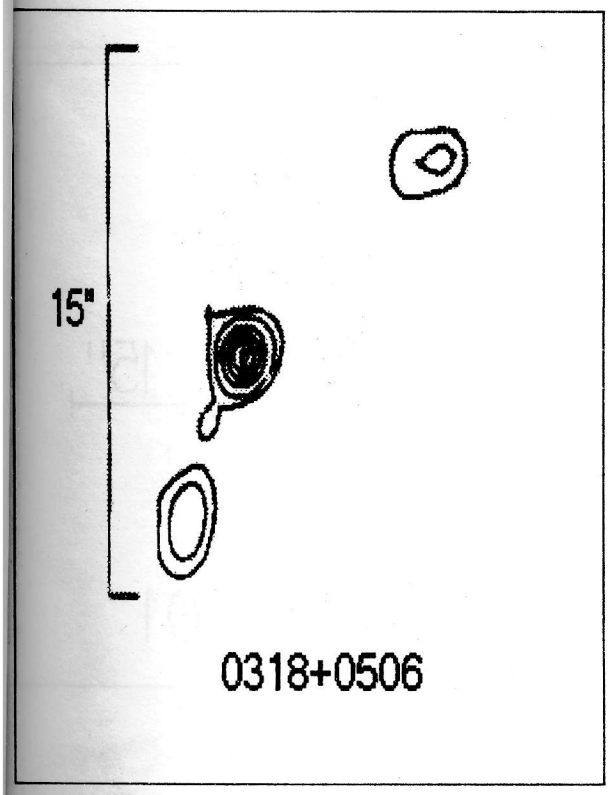
15"
0318+0506

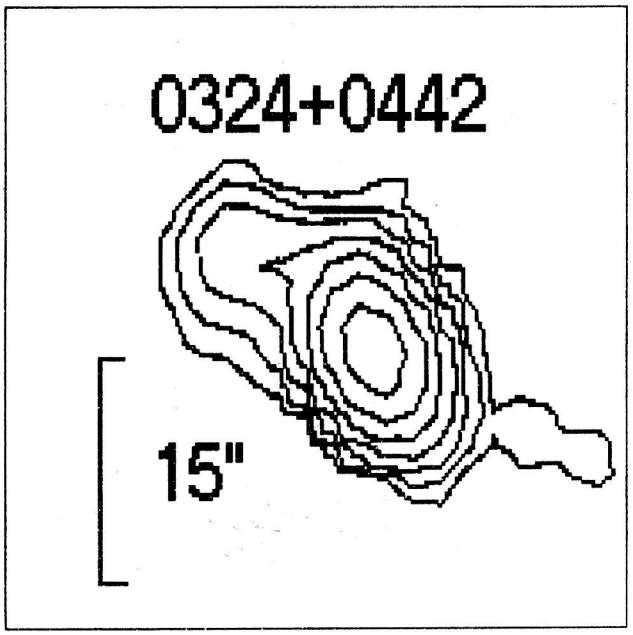
0324+0442
15"

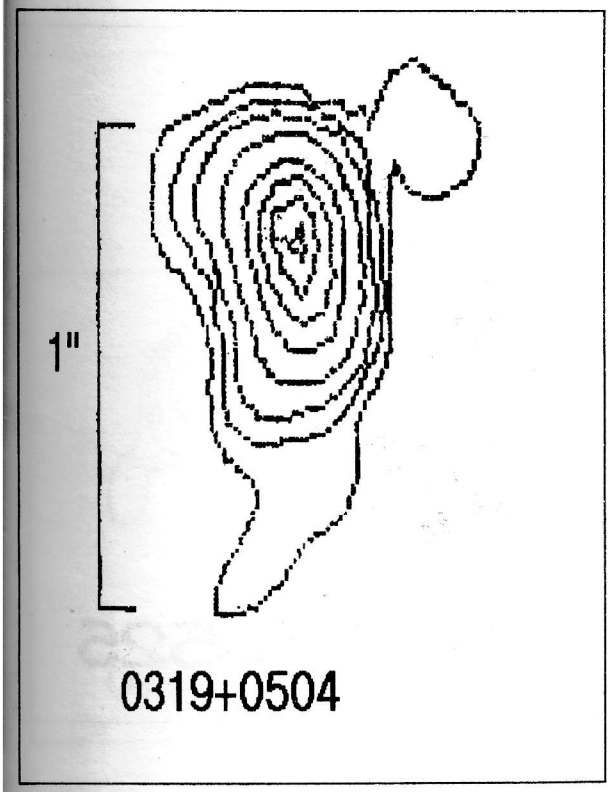
1"
0319+0504

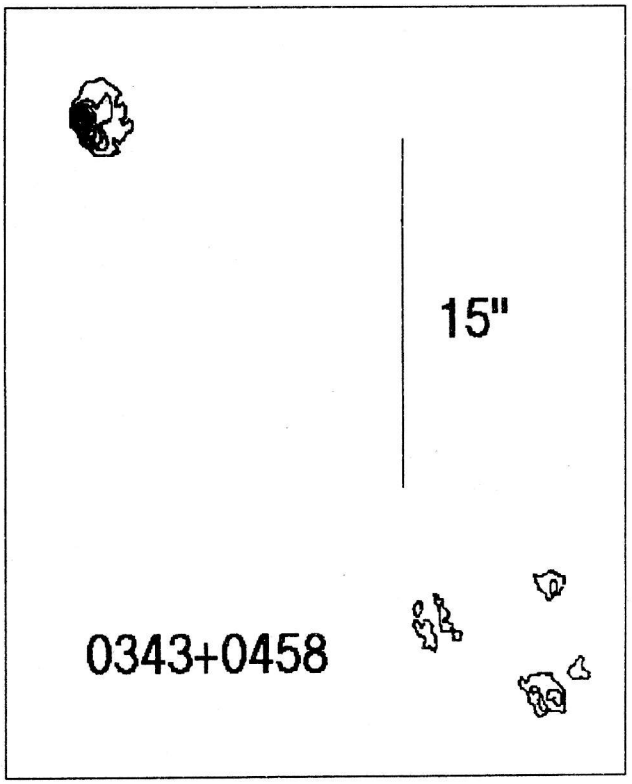
15"
0343+0458

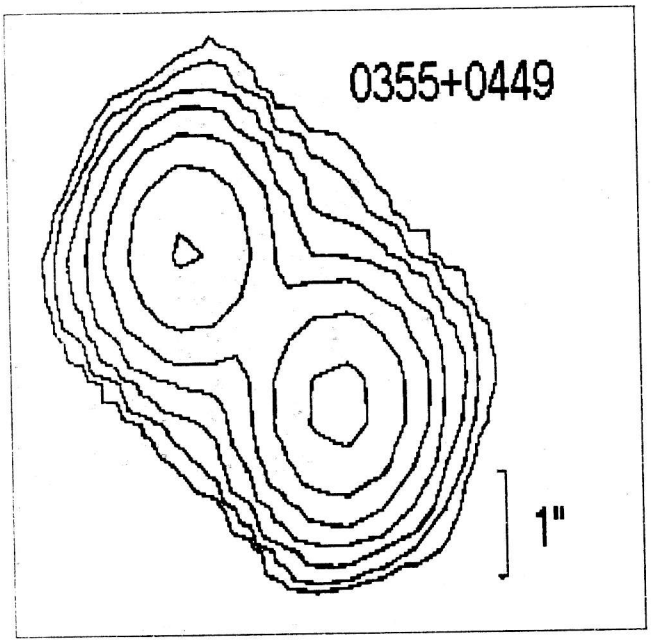
0355+0449
1"

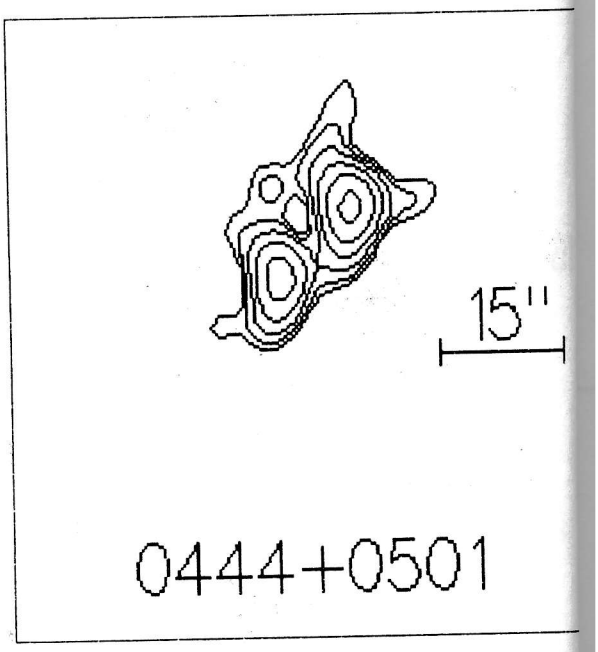
15"
0444+0501

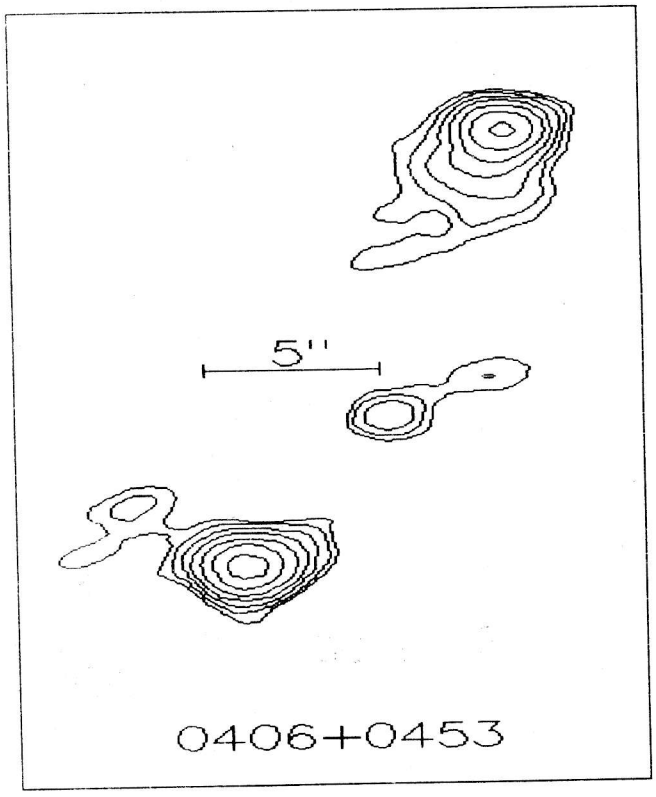
5"
0406+0453


5"
0446+0525

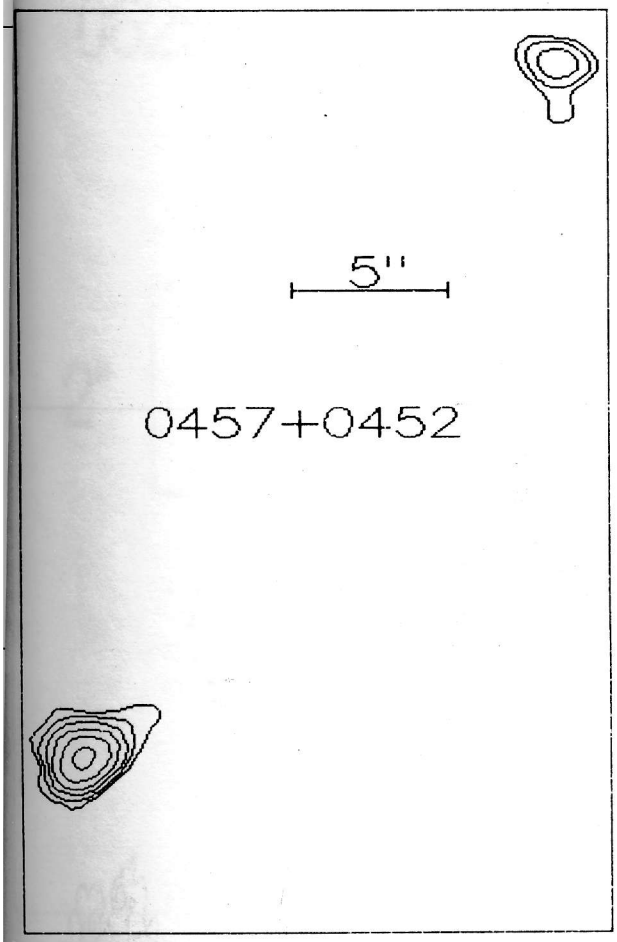
5''
0457+0452

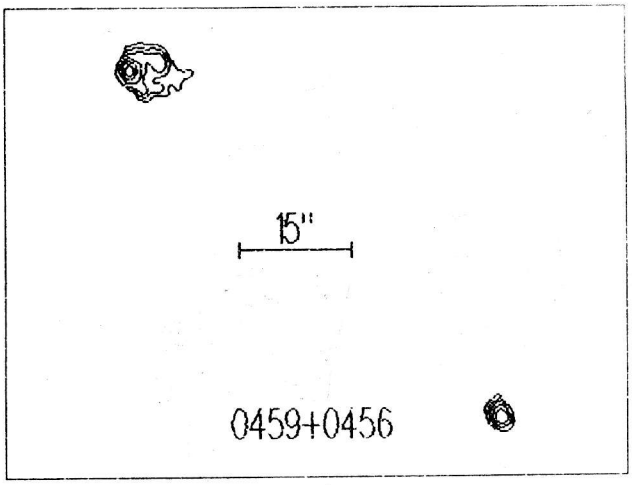
15''
0459+0456

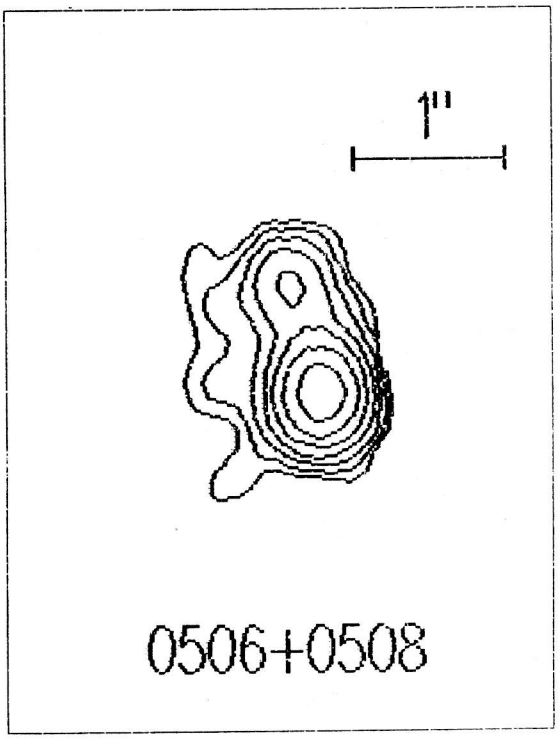
1''
0506+0508

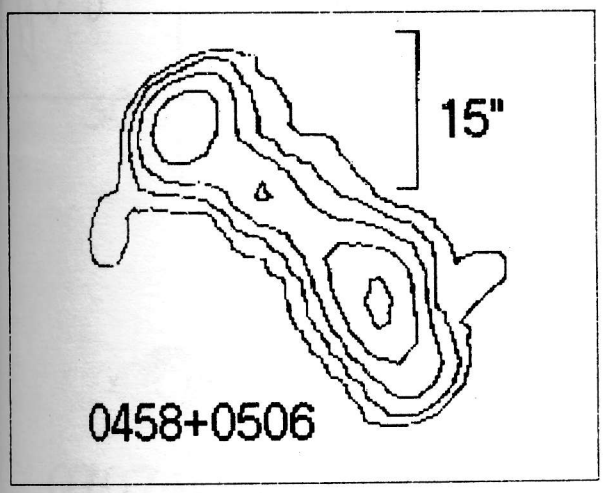
15"
0458+0506

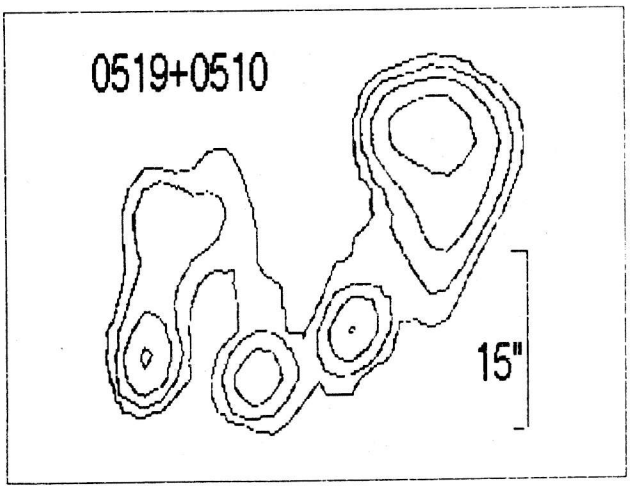
0519+0510
15"

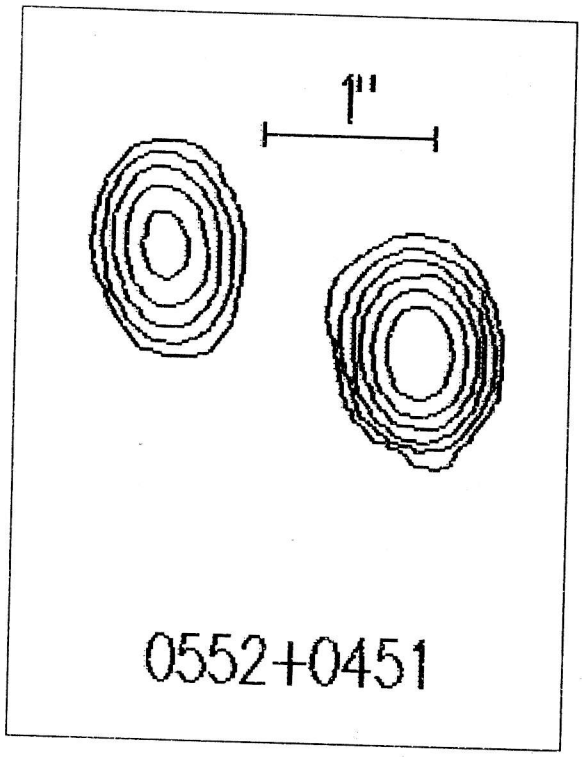
1"
0552+0451

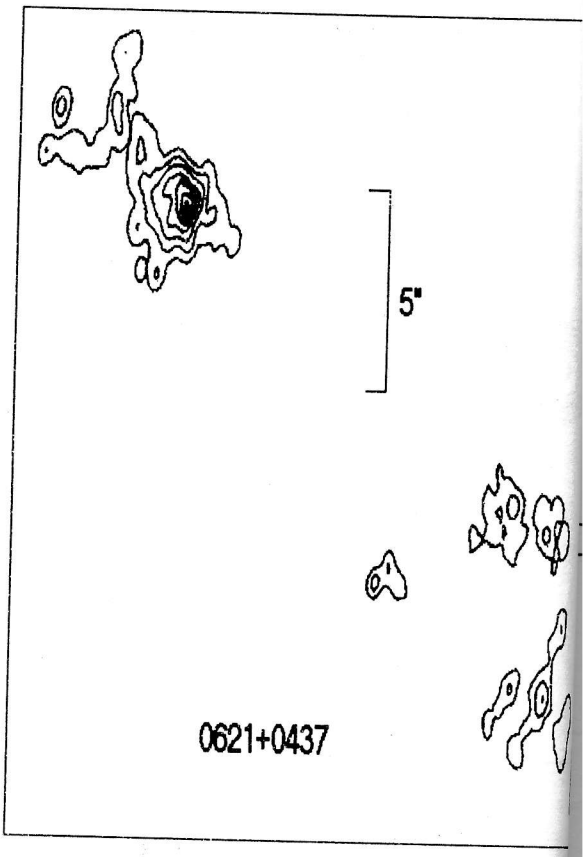
5"
0621+0437

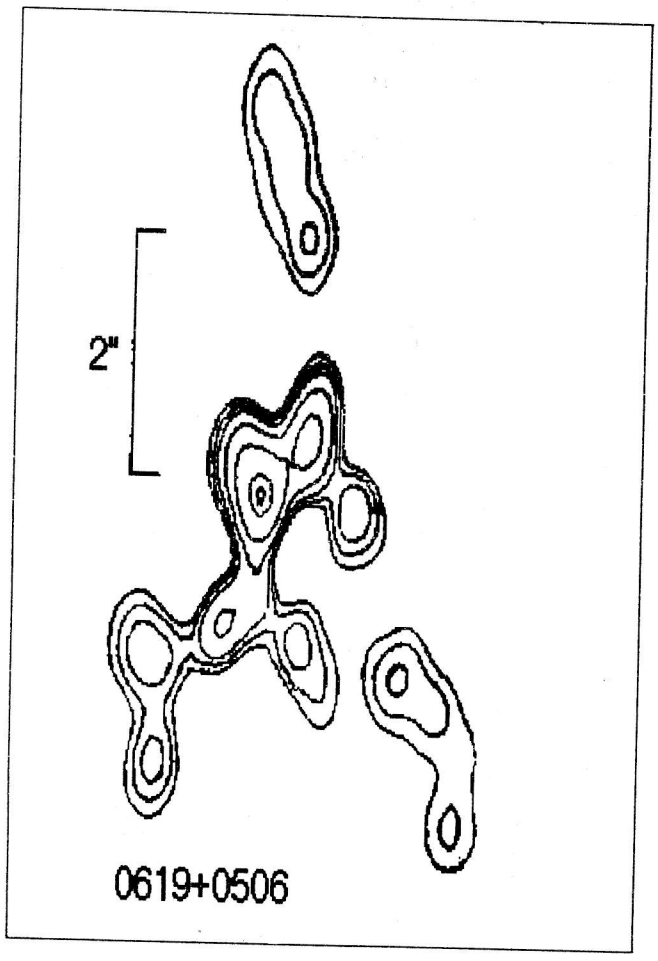
2"
0619+0506

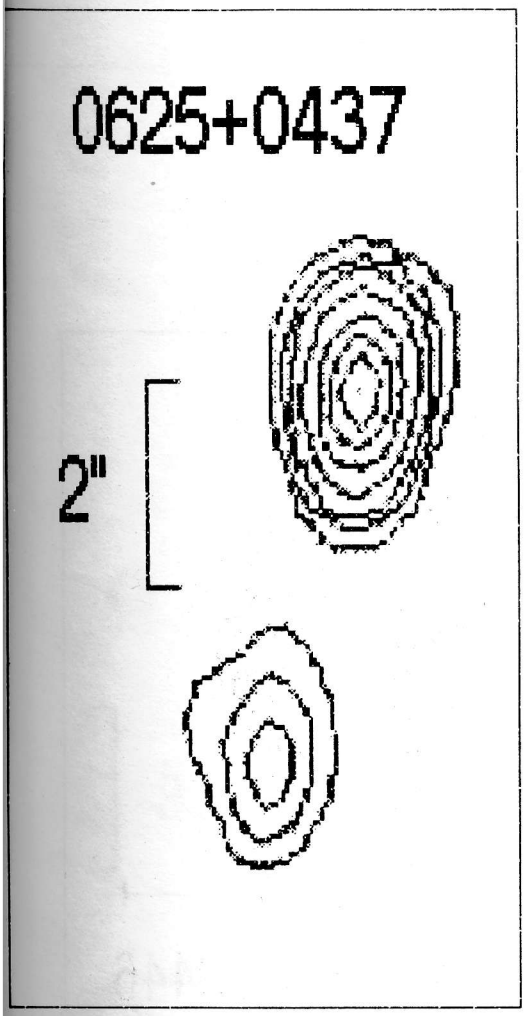
0625+0437
2"

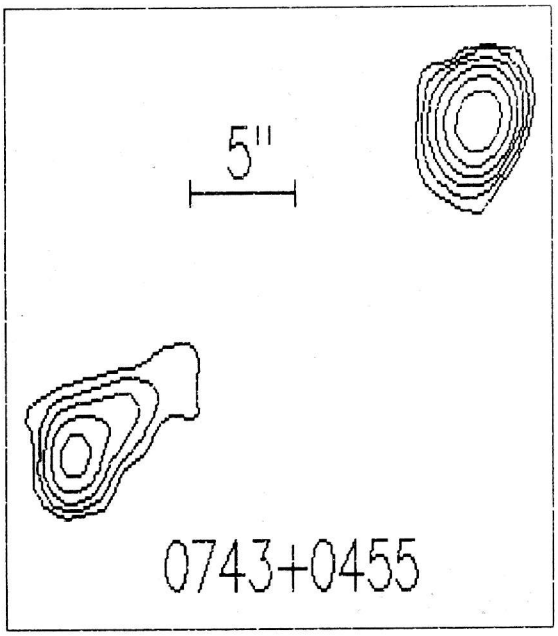
5"
0743+0455

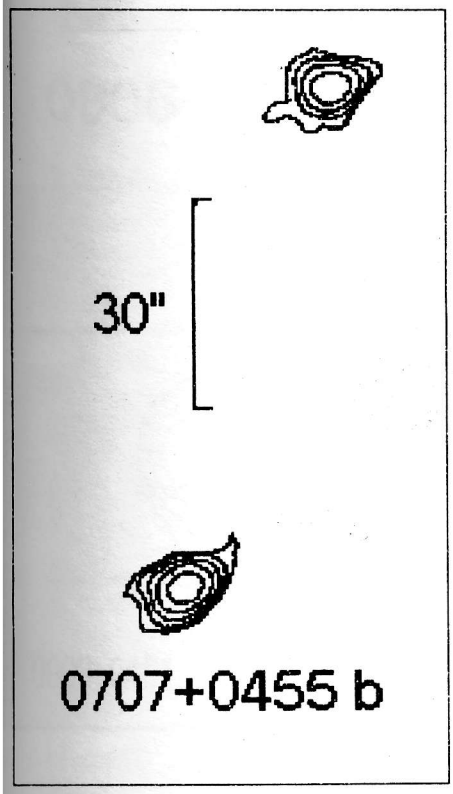
30"
0707+0455 b

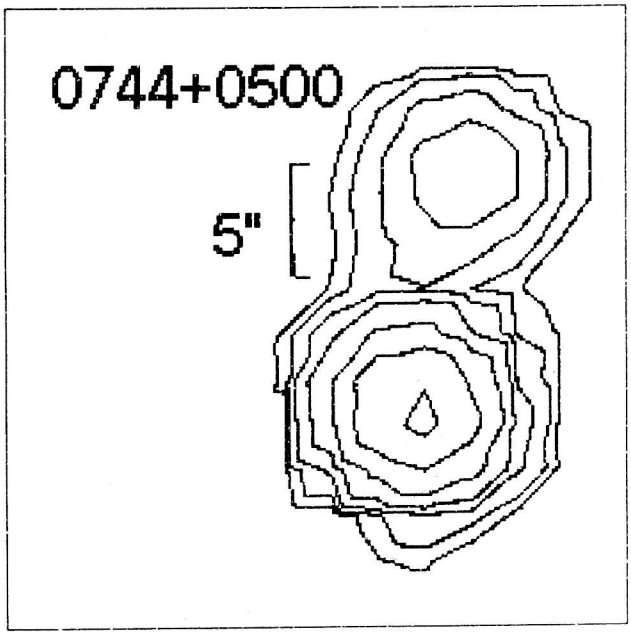
0744+0500
5"

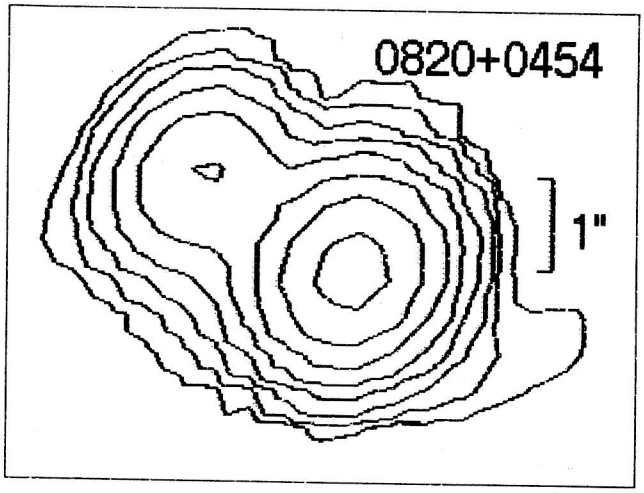
0820+0454
1"

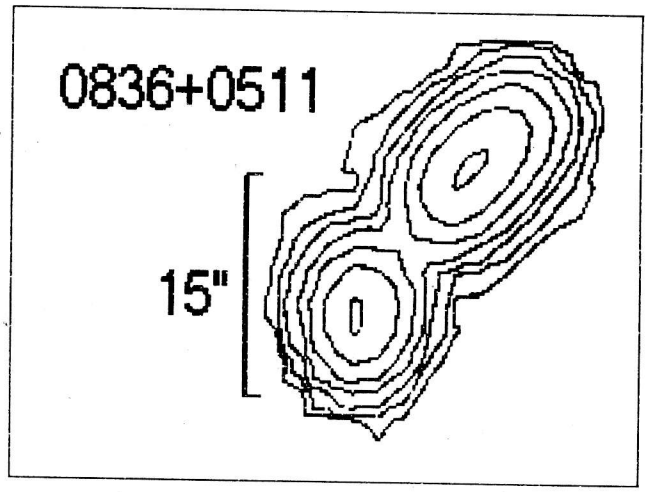
0836+0511
15"

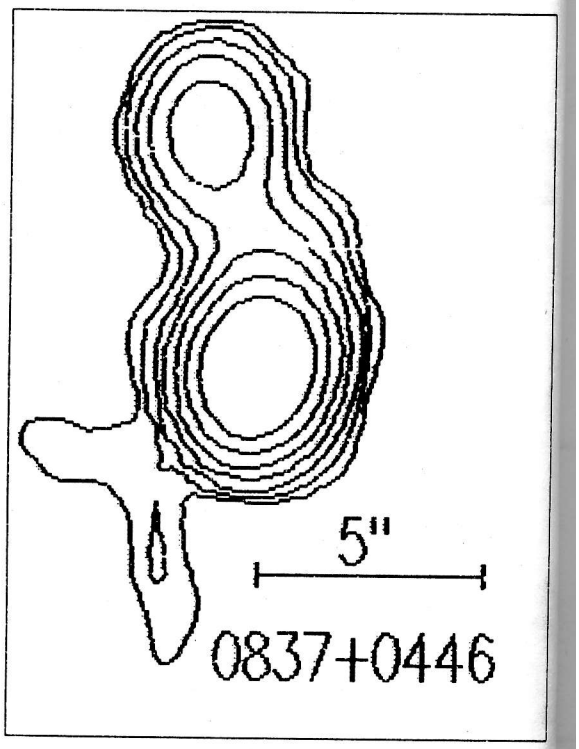
5"
0837+0446

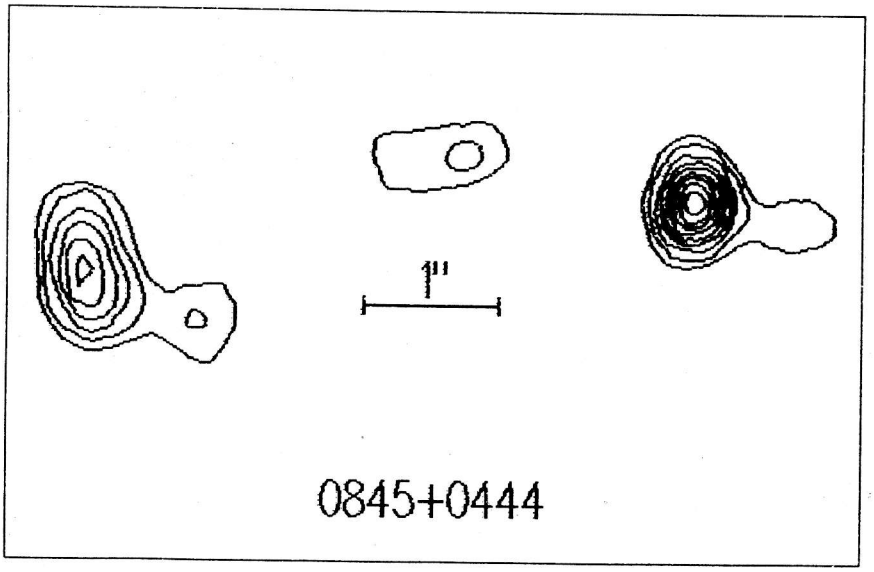
1"
0845+0444

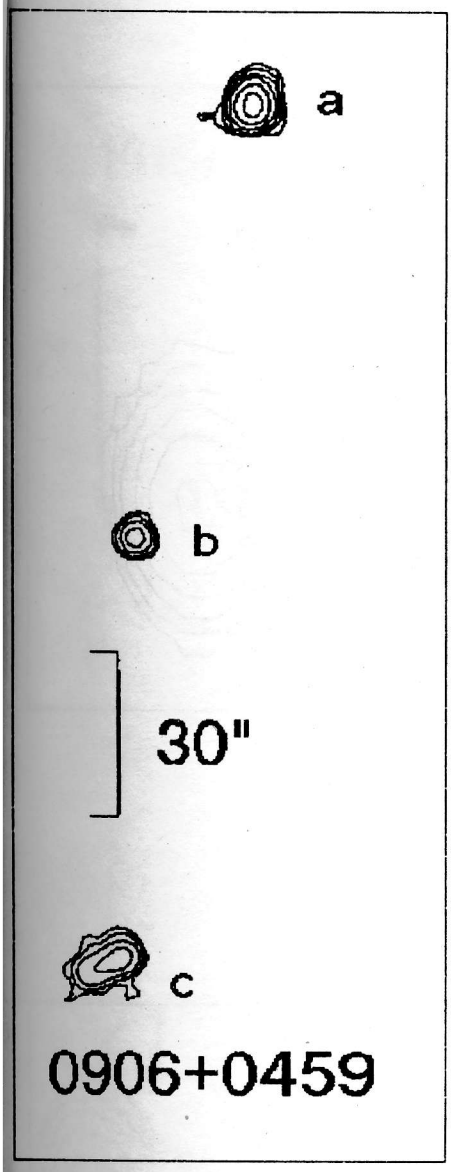
a
b
30"
c
0906+0459

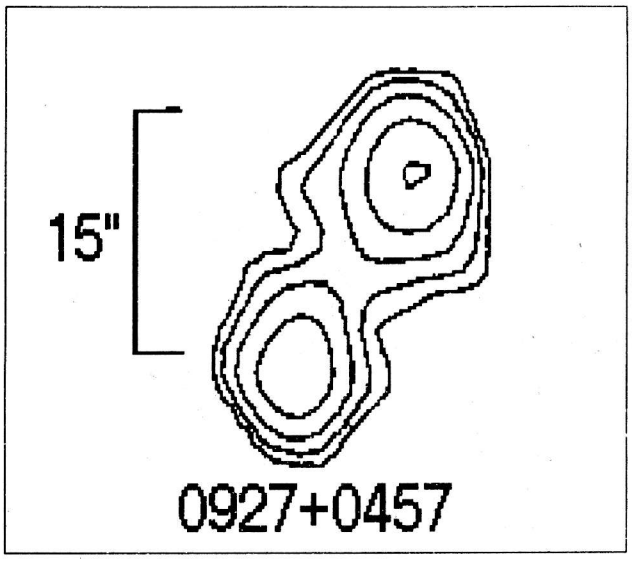
15"
0927+0457

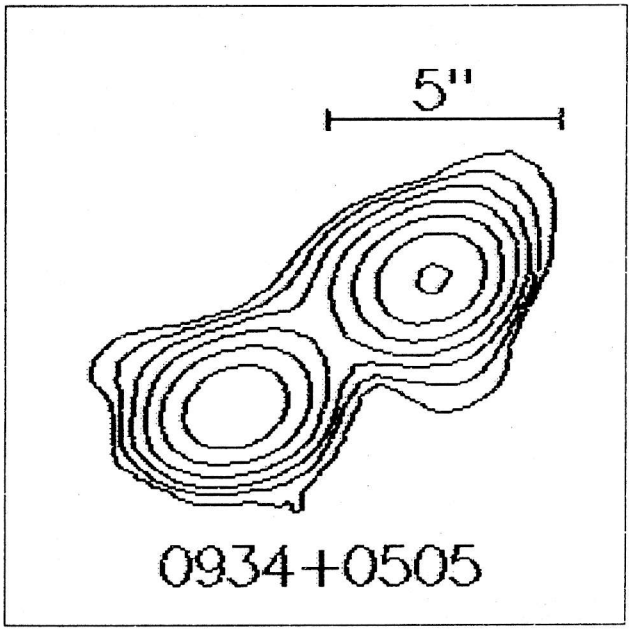
5"
0934+0505

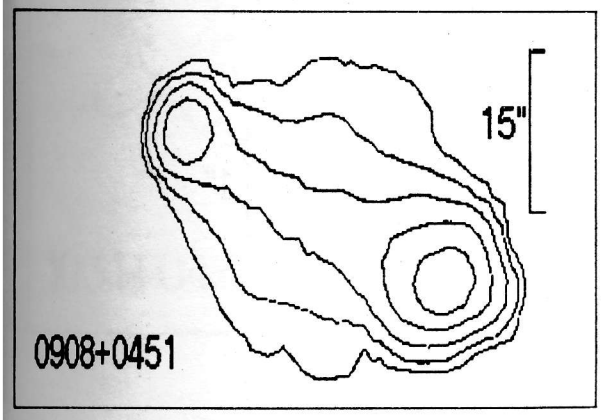
15"
0908+0451

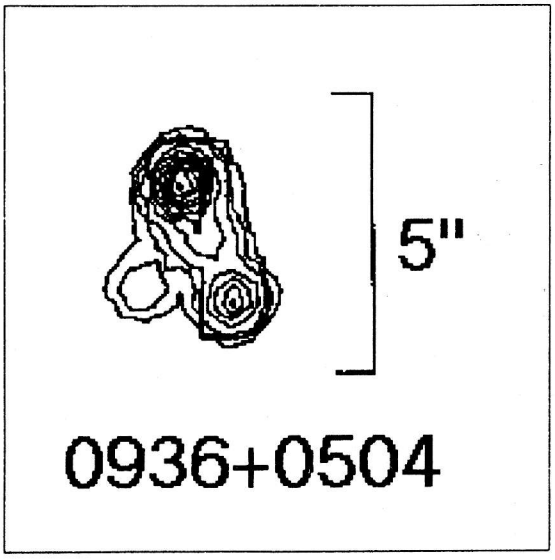
5"
0936+0504

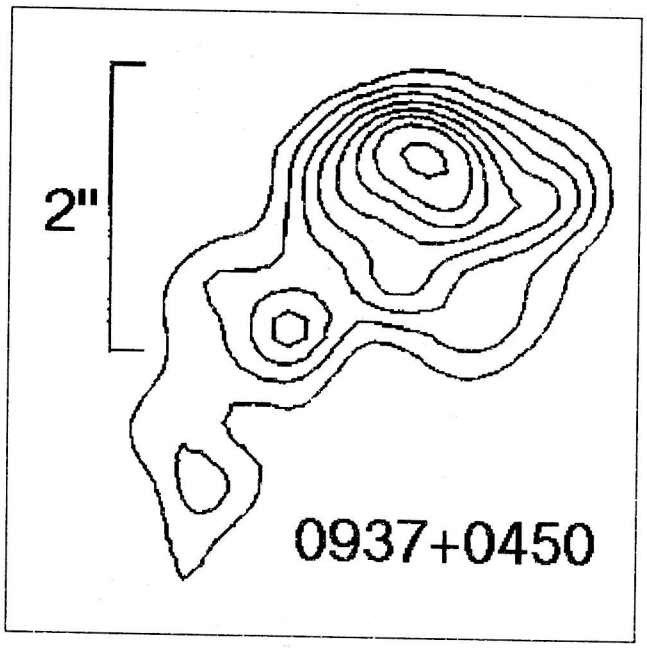
2"
0937+0450

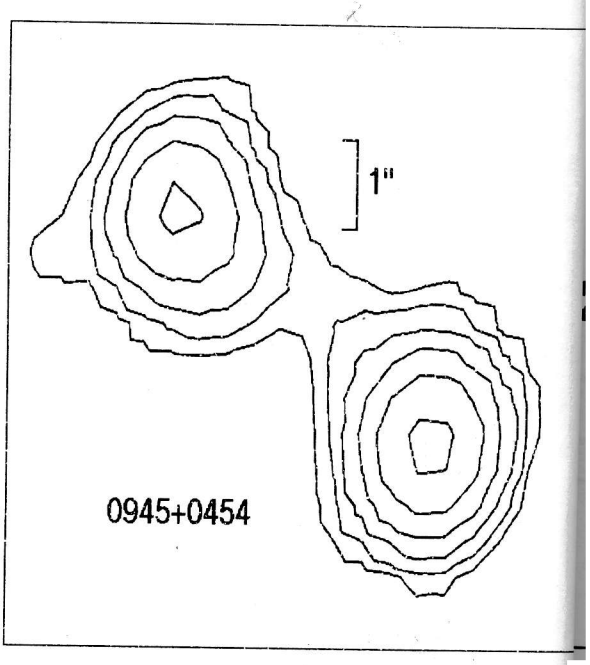
1"
0945+0454

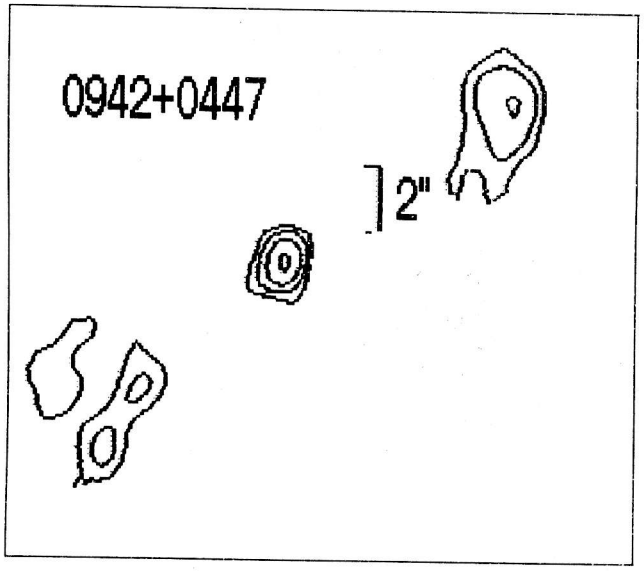
0942+0447
2"

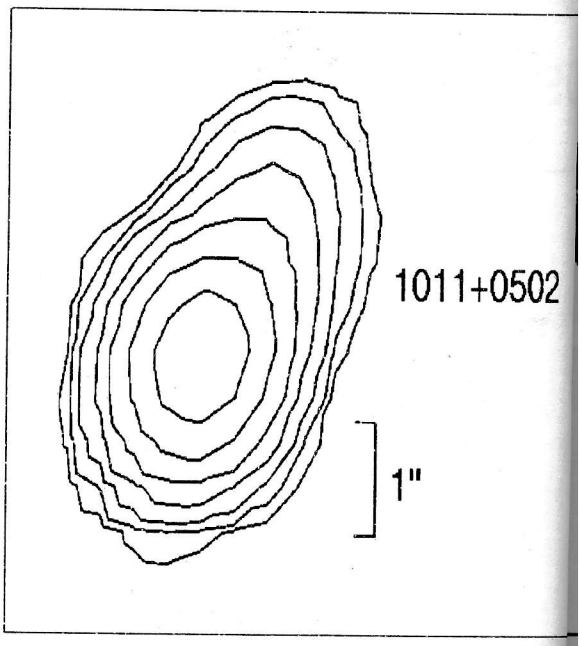
1011+0502
1"

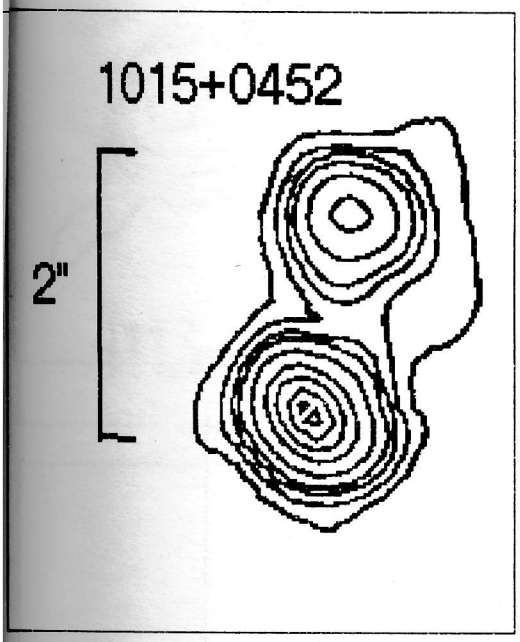
1015+0452
2"

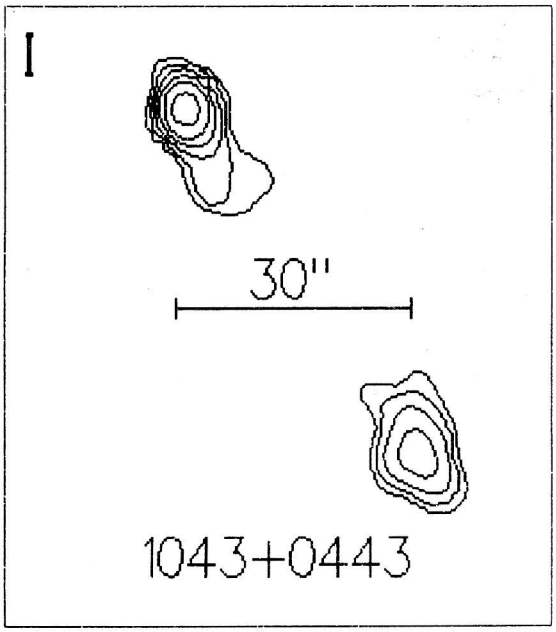
30"
1043+0443

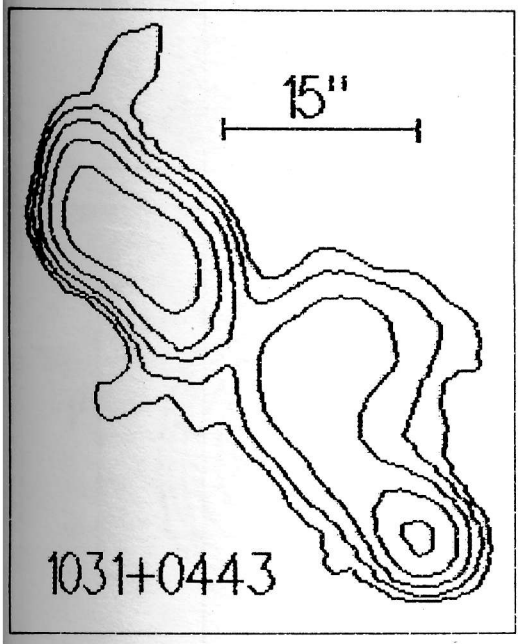
15"
1031+0443

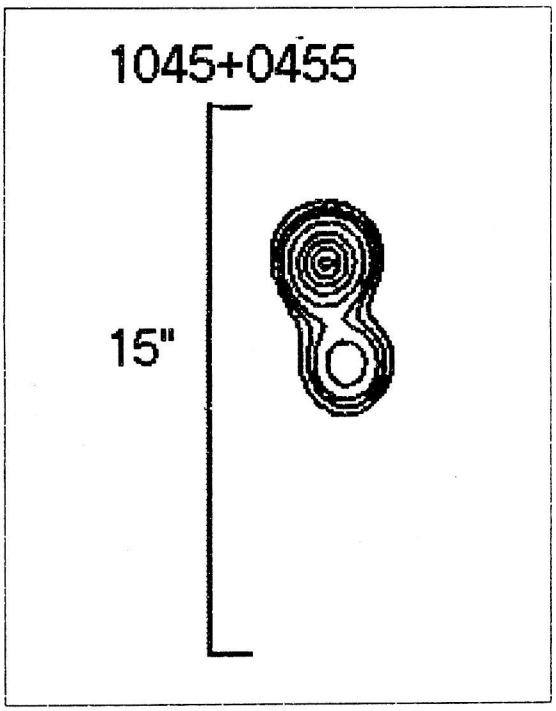
1045+0455
15"

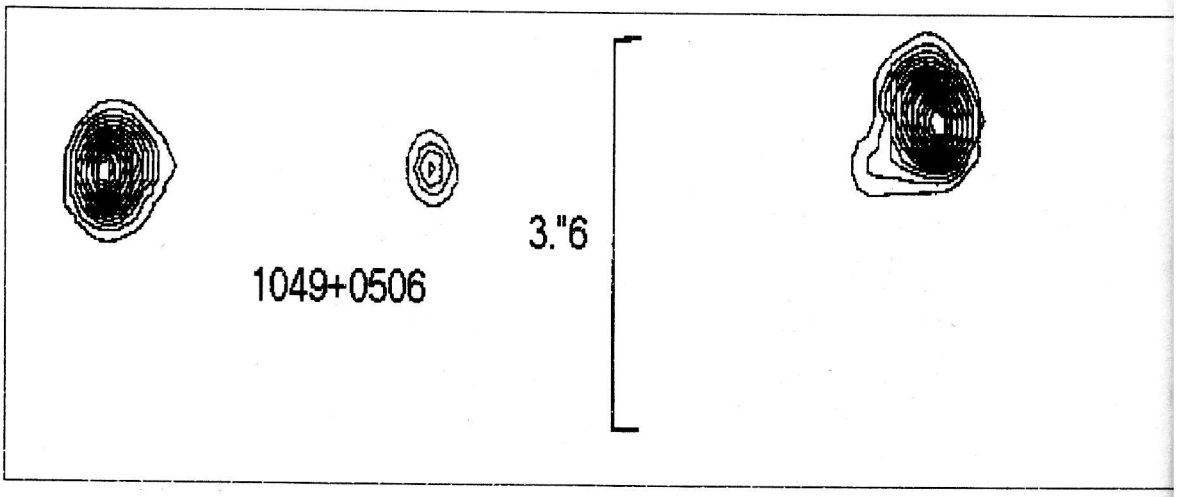
3."6
1049+0506

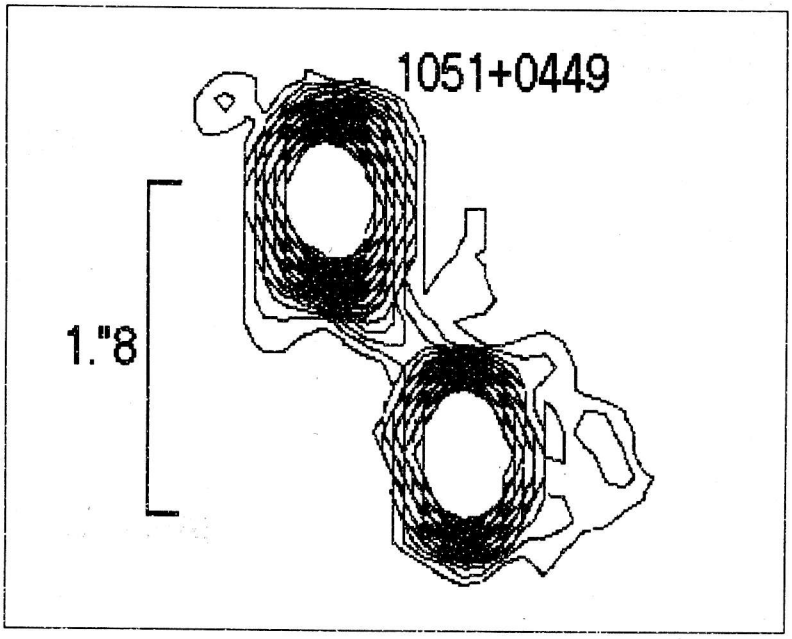
1051+0449
1."8

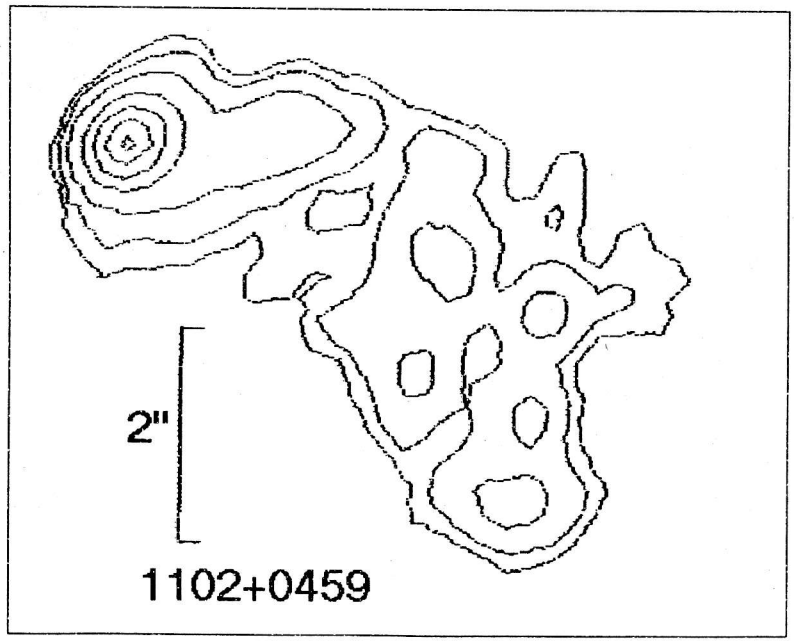
2"
1102+0459

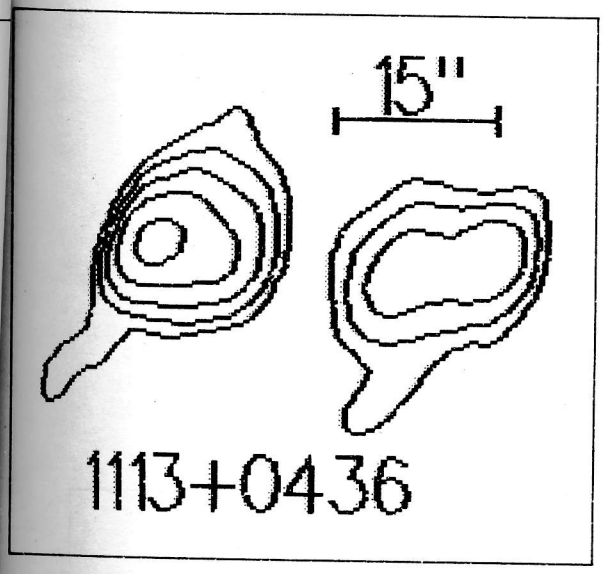
15"
1113+0436

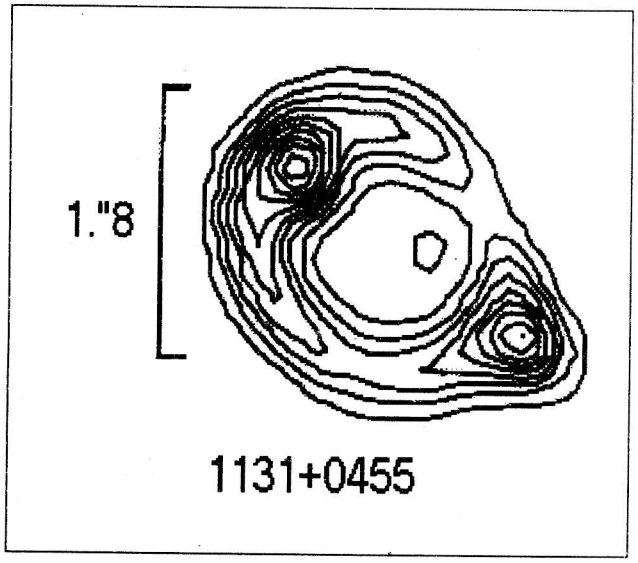
1."8
1131+0455

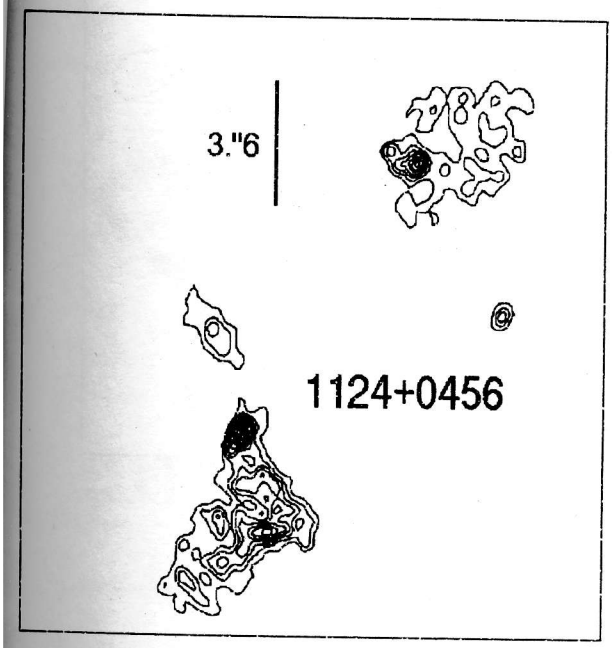
3."6
1124+0456

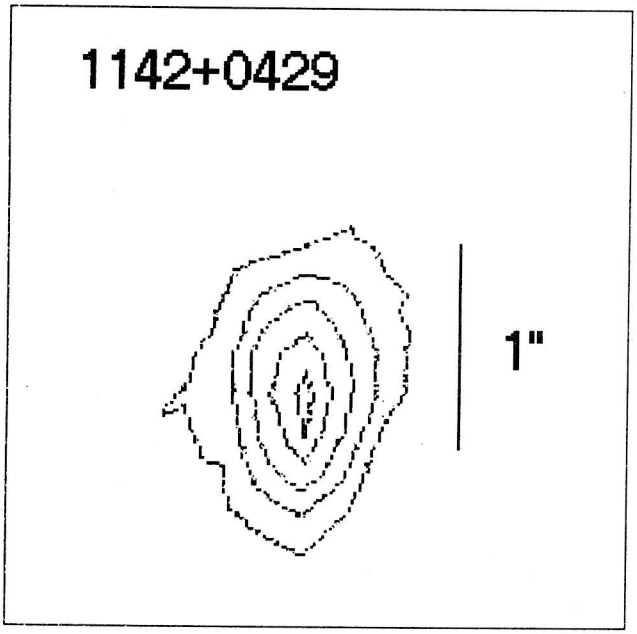
1142+0429
1"

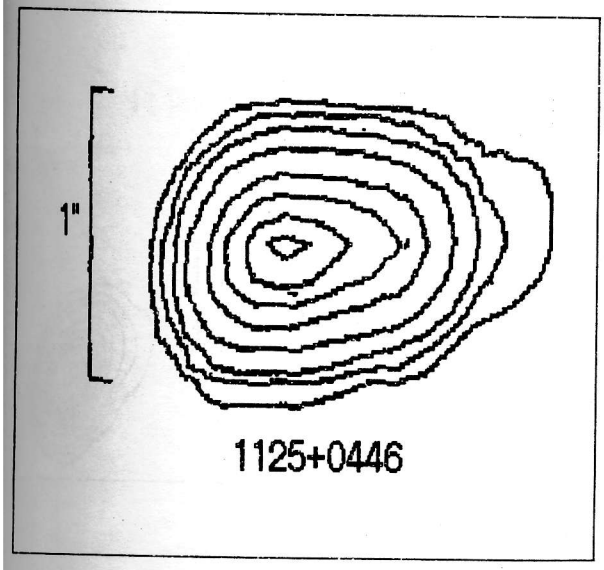
1"
1125+0446

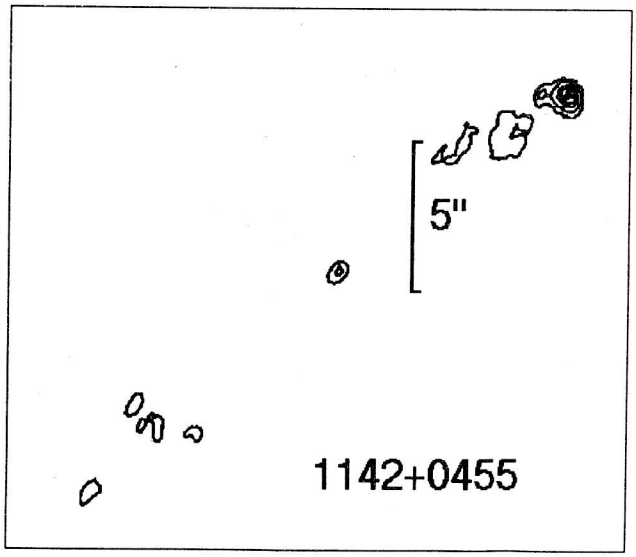
5"
1142+0455

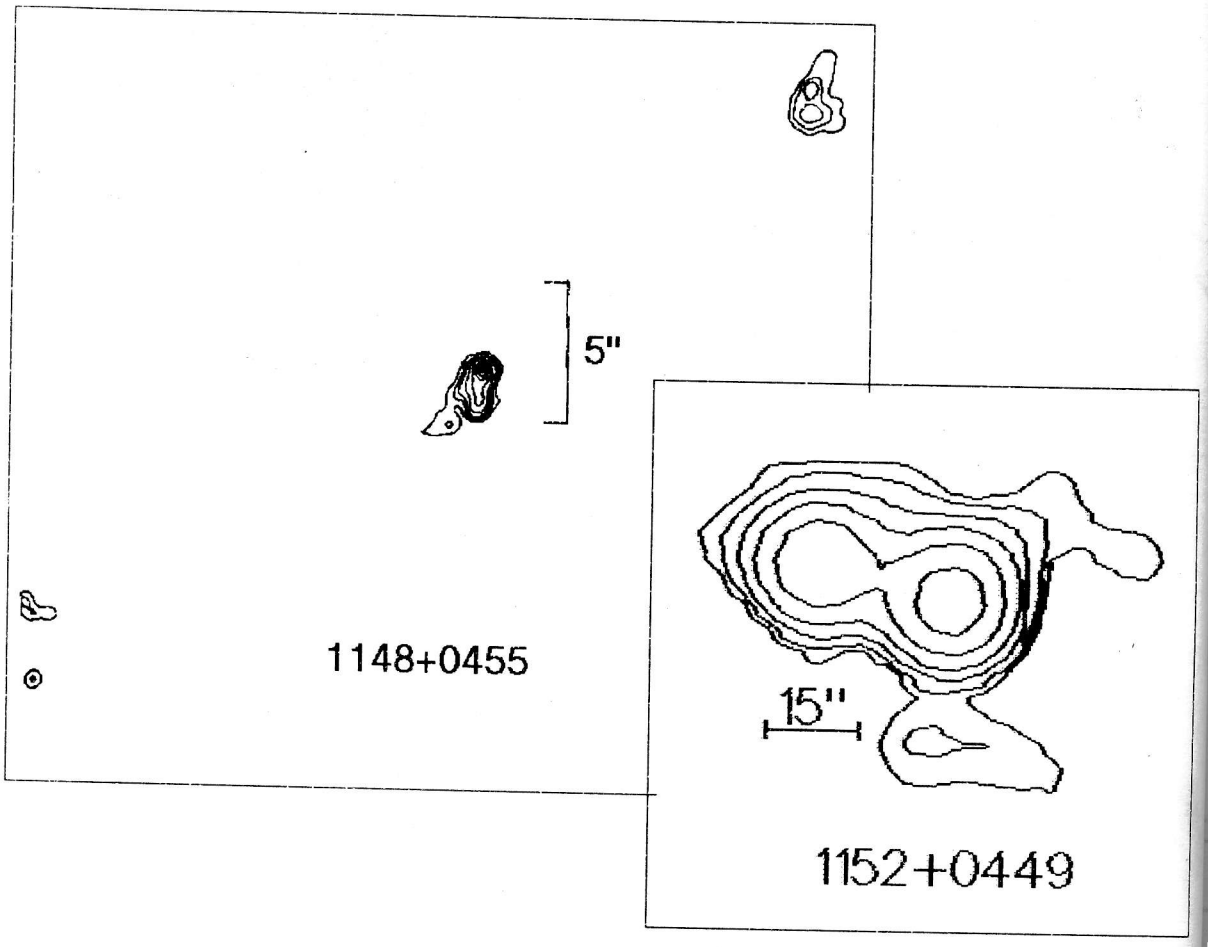
5"
1148+0455
15"
1152+0449

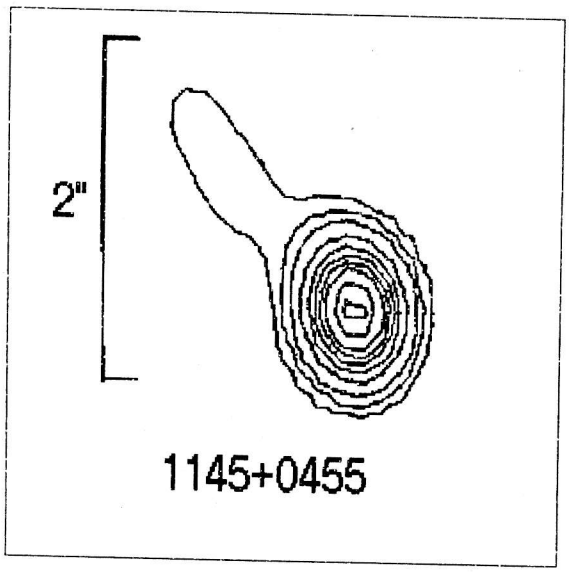
2"
1145+0455

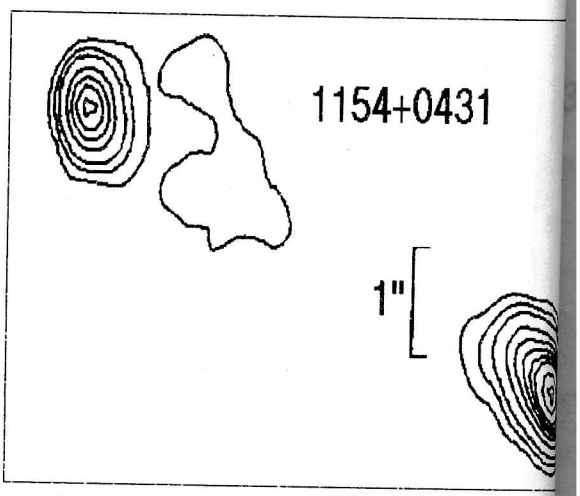
1154+0431
1"

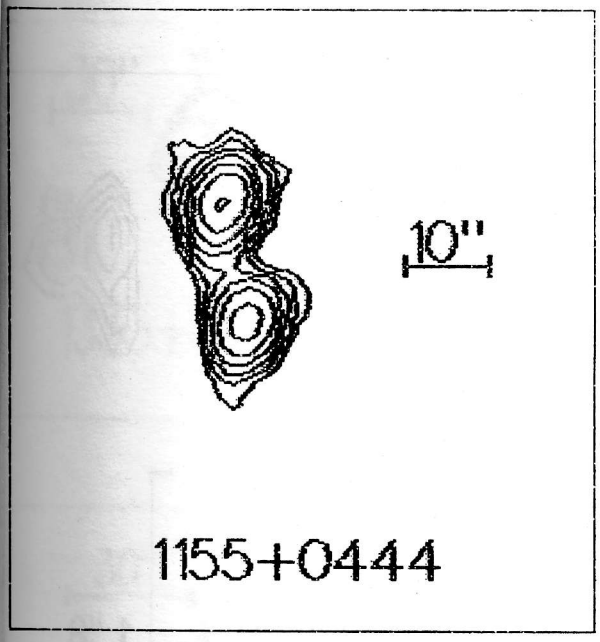
10''
1155+0444

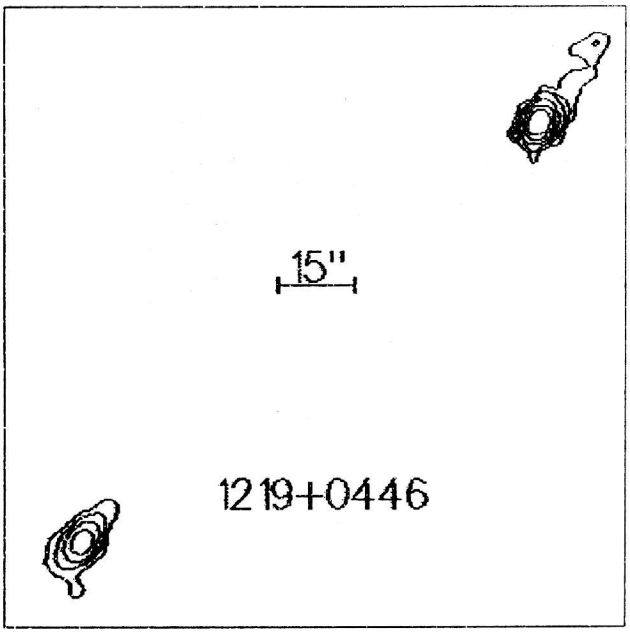
15''
1219+0446

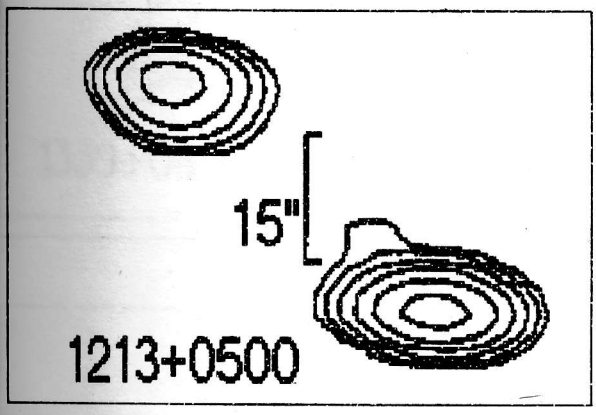
15''
1213+0500

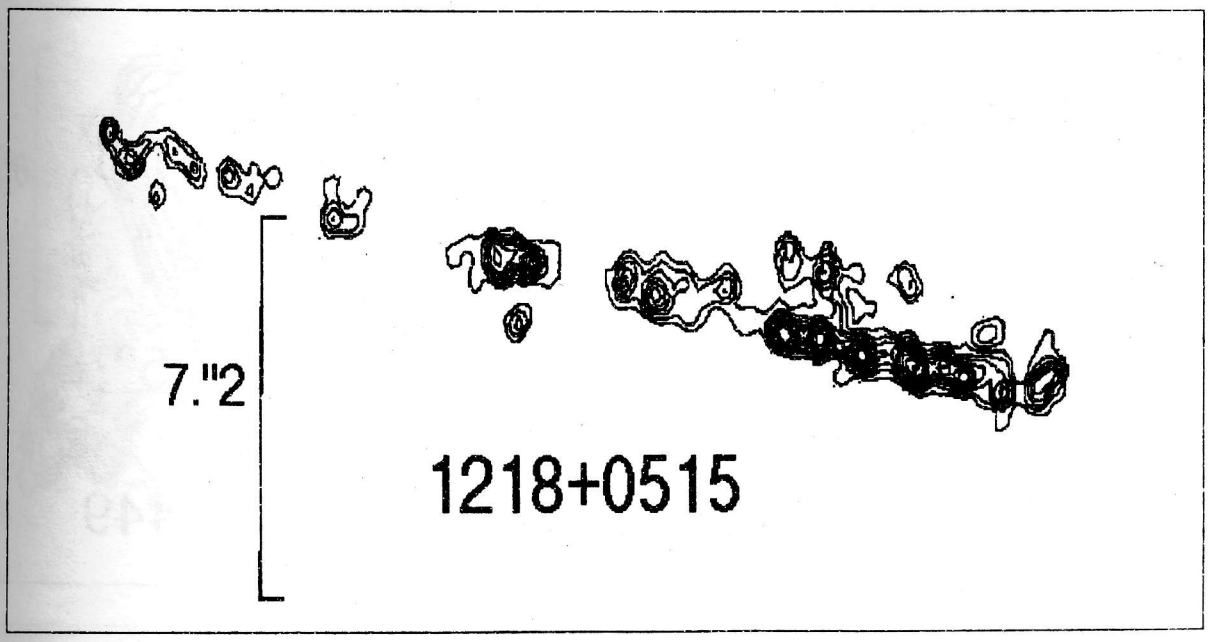
7.''2
1218+0515

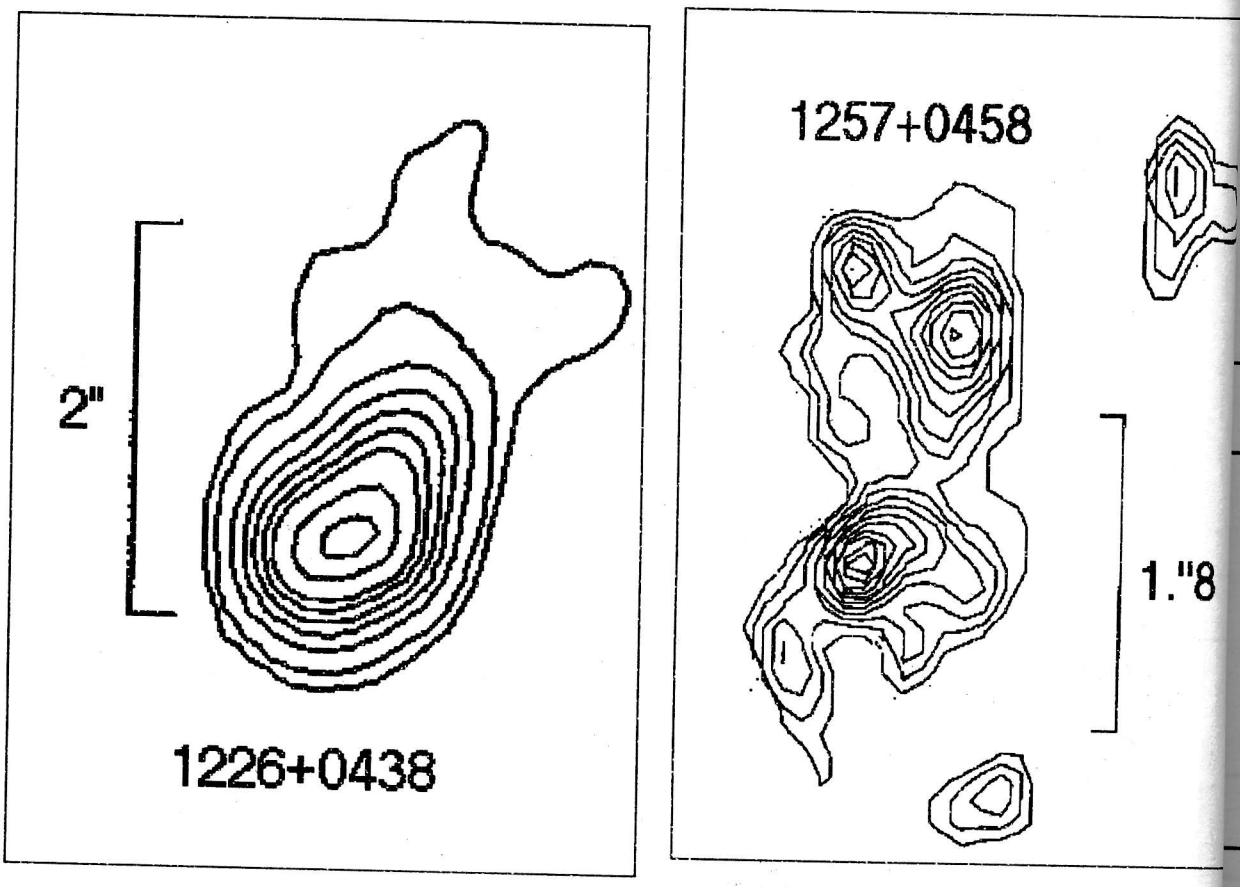
2"
1226+0438
1257+0458
1."8

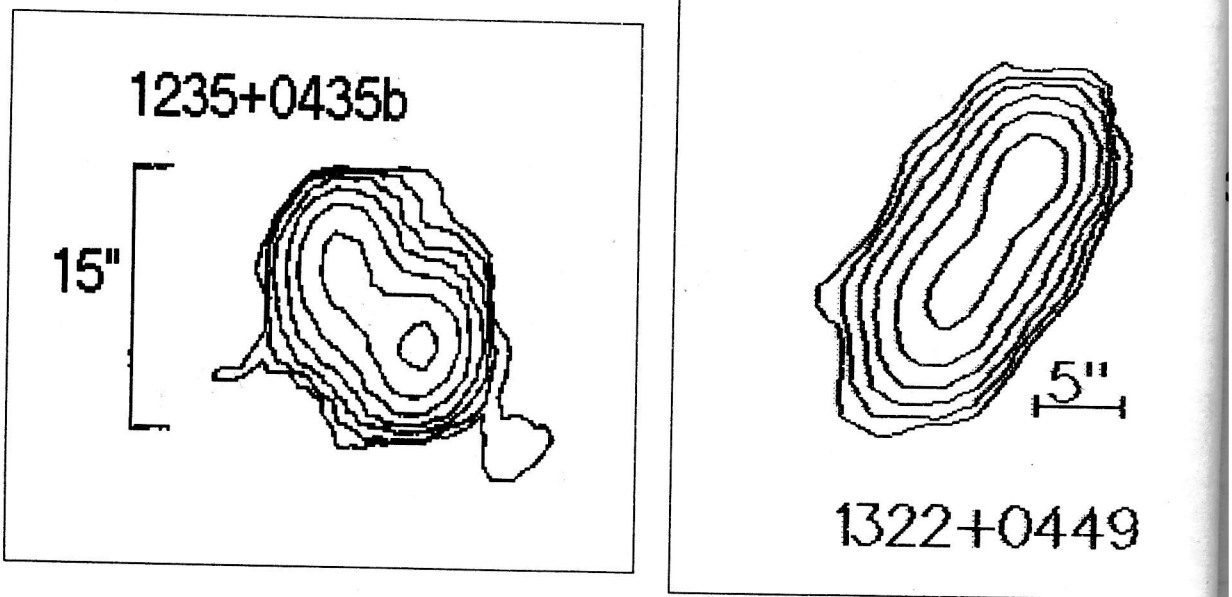
1235+0435b
15"
5"
1322+0449

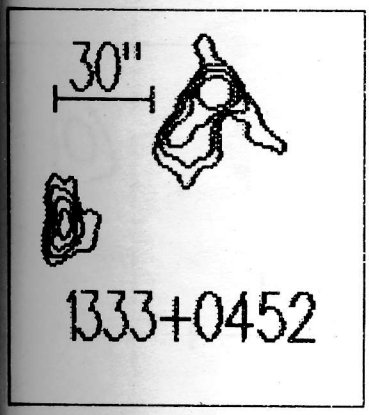
30"
1333+0452

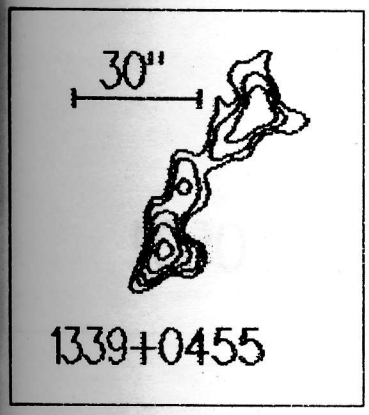
30"
1339+0455

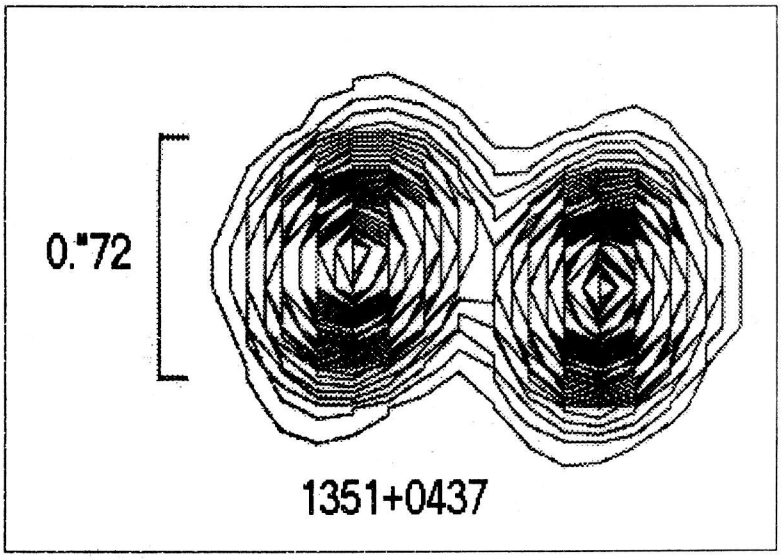
0."72
1351+0437

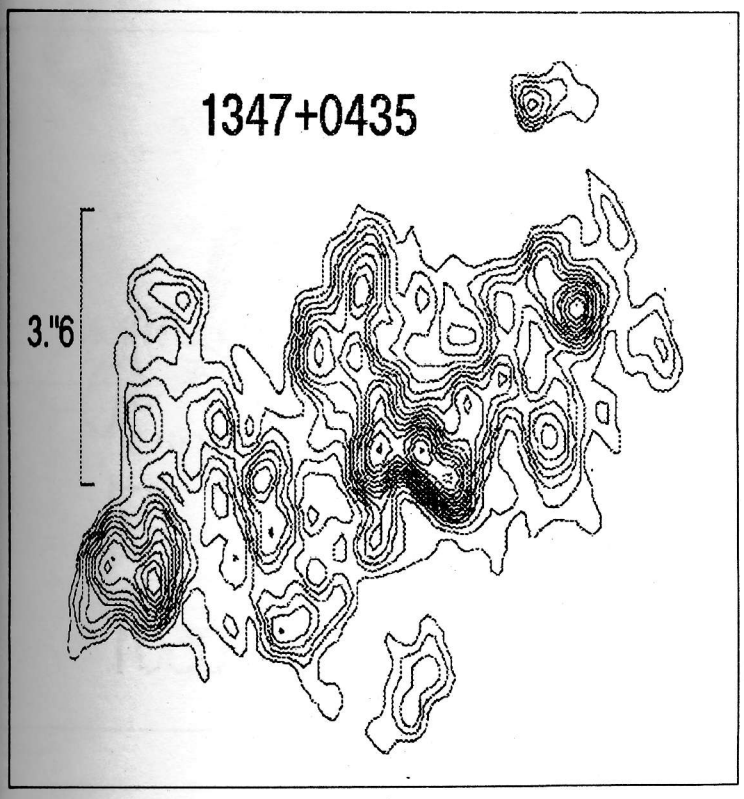
1347+0435
3."6

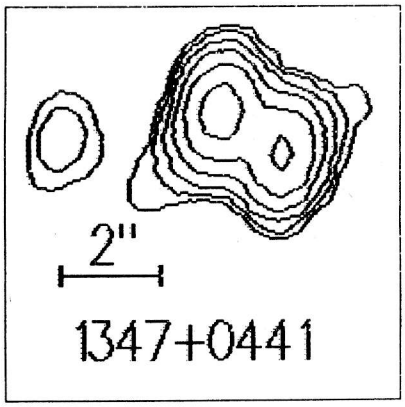
2"
1347+0441

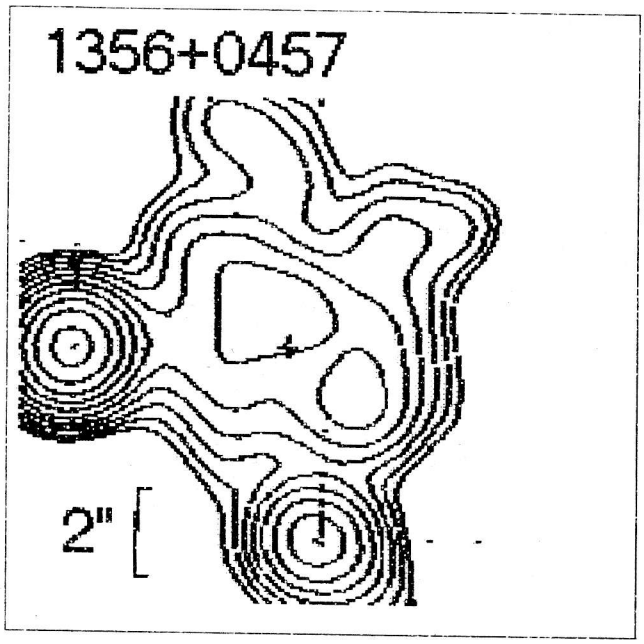
1356+0457
2"

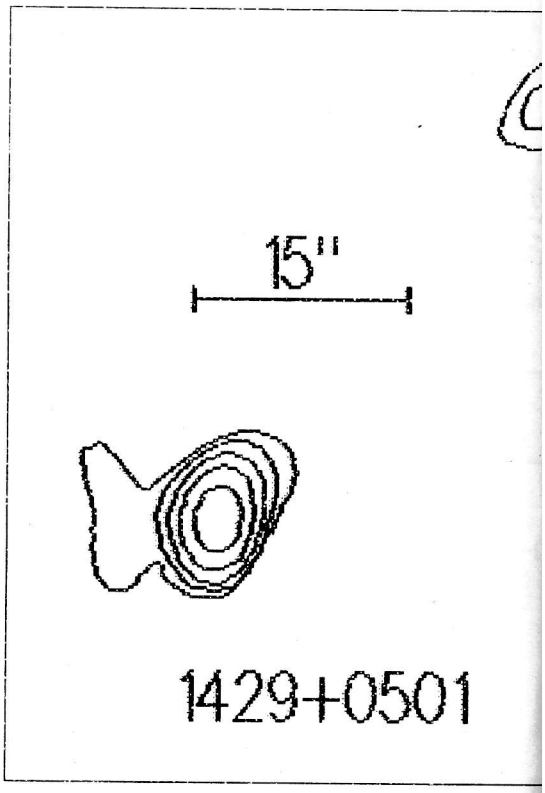
15"
1429+0501

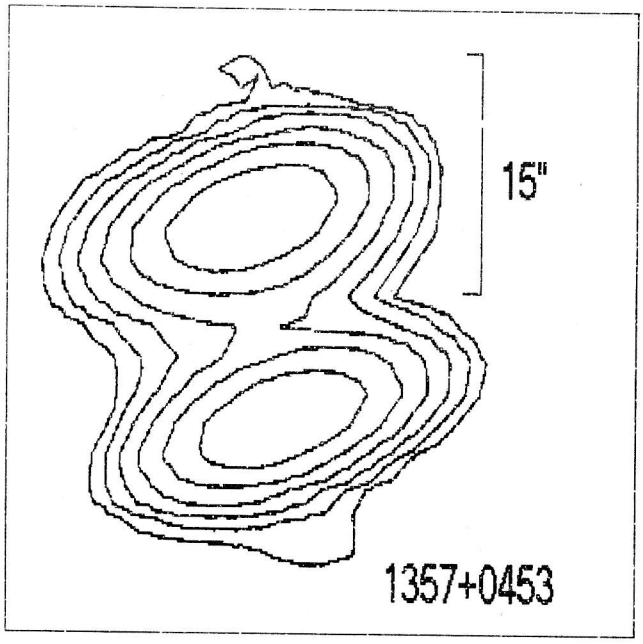
15"
1357+0453

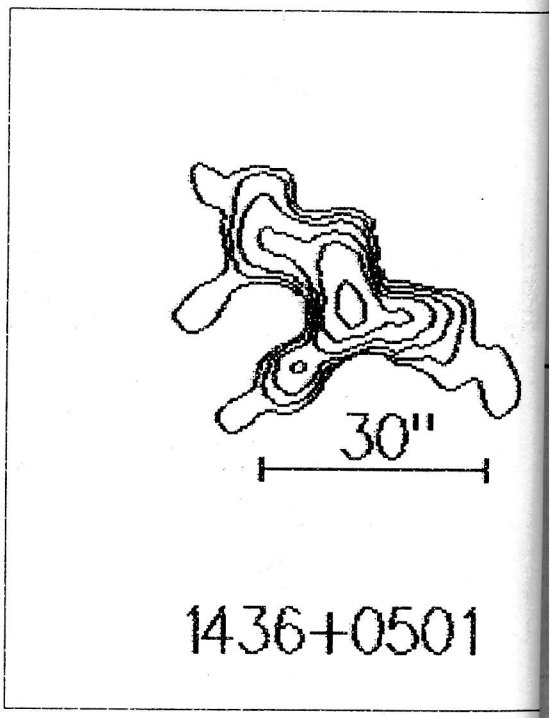
30"
1436+0501

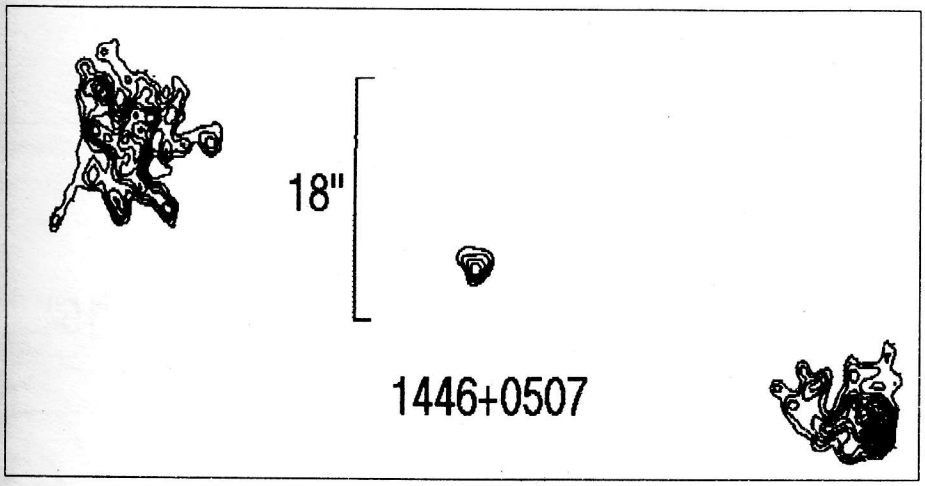
18"
1446+0507

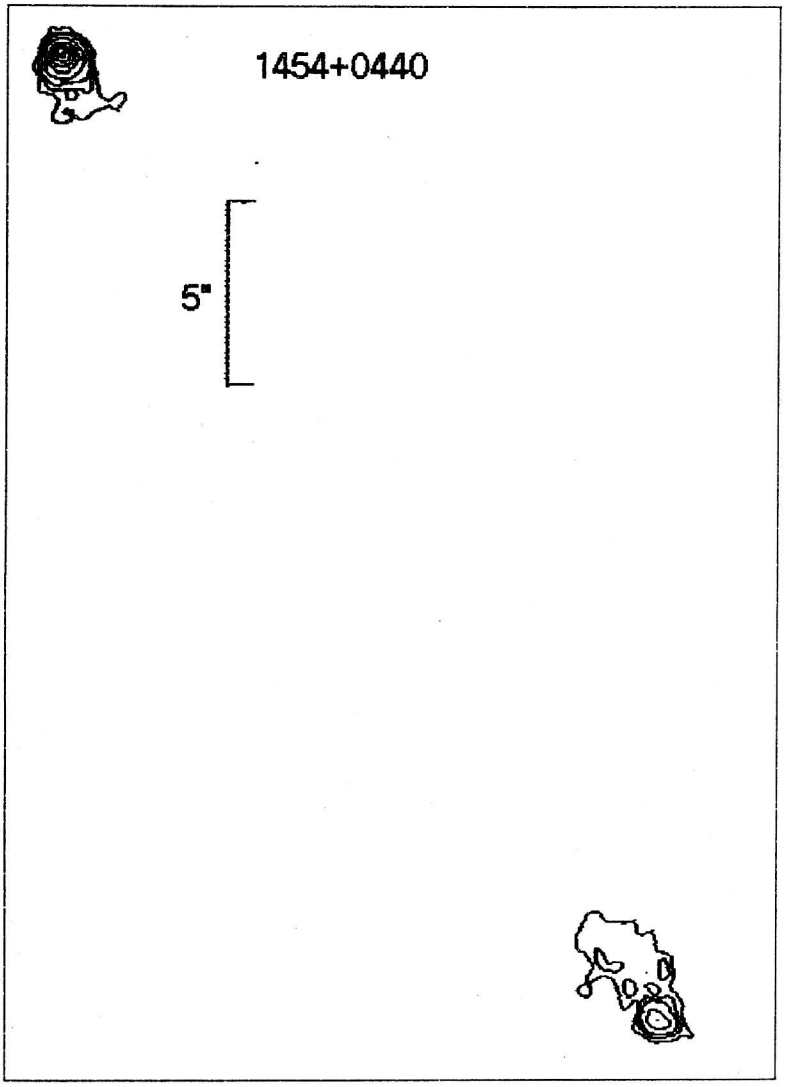
1454+0440
5"

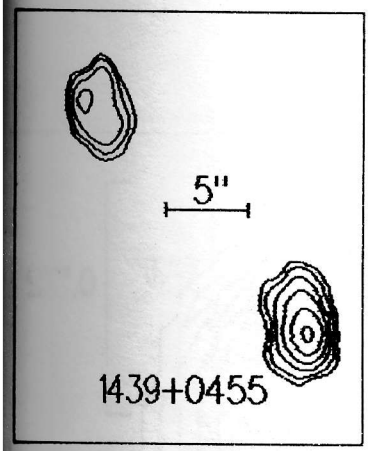
5"
1439+0455

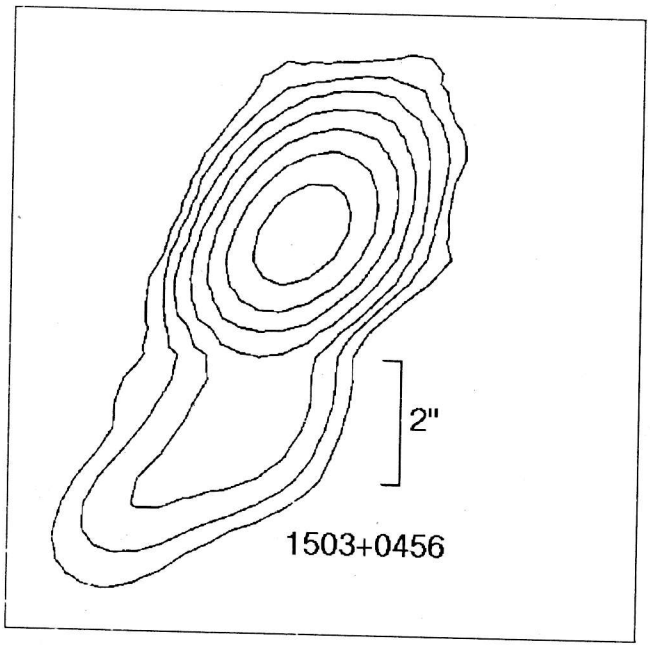
2"
1503+0456

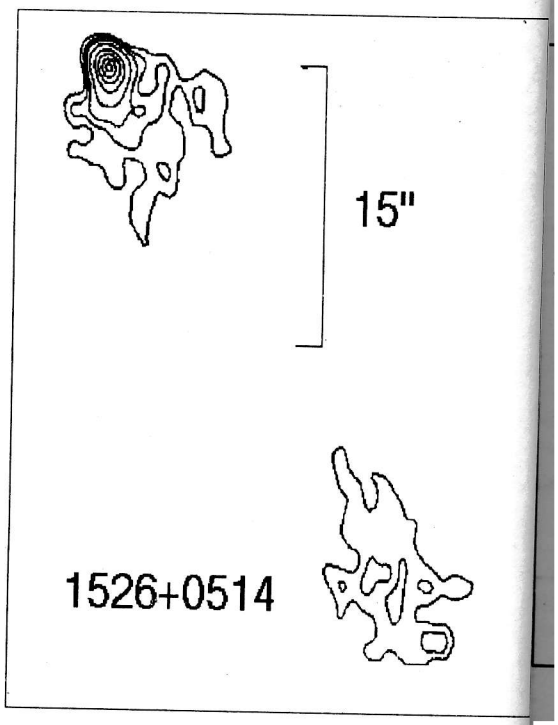
15"
1526+0514

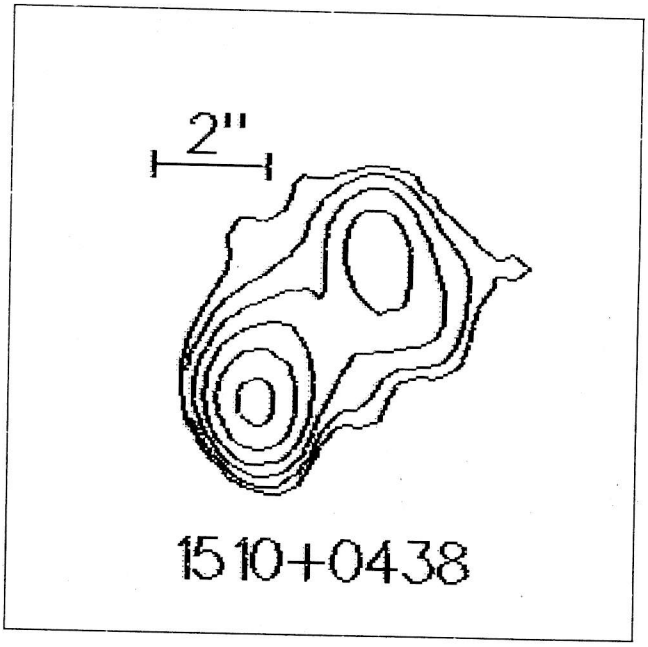
2"
1510+0438

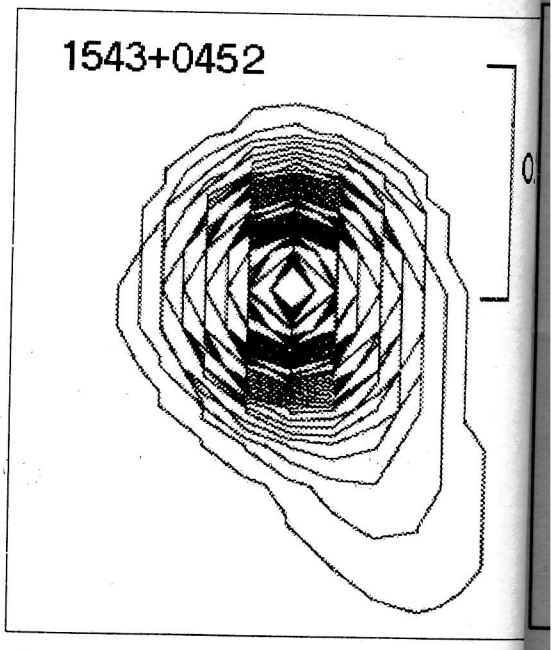
1543+0452

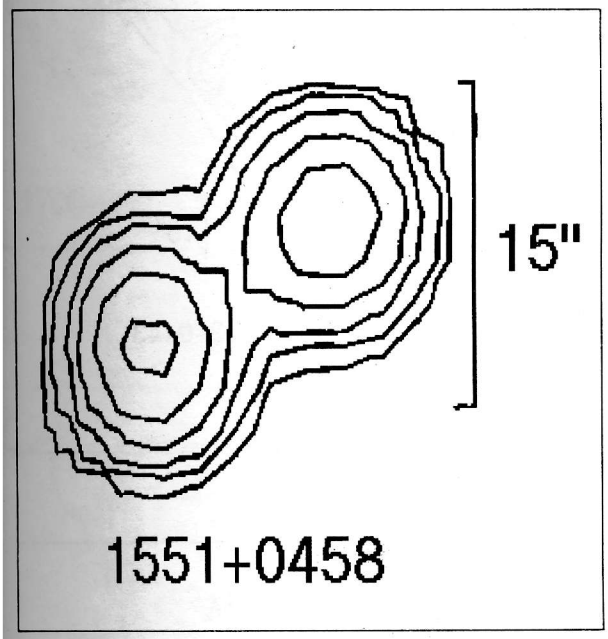
15"
1551+0458

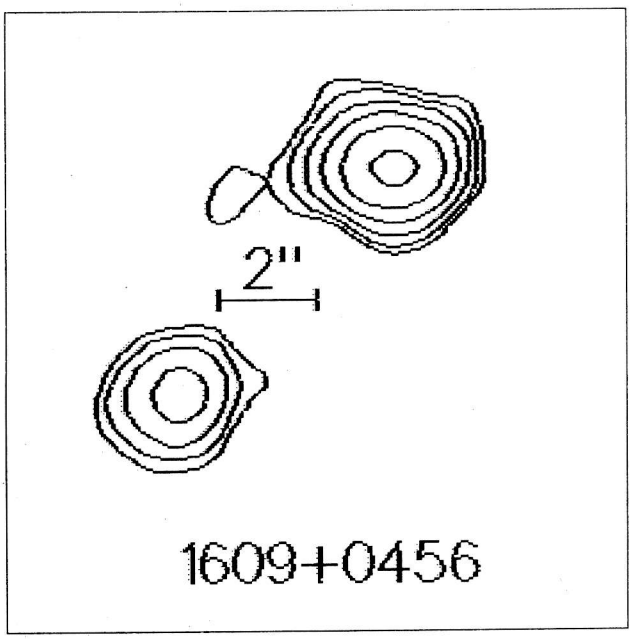
2"
1609+0456

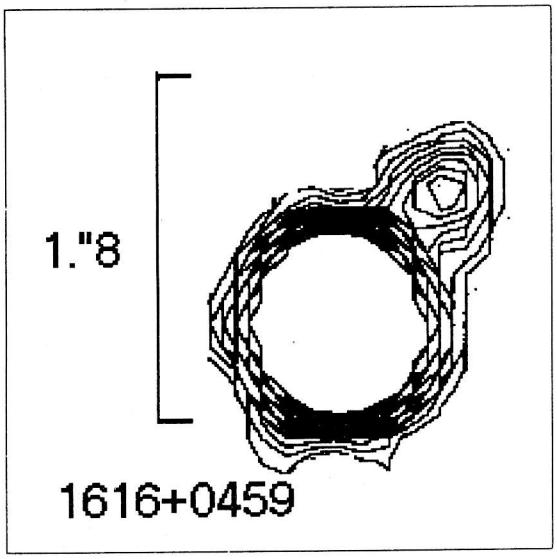
1."8
1616+0459

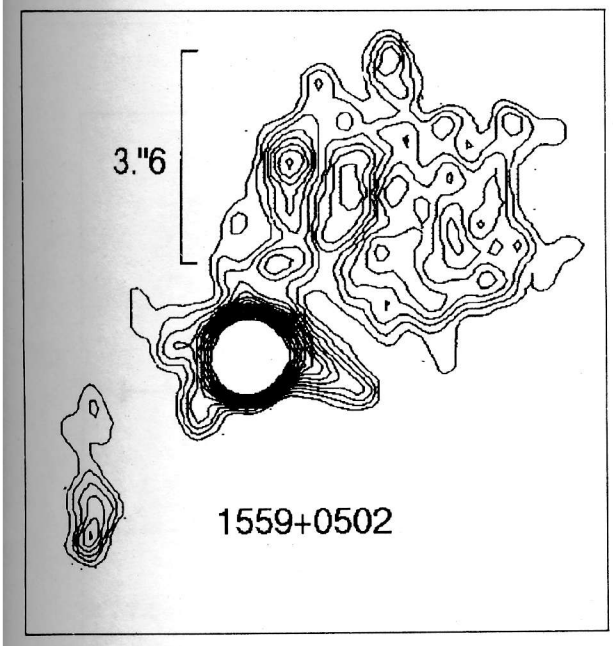
3."6
1559+0502

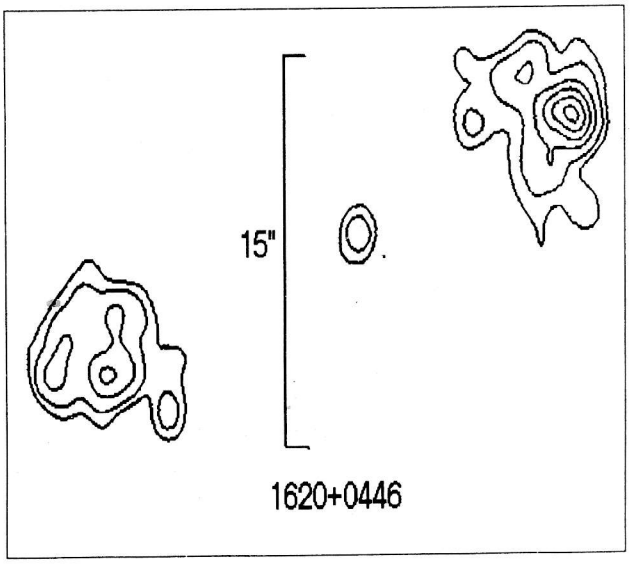
15"
1620+0446

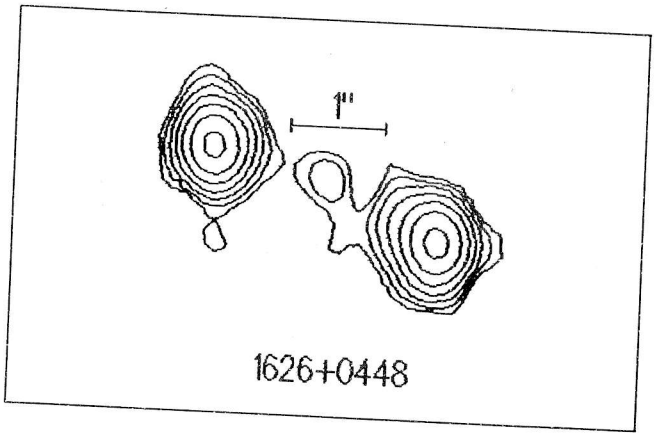
1"
1626+0448

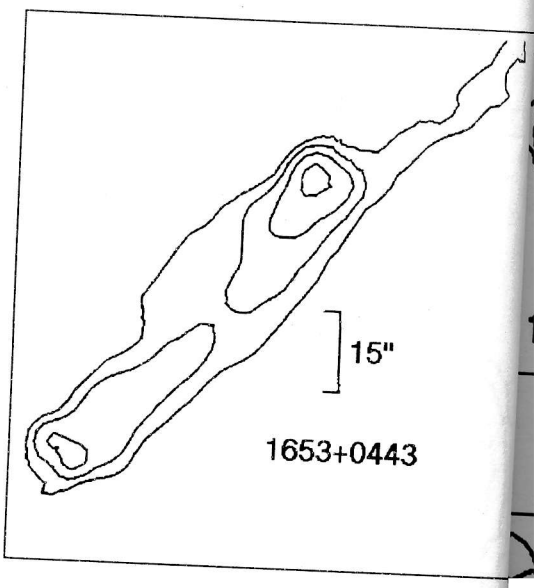
15"
1653+0443

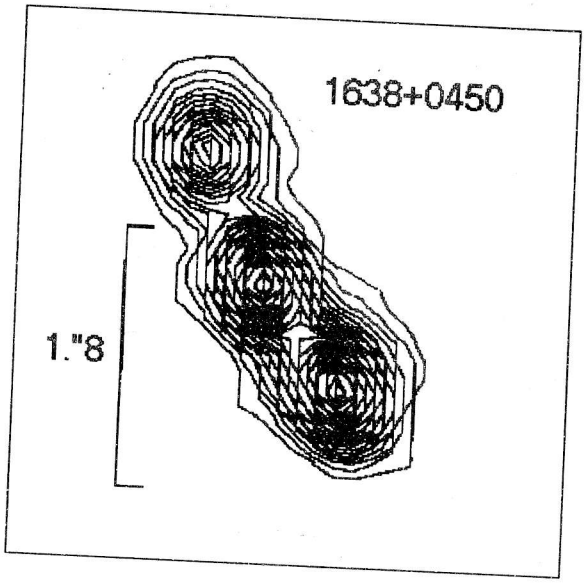
1638+0450
1."8

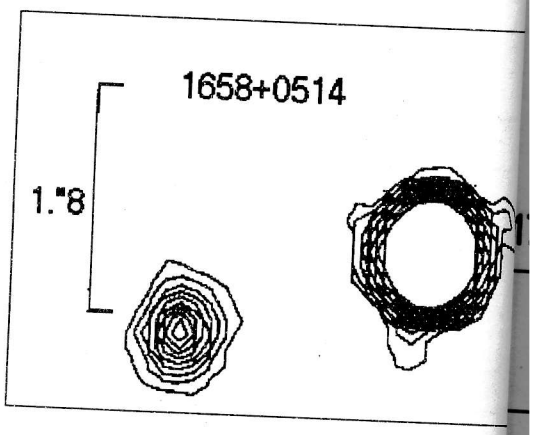
1658+0514
1."8

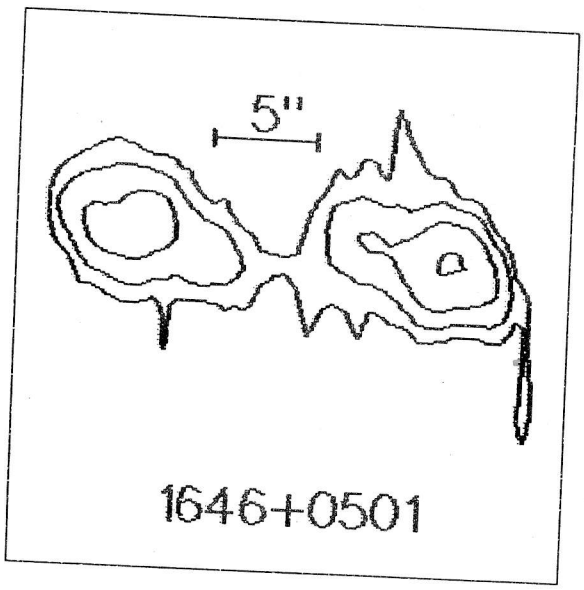
5"
1646+0501

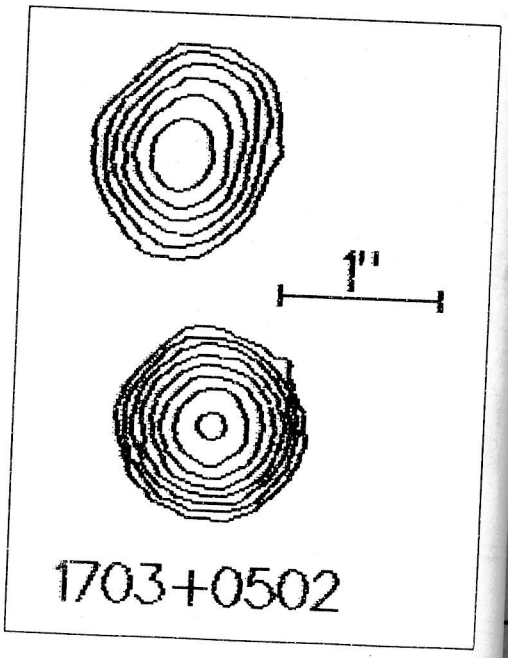
1"
1703+0502

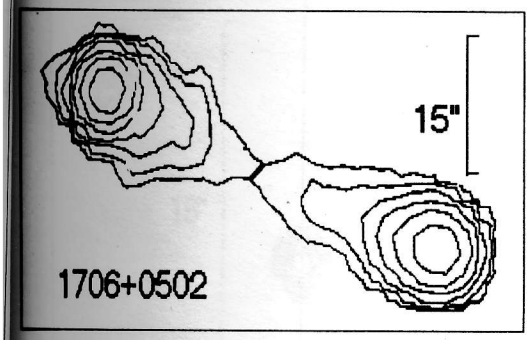
15"
1706+0502

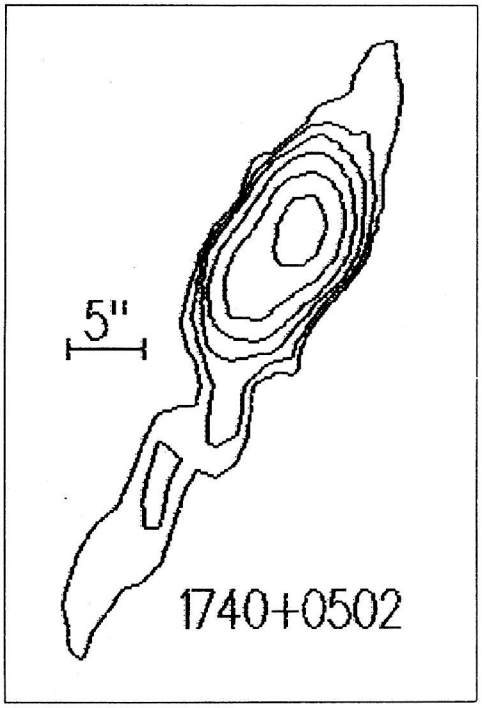
5"
1740+0502

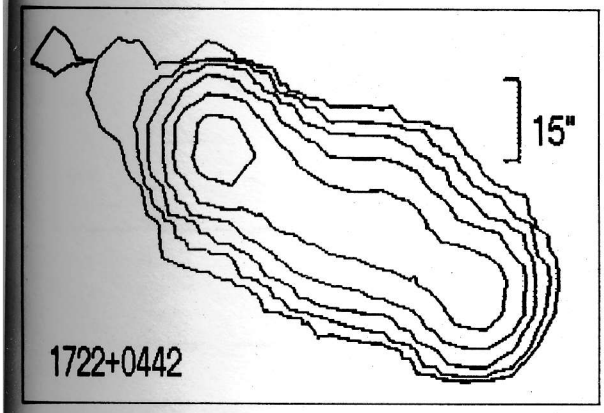
15"
1722+0442

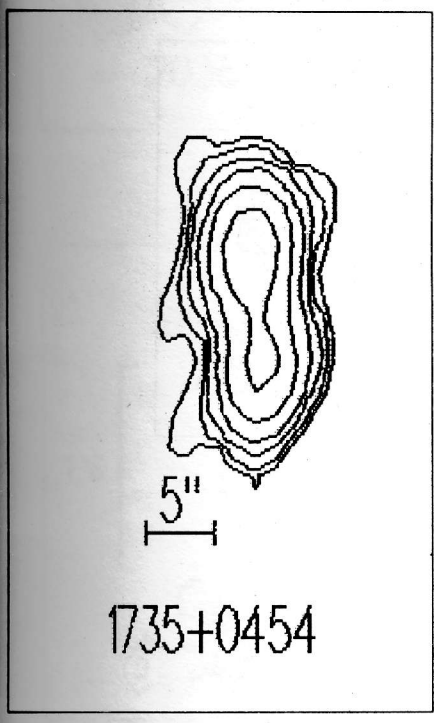
5"
1735+0454

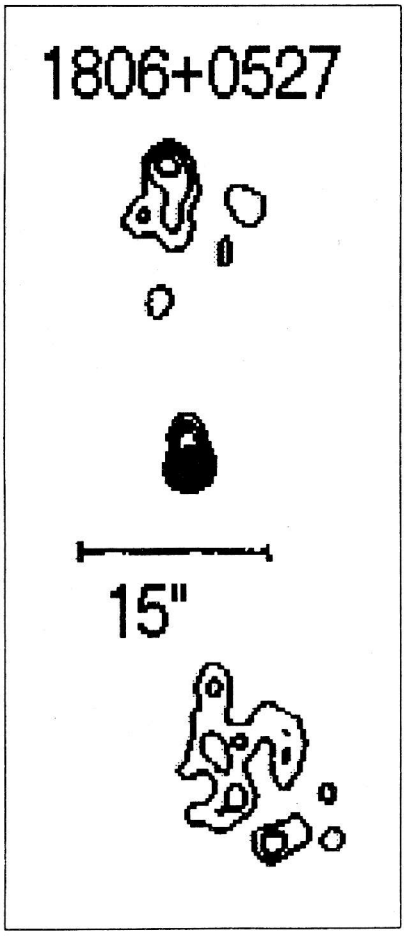
1806+0527
15"

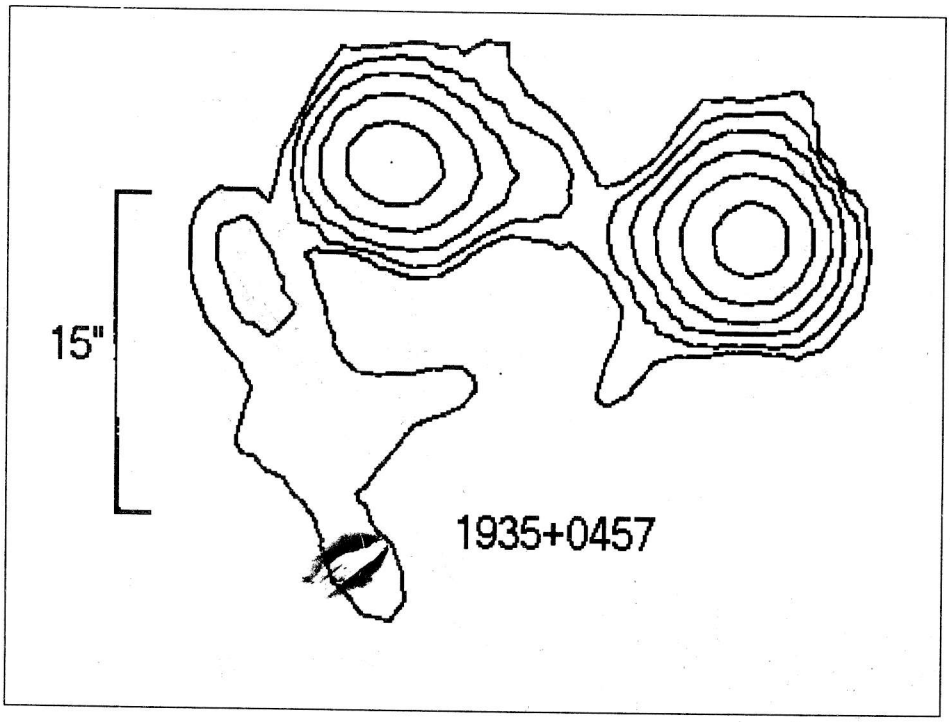
15"
1935+0457

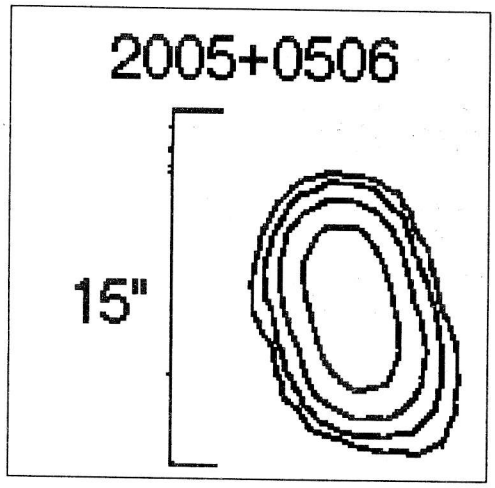
2005+0506
15"

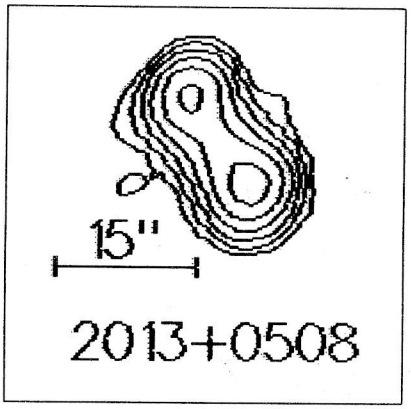
15"
2013+0508

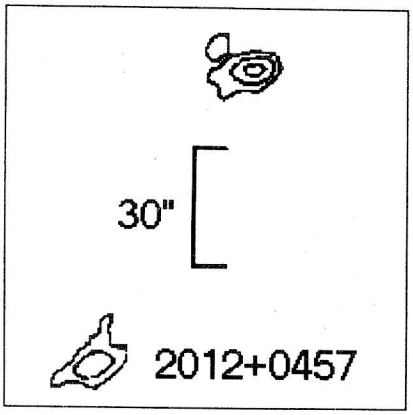
30"
2012+0457

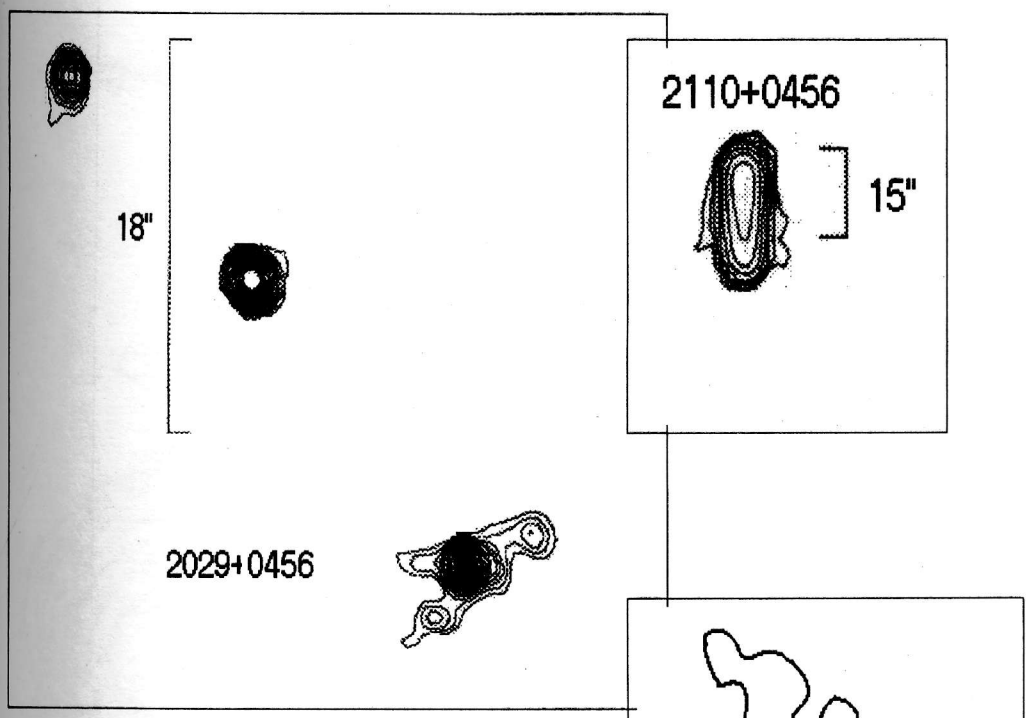
18"
2029+0456

2110+0456
15"

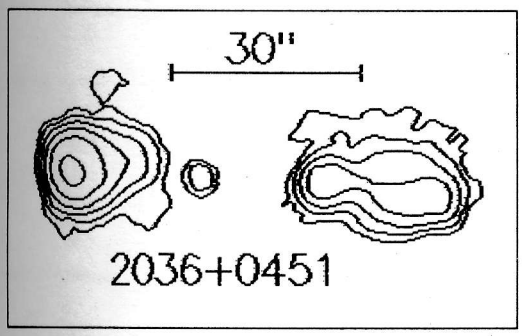
30"
2036+0451

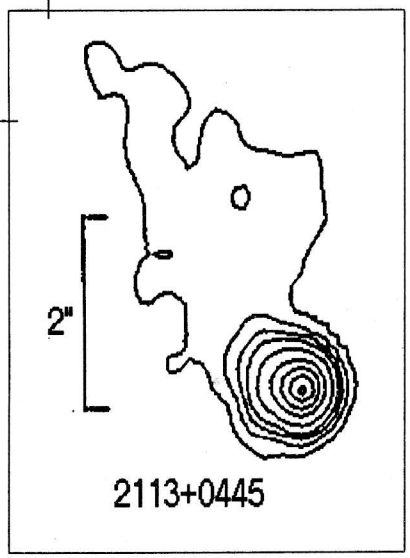
2"
2113+0445

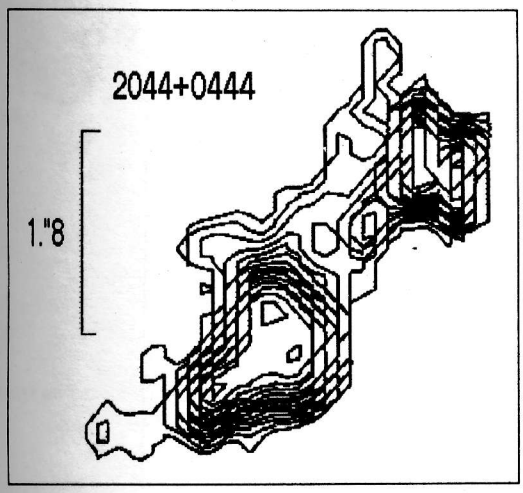
2044+0444
1."8

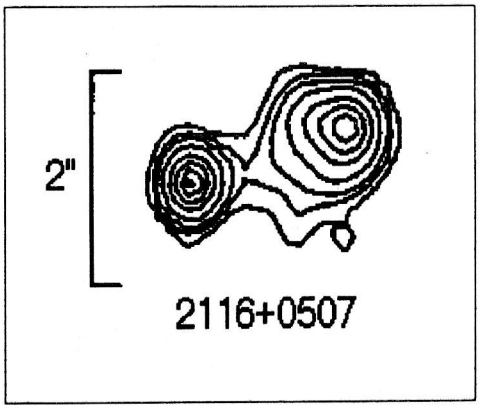
2"
2116+0507

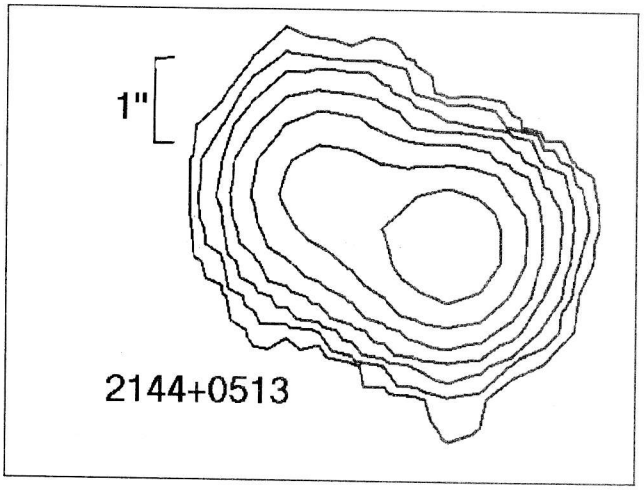
1"
2144+0513

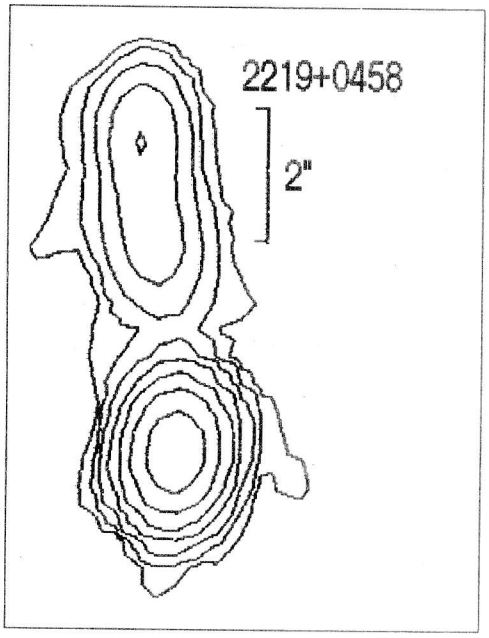
2219+0458
2"

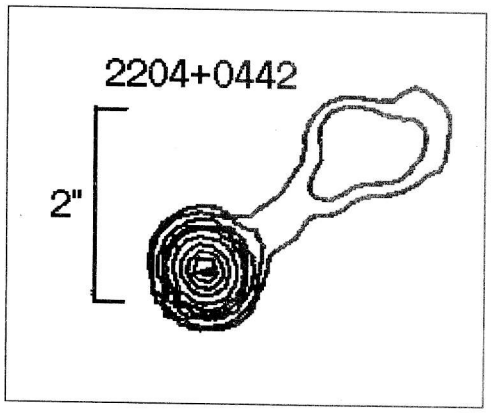
2204+0442
2"

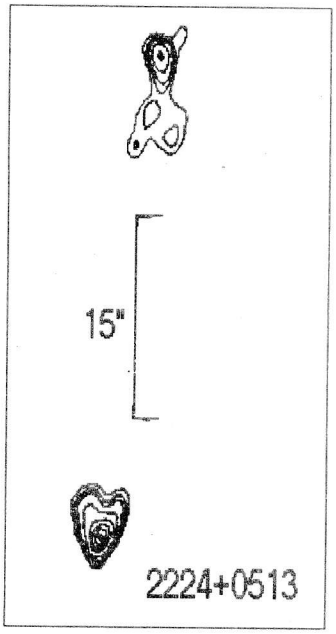
15"
2224+0513

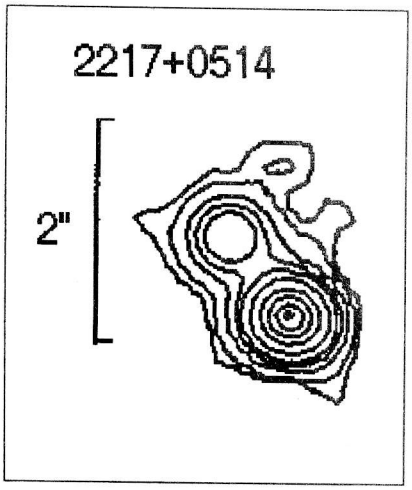
2217+0514
2"

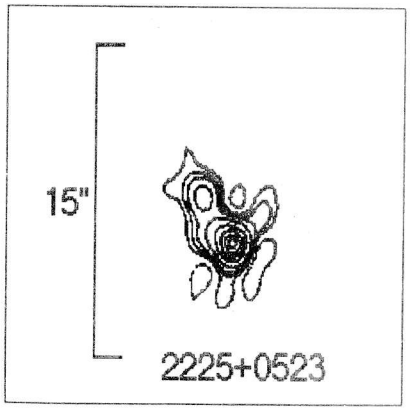
15"
2225+0523

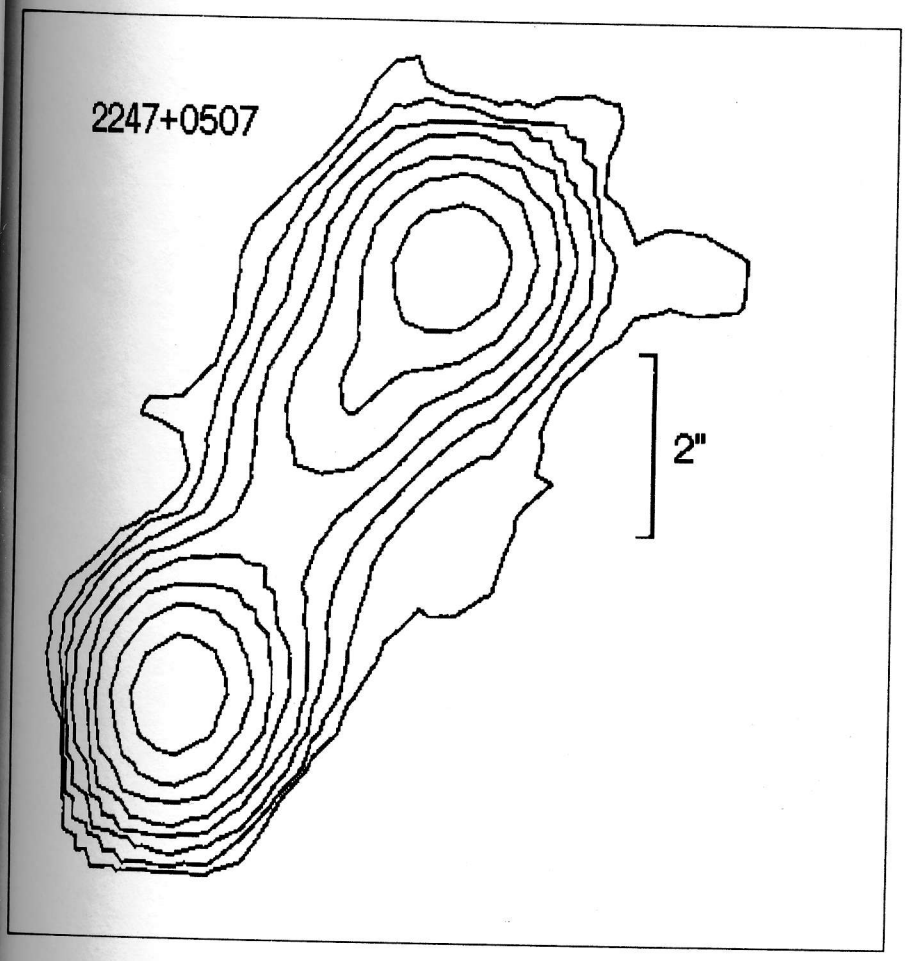
2247+0507
2"

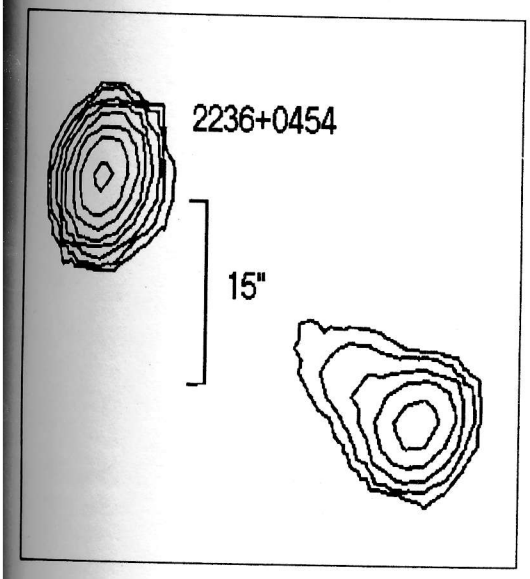
2236+0454
15"

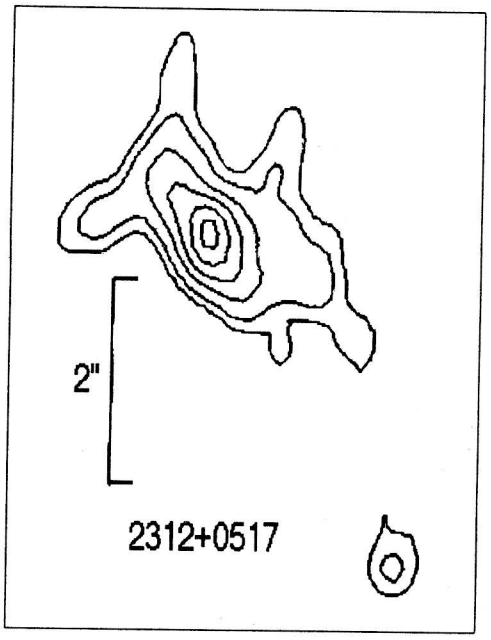
2"
2312+0517

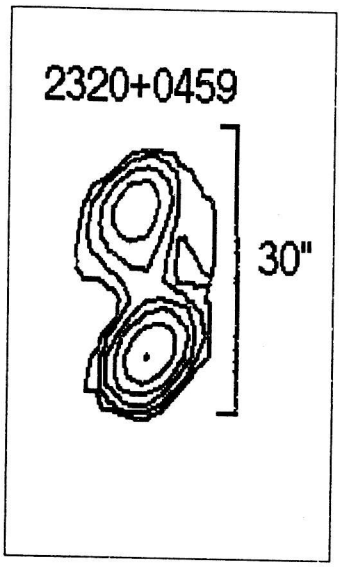
2320+0459
30"

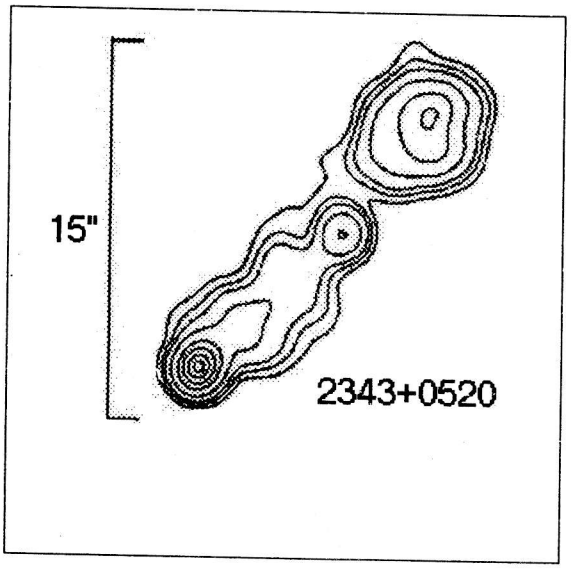
15"
2343+0520

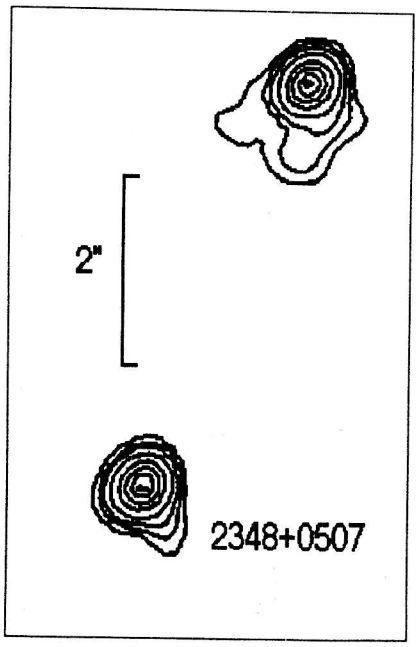
2"
2348+0507

Figure 9: CCD images of RC objects in R-filter

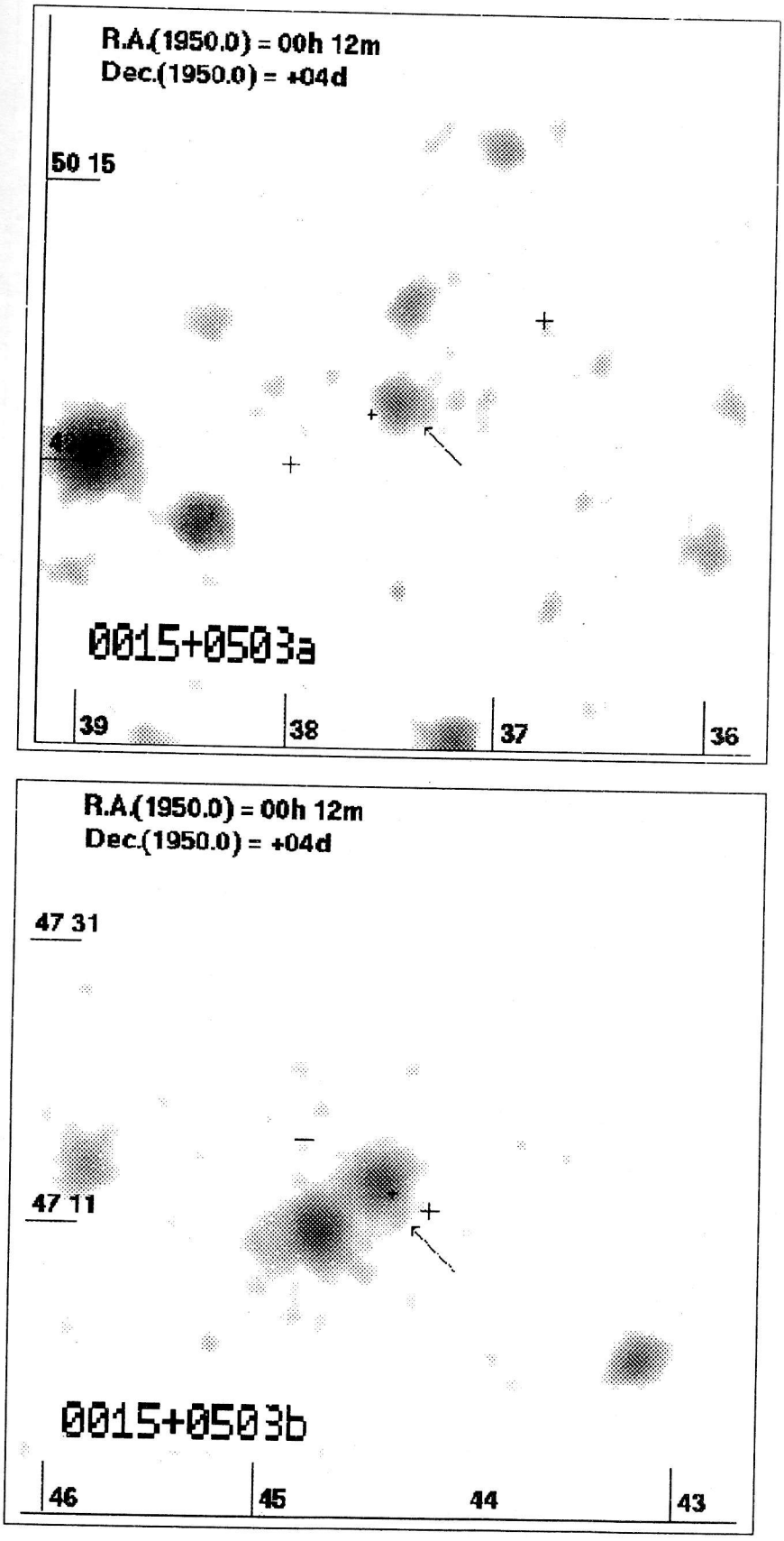

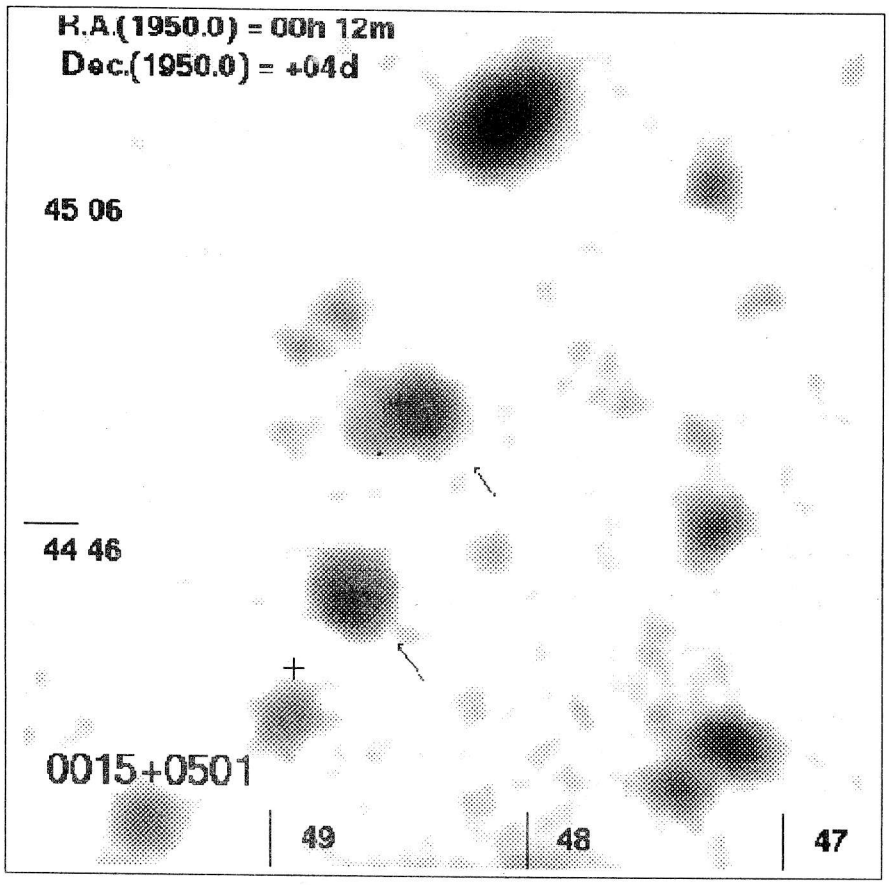
R.A.(1950.0) = 00h 12m
Dec.(1950.0) = +04d
45 06
44 46
0015+0501
49
48
47

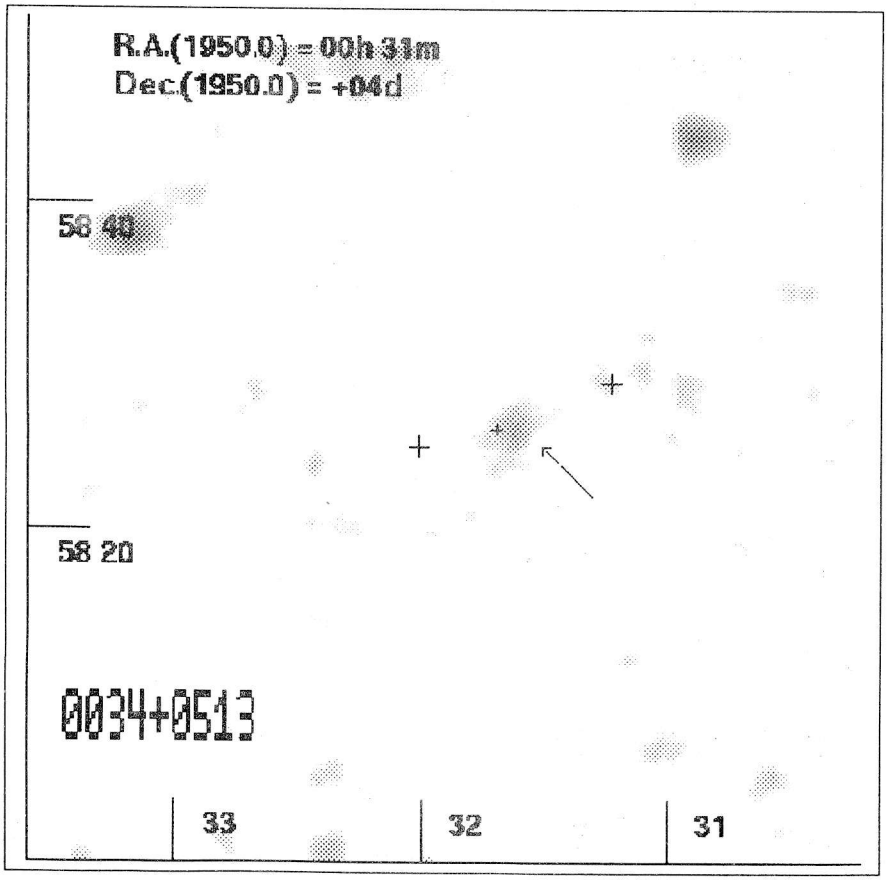
R.A.(1950.0) = 00h 31m
Dec.(1950.0) = +04d
58 40
58 20
0034+0513
33
32
31

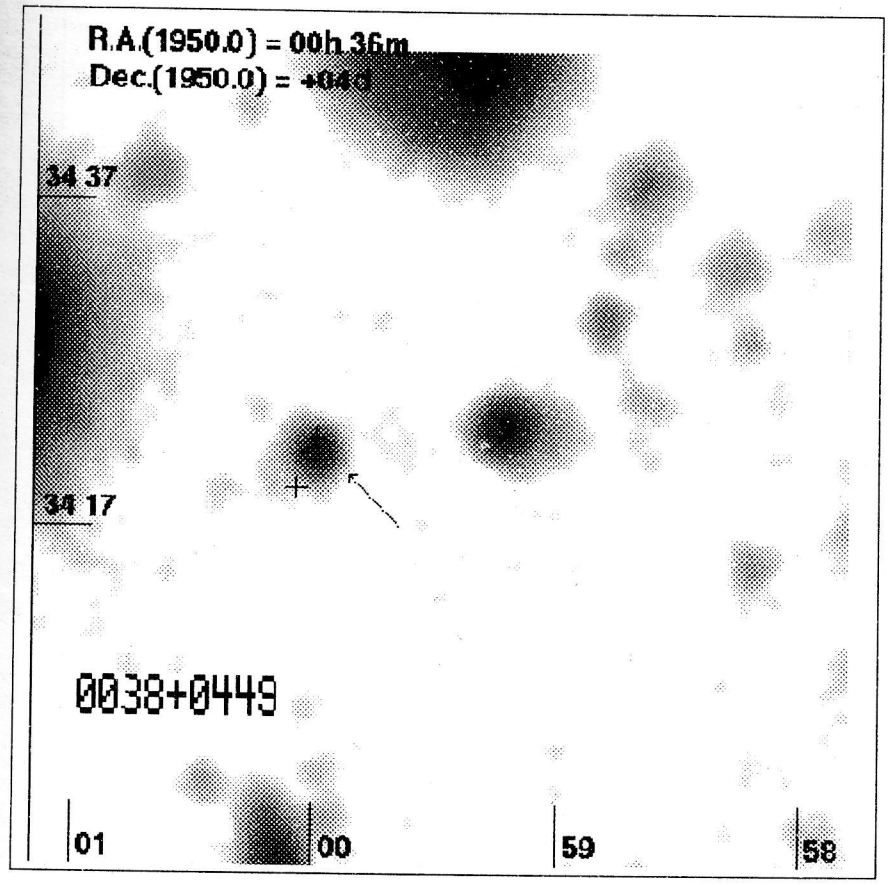
R.A.(1950.0) = 00h 36m
Dec.(1950.0) = +04d
34 37
34 17
0038+0449
01
00
59
58

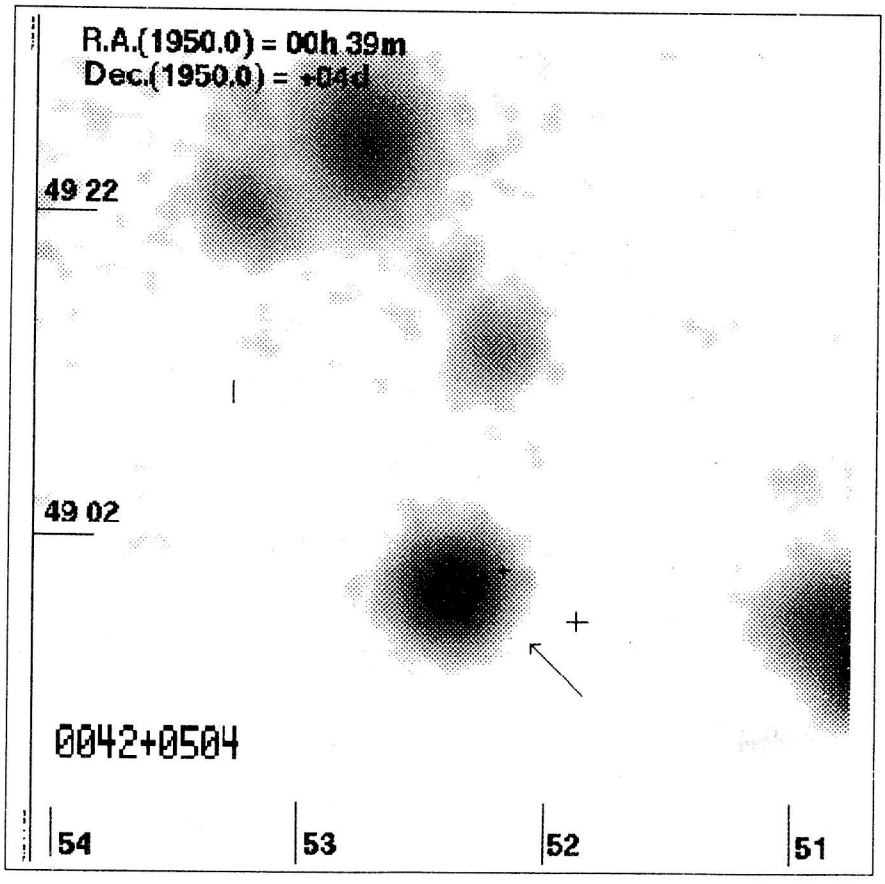
R.A.(1950.0) = 00h 39m
Dec.(1950.0) = +04d
49 22
49 02
0042+0504
54
53
52
51

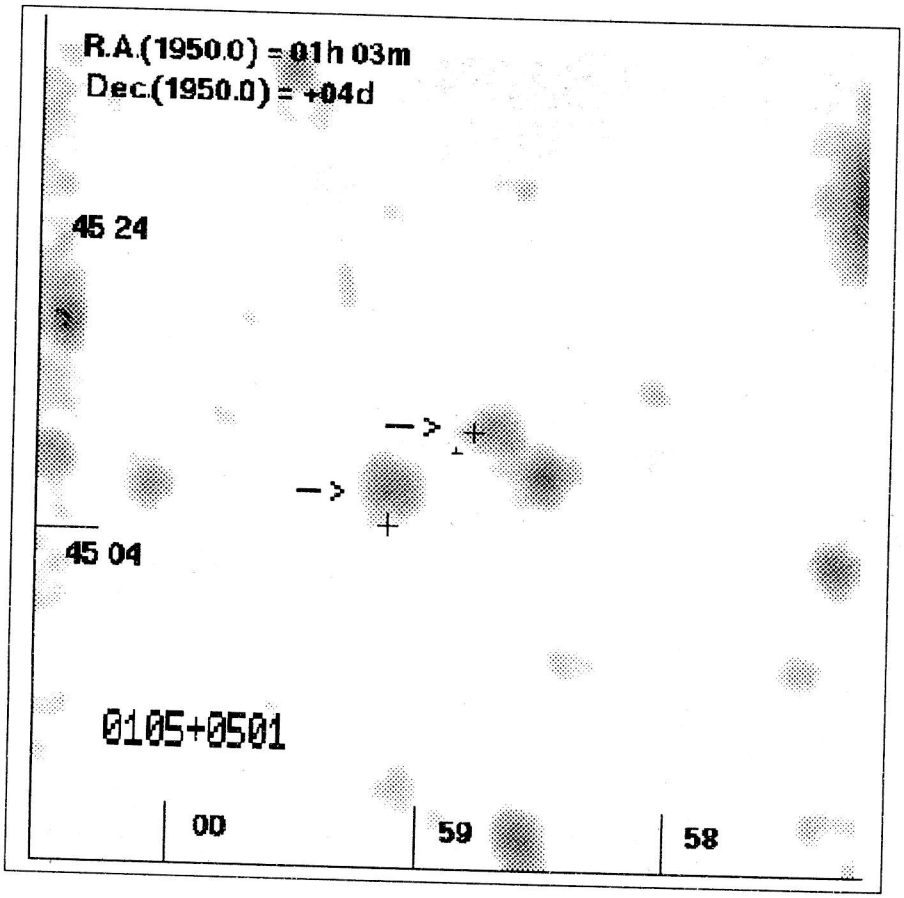
R.A.(1950.0) = 01h 03m
Dec.(1950.0) = +04d
45 24
45 04
0105+0501
00
59
58

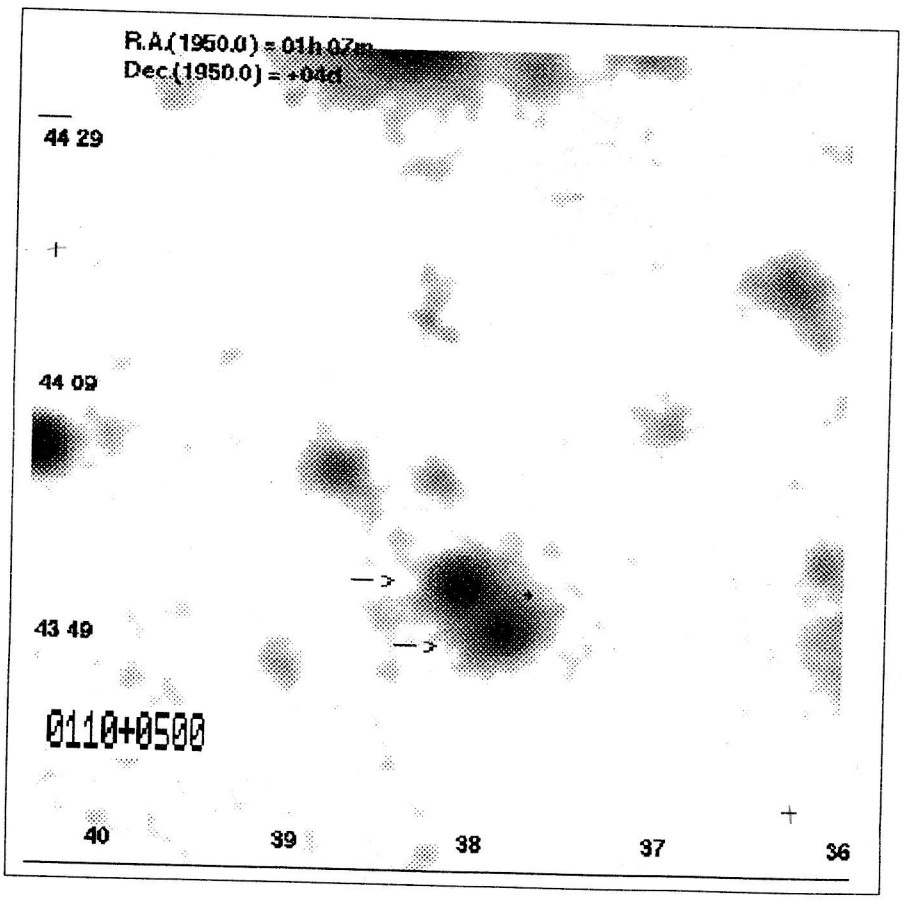
R.A.(1950.0) = 01h 07m
Dec.(1950.0) = +04d
44 29
44 09
43 49
0110+0500
40
39
38
37
36

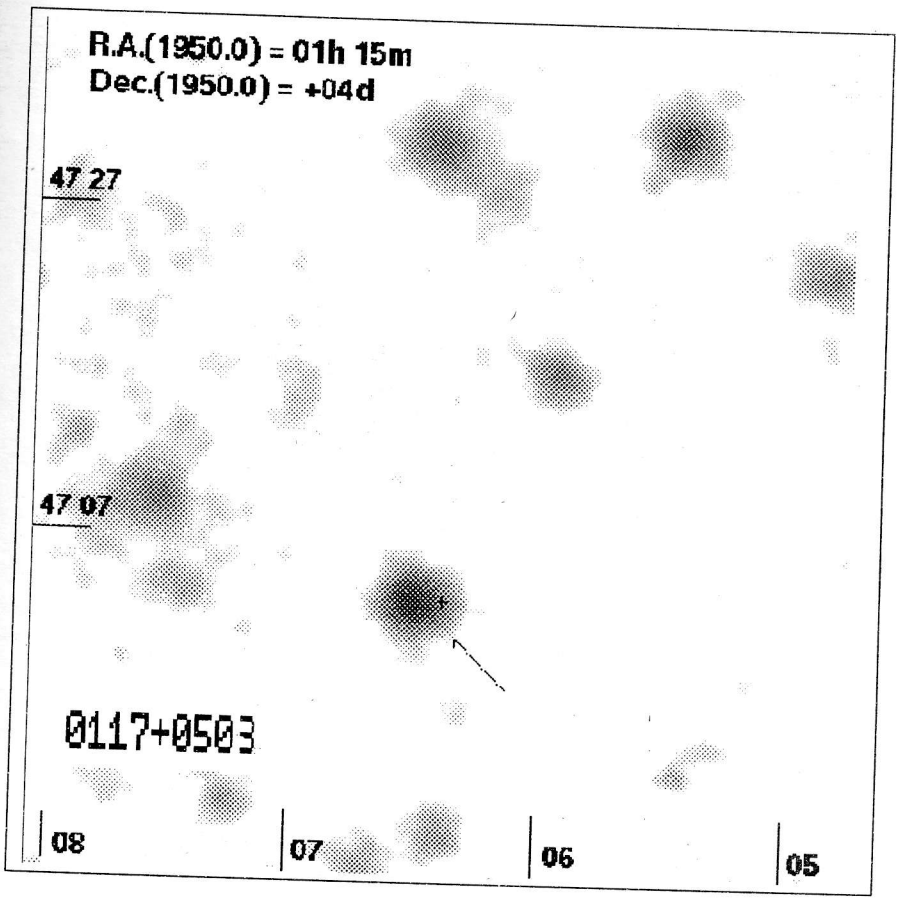
R.A.(1950.0) = 01h 15m
Dec.(1950.0) = +04d
47 27
47 07
0117+0503
08
07
06
05

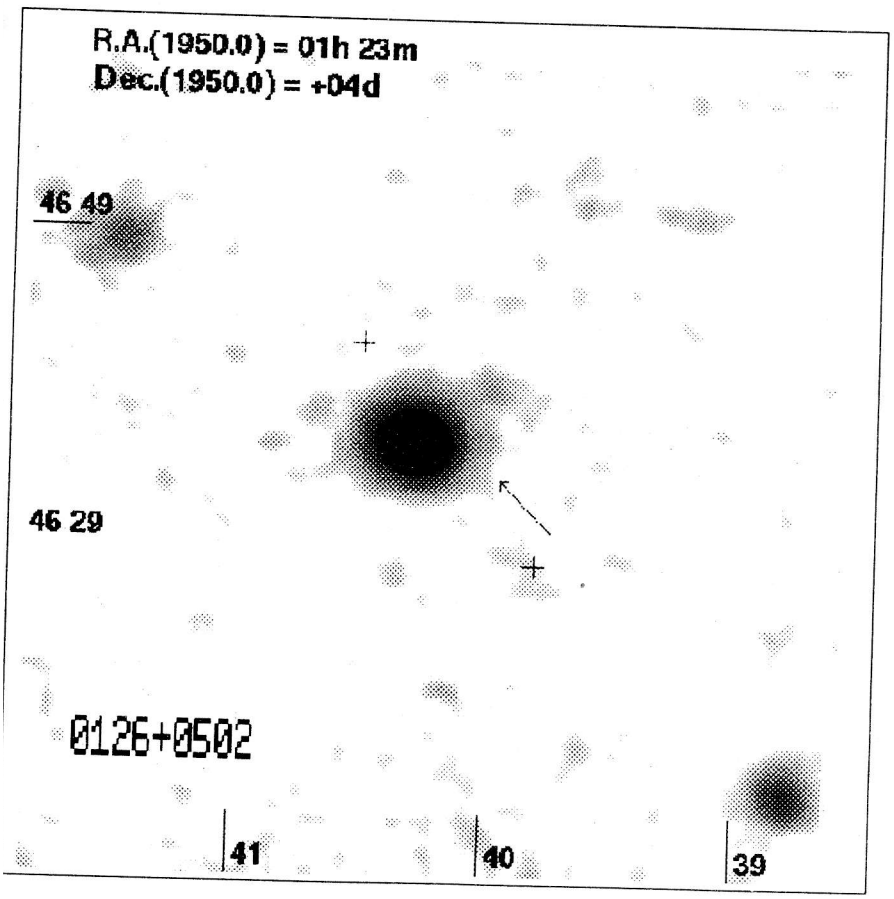
R.A.(1950.0) = 01h 23m
Dec.(1950.0) = +04d
46 49
46 29
0126+0502
41
40
39

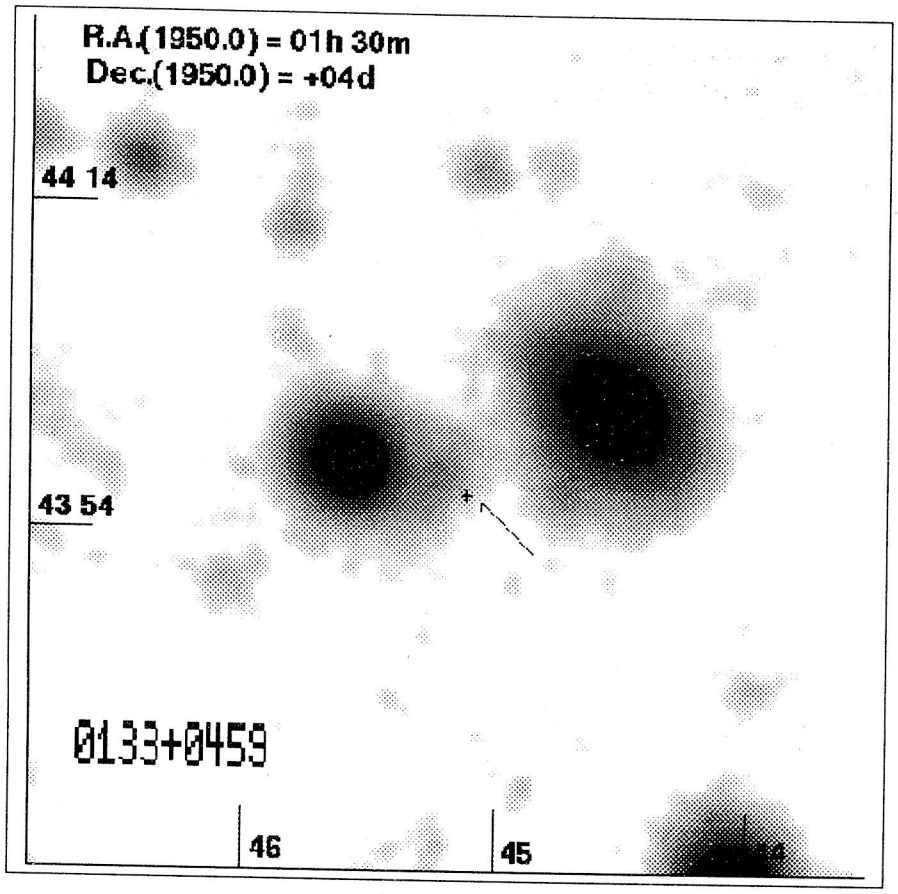
R.A.(1950.0) = 01h 30m
Dec.(1950.0) = +04d
44 14
43 54
0133+0459
46
45

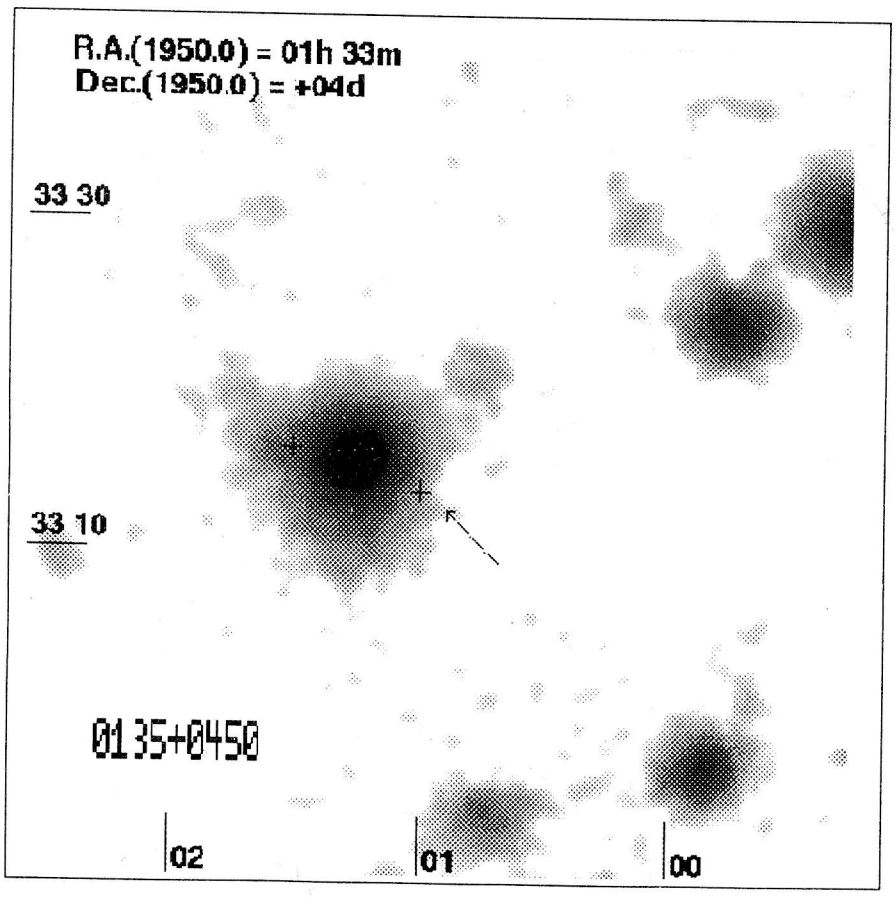
R.A.(1950.0) = 01h 33m
Dec.(1950.0) = +04d
33 30
33 10
0135+0450
02
01
00

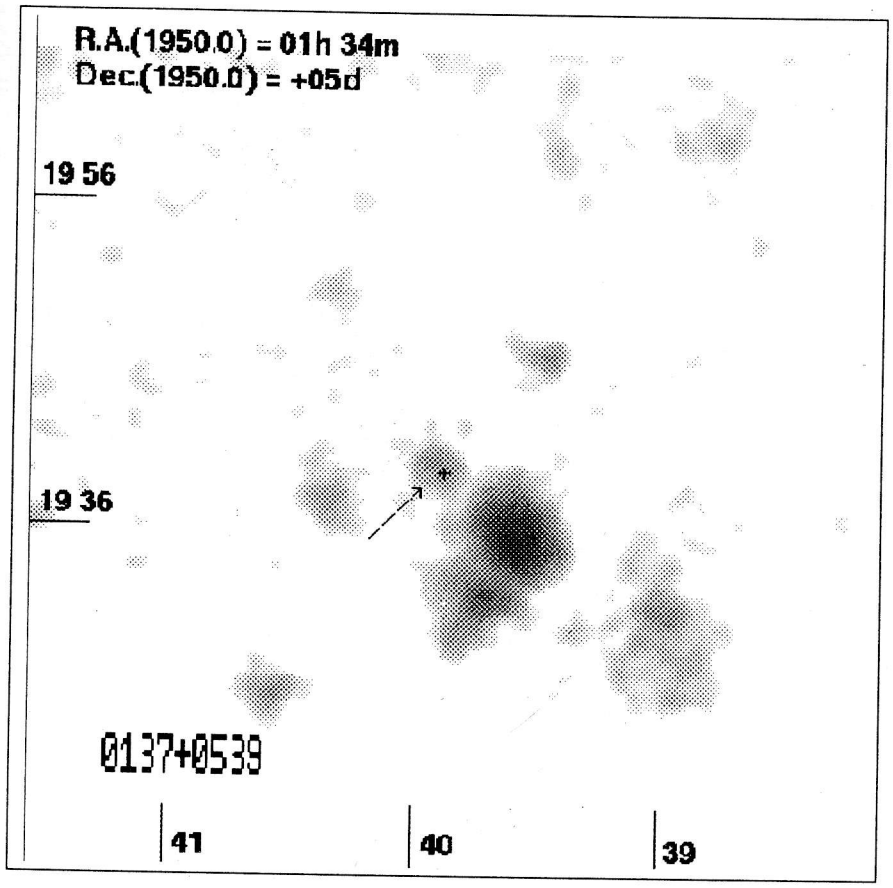
R.A.(1950.0) = 01h 34m
Dec.(1950.0) = +05d
19 56
19 36
0137+0539
41
40
39

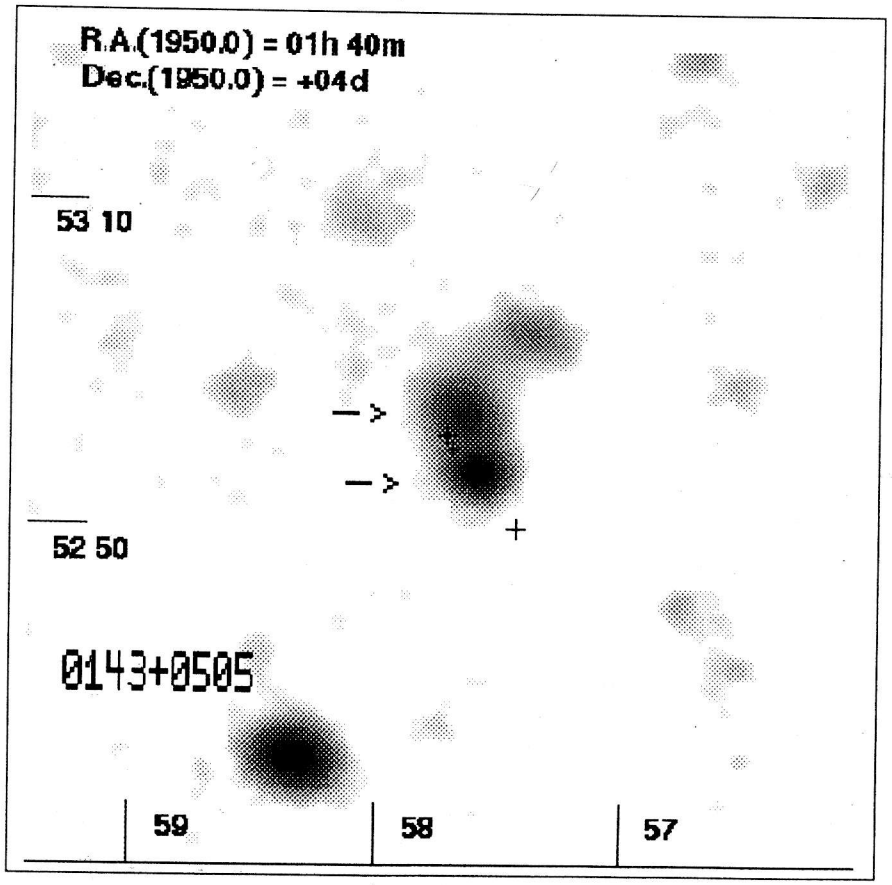
R.A.(1950.0) = 01h 40m
Dec.(1950.0) = +04d
53 10
52 50
0143+0505
59
58
57

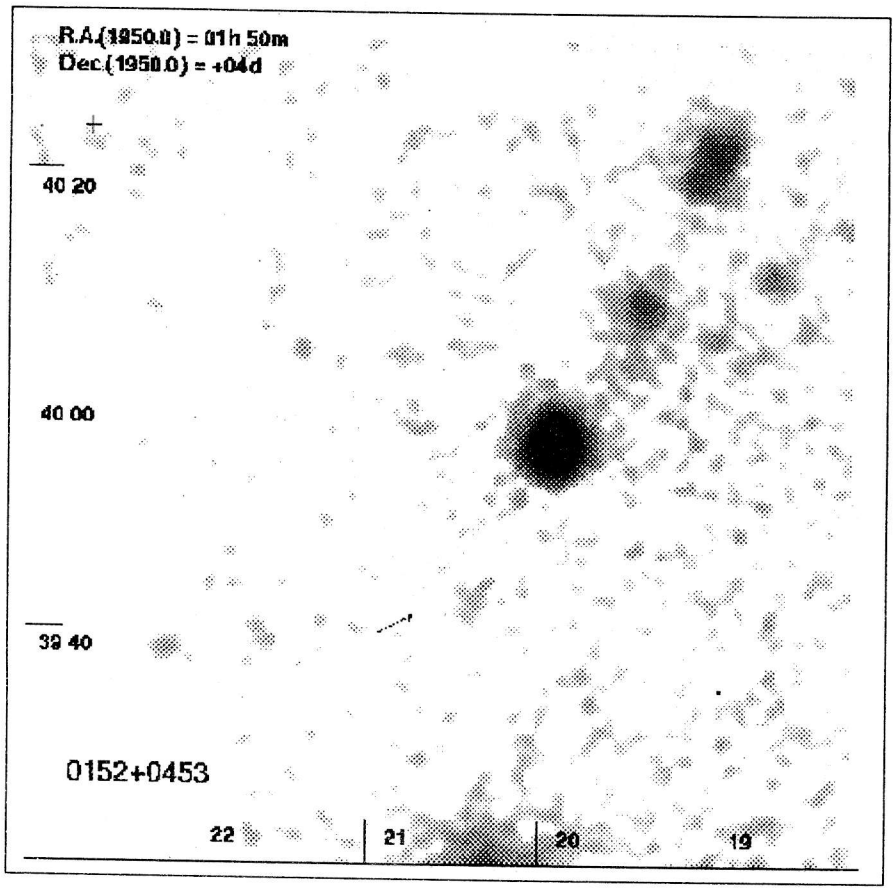
R.A.(1950.0) = 01h 50m
Dec.(1950.0) = +04d
40 20
40 00
39 40
0152+0453
22
21
20
19

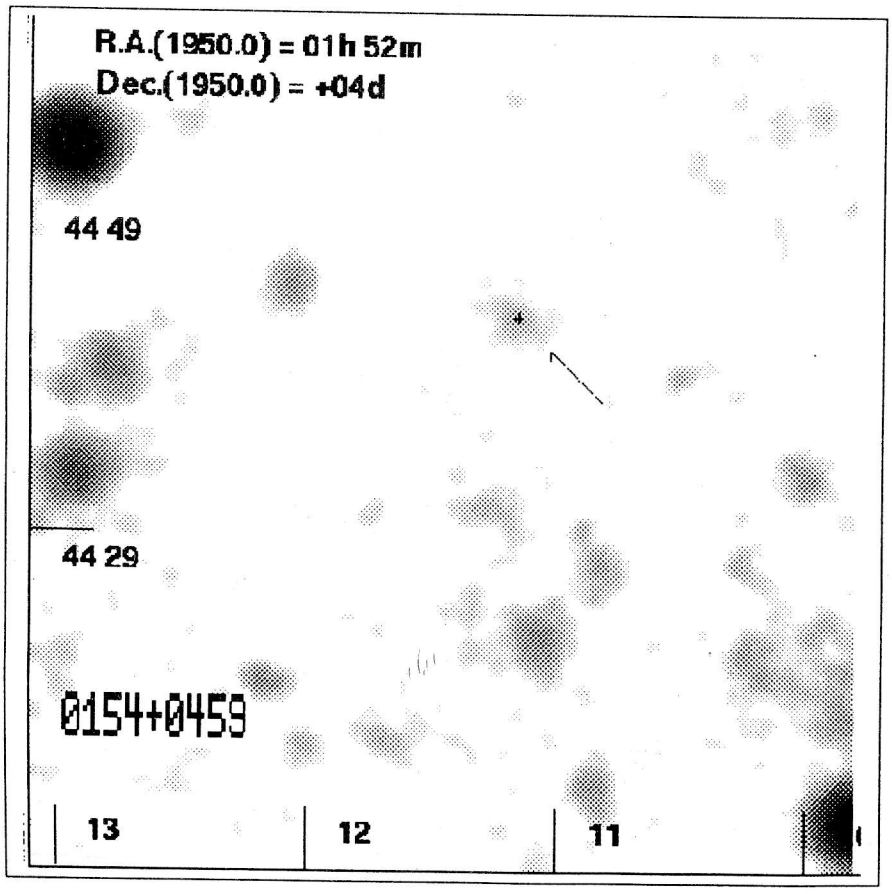
R.A.(1950.0) = 01h 52m
Dec.(1950.0) = +04d
44 49
44 29
0154+0459
13
12
11

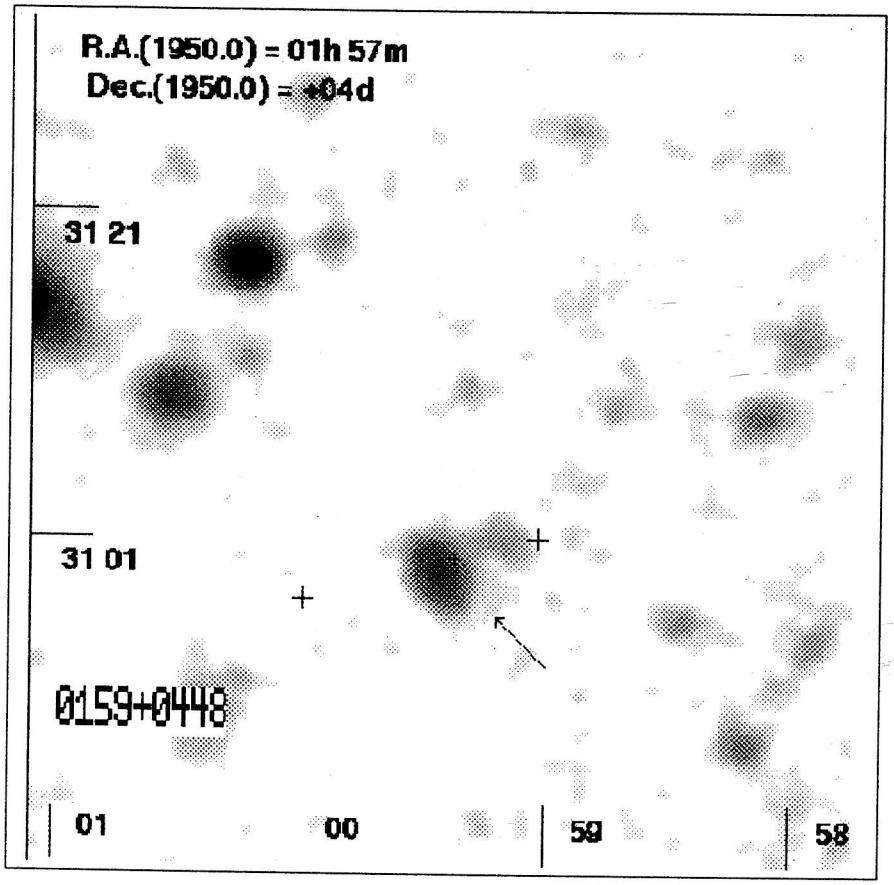
R.A.(1950.0) = 01h 57m
Dec.(1950.0) = +04d
31 21
31 01
0159+0448
01
00
59
58

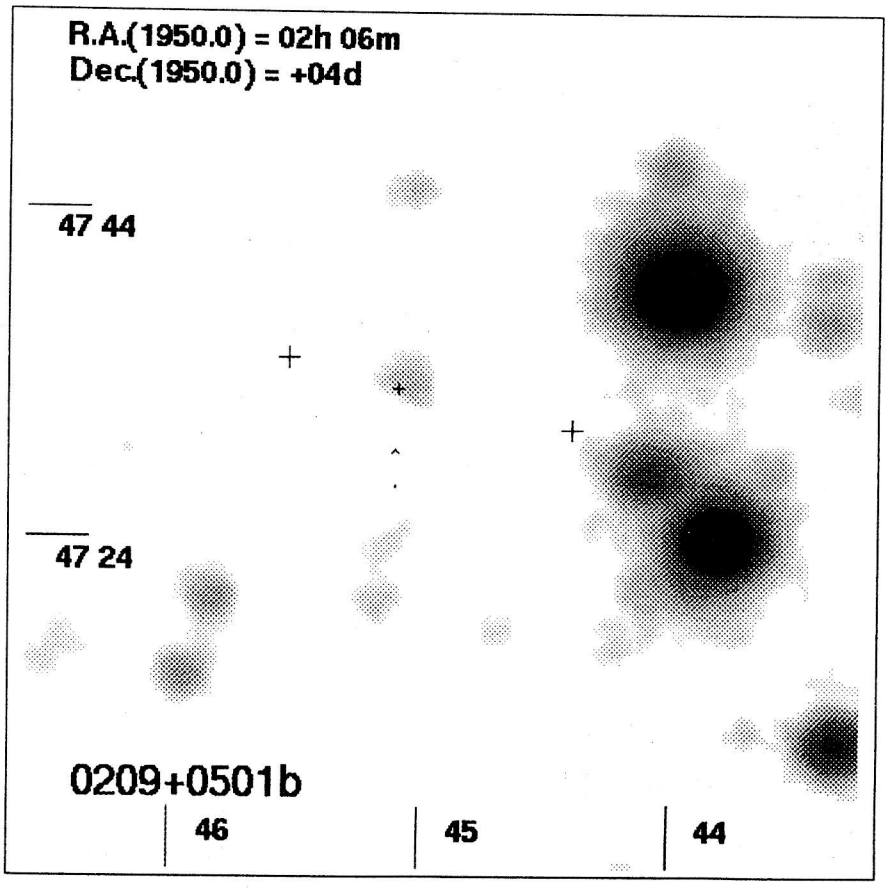
R.A.(1950.0) = 02h 06m
Dec.(1950.0) = +04d
47 44
47 24
0209+0501b
46
45
44

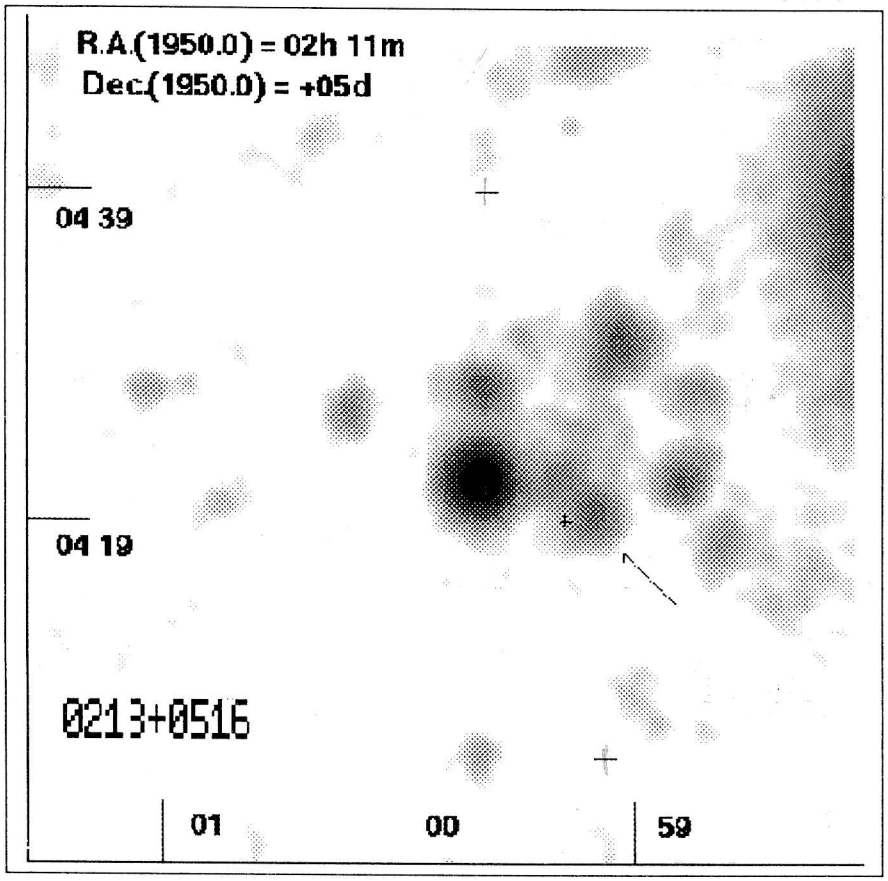
R.A.(1950.0) = 02h 11m
Dec.(1950.0) = +05d
04 39
04 19
0213+0516
01
00
59

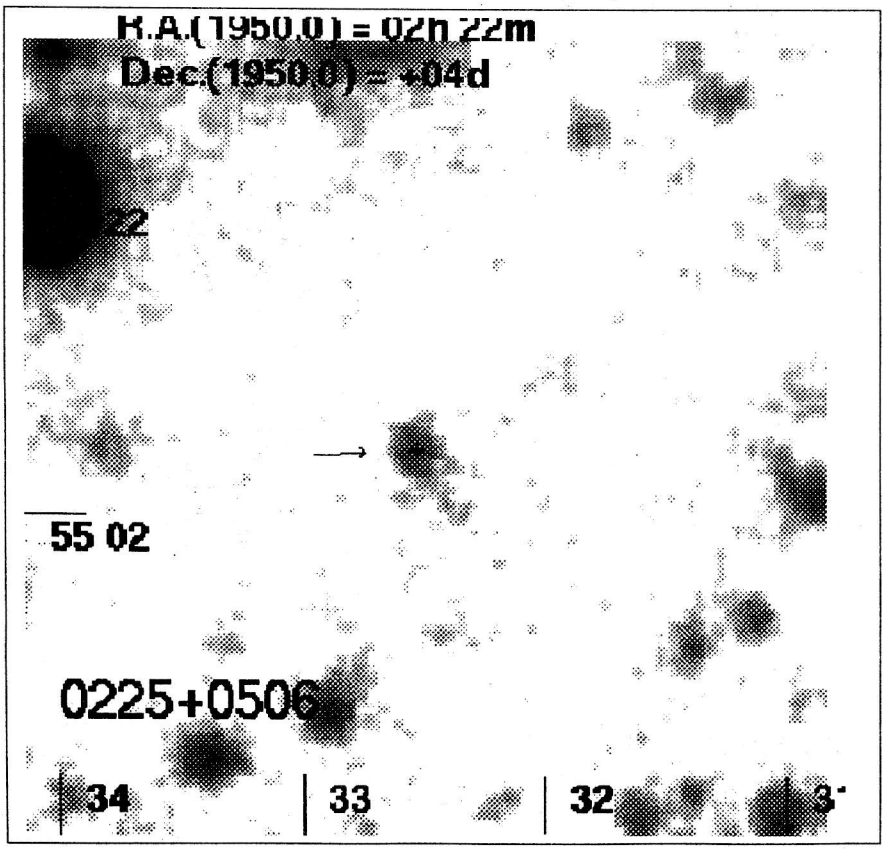
R.A.(1950.0) = 02h 22m
Dec.(1950.0) = +04d
22
55 02
0225+0506
34
33
32

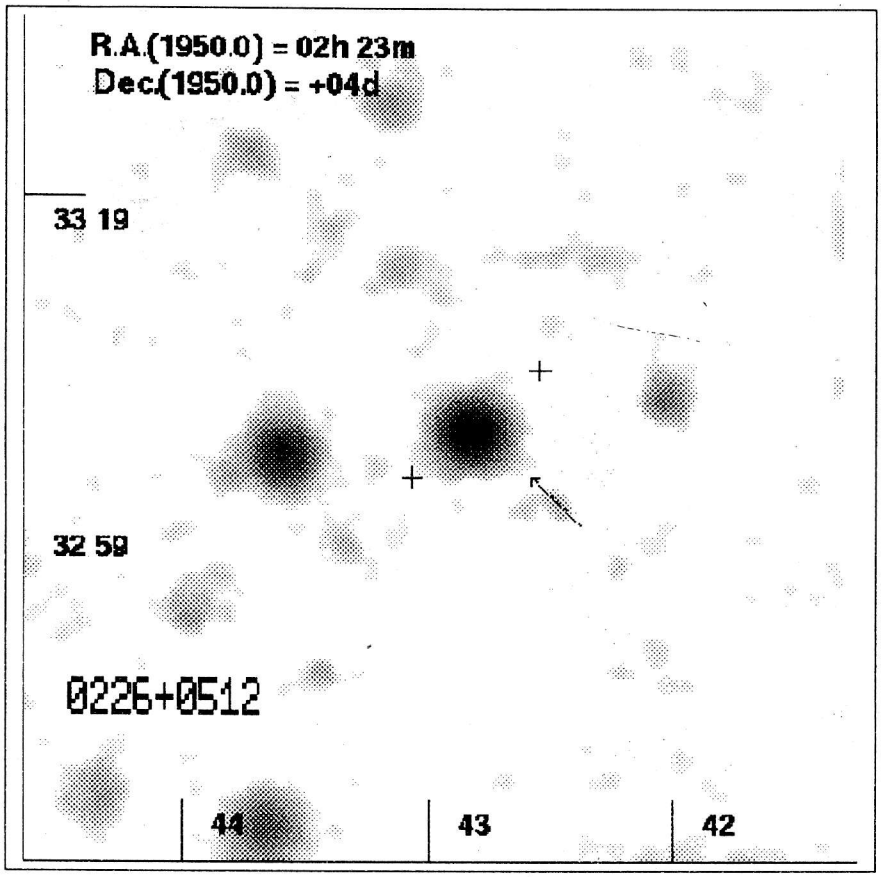
R.A.(1950.0) = 02h 23m
Dec.(1950.0) = +04d
33 19
32 59
0226+0512
44
43
42

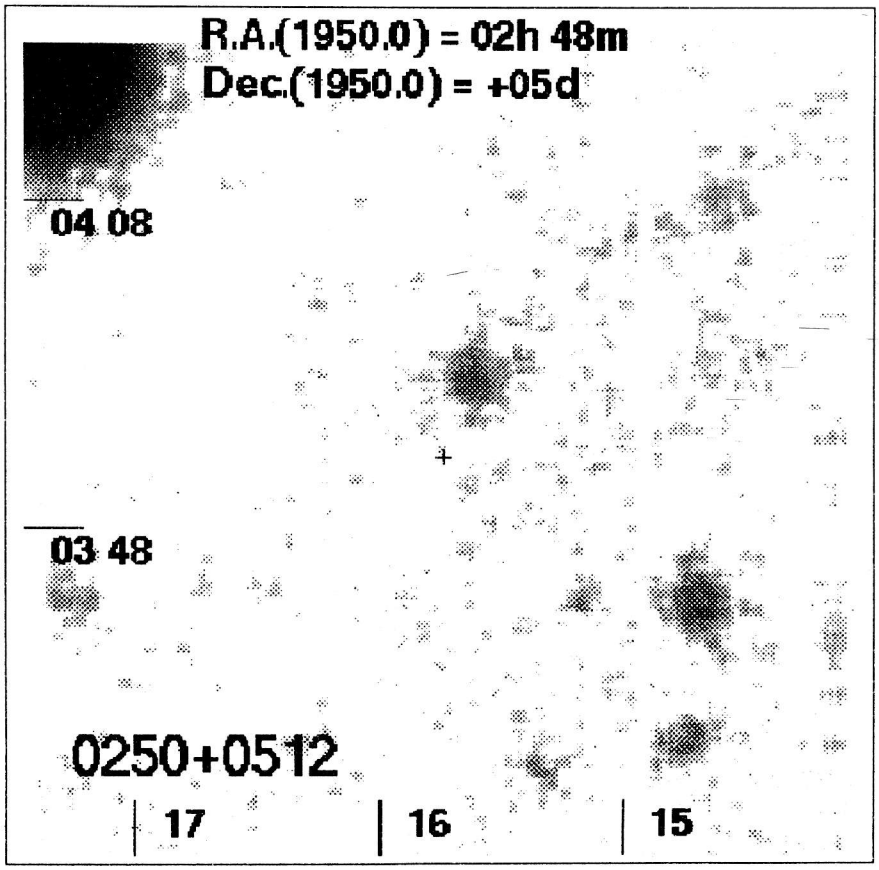
R.A.(1950.0) = 02h 48m
Dec.(1950.0) = +05d
04 08
03 48
0250+0512
17
16
15

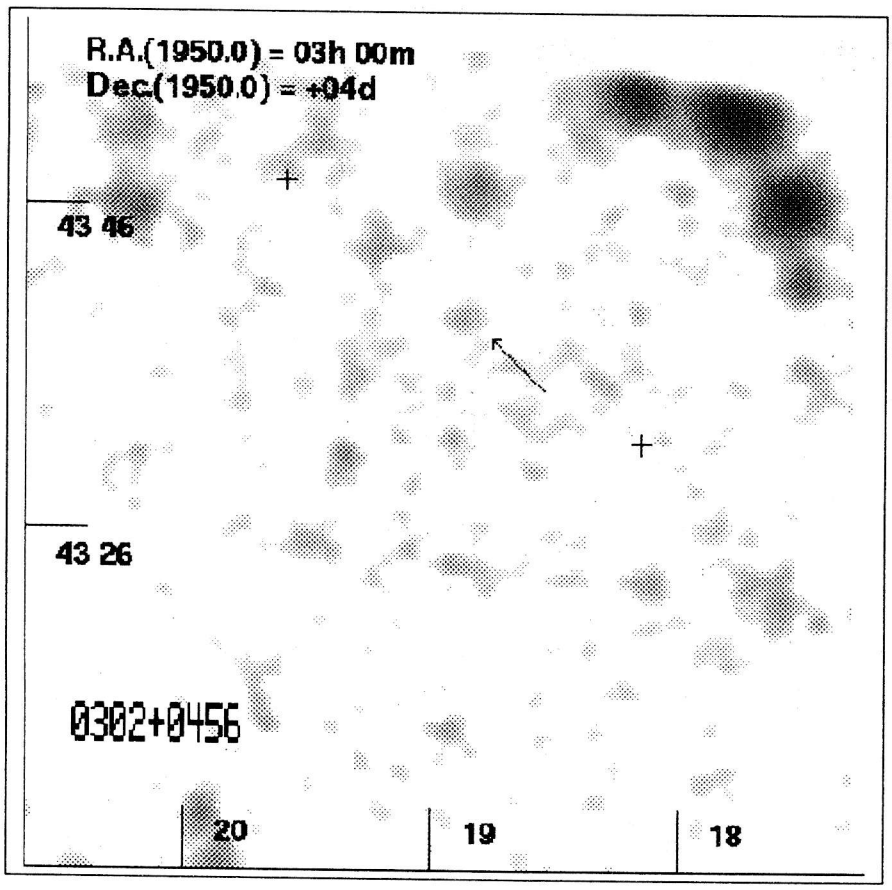
R.A.(1950.0) = 03h 00m
Dec.(1950.0) = +04d
43 46
43 26
0302+0456
20
19
18

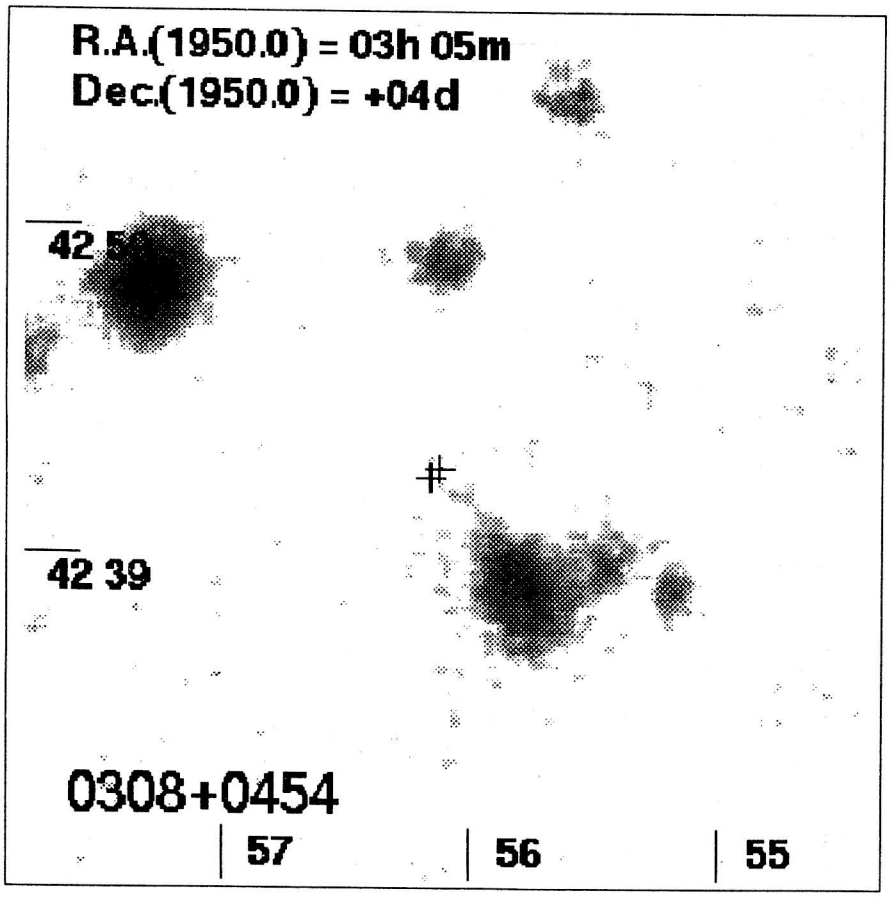
R.A.(1950.0) = 03h 05m
Dec.(1950.0) = +04d
42 39
0308+0454
57
56
55

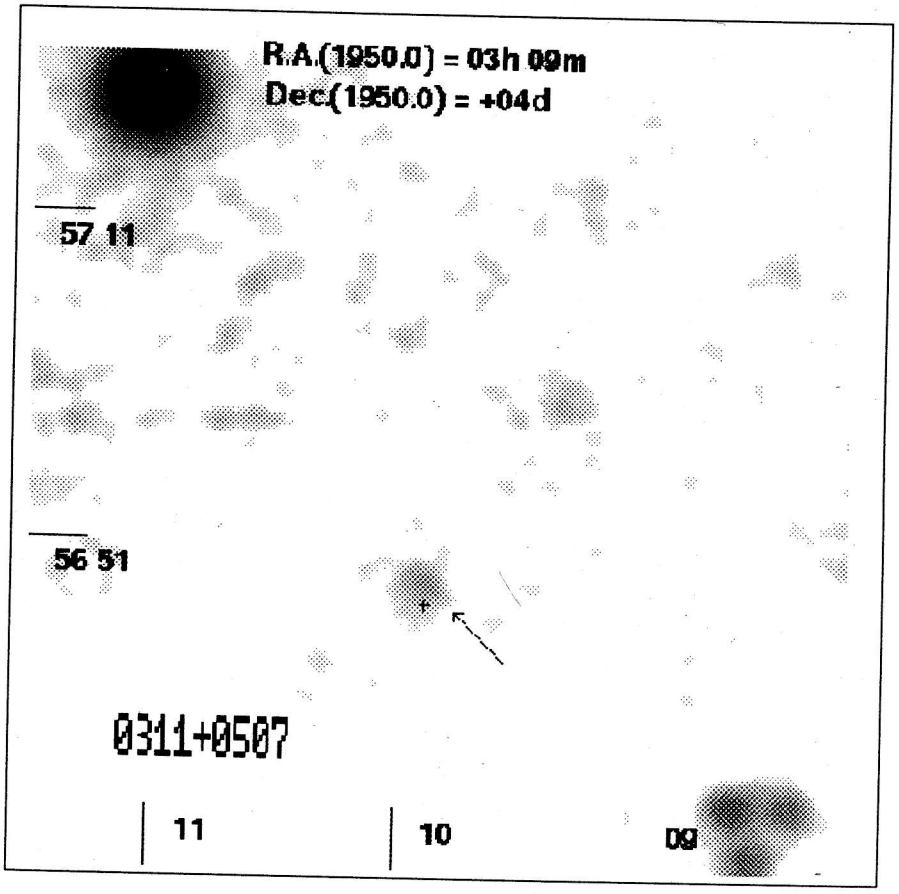
R.A.(1950.0) = 03h 09m
Dec.(1950.0) = +04d
57 11
56 51
0311+0507
11
10
09

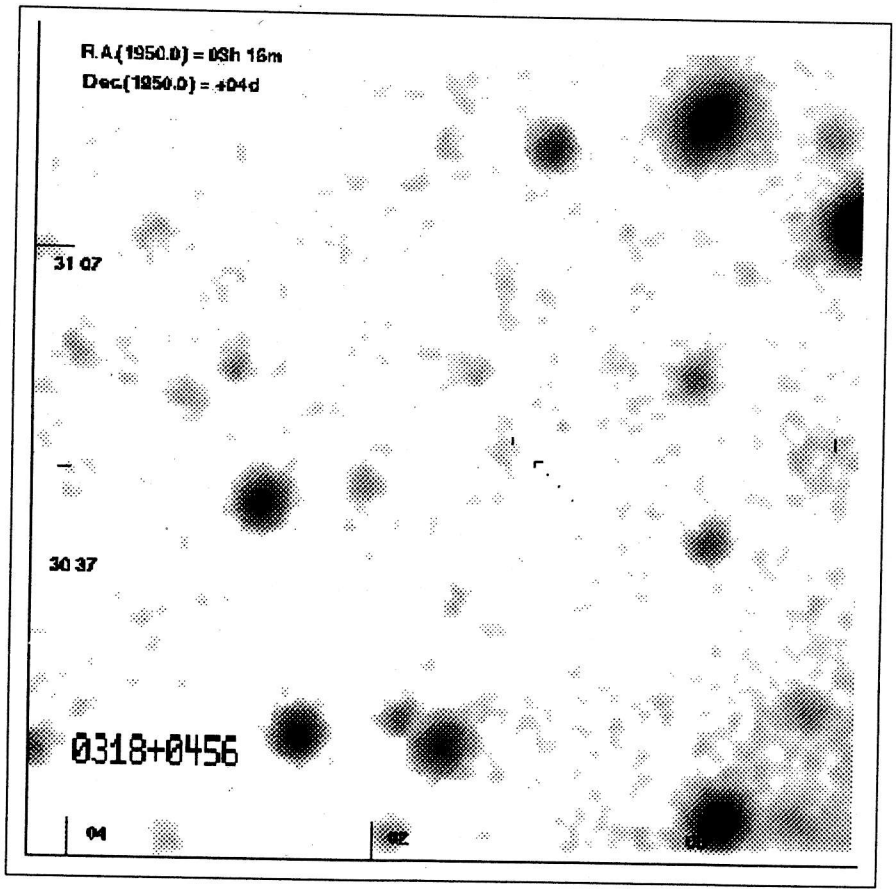
R.A.(1950.0) = 03h 16m
Dec.(1950.0) = +04d
31 07
30 37
0318+0456
04
02

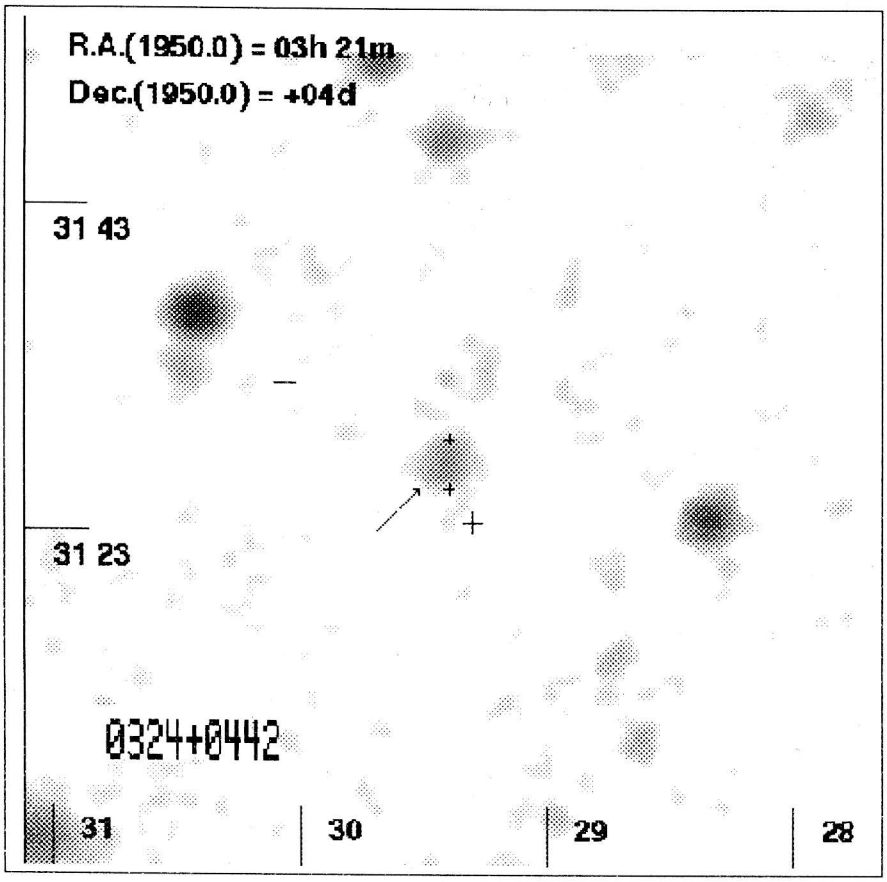
R.A.(1950.0) = 03h 21m
Dec.(1950.0) = +04d
31 43
31 23
0324+0442
31
30
29
28

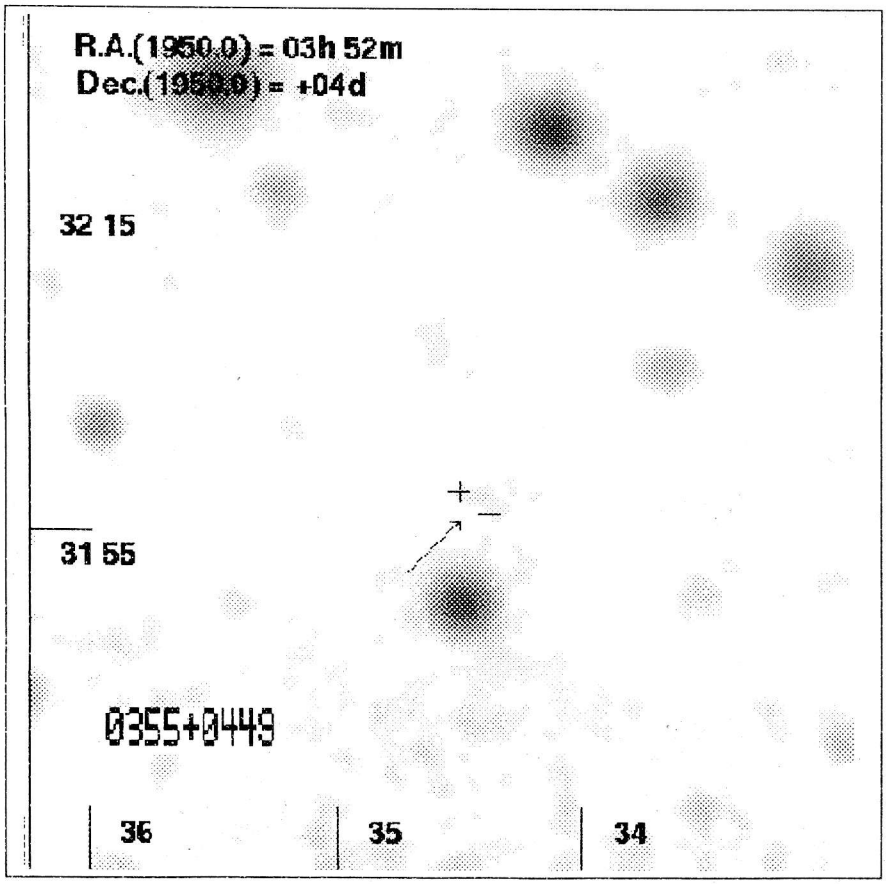
R.A.(1950.0) = 03h 52m
Dec.(1950.0) = +04d
32 15
31 55
0355+0449
36
35
34

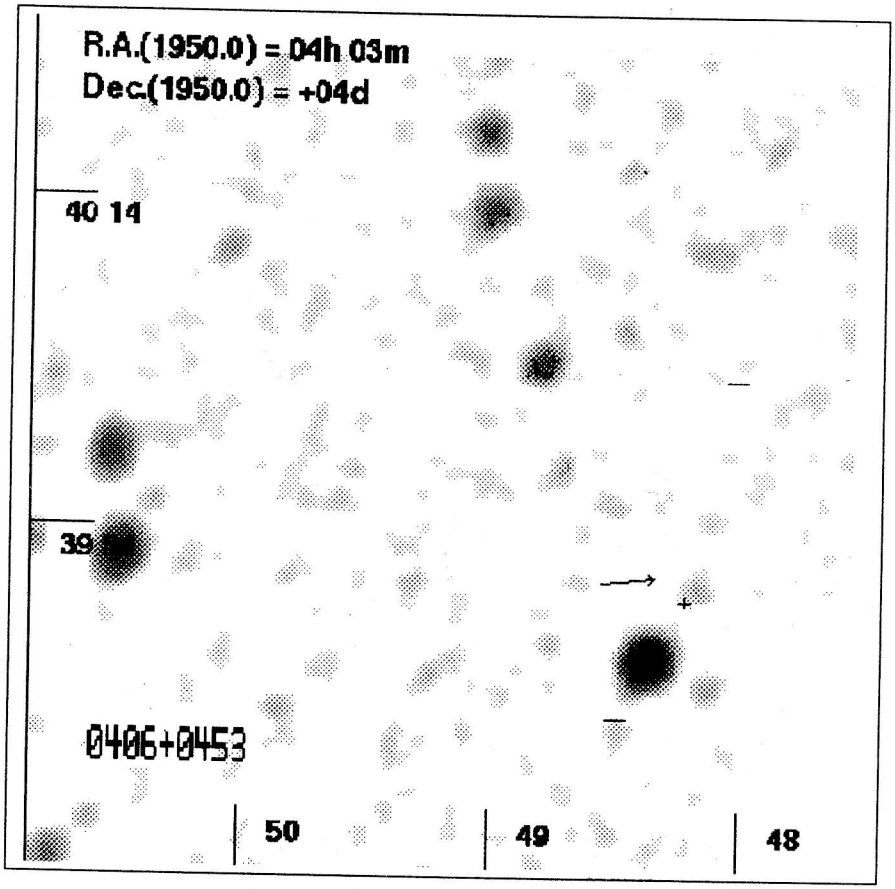
R.A.(1950.0) = 04h 03m
Dec.(1950.0) = +04d
40 14
39
0406+0453
50
49
48

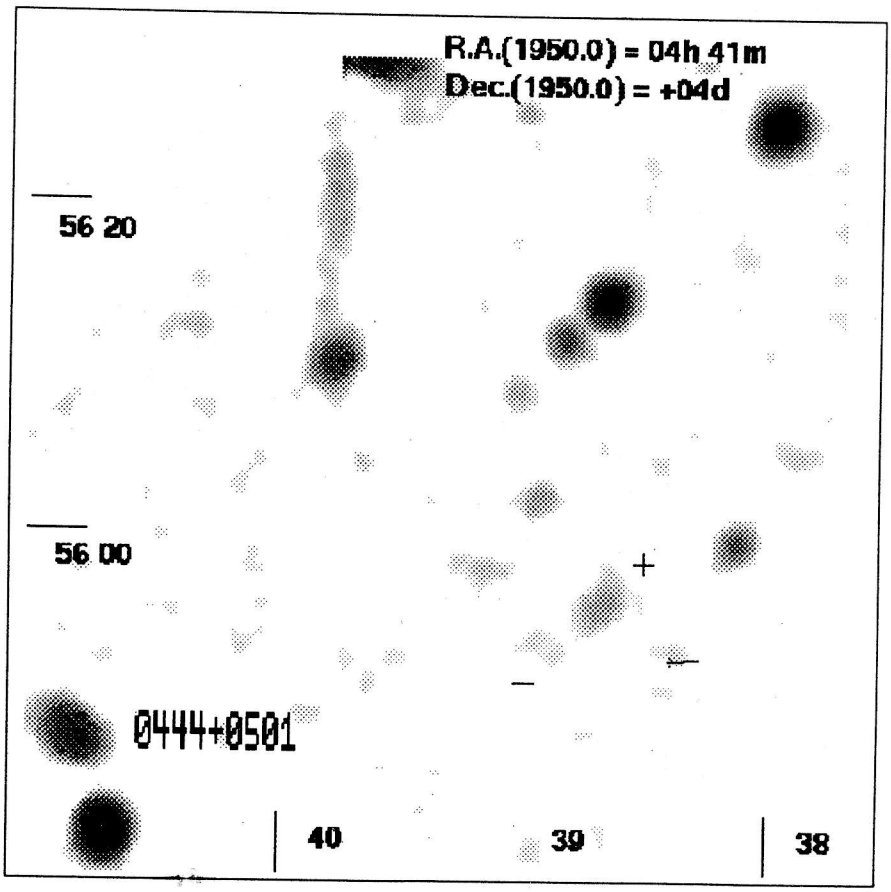
R.A.(1950.0) = 04h 41m
Dec.(1950.0) = +04d
56 20
56 00
0444+0501
40
39
38

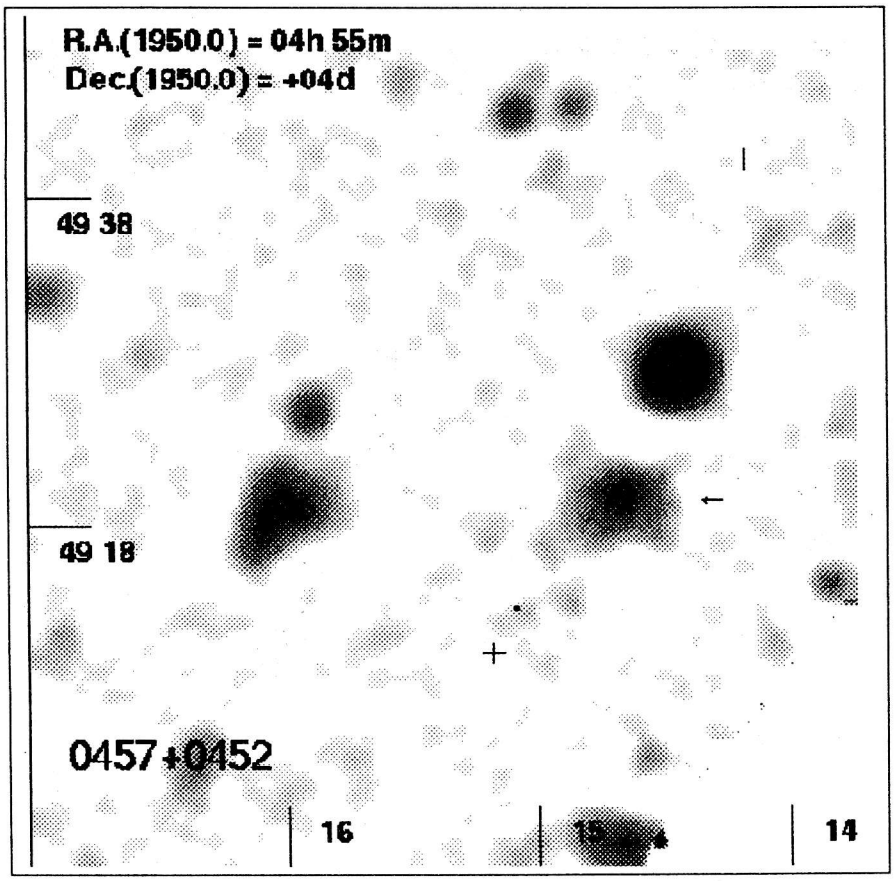
R.A.(1950.0) = 04h 55m
Dec.(1950.0) = +04d
49 38
49 18
0457+0452
16
14

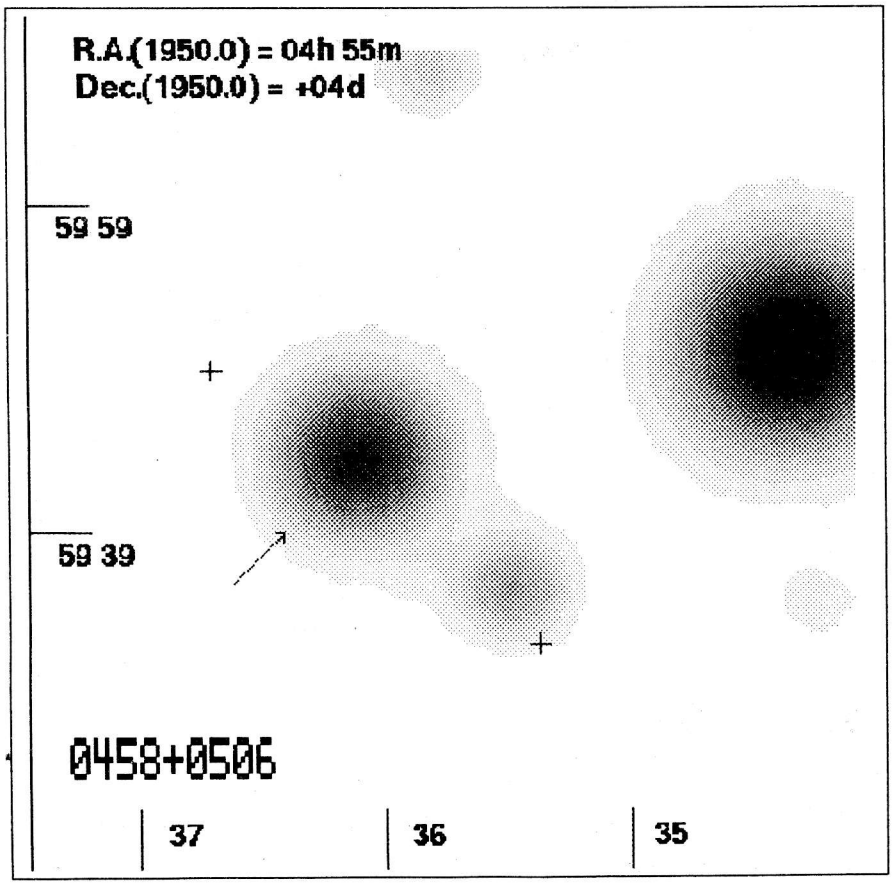
R.A.(1950.0) = 04h 55m
Dec.(1950.0) = +04d
59 59
59 39
0458+0506
37
36
35

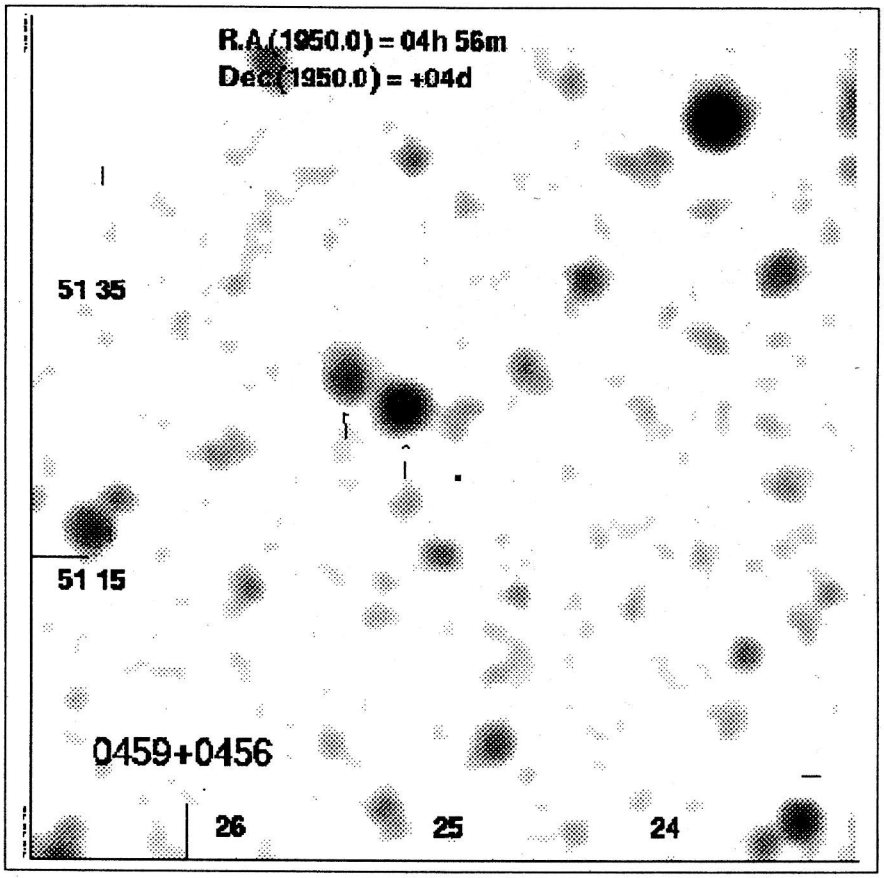
R.A.(1950.0) = 04h 56m
Dec.(1950.0) = +04d
51 35
51 15
0459+0456
26
25
24

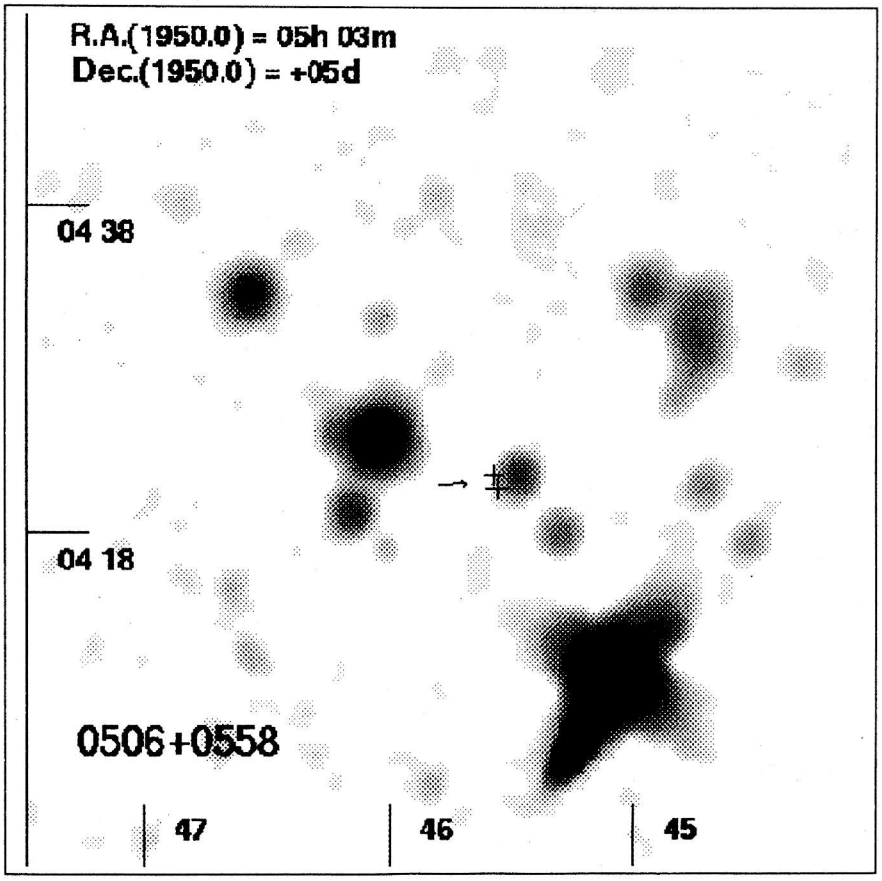
R.A.(1950.0) = 05h 03m
Dec.(1950.0) = +05d
04 38
04 18
0506+0558
47
46
45

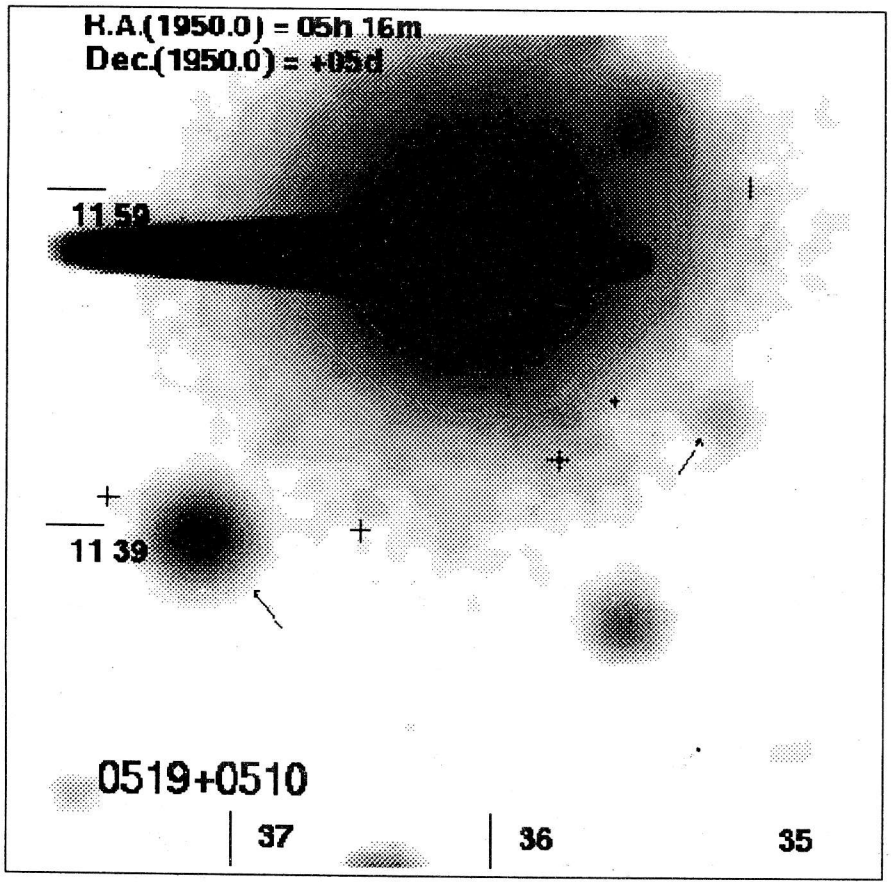
R.A.(1950.0) = 05h 16m
Dec.(1950.0) = +05d
11 59
11 39
0519+0510
37
36
35

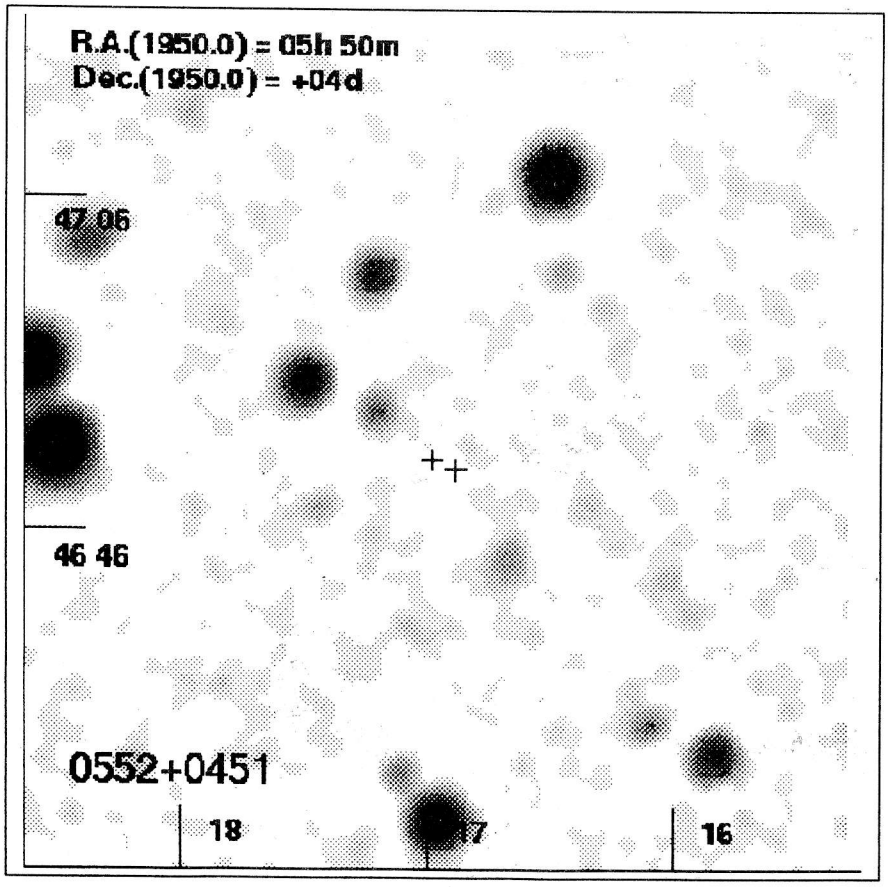
R.A.(1950.0) = 05h 50m
Dec.(1950.0) = +04d
47 06
46 46
0552+0451
18
17
16

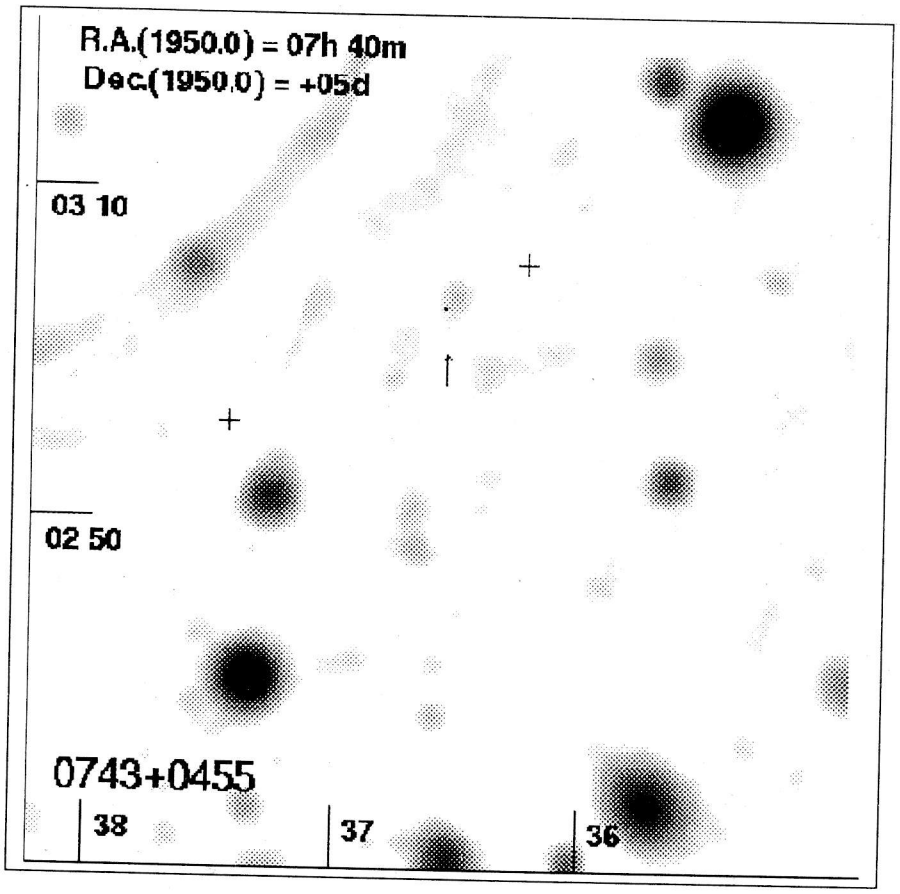
R.A.(1950.0) = 07h 40m
Dec.(1950.0) = +05d
03 10
02 50
0743+0455
38
37
36

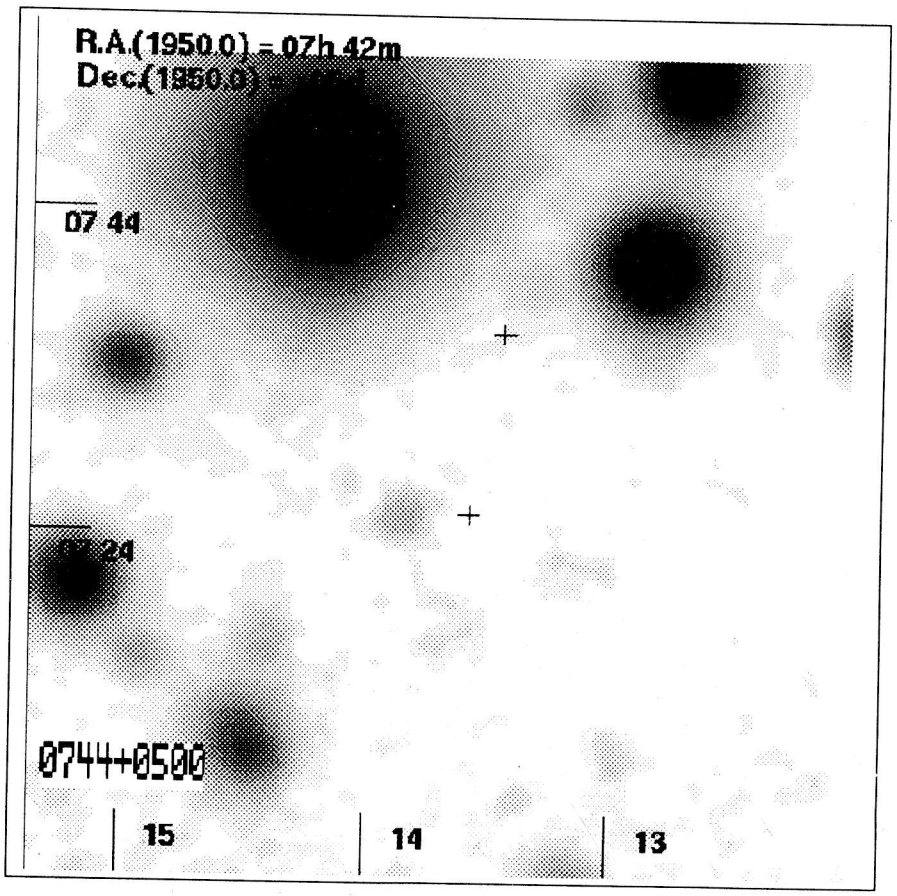
R.A.(1950.0) = 07h 42m
07 44
07 24
0744+0500
15
14
13

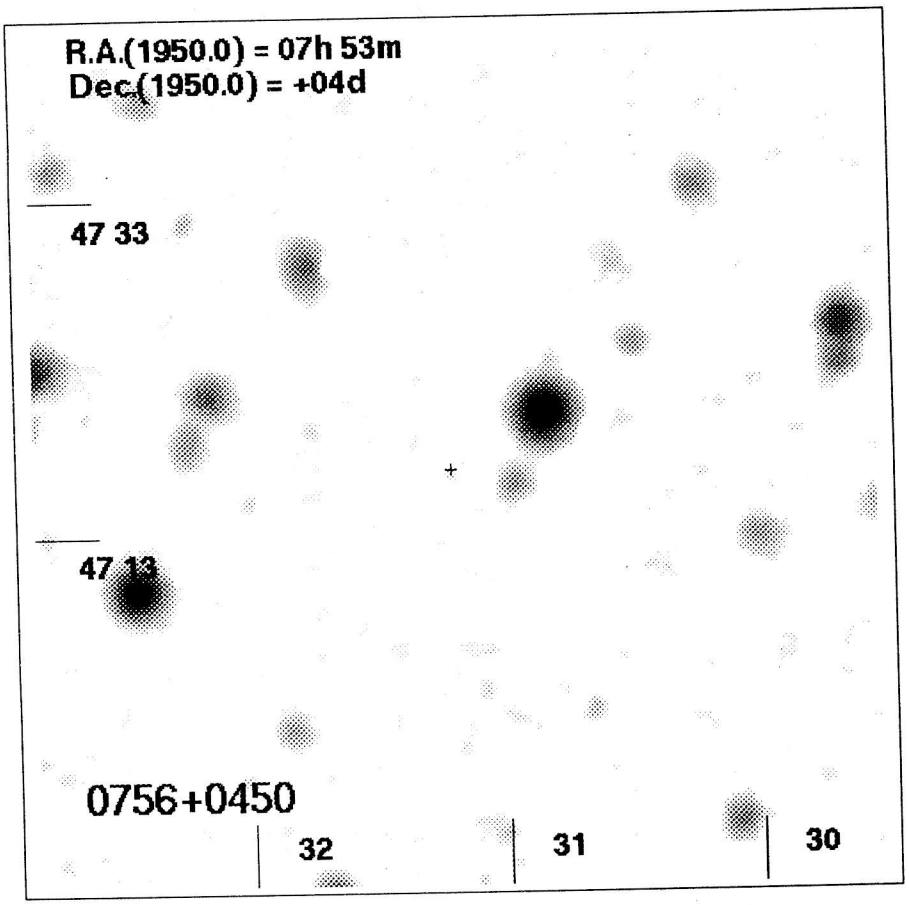
R.A.(1950.0) = 07h 53m
Dec.(1950.0) = +04d
47 33
47 13
0756+0450
32
31
30

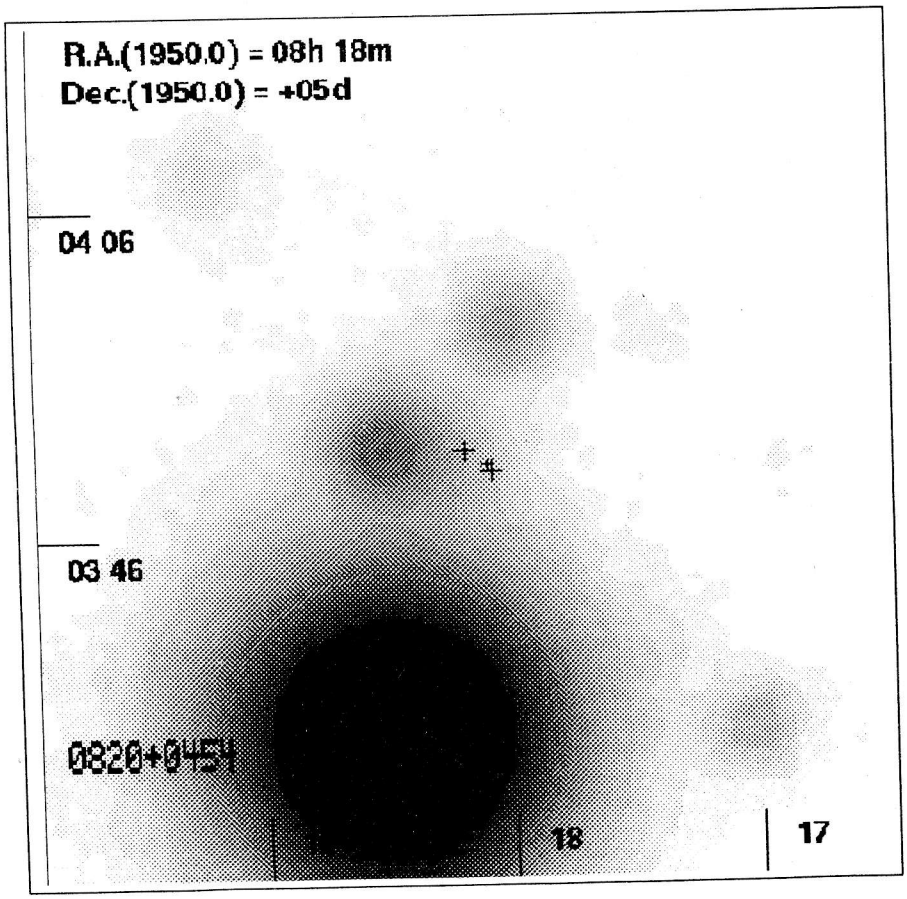
R.A.(1950.0) = 08h 18m
Dec.(1950.0) = +05d
04 06
03 46
0820+0454
18
17

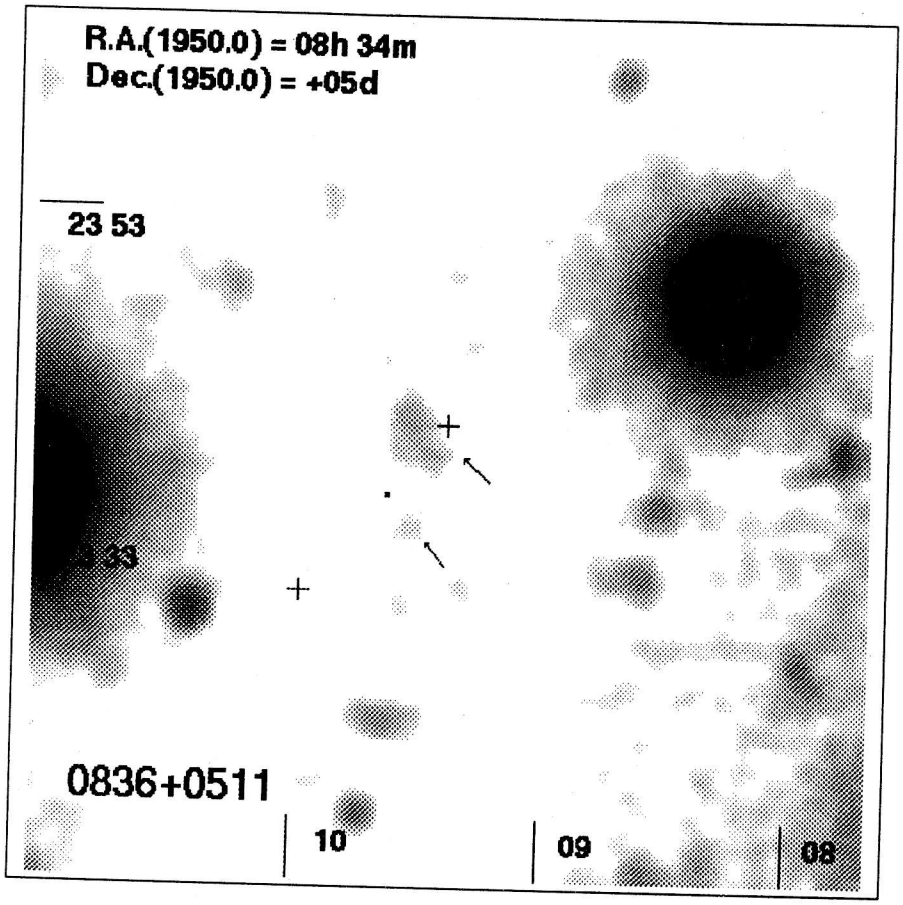
R.A.(1950.0) = 08h 34m
Dec.(1950.0) = +05d
23 53
33
0836+0511
10
09
08

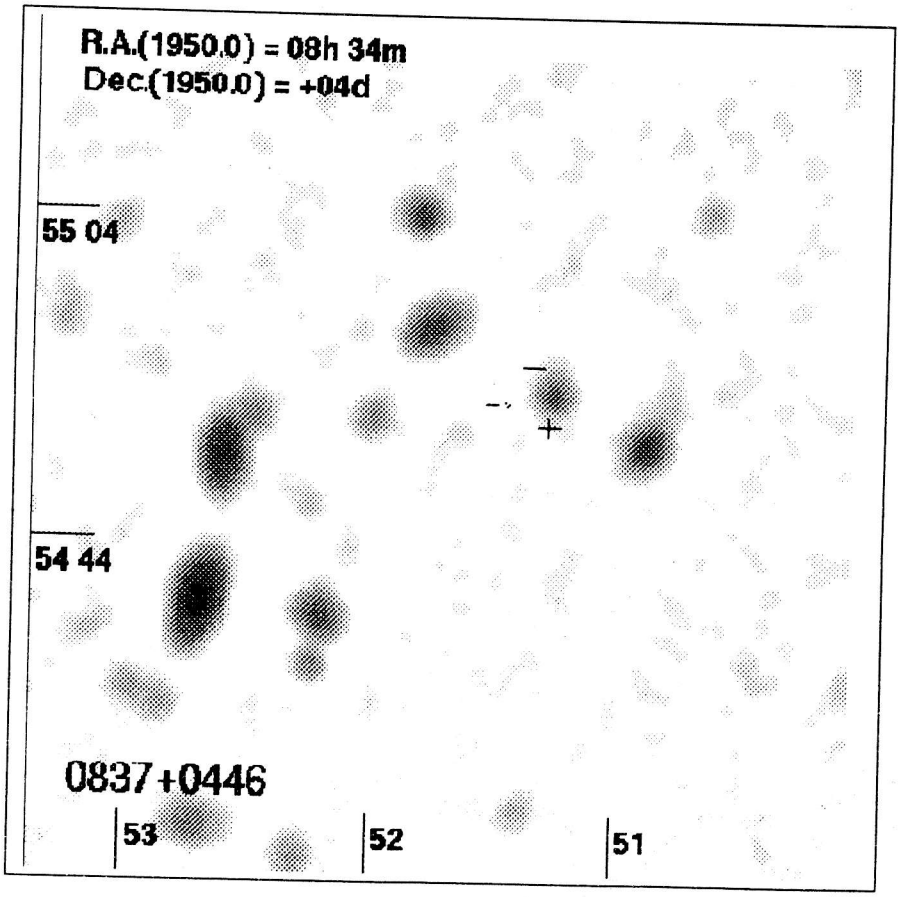
R.A.(1950.0) = 08h 34m
Dec.(1950.0) = +04d
55 04
54 44
0837+0446
53
52
51

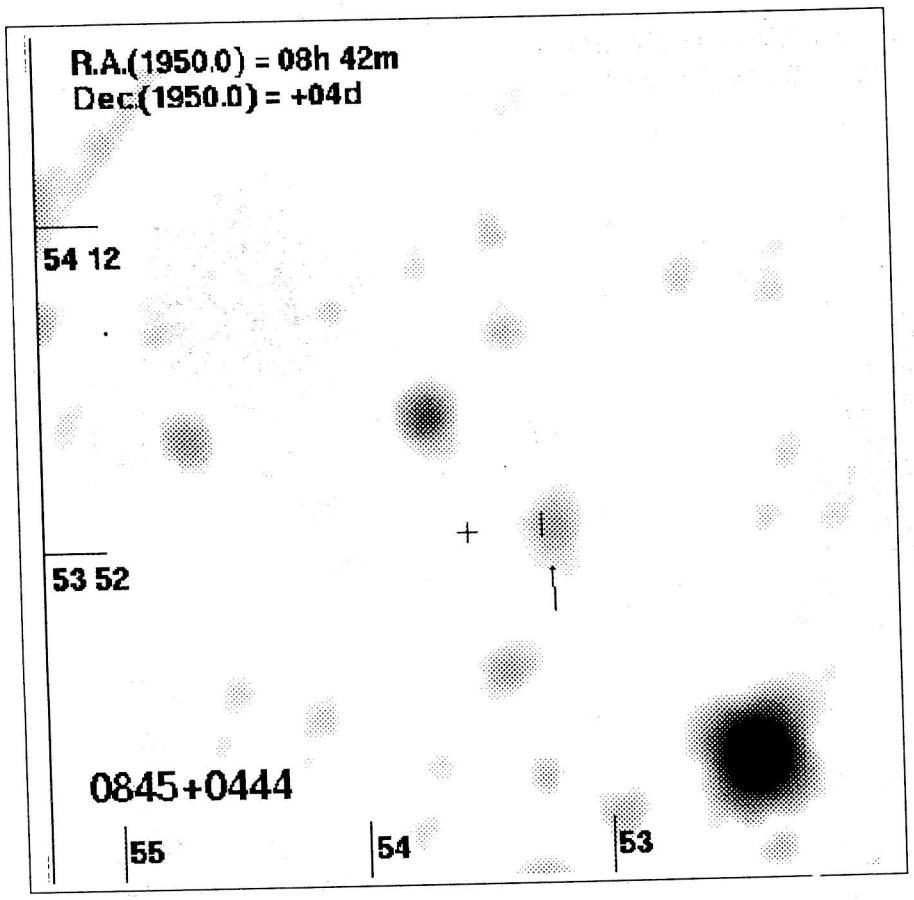
R.A.(1950.0) = 08h 42m
Dec.(1950.0) = +04d
54 12
53 52
0845+0444
55
54
53

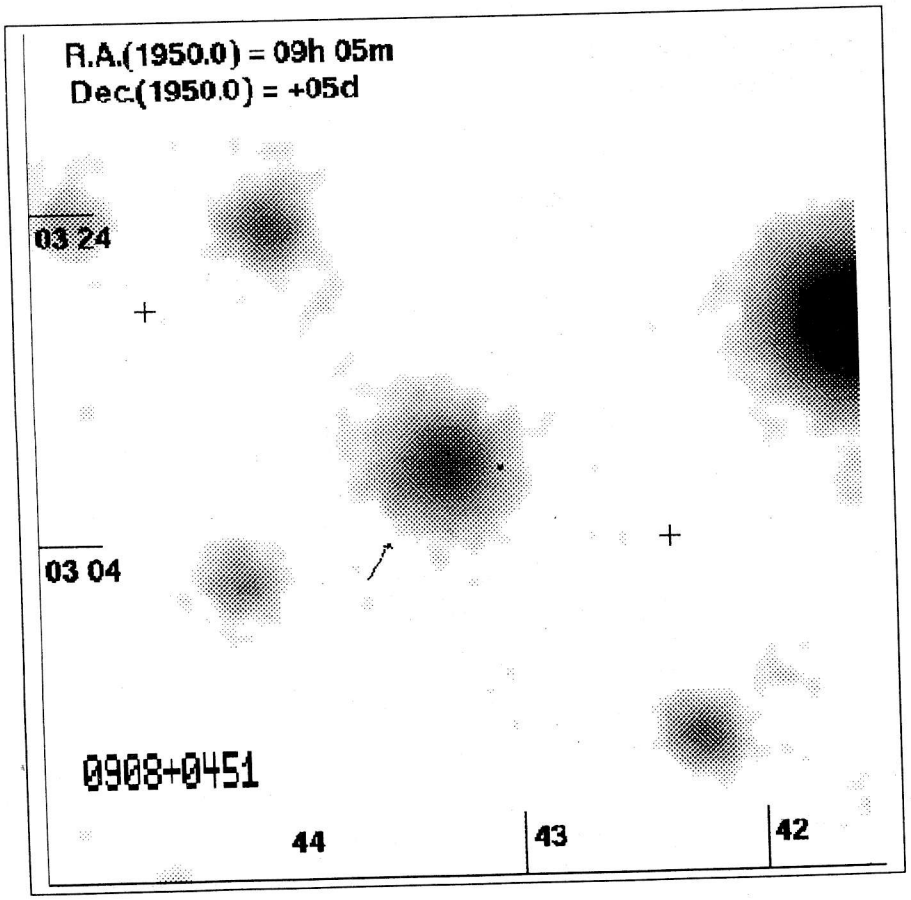
R.A.(1950.0) = 09h 05m
Dec.(1950.0) = +05d
03 24
03 04
0908+0451
44
43
42

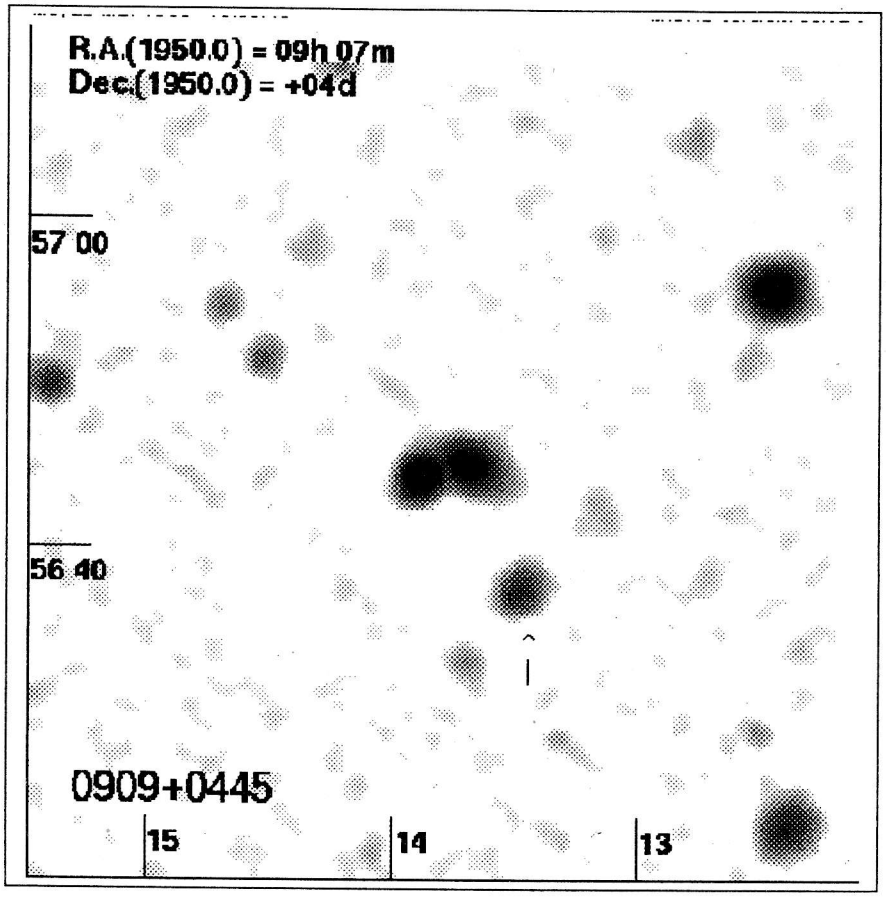
R.A.(1950.0) = 09h 07m
Dec.(1950.0) = +04d
57 00
56 40
0909+0445
15
14
13

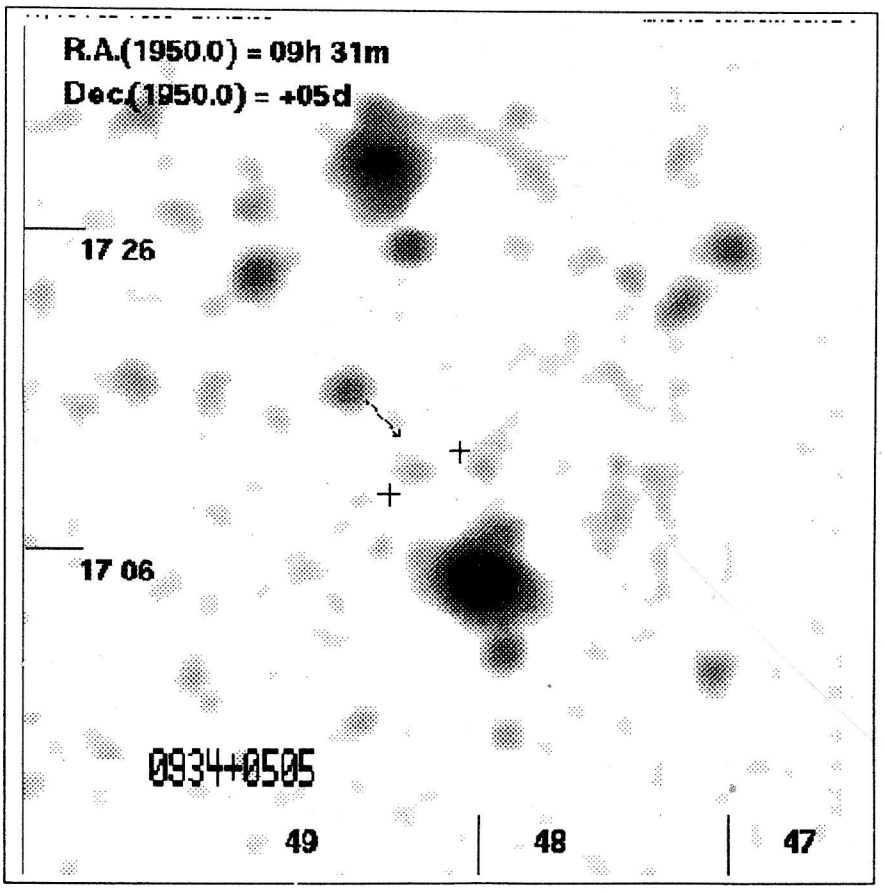
R.A.(1950.0) = 09h 31m
Dec.(1950.0) = +05d
17 26
17 06
0934+0505
49
48
47

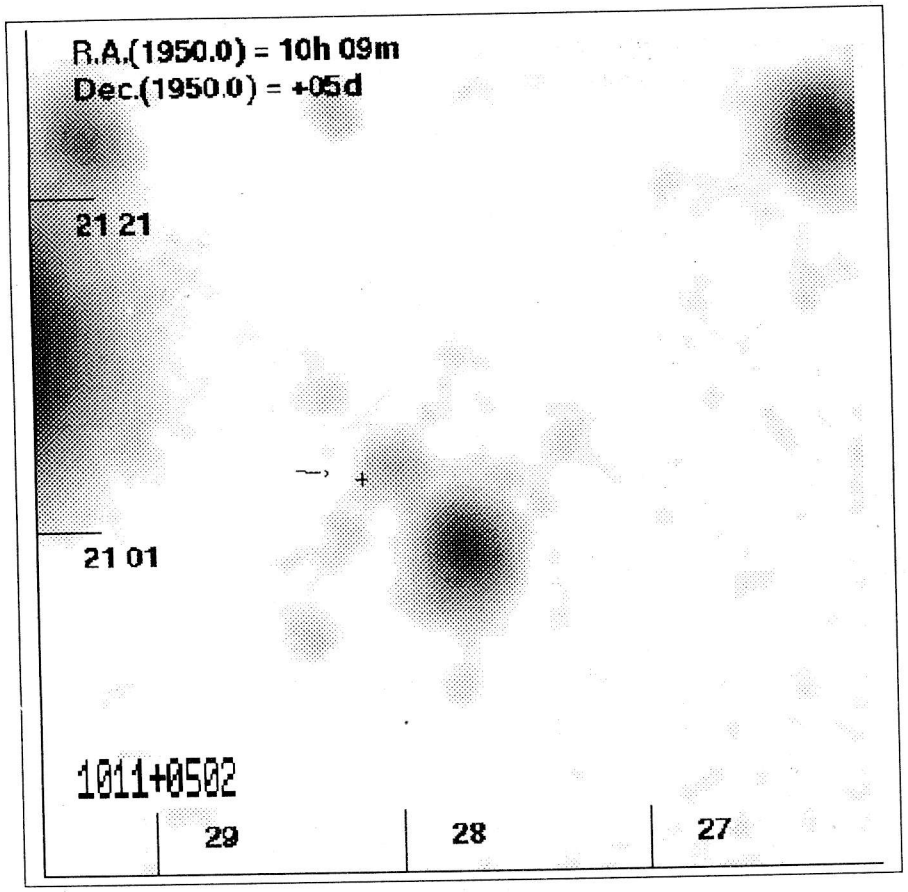
R.A.(1950.0) = 10h 09m
Dec.(1950.0) = +05d
21 21
21 01
1011+0502
29
28
27

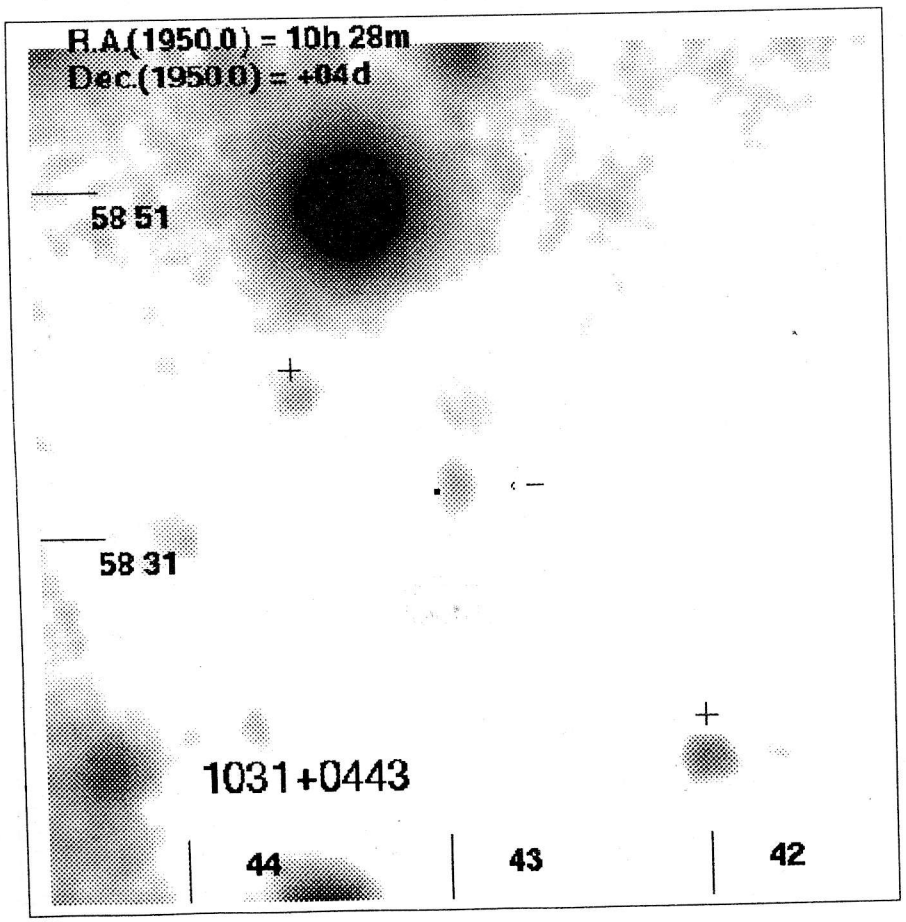
R.A.(1950.0) = 10h 28m
Dec.(1950.0) = +04d
58 51
58 31
1031+0443
44
43
42

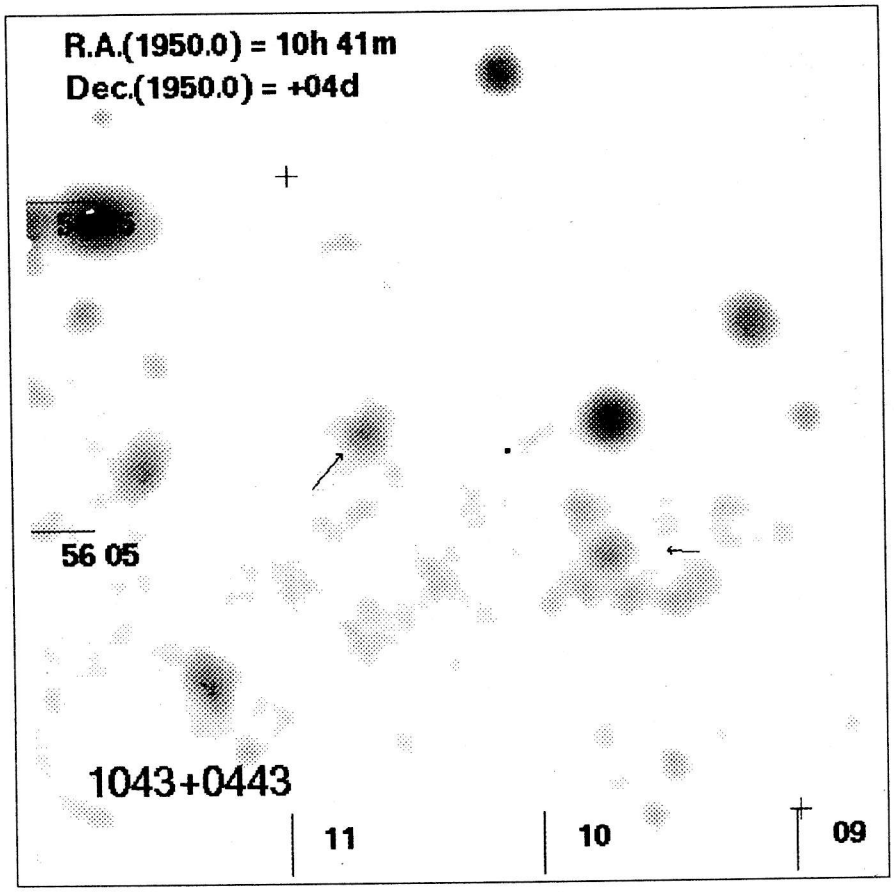
R.A.(1950.0) = 10h 41m
Dec.(1950.0) = +04d
56 05
1043+0443
11
10
09

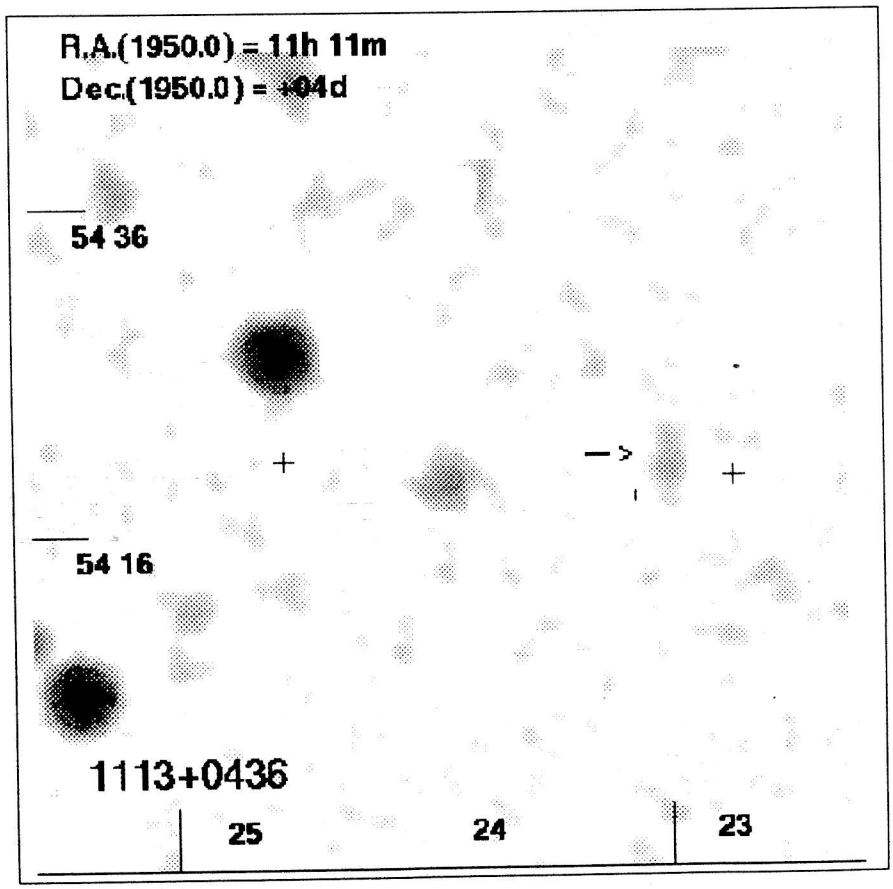
R.A.(1950.0) = 11h 11m
Dec.(1950.0) = +04d
54 36
54 16
1113+0436
25
24
23

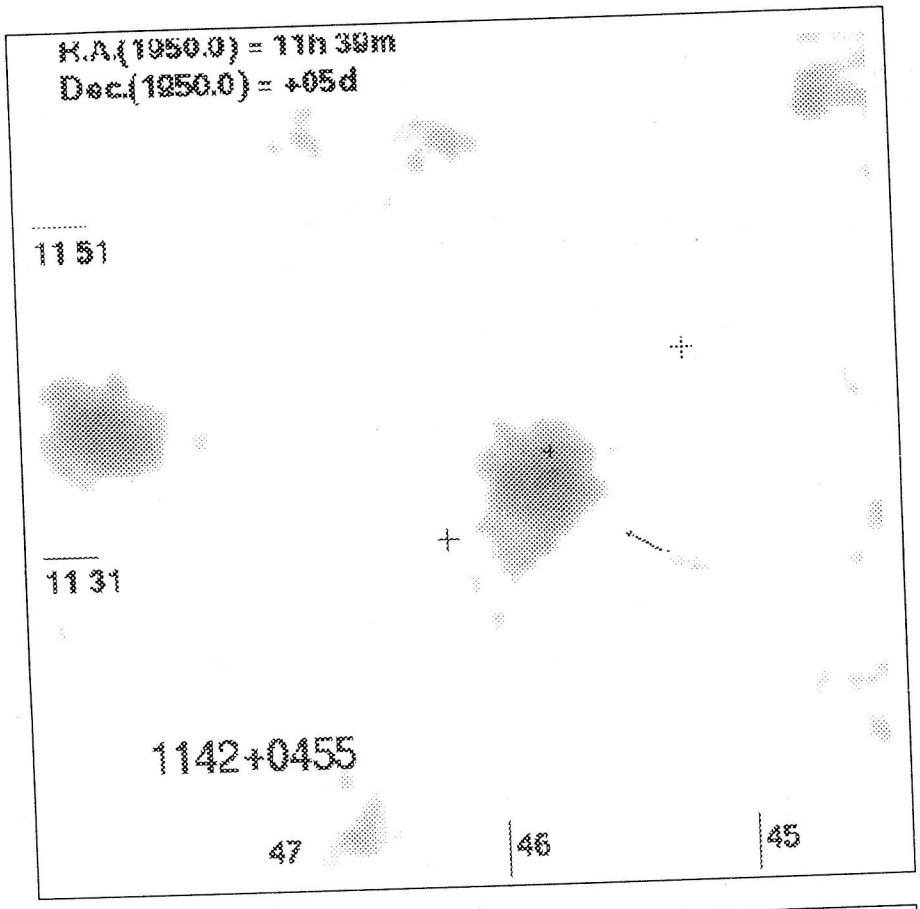
R.A.(1950.0) = 11h 39m
Dec.(1950.0) = +05d
11 51
11 31
1142+0455
47
46
45

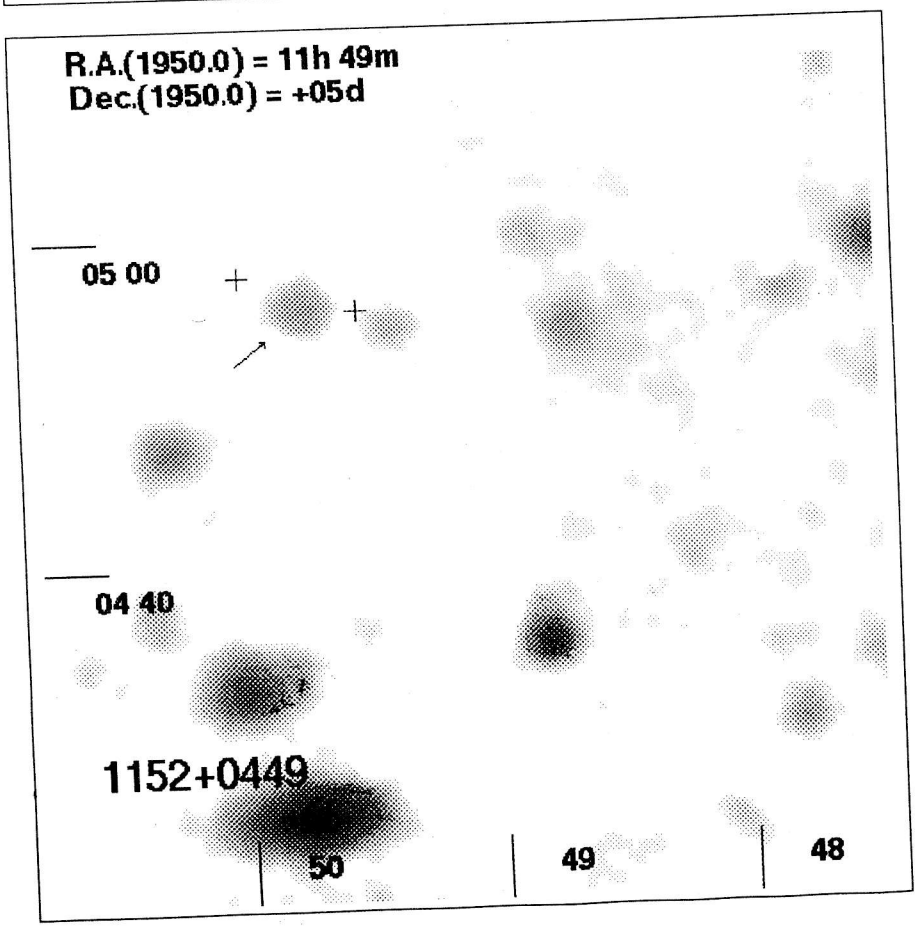
R.A.(1950.0) = 11h 49m
Dec.(1950.0) = +05d
05 00
04 40
1152+0449
50
49
48

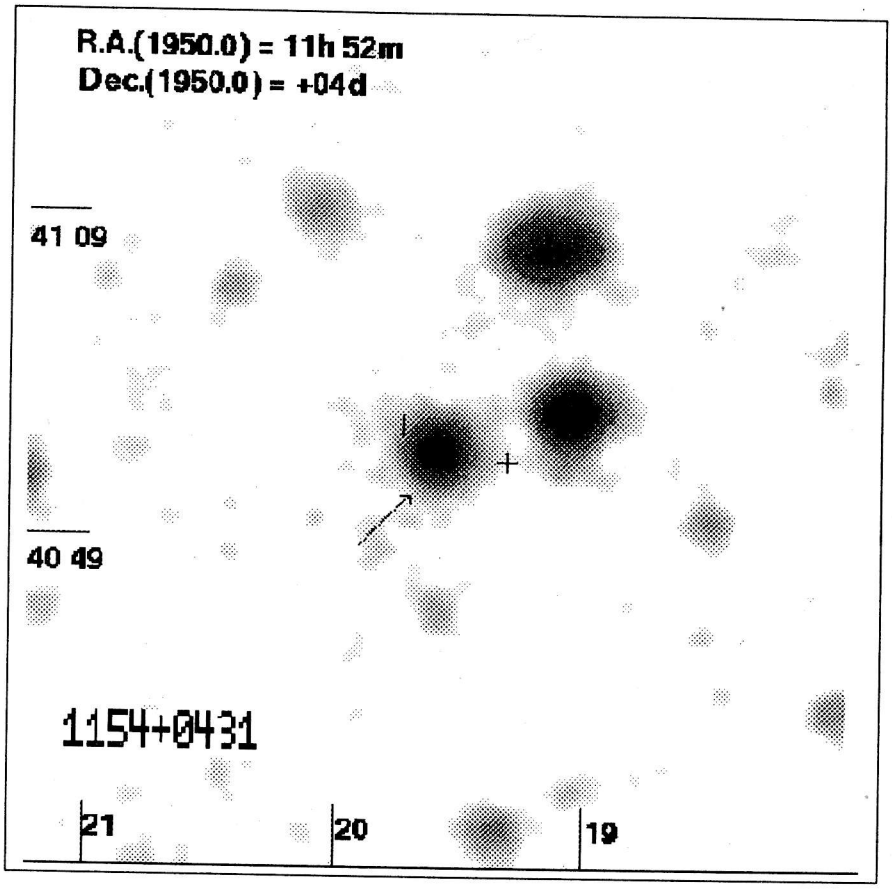
R.A.(1950.0) = 11h 52m
Dec.(1950.0) = +04d
41 09
40 49
1154+0431
21
20
19

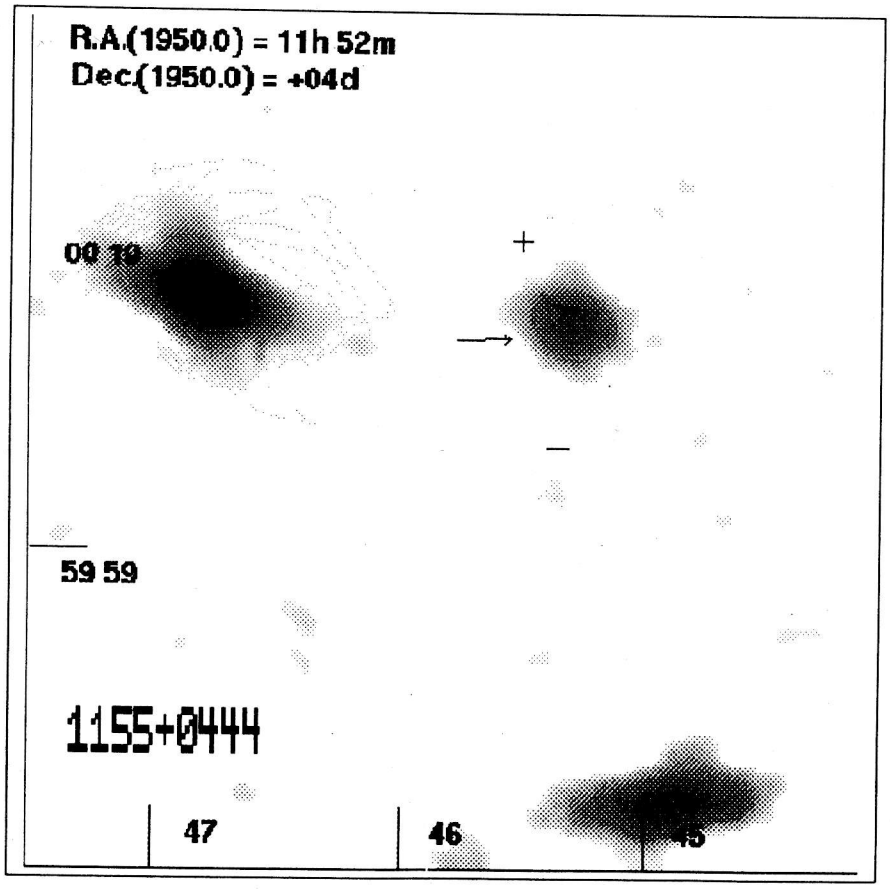
R.A.(1950.0) = 11h 52m
Dec.(1950.0) = +04d
59 59
1155+0444
47
46

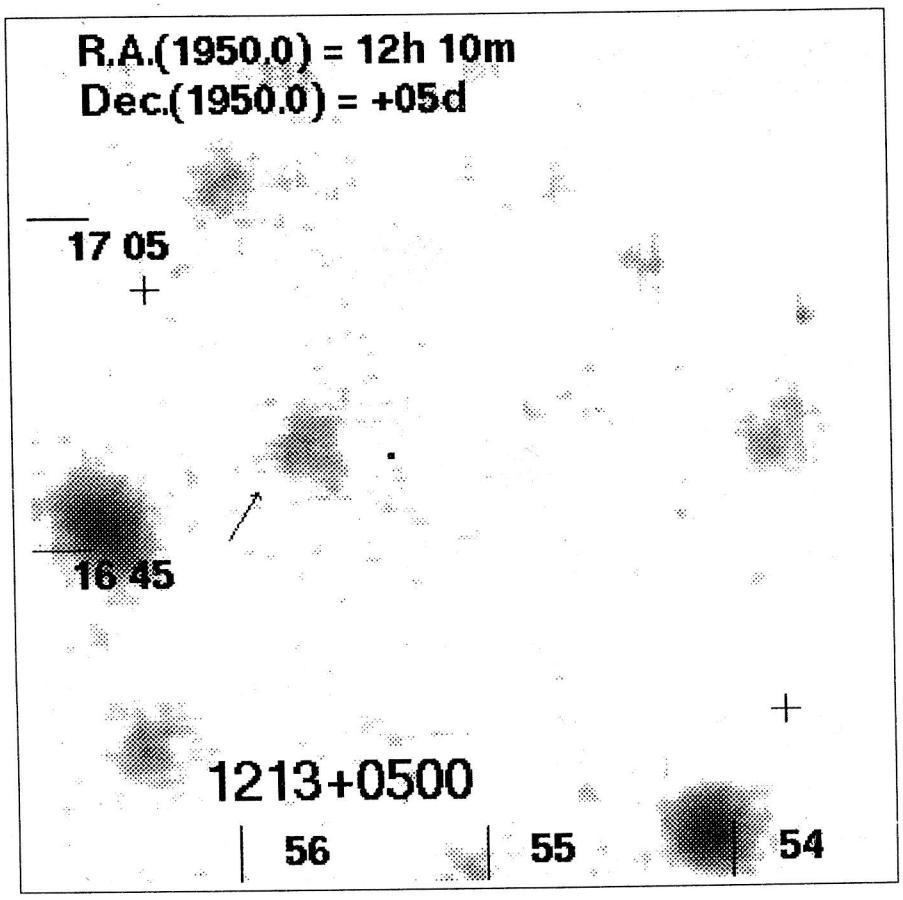
R.A.(1950.0) = 12h 10m
Dec.(1950.0) = +05d
17 05
16 45
1213+0500
56
55
54

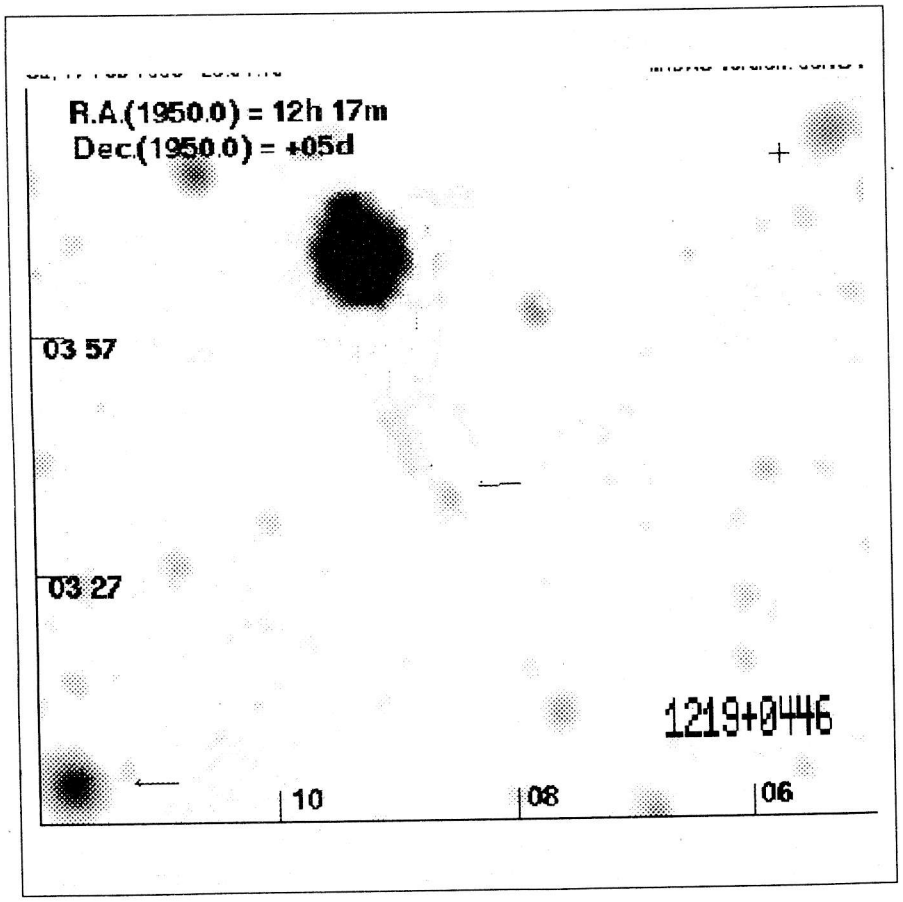
R.A.(1950.0) = 12h 17m
Dec.(1950.0) = +05d
03 57
03 27
1219+0446
10
08
06

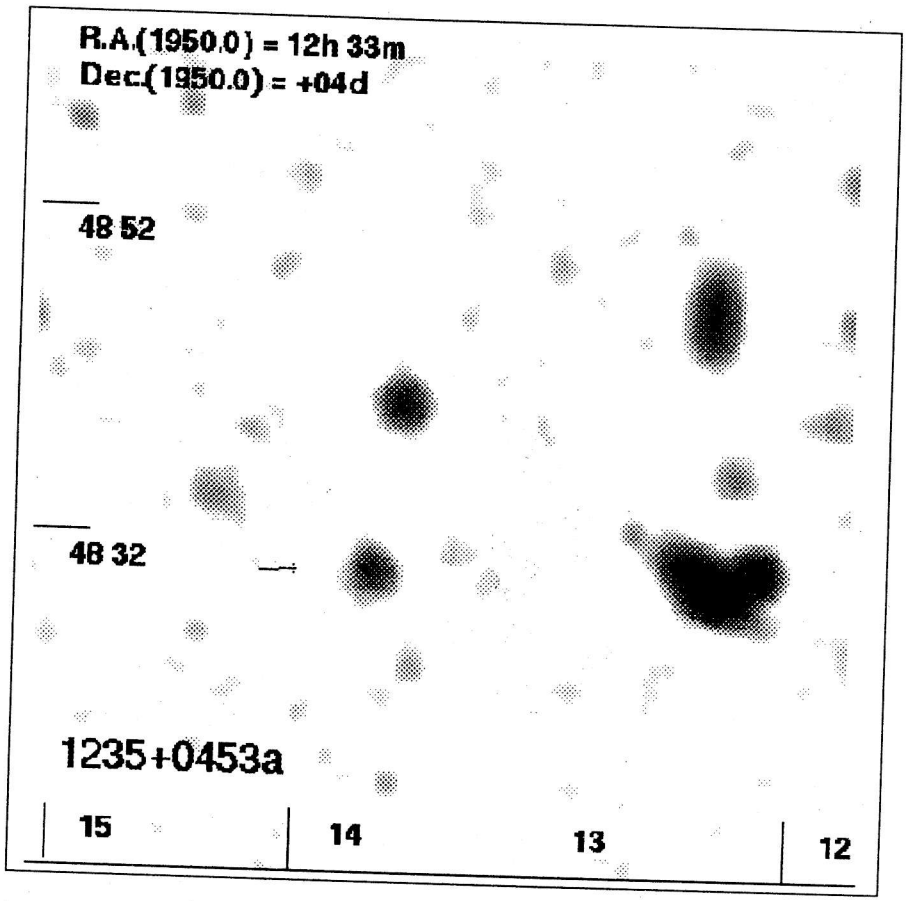
R.A.(1950.0) = 12h 33m
Dec.(1950.0) = +04d
48 52
48 32
1235+0453a
15
14
13
12

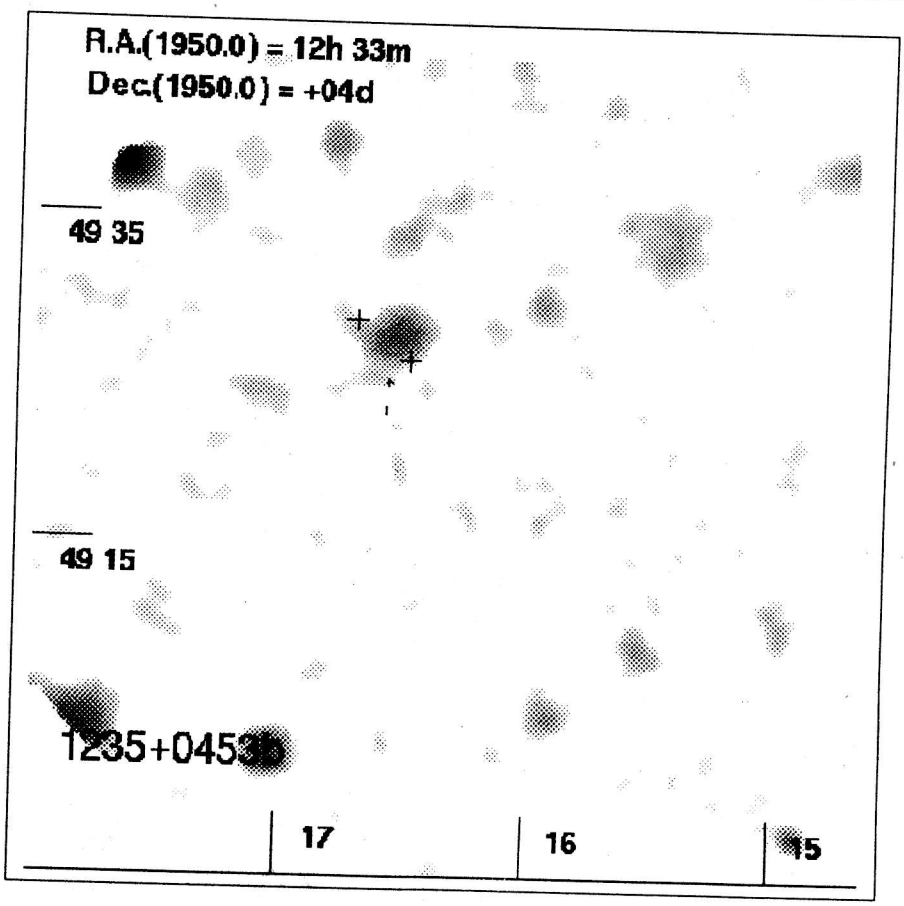
R.A.(1950.0) = 12h 33m
Dec.(1950.0) = +04d
49 35
49 15
17
16
15

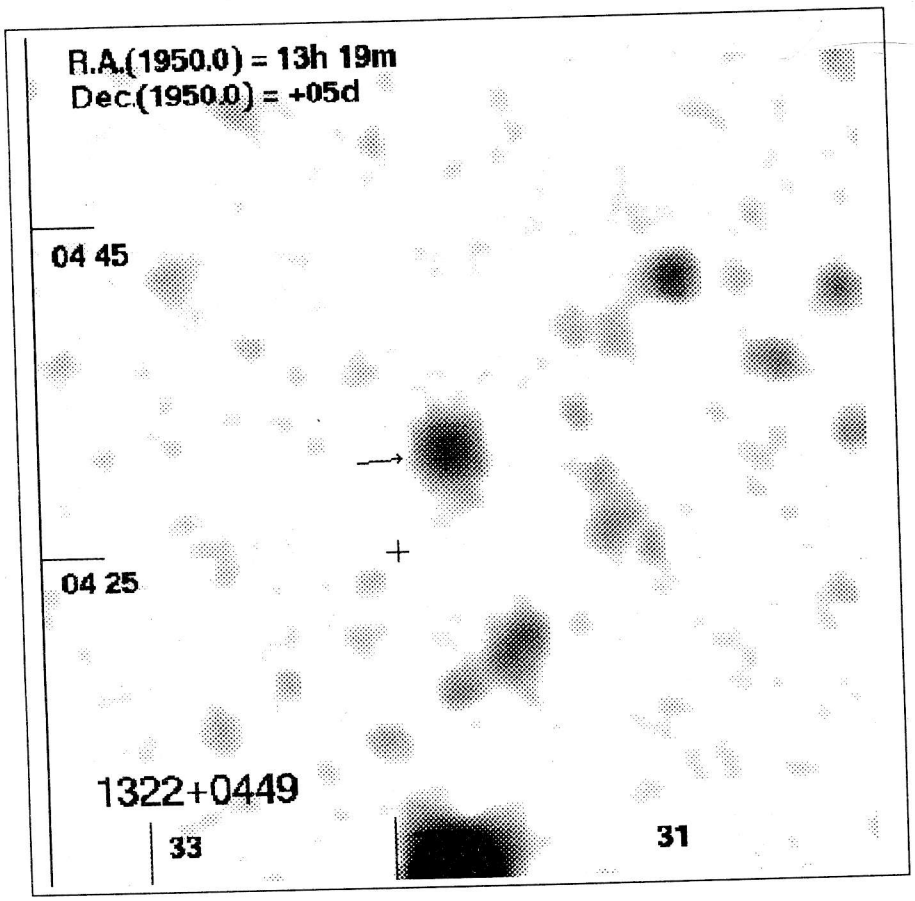
R.A.(1950.0) = 13h 19m
Dec.(1950.0) = +05d
04 45
04 25
1322+0449
33
31

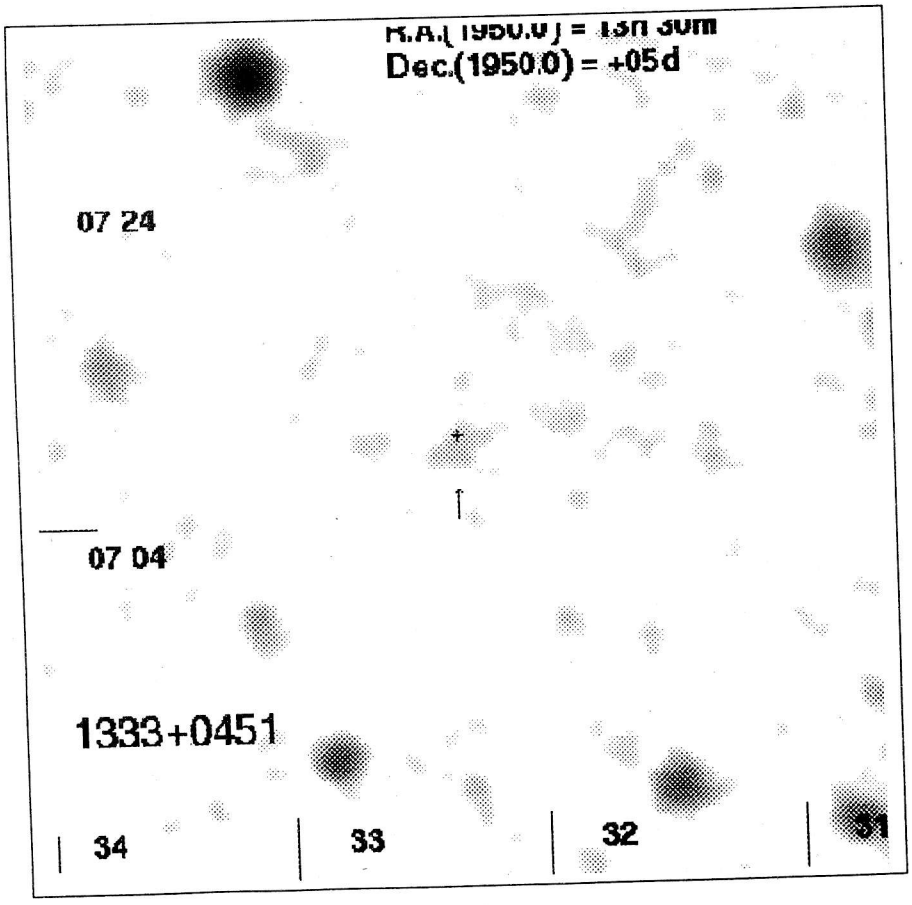
Dec.(1950.0) = +05d
07 24
07 04
1333+0451
34
33
32
31

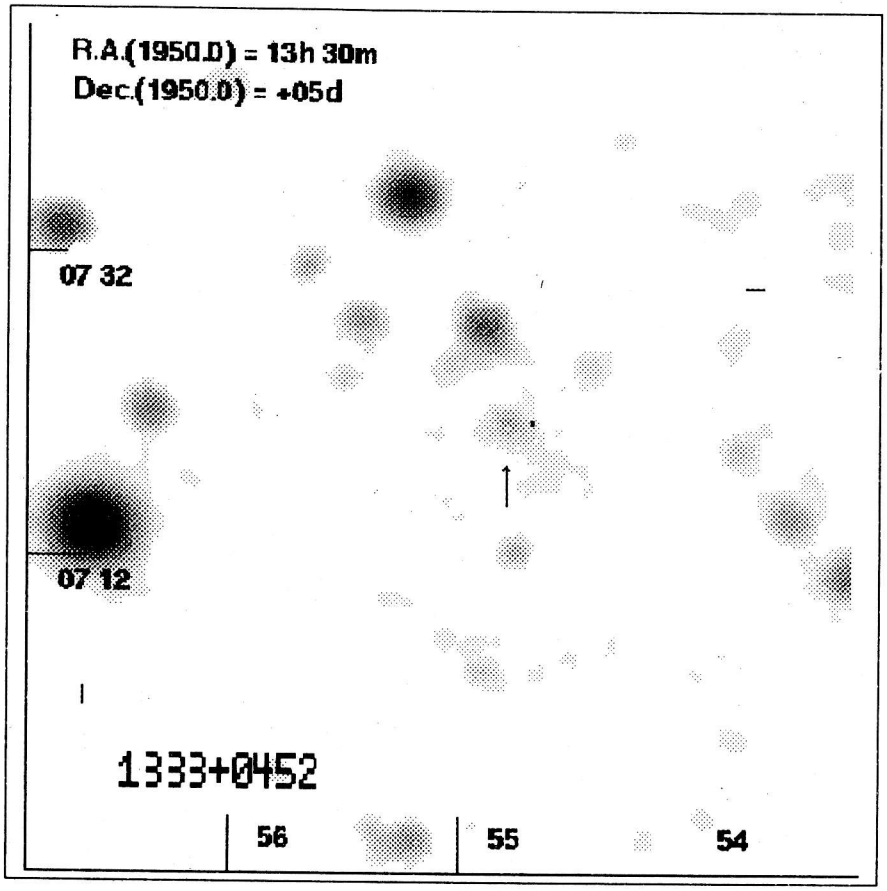
R.A.(1950.0) = 13h 30m
Dec.(1950.0) = +05d
07 32
07 12
1333+0452
56
55
54

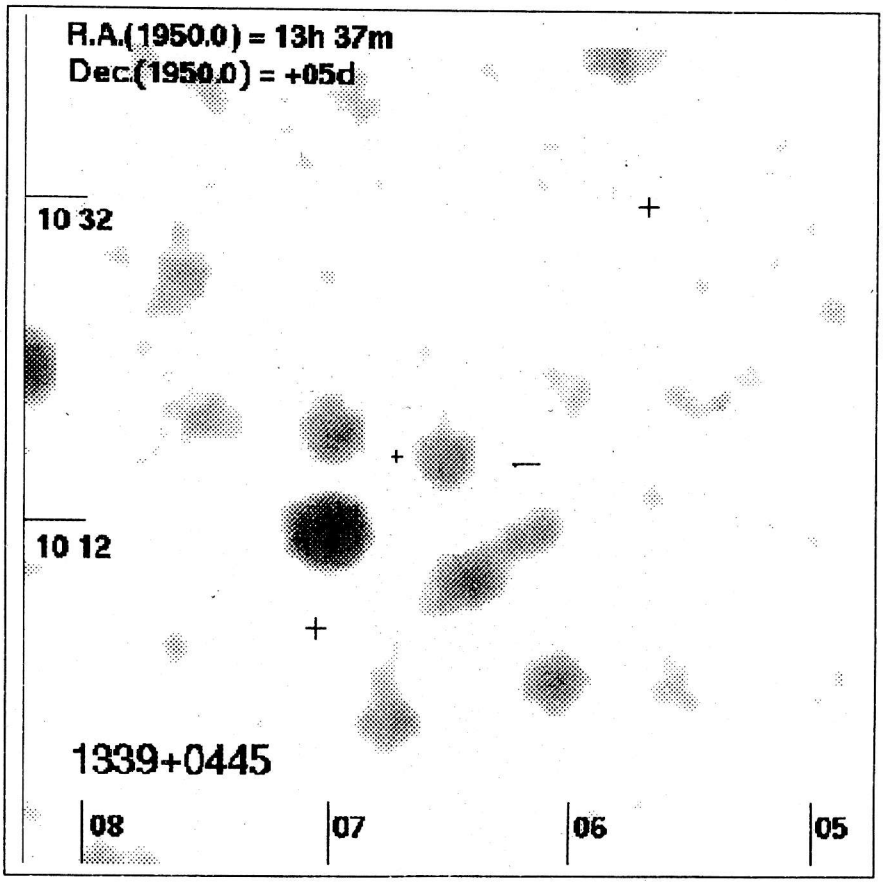
R.A.(1950.0) = 13h 37m
Dec.(1950.0) = +05d
10 32
10 12
1339+0445
08
07
06
05

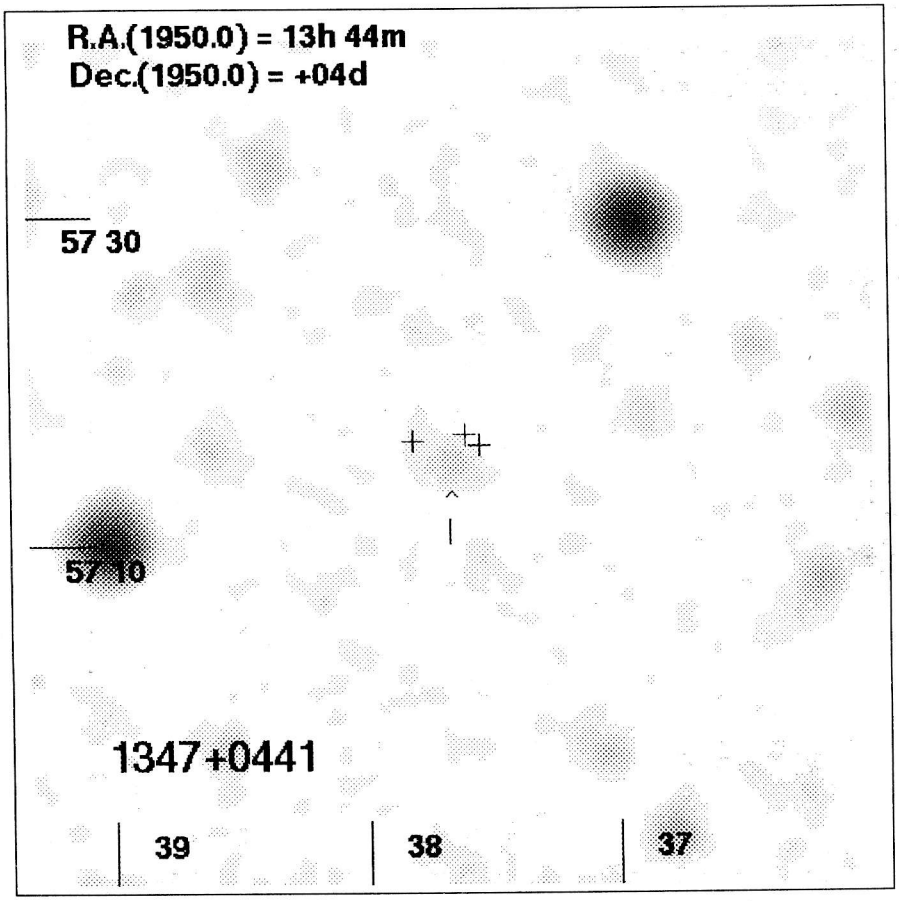
R.A.(1950.0) = 13h 44m
Dec.(1950.0) = +04d
57 30
57 10
1347+0441
39
38
37

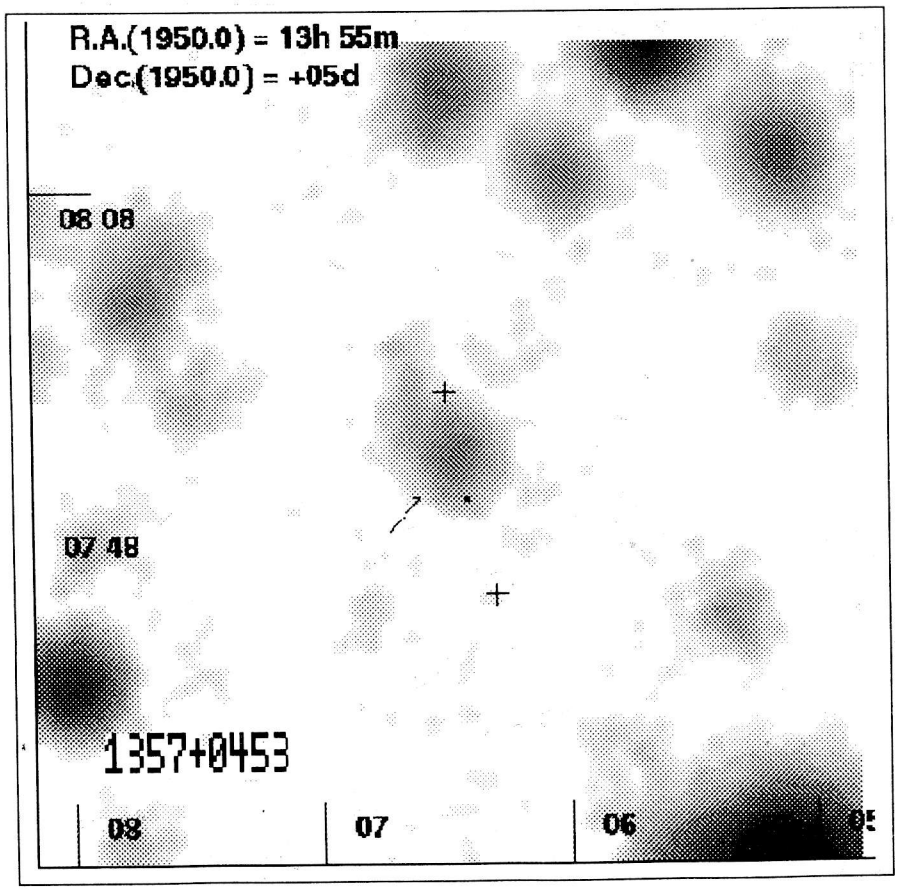
R.A.(1950.0) = 13h 55m
Dec.(1950.0) = +05d
08 08
07 48
1357+0453
08
07
06

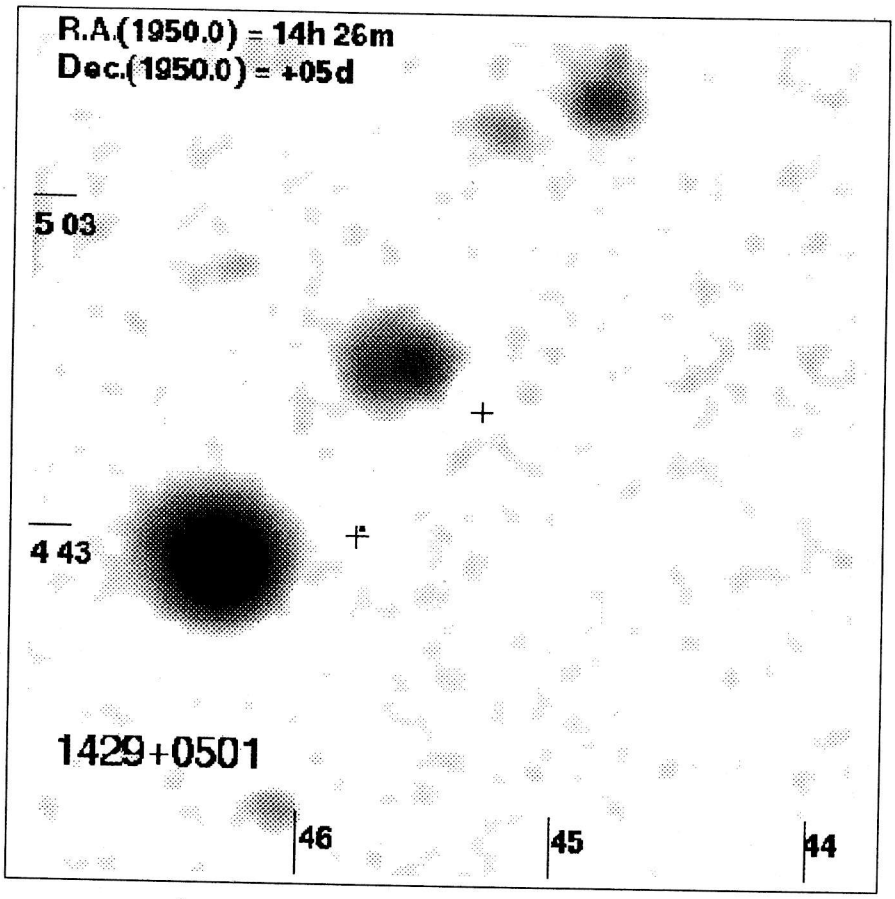
R.A.(1950.0) = 14h 26m
Dec.(1950.0) = +05d
5 03
4 43
1429+0501
46
45
44

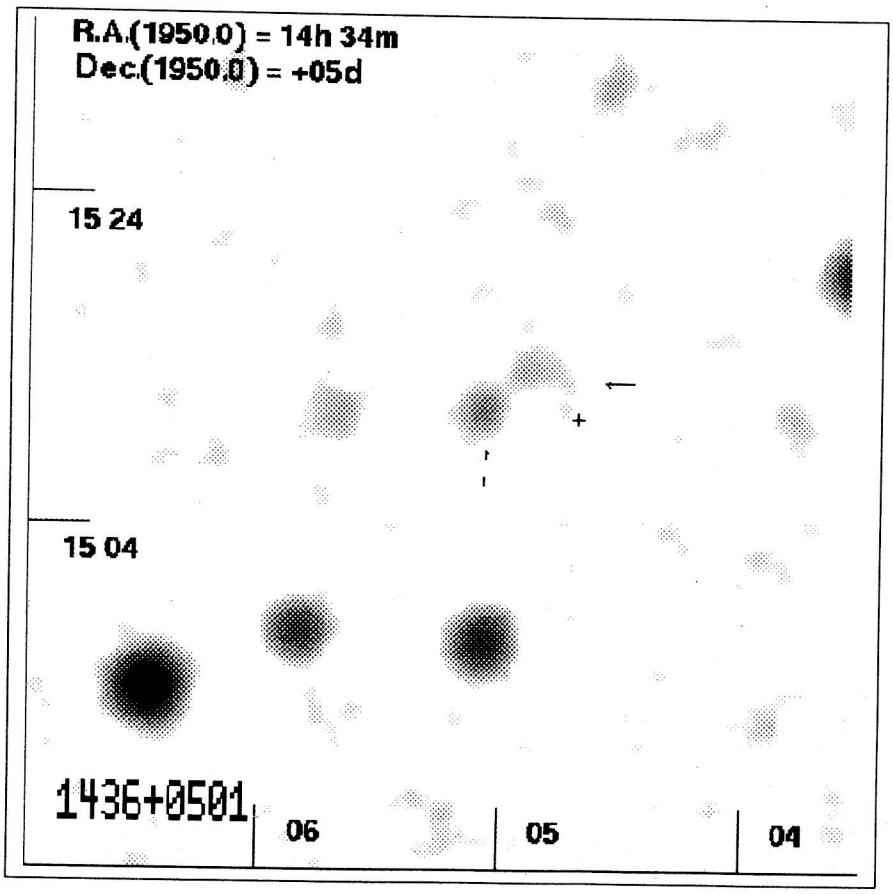
R.A.(1950.0) = 14h 34m
Dec.(1950.0) = +05d
15 24
15 04
1436+0501
06
05
04

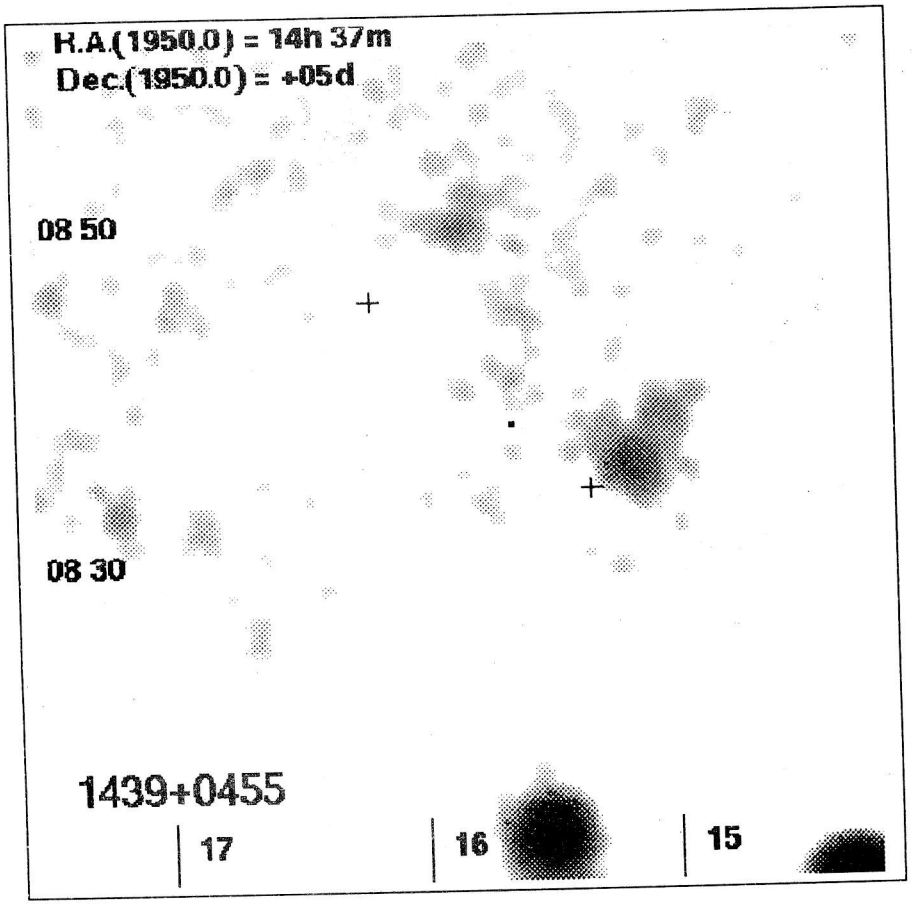
R.A.(1950.0) = 14h 37m
Dec.(1950.0) = +05d
08 50
08 30
1439+0455
17
16
15

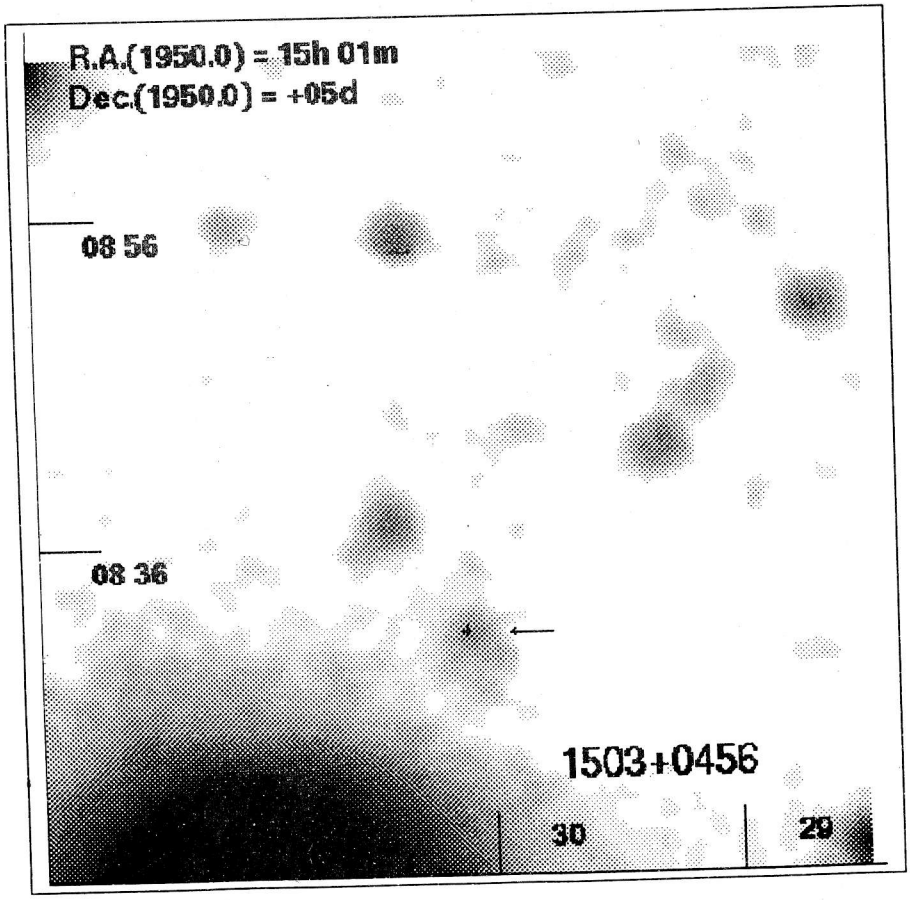
R.A.(1950.0) = 15h 01m
Dec.(1950.0) = +05d
08 56
08 36
1503+0456
30
29

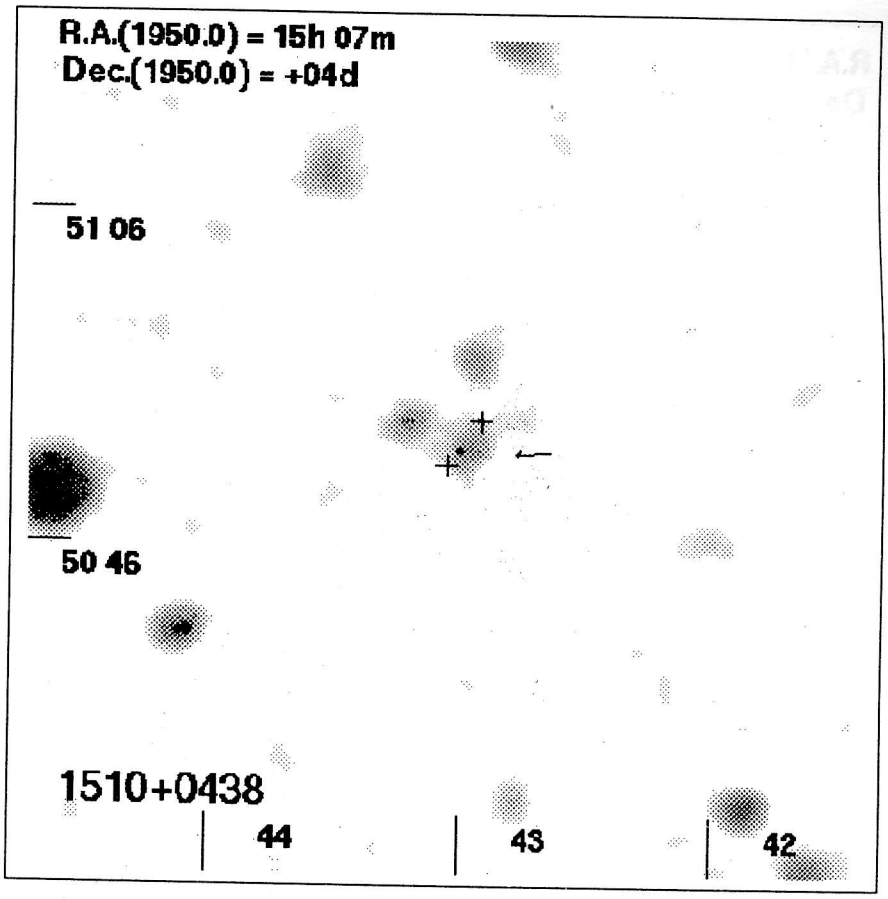
R.A.(1950.0) = 15h 07m
Dec.(1950.0) = +04d
51 06
50 46
1510+0438
44
43
42

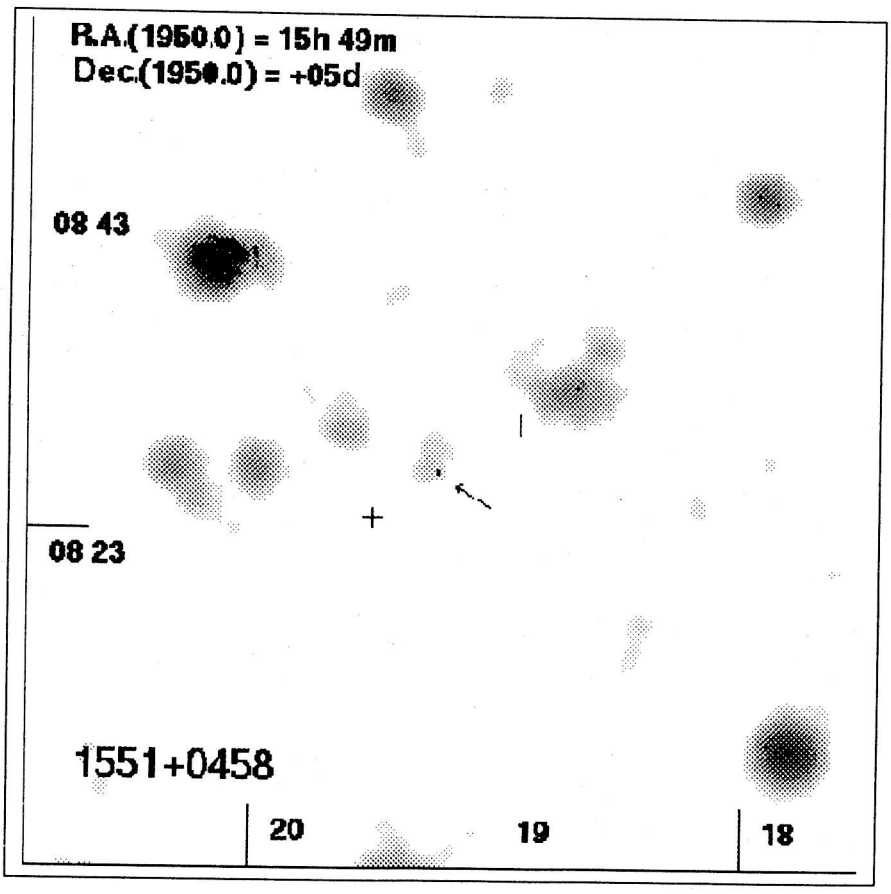
R.A.(1950.0) = 15h 49m
Dec.(1950.0) = +05d
08 43
08 23
1551+0458
20
19
18

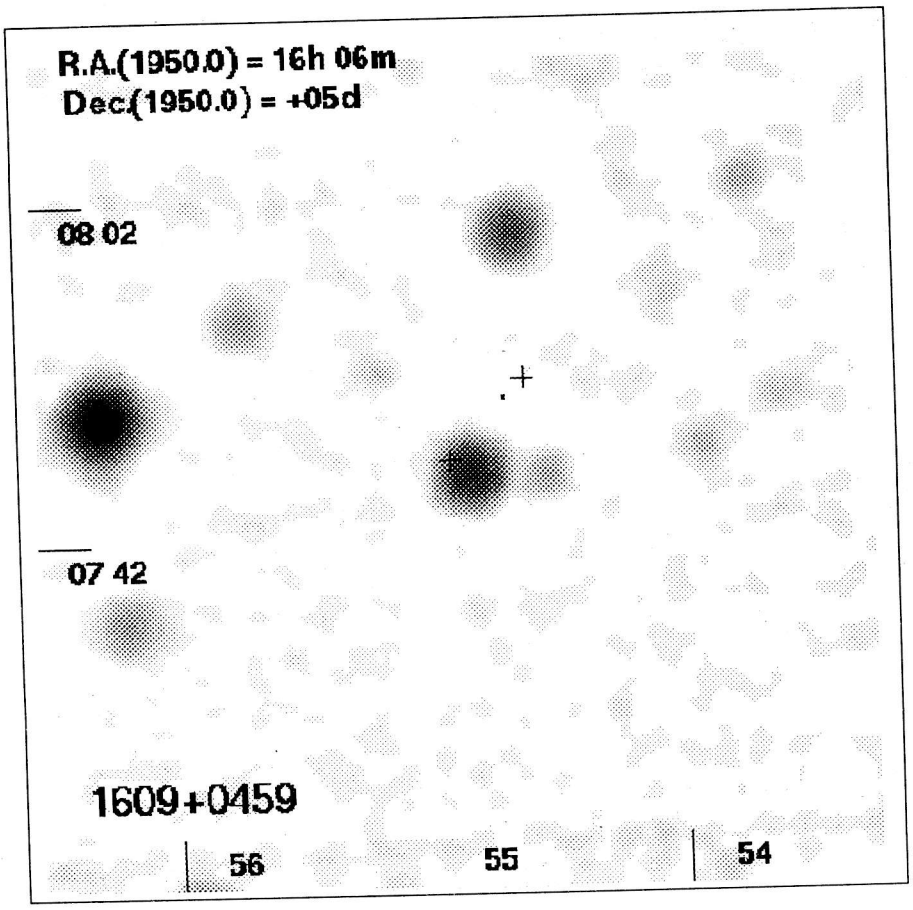
R.A.(1950.0) = 16h 06m
Dec.(1950.0) = +05d
08 02
07 42
1609+0459
56
55
54

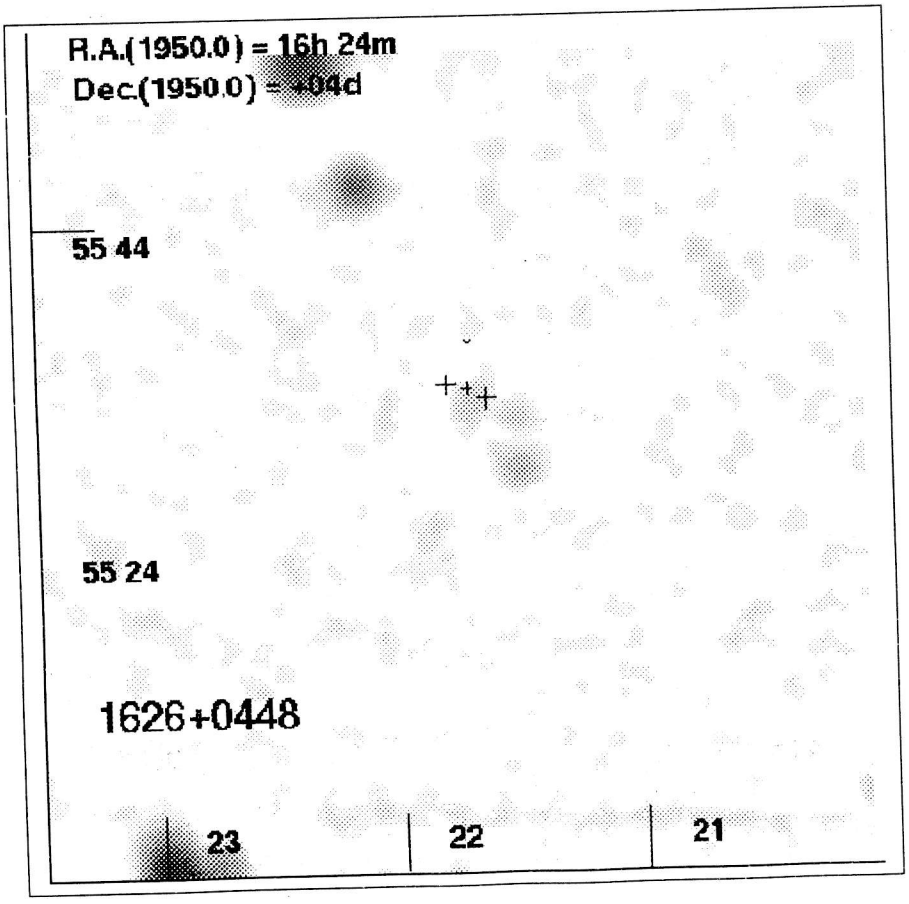
R.A.(1950.0) = 16h 24m
Dec.(1950.0) = +04d
55 44
55 24
1626+0448
23
22
21

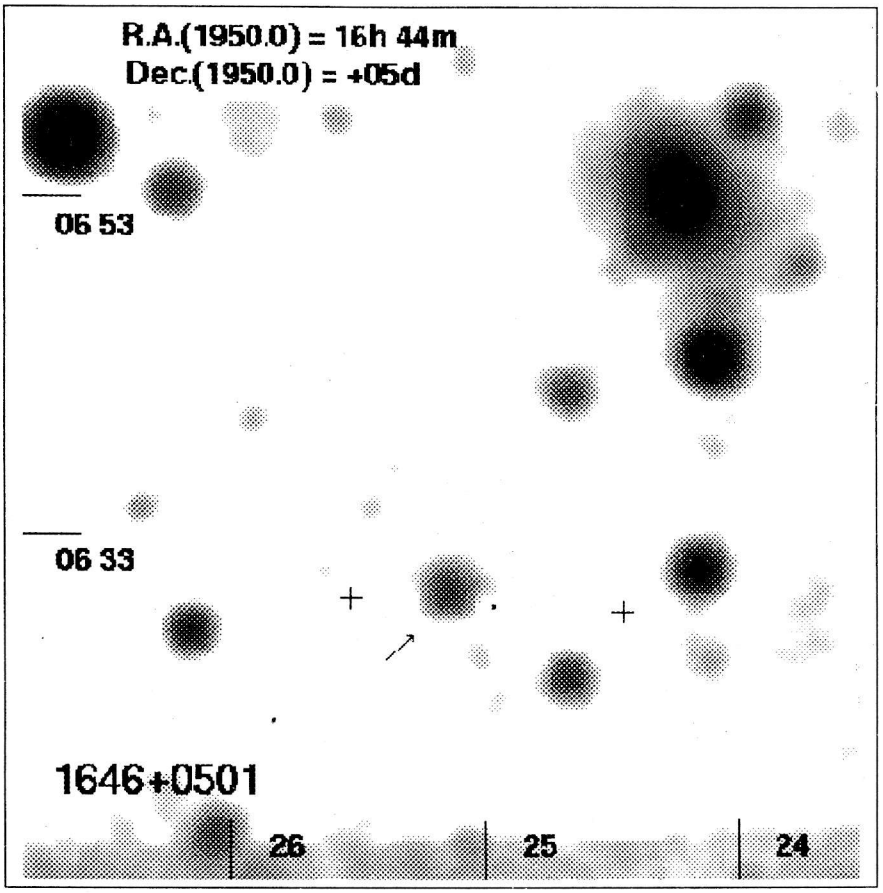
R.A.(1950.0) = 16h 44m
Dec.(1950.0) = +05d
06 53
06 33
1646+0501
26
25
24

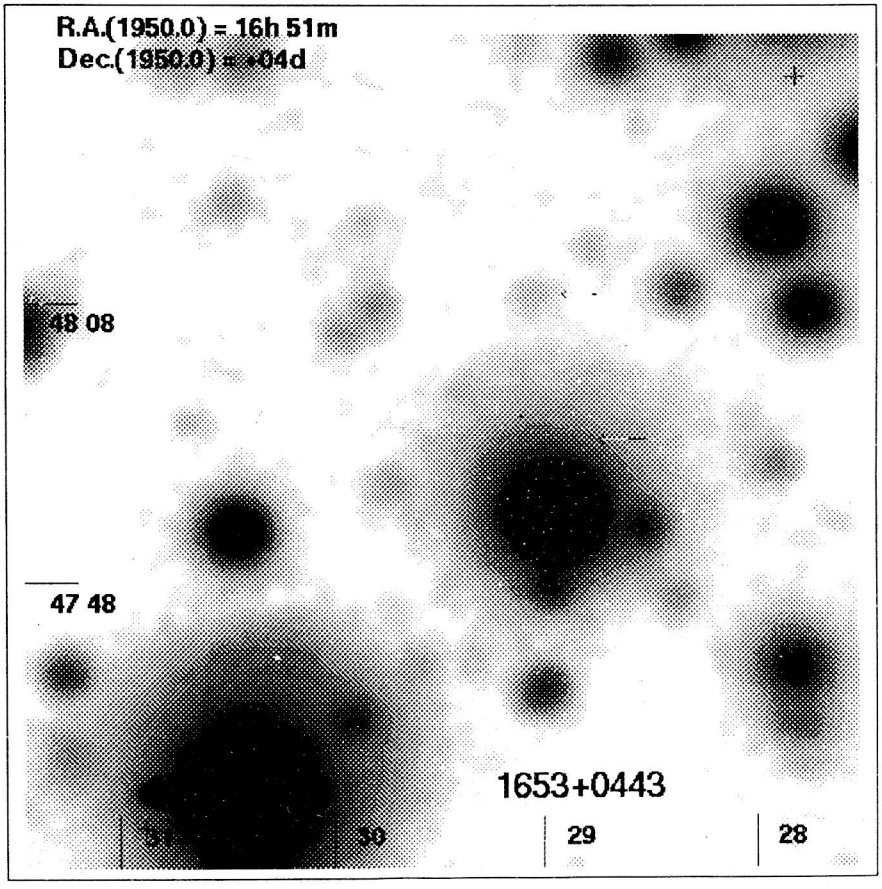
R.A.(1950.0) = 16h 51m
Dec.(1950.0) = +04d
48 08
47 48
1653+0443
29
28

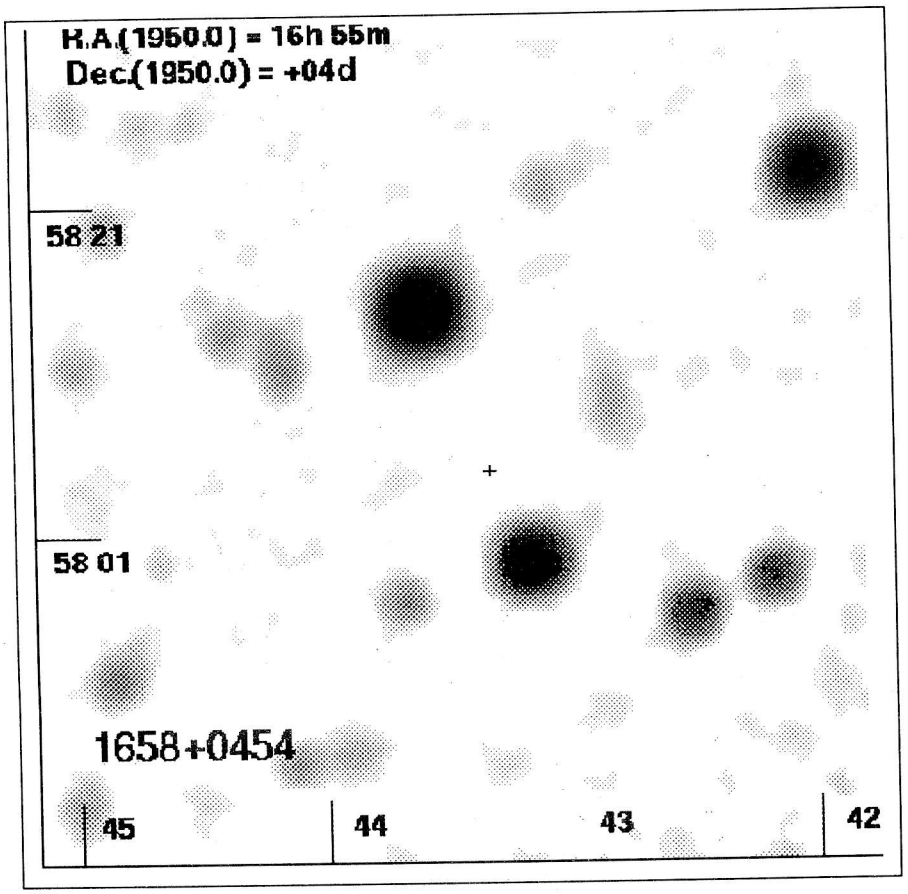
R.A.(1950.0) = 16h 55m
Dec.(1950.0) = +04d
58 21
58 01
1658+0454
45
44
43
42

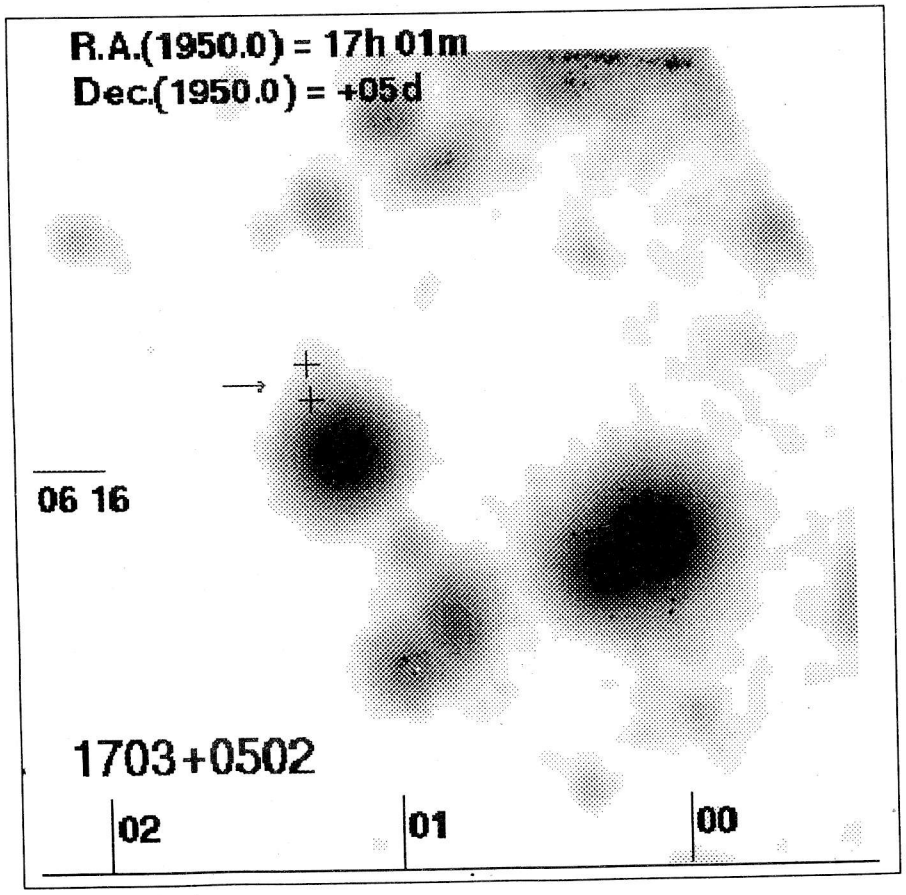
R.A.(1950.0) = 17h 01m
Dec.(1950.0) = +05d
06 16
1703+0502
02
01
00

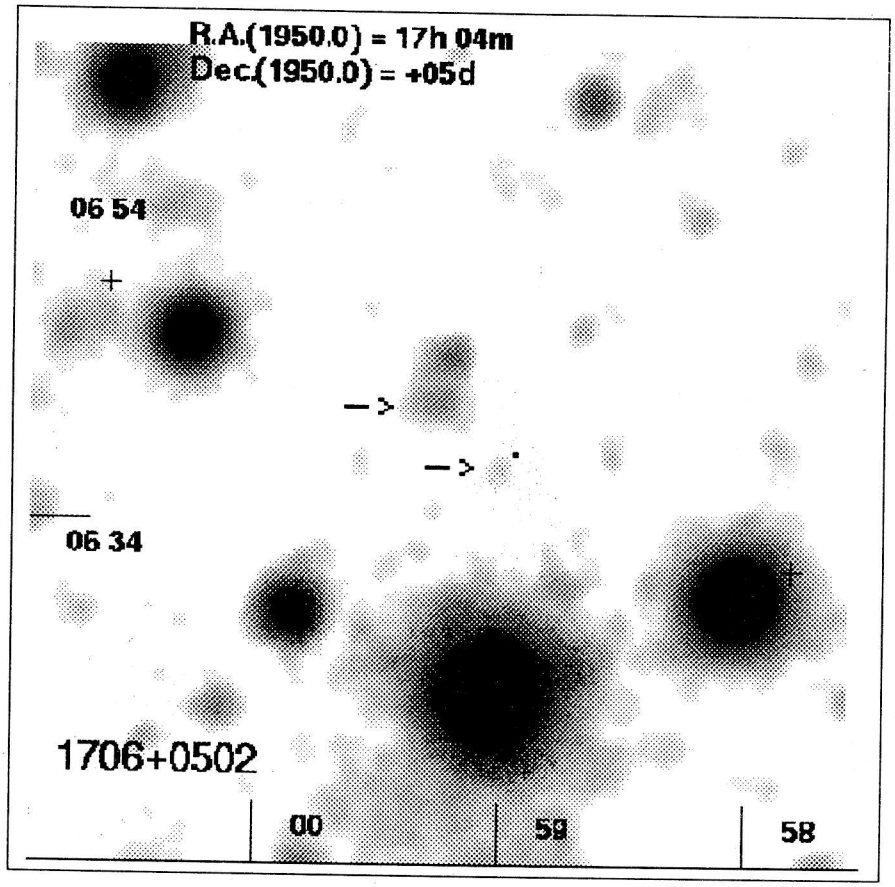
R.A.(1950.0) = 17h 04m
Dec.(1950.0) = +05d
06 54
06 34
1706+0502
00
59
58

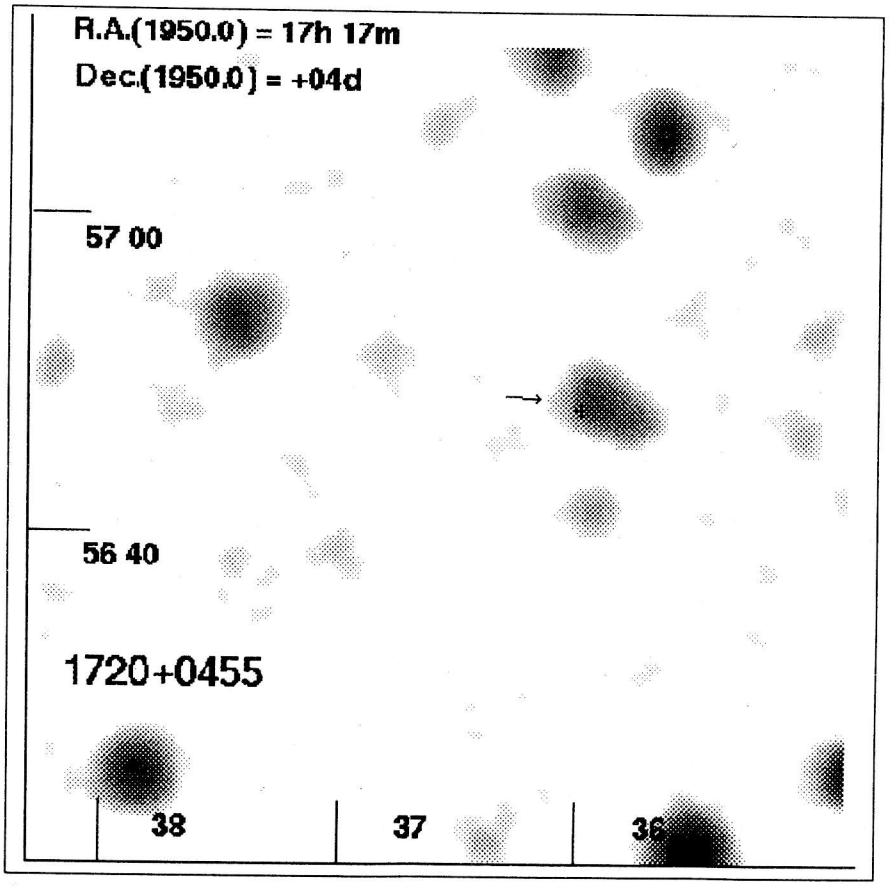
R.A.(1950.0) = 17h 17m
Dec.(1950.0) = +04d
57 00
56 40
1720+0455
38
37
36

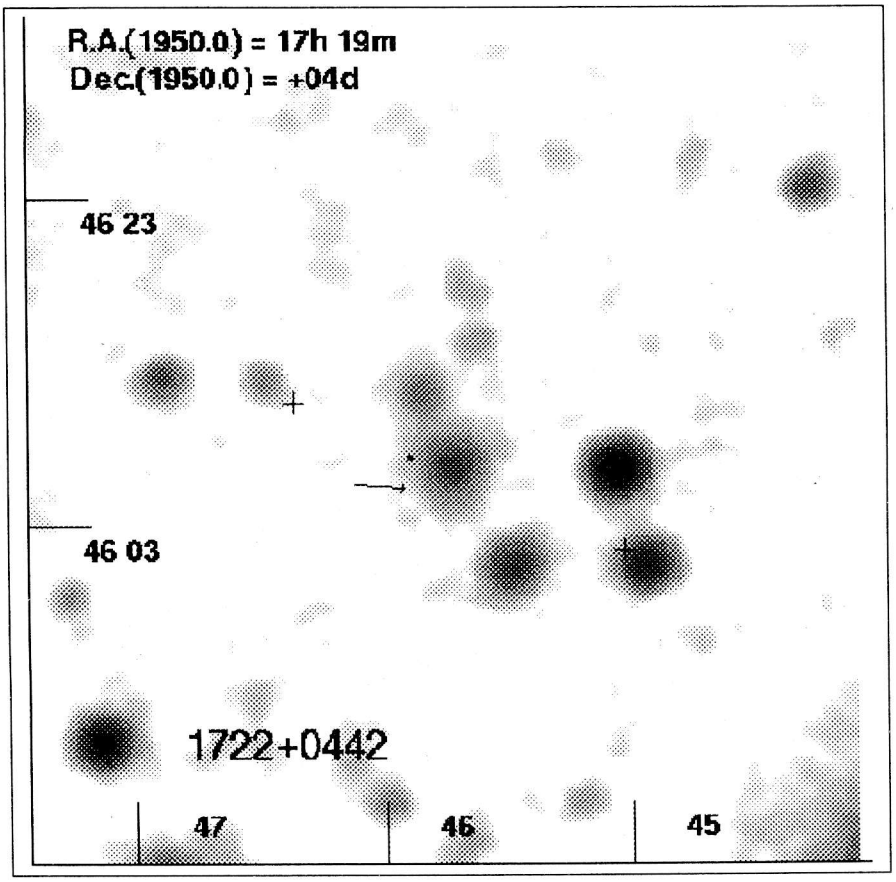
R.A.(1950.0) = 17h 19m
Dec.(1950.0) = +04d
46 23
46 03
1722+0442
47
46
45

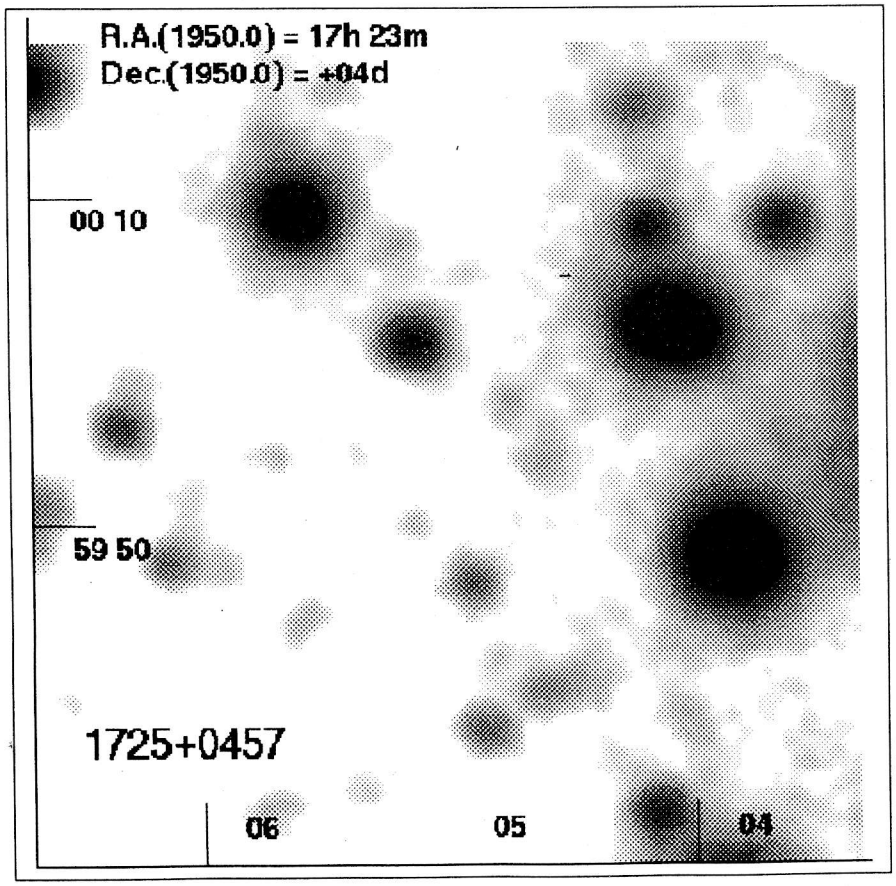
R.A.(1950.0) = 17h 23m
Dec.(1950.0) = +04d
00 10
59 50
1725+0457
06
05
04

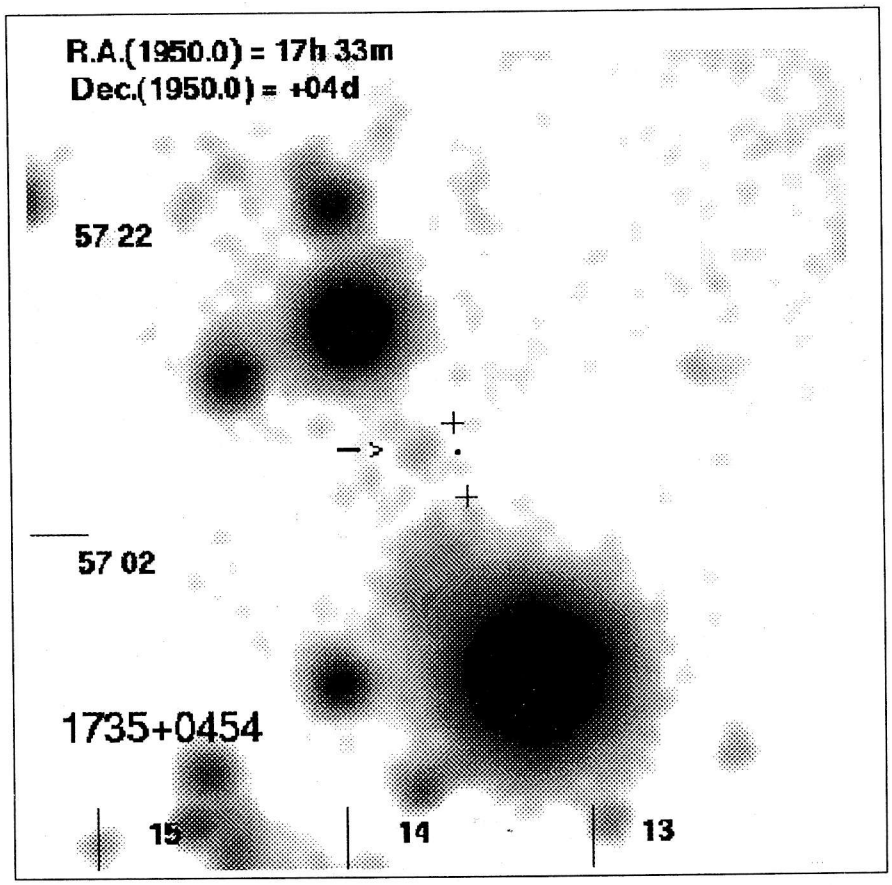
R.A.(1950.0) = 17h 33m
Dec.(1950.0) = +04d
57 22
57 02
1735+0454
15
14
13

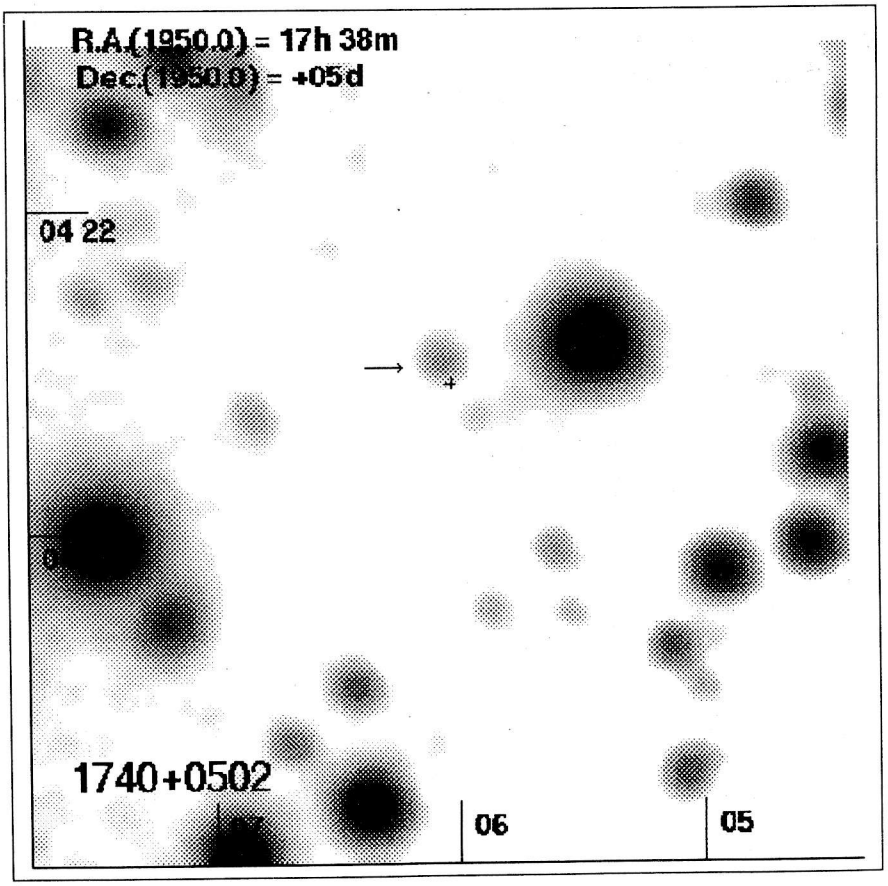
R.A.(1950.0) = 17h 38m
Dec.(1950.0) = +05d
04 22
1740+0502
06
05

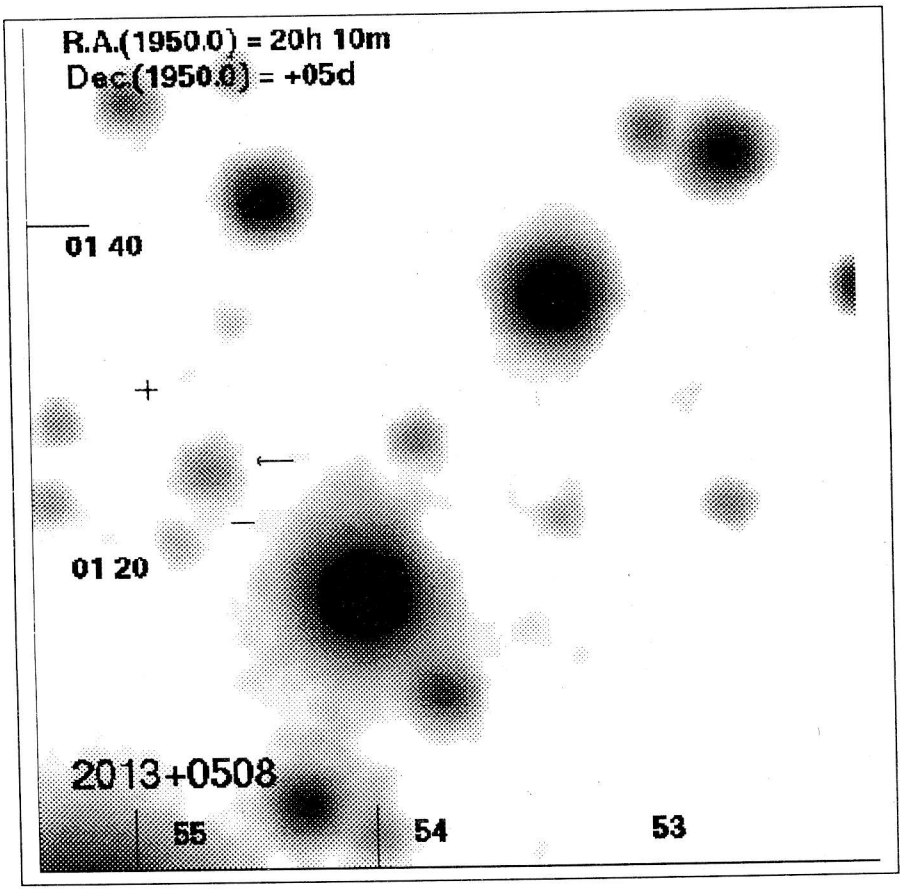
R.A.(1950.0) = 20h 10m
Dec.(1950.0) = +05d
01 40
01 20
2013+0508
55
54
53

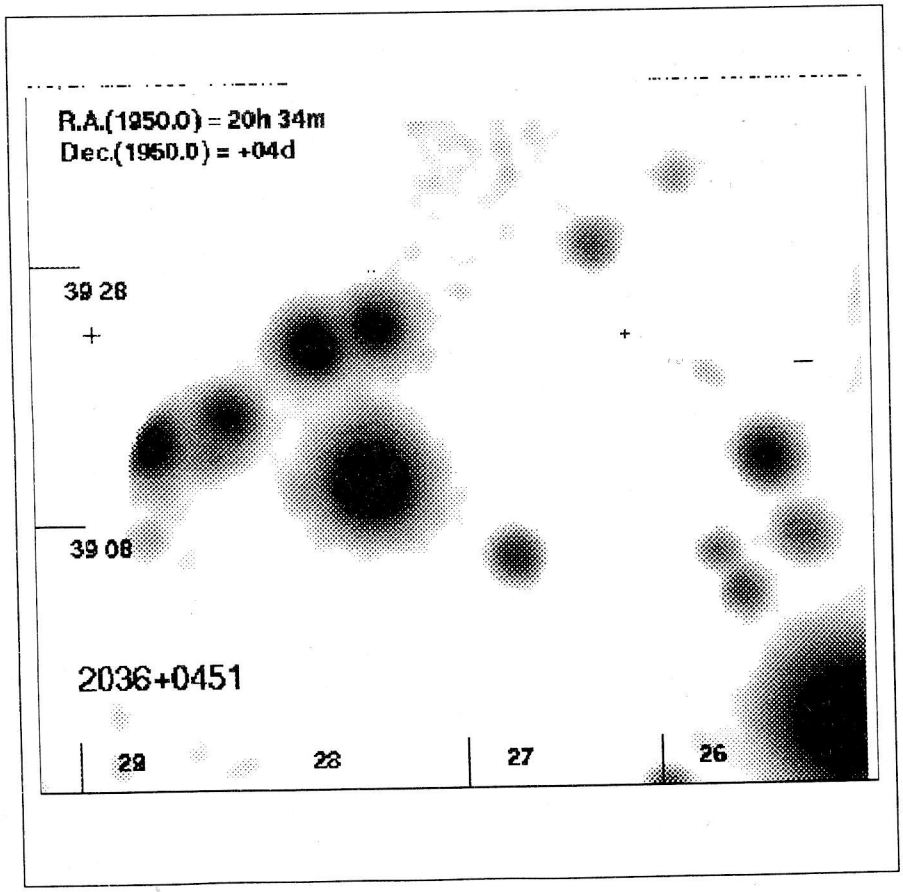
R.A.(1950.0) = 20h 34m
Dec.(1950.0) = +04d
39 28
39 08
2036+0451
29
28
27
26

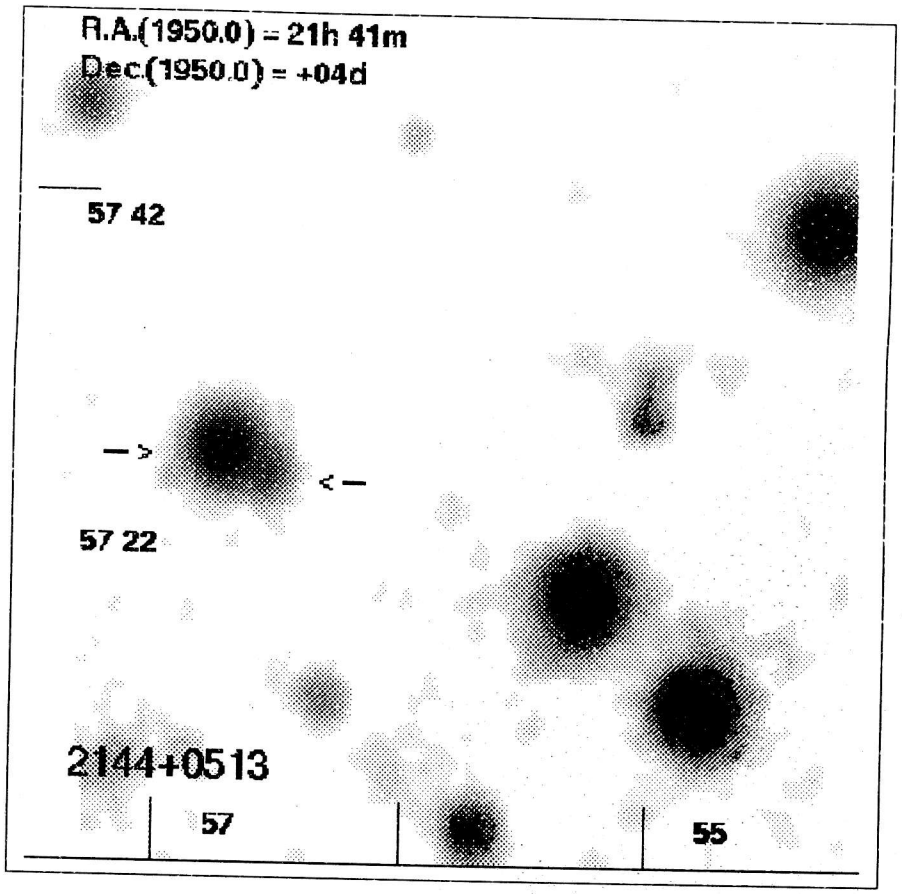
R.A.(1950.0) = 21h 41m
Dec.(1950.0) = +04d
57 42
57 22
2144+0513
57
55

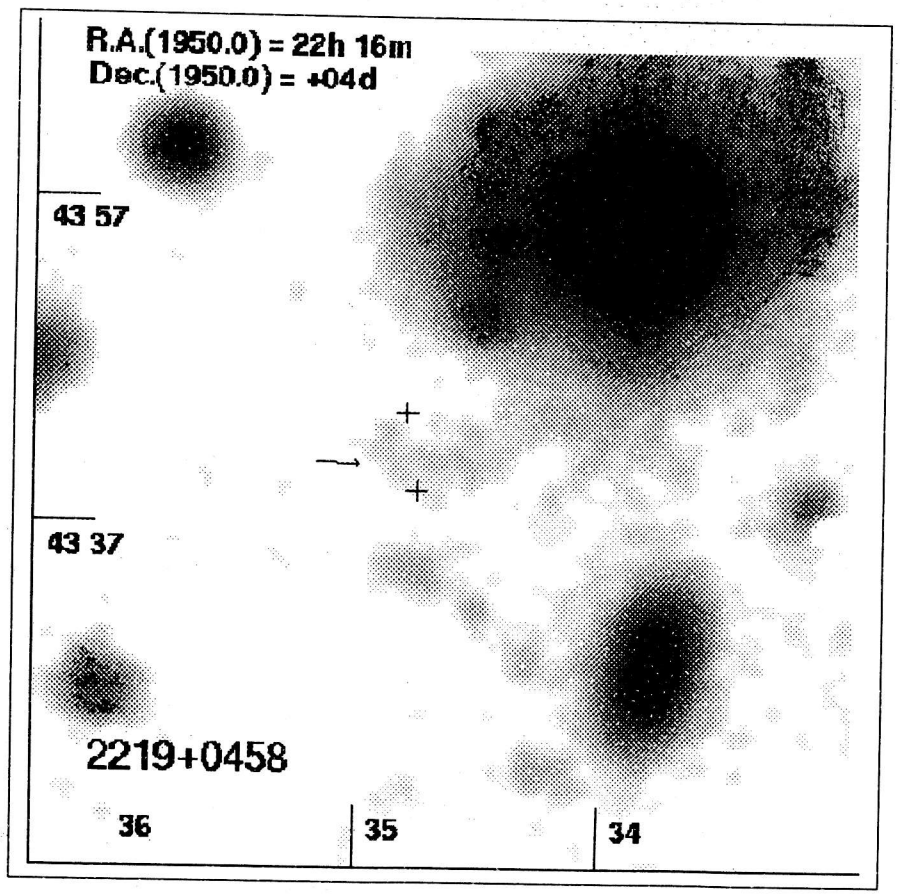
R.A.(1950.0) = 22h 16m
Dec.(1950.0) = +04d
43 57
43 37
2219+0458
36
35
34

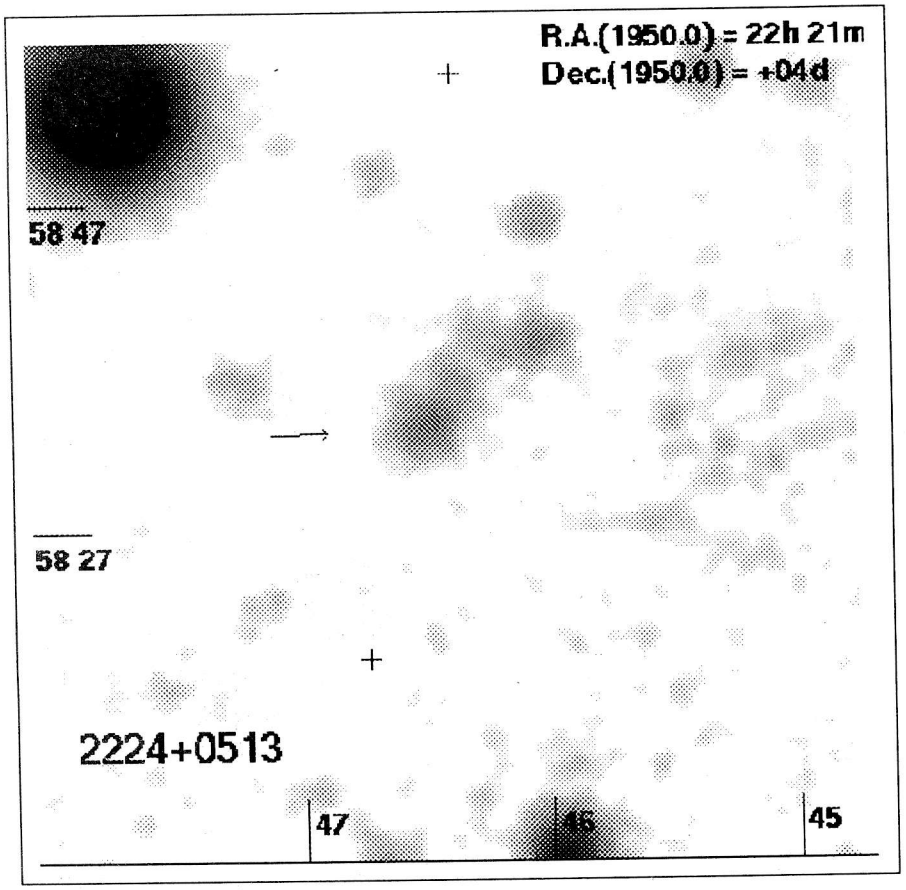
R.A.(1950.0) = 22h 21m
Dec.(1950.0) = +04d
58 47
58 27
2224+0513
47
45
45

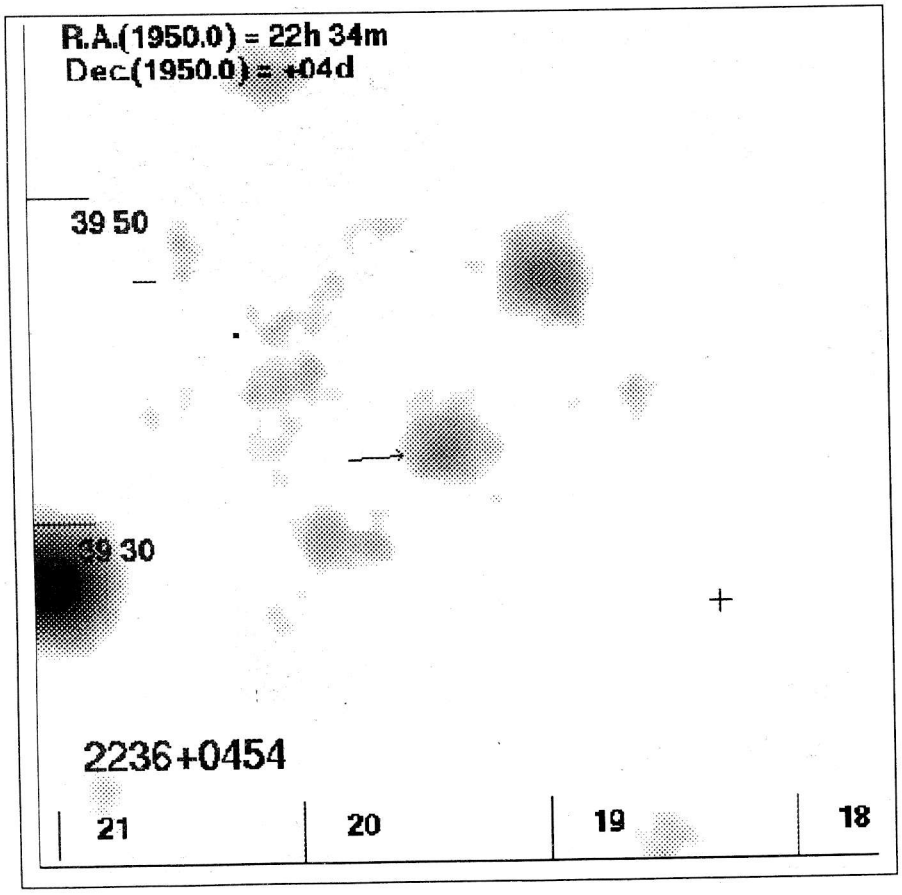
R.A.(1950.0) = 22h 34m
Dec.(1950.0) = +04d
39 50
39 30
2236+0454
21
20
19
18

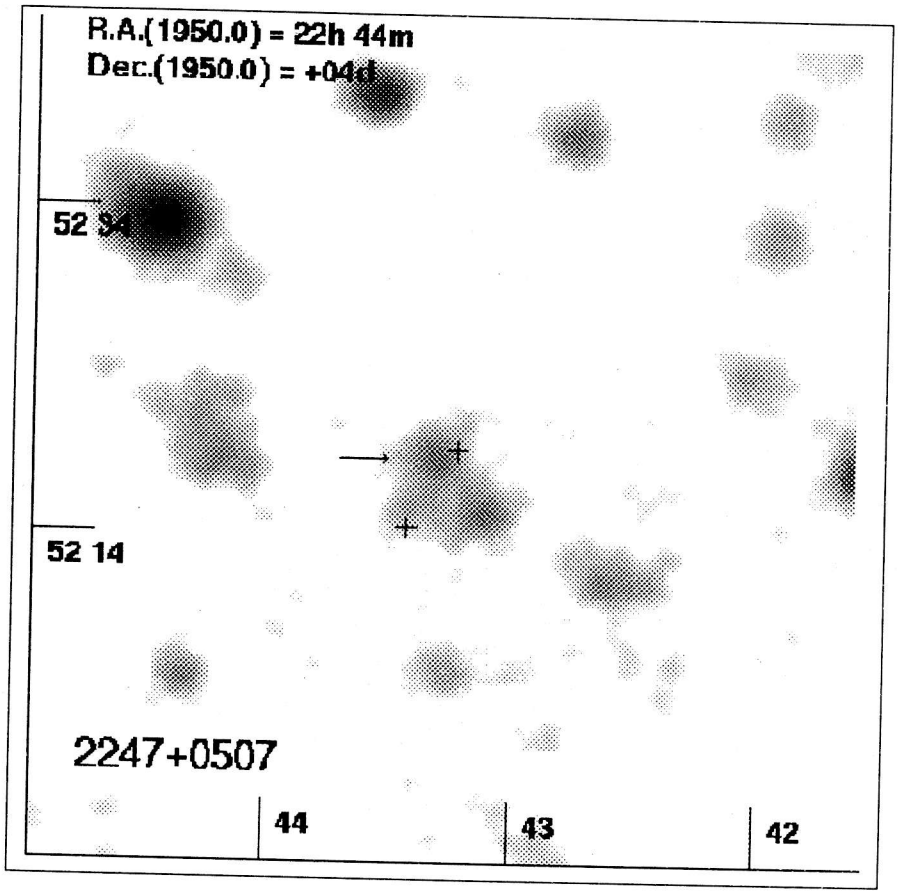
R.A.(1950.0) = 22h 44m
Dec.(1950.0) = +04d
52 24
52 14
2247+0507
44
43
42

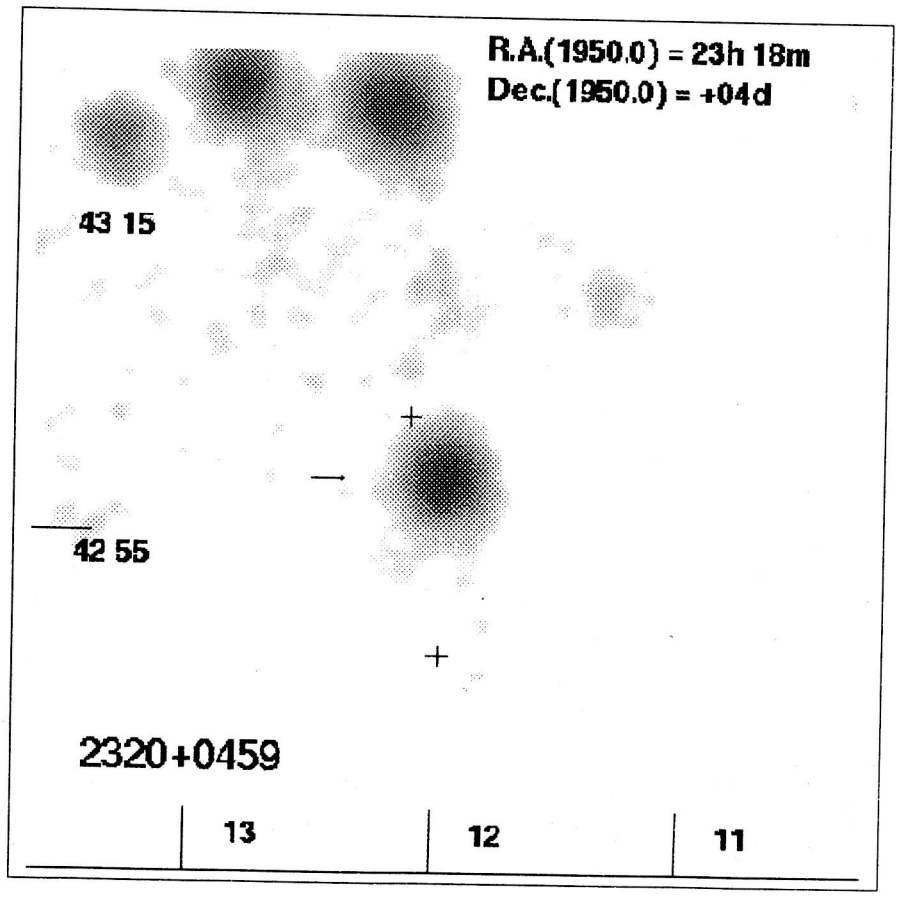
R.A.(1950.0) = 23h 18m
Dec.(1950.0) = +04d
43 15
42 55
2320+0459
13
12
11

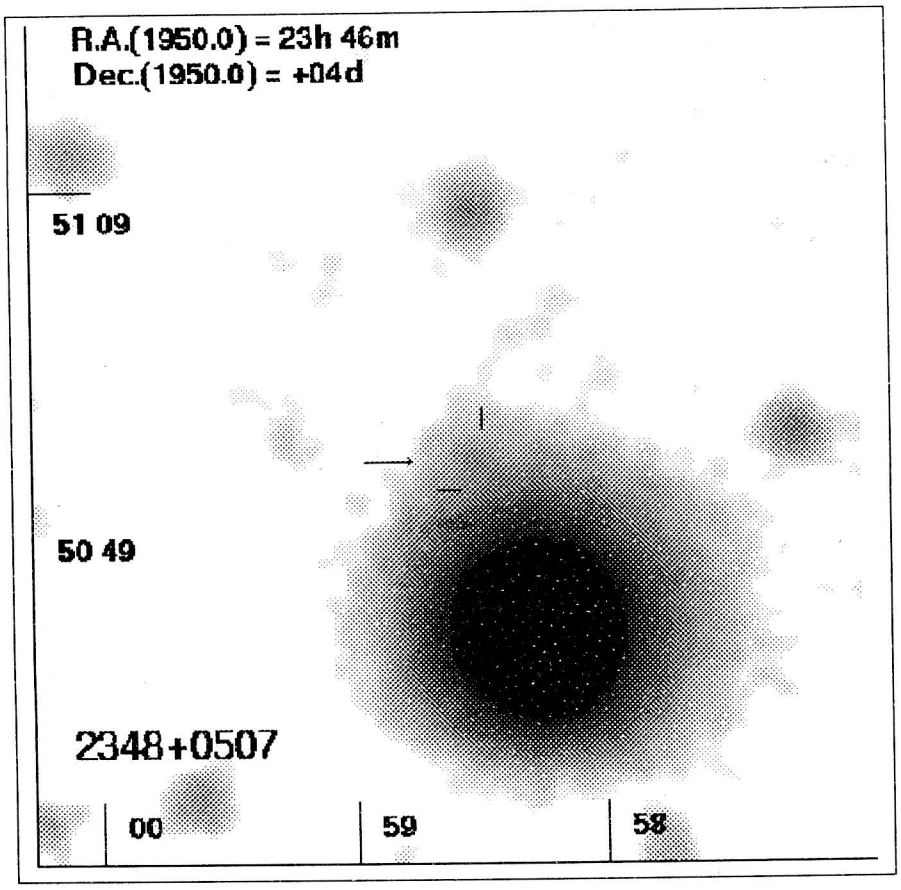
R.A.(1950.0) = 23h 46m
Dec.(1950.0) = +04d
51 09
50 49
2348+0507
00
59
58

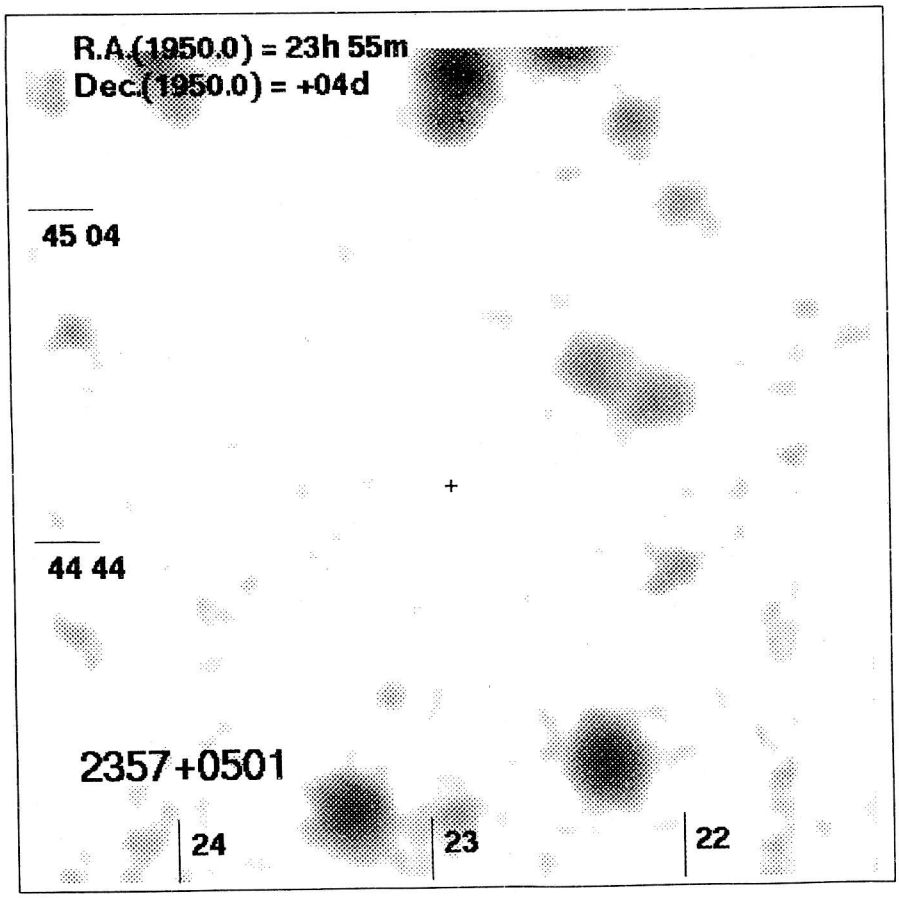
R.A.(1950.0) = 23h 55m
Dec.(1950.0) = +04d
45 04
44 44
2357+0501
24
23
22